TECHNISCHE UNIVERSITÄT MÜNCHEN

Lehrstuhl für Bauchemie

A Comprehensive Study of Interactions Occurring Between Superplasticizers and Clays, and Superplasticizers and Cement

Lei Lei

Vollständiger Abdruck der von der Fakultät für Chemie der Technischen Universität München zur Erlangung des akademischen Grades eines

Doktors der Naturwissenschaften (Dr. rer. nat.)

genehmigten Dissertation.

Vorsitzender:	**Univ.-Prof. Dr. Klaus Köhler**
Prfer der Dissertation:	**1. Univ.-Prof. Dr. Johann P. Plank**
	2. apl.Prof. Dr. Anton Lerf
	3. Univ.-Prof. Dr.-Ing. Karl-Christian Thienel
	Universität der Bundeswehr München

Die Dissertation wurde am 26.02.2016 bei der Technischen Universität München eingereicht und durch die Fakultät für Chemie am 30.03.2016 angenommen.

I have no trace of wings in the air,

but I am glad I have had my flight.

Firefiles
Rabindranath Tagore

Acknowledgements

First and foremost I would like to express my deep gratitude to my supervisor,

Prof. Dr. Johann Peter Plank

who has given me such a wonderful opportunity for conducting my doctoral work here at the Chair for Construction Chemistry, Technische Universität München. He has been a tremendous mentor for me. With his continuous support, encouragement, and immense knowledge, he provided my first exposure to the world of advanced scientific research and guided me throughout my Ph.D. work. Without his input it would not have been possible to complete this thesis. I greatly appreciate the precious opportunities he has offered to attend and present at international conferences. I really benefited tremendously from listening to the lectures and conversing with experts in the construction chemistry field.

I want to thank **TUM Center for Advanced PCE Studies** for providing me the laboratory and analytical instruments.

I would also like to thank the **Jürgen Manchot Stiftung** for generously providing a scholarship to finance my research and stay at TU München. Additionally, they have graciously covered my expenses for several conference trips.

The great appreciation also goes to **Deutsches Zentrum für Luft- und Raumfahrt (DLR)** for financing our parabolic flight experiments. I would like to thank especially **Dr. Ulrike Friedrich** and **Dr. Rainer Forke** for their support!

I want to thank **Dr. Wolfgang Eisenreich** for performing Diffusion-Ordered NMR measurements for me.

My heartfelt gratitude goes to **Gebhard Riepl** & **Angelika Busch** for providing me a warm home on the first day I arrived in Germany, and for always being my family.

Special mention goes to **Dr. Alex Lange** for guidance, especially at the beginning of my study, and all the help during the course of my thesis. Similar gratitude goes to **Markus Meier**, **Dr. Stefan Baueregger** and **Alexander Rinkenburger**, for their experimental contributions. Also, I would like to express my gratitude to **Dr. Oksana Storcheva** for her encouragement and support. My special thanks also go to our secretaries **Tim Dannemann** and **Anke Kloiber** for all their administrative work.

I also want to take this opportunity to thank all my other colleagues at the chair: **Timon Echt**, **Thomas Hurnaus**, **Thomas Pavlitschek**, **Vipasri Kanchanason**, **Somruedee Klaithong**, **Stefanie Gruber**, **Johannes Stecher**, **Johanna de Reese**, **My Linh Vo**, **Huiqun Li**, **Maike Müller**, **Manuel Ilg**, **Markus Schönlein**, **Mouala Moumin**, **Dr. Nan Zou**, **Dr. Salami Taye**, **Dr. Constantin Tiemeyer**, **Dr. Ahmad Habbaba**, **Dr. Julia Pickelmann**, **Dr. Hang Bian** and **Dagmar Lettrich**.

Last but not the least, I would like to thank my family with all my heart – my father **Lei Yongle**, my mother **Zhang Huaping** and my brother **Lei Shaohui**. With their unconditional support and encouragement, my world is full of love.

List of papers

This thesis is based on a total of 13 papers which are listed in the following:

Peer reviewed SCI(E) journal and conference papers

1) **L. Lei** and J. Plank.
"Synthesis and Properties of a Vinyl Ether-Based Polycarboxylate Superplasticizer for Concrete Possessing Clay Tolerance"
Industrial and Engineering Chemistry Research, 53 (3), (**2014**) 1048–1055.

2) **L. Lei** and J. Plank.
"A study on the impact of different clay minerals on the dispersing force of conventional and modified vinyl ether based polycarboxylate superplasticizers"
Cement and Concrete Research, 60 (**2014**) 1–10.

3) **L. Lei** and J. Plank.
"A Simplified Preparation Method for PCEs Involving Macroradicals"
in: V. M. Malhotra (Ed.), 11th International Conference on Superplasticizers and Other Chemical Admixtures in Concrete (CANMET/ACI), July 12–15, **2015**, Ottawa (ON / Canada), Proceedings, SP-302-12, 155–168.

4) **L. Lei**, M. R. Meier, B. Zheng, L. Fu and J. Plank.
"Early Hydration of Portland Cement Admixed with Polycarboxylates Under Microgravity Conditions"
Journal of Advanced Concrete Technology, 14(3), (**2016**) 102-107.

5) A. Lange, **L. Lei** and J. Plank.

"Cement Compatibility of PCE Superplasticizers"
14th International Congress on the Chemistry of Cement (ICCC), October 13–16, **2015**, Beijing, China.

6) S. Baueregger, **L. Lei**, M. Perello, J. Plank.
"Use of a Nano Clay for Early Strength Enhancement of Portland Cement"
5th International Symposium on Nanotechnology in Construction (NICOM5), May 24–26, **2015**, Chicago (USA). Proceedings, 199–206.

Non-reviewed conference papers

7) **L. Lei**, J. Plank.
"Impact of Different Clay Minerals on the Dispersing Force of Vinyl Ether Based Polycarboxylate Superplasticizers and Respective Mitigation Strategies"
Tagung der GDCh-Fachgruppe Bauchemie, October 6–8, **2014**, Kassel (Germany), GDCh-Monographie 47, 84–87.

8) **L. Lei**, J. Plank.
"A Study on the Impact of Different Clay Minerals on the Dispersing Force of Conventional and Modified Vinyl Ether Based Polycarboxylate Superplasticizers"
in: P. Gupta (Ed.), 11th International Conference on Superplasticizers and Other Chemical Admixtures in Concrete (CANMET/ACI), July 12–15, **2015**, Ottawa (ON / Canada), Supplementary Papers, 145–159.

9) **L. Lei**, J. Plank.
"A Study on the Sensibility of Conventional Vinyl Ether-based Polycarboxylate superplasticizers Toward Different Clay Minerals"
in: C. Shi, Z. Ou, K. H. Khayat (Eds.), Design, Performance and Use of Self-Consolidating Concrete (SCC'2014), Proceedings of the 3rd International Symposium, Xiamen (China), June 5–8, **2014**, RILEM Publications S.A.R.L., Bagneux (F), p. 126.

10) **L. Lei**, J. Plank.
"Synthesis, characterization of a vinyl ether based Polycarboxylate Possessing Clay Tolerance"
1st International Conference on the Chemistry of Construction Materials, Berlin (Germany), October 7–9, **2013**, GDCh-Monographie 46, 297–300.

11) **L. Lei**, J. Plank.
"A novel type of PCE superplasticizer exhibiting clay tolerance"
4th National Conference on Polycarboxylate Superplasticizer and Application Technology, June 18–20, **2013**, Beijing (China), in: Polycarboxylate superplasticizers – New progress in preparation, performance and application technology, Beijing Institute of Technology Press, 58 – 65.

12) **L. Lei**, J. Plank.
"Preparation and characterization of a novel polycarboxylate montmorillonite nanocomposite"
18th International Symposium on Intercalation Compounds (ISIC18), Strasbourg (France), May 31–June 4, **2015**, Compilation of Abstracts p. 86.

13) **L. Lei**, J. Plank, M. R. Meier.
"Impact of Polycarboxylate Superplasticizers on Ettringite Crystallization at Very Early Cement Hydration Stages Under Zero Gravity"
5th National Conference on Polycarboxylate Superplasticizer and Application Technology, June 15–17, **2015**, Beijing, China. Proceedings, 45–49.

List of abbreviations

Cement chemistry notation:

In order to simplify the formulas of cement minerals, and compounds, an abbreviated cement chemistry notation has been developed. There, shorthand notations that leave out the oxygen are used.

Notation	Chemical formula	Mineral name
C	CaO	Calcium oxide
S	SiO_2	Silicon dioxide
A	Al_2O_3	Aluminium oxide
F	Fe_2O_3	Iron oxide
H	H_2O	Water
$\bar{S}$	SO_3	Sulfur trioxide
C_3S	$3CaO{\cdot}SiO_2$	Tricalcium silicate
C_2S	$2CaO{\cdot}SiO_2$	Dicalcium silicate
C_3A	$3CaO{\cdot}Al_2O_3$	Tricalcium aluminate
C_4AF	$4CaO{\cdot}Al_2O_3{\cdot}SiO_2$	Tetracalcium alumino ferrite
$C_3A\bar{S}_3H_{32}/AF_t$	$3CaO{\cdot}Al_2O_3{\cdot}3CaSiO_4{\cdot}32H_2O$	Ettringite
$C_3A\bar{S}H_{12}/AF_m$	$3CaO{\cdot}Al_2O_3{\cdot}CaSiO_4{\cdot}12H_2O$	Monosulfate

General abbreviations:

AA	Acrylic acid
AFS	Acetone formaldehyde sulfite resin
APEG	α-allyl-ω-methoxy or hydroxy poly(ethylene glycol)
BNS	Sulfonated naphthalene formaldehyde resin
bwoc	by weight of cement
bwo clay	by weight of clay
EO	Ethylene oxide
ESEM	Environmental scanning electron microscope (y)
GPC	Gel permeation chromatography
HPEG	α-methallyl-ω-methoxy or -ω-hydroxy poly(ethylene glycol) ether
IPEG	Isoprenyl oxy poly(ethylene glycol) ether
MA	Methacrylic acid
MPEG	Methoxy poly(ethylene glycol)
MPEG-MA	ω-methoxy poly(ethylene glycol) methacrylate ester
PCE	Polycarboxylate ether/ ester
PDI	Polydispersity index
PEG	Poly(ethylene glycol)
PEO	Poly(ethylene oxide)
PMS	Sulfonated melamine formaldehyde resin
SEC	Size Exclusion Chromatography
SEM	Scanning electron microscope (y)
SPF	Sulfanilic acid phenol formaldehyde resin
TGA	Thermogravimetric analysis
TOC	Total Organic Carbon
VPEG	α-vinyl-ω-hydroxy poly(ethylene glycol) ether
w/c	Water-to-cement ratio
XRD	X-ray diffraction

Contents

1 Introduction

Concrete admixtures present key components of modern concrete. The most recent technological breakthroughs originate from the invention of novel admixtures while cement manufacturing itself has matured somewhat [1, 2].

Concrete superplasticizers are widely used in the construction industry and present a very important class within in the admixture family. With the help of modern superplasticizers, concrete of extremely high fluidity with much reduced water-to-cement ratio can be produced. Among the different superplasticizers based on various chemical structures, polycarboxylate based superplasticizers (PCEs) became extremely popular due to their high effectiveness at low w/c ratios and the easy modification of their chemical properties and performance characteristics.

The comb-shaped polycarboxylate copolymers consist of a negatively charged backbone and grafted hydrophilic side chains, typically from polyethylene glycol [3–5]. Due to the high flexibility in their chemistry which makes tailored molecular design possible, various PCE products based on different chemical compositions are available nowadays on the market. Through the modification of PCE molecular architecture, different application purposes can be satisfied.

In this thesis, different synthesis approaches to achieve different types of PCE polymers are elaborated and, in addition, the advantages and drawbacks of these synthetic routes are highlighted. In the industry, free radical copolymerization where macromonomers are involved presents the most widely applied synthetic method. Here, the quality of the macromonomers greatly determines the performance of the final PCE products, thus the ability to provide good quality macromonomers is of great importance. Generally, they can be produced in a one-step synthesis process by reacting an unsaturated alcohol with ethylene oxide. For methacrylate ester macromonomers in particular it is very critical to

control their di-ester content (typically < 3 %) to avoid occurrence of cross linking during PCE synthesis.

In spite of the great benefits from PCE technology, still some limitations and problems exist which need to be improved. Those include:

- Clay sensitivity

It has been reported that PCE superplasticizers exhibit a strong sensitivity to clay contaminants occurring in aggregates [6–9]. Because of this effect the dispersing performance of PCEs can be reduced significantly. To make it even more complicated, the negative effect from clay contaminants varies from case to case depending on the type of clay. For example, montmorillonite, due to its expanding lattice and strong water swelling capacity, causes a much higher loss in workability than other types of clays [10, 11]. PCEs can be consumed by clays in two different ways, namely through surface adsorption and chemical intercalation. Adsorption of Ca^{2+} ions from cement pore solution onto the negative aluminosilicate layers induces a charge reversal on the clay surface, then PCE polymers can adsorb on the positively charged clay particles. Moreover, PCE molecules can become entrapped in the interlayer region of the clay lattice (typically of swelling clays such as smectites) through intercalation. The driving force behind such chemisorption is the affinity of the aluminosilicate layers for PEG chains which are a major constitute in PCE molecules. Through these two mechanisms, PCE polymers can be depleted from the cement pore solution, thus the dispersing force is much reduced or even lost completely. Consequently, new PCE superplasticizers possessing modified chemical structures for enhanced robustness towards clay minerals need to be developed and studied.

Here, in this study, the mode of interaction between PCE polymers and clays was clarified. It was found that based on their different lattice structures, the interaction between PCEs and clays can be only surface adsorption or include both physical and chemical interaction. Moreover, PCE structures exhibiting enhanced clay tolerance were proposed and successfully synthesized.

- Cement compatibility

It has been noticed by PCE applicators that some PCEs can show great sensitivity towards different cement compositions. The fluctuations in the dispersing performance

signify the compatibility problem between some cements and PCEs. Several factors such as the cement and superplasticizer composition or the free sulfate content alone or synergistically can cause the incompatibility problem [12].

C_3A plays a crucial role in cement compatibility of PCE superplasticizers. From mechanistic studies it is known that the dispersing force of PCEs originates from the adsorption of negatively charged anchor groups on the clinker phase C_3A or its early hydration products, namely ettringite (AF_t) and calcium monosulfoaluminate (AF_m). Consequently, cements with high C_3A contents require much higher PCE dosages due to the larger surface areas to cover [13–15].

Free soluble alkali sulfates are another factor which can influence the compability between cement and PCEs. Owed to their presence, competitive adsorption between the PCEs and sulfate on cement particles can occur whereby the rheology of the cement paste is negatively affected [16]. The problem was solved by modifying the PCE molecular architecture. To be more specific, PCEs incorporating blocks of highly negative charge along the trunk chain or containing stronger anchor groups such as phosphates or phosphonates have been demonstrated to be more sulfate tolerant [17].

Regarding PCE polymers, their type, dosage, chemical composition and molecular structure can greatly influence the rheological properties of cement pastes. It has been reported before that superplasticizers act as morphological catalyst for ettringite crystals which presents the most early cement hydrate and also the main anchoring phase for superplasticizers [18]. As for PCE molecules, they can also change the morphology of ettringite e.g. to much smaller needles, consequently the compatibility between PCEs and cement can be affected.

Here, the incompatibility phenomenon occurring between most PCE polymers and specific cements was investigated. A wide range of ordinary Portland cements (OPCs) and structurally different PCE superplasticizer samples were chosen to probe their cement compatibility via the 'mini slump' test. The morphology of the ettringite crystals was observed under the SEM, and the role of the PCE polymers as morphological catalyst was elucidated.

2 Aims and scope

This PhD work is dealing with five different research topics. In the following, a brief summary of each topic is provided.

2.1 Impact of different clay minerals on the dispersing force of PCEs & synthesis of clay tolerant PCEs

The aim of this part was to fundamentally understand the interaction mechanism between different clay minerals and PCE polymers. First of all, three most frequently occurring clay minerals (montmorillonite, kaolin, muscovite) were characterized via methylene blue test, thermogravimetric analysis and zeta potential measurement in order to obtain their cation exchange capacity, overall water uptake and Ca^{2+} sorption capacity.

From previous studies it was known that the PEG side chain existing in PCE polymers present the reason for intercalation into the layer structure of clays which leads to a huge loss in paste flow. Subsequently, new PCE structures incorporating hydroxyalkyl pendant chains were synthesized, and in a mechanistic study, conventional PCEs were also synthesized for comparison as well. For both polymers, the dispersing force in cement pastes containing different clay minerals was tested. To specify their different modes of interaction with these three different clay minerals, XRD analysis, adsorption and zeta potential measurements were carried out.

2.2 A new synthetic route for PCEs involving macroradicals

The most common industrial synthesis methods of (meth)acrylate ester-based PCEs include aqueous free radical copolymerization and grafting (esterification) reaction. Most often, the process of radical copolymerization is applied, however its limitation is the requirement for macromonomers which may not be easily available in some countries and areas. The alternate method via esterification reaction can produce PCEs with more regular structures, however its disadvantage is the difficulty in preparing short-chain poly(meth)acrylic acid as backbone.

The goal of this study was to develop a new synthesis route for MPEG PCEs utilizing easily accessible raw materials such as maleic anhydride and ω-methoxy poly(ethylene glycol). To achieve this, different synthesis approaches were probed and a facile process will be suggested. Furthermore, the synthesized polymers were characterized via GPC and charge titration measurements. Their dispersing power was evaluated via 'mini slump' test. The specific reaction mechanism occurring there was also studied.

2.3 Study of cement – PCE incompatibility

The fluctuating dispersing performance of PCEs with different cements was studied in this part. The incompatibility problem observed from some cements was not only related to the C_3A content in the cement samples, but also to the potential role of PCEs as morphological catalysts which can greatly decrease the size of ettringite crystals. For this purpose, the initial hydration products generated in the presence or absence of PCE polymers were investigated under the SEM.

2.4 Influence of PCE polymers on early ettringite crystallization

As discussed above, PCE polymers can act as morphological catalysts for ettringite. The aim of this work was to establish a better understanding of the nucleation and

crystal growth of ettringite, thus the interaction of such polymers with ettringite could be clarified.

Due to the complexity of the initial crystallization process of ettringite, very few studies have been carried out so for on this topic. Here, the formation of ettringite was investigated under zero gravity conditions where only diffusion dependent crystallization could occur. These experiments were performed on parabolic flights which produce microgravity conditions for 22 s. The morphology of ettringite crystals formed under zero gravity was compared with those produced in the earth's gravity field.

2.5 Nano clays as enhancer for the early strength of cement

Common cement hydration accelerators boost the early strength of cement while sacrificing the final strength. In this part, two nano clay samples possessing different sizes were tested for their potential effectiveness on increasing the 16 h strength of Portland cement. A thorough mechanistic study was also carried out to explain the strength enhancing effect observed. A correlation between the strength enhancement and particle size of nano clay was established.

3 Theoretical background and state of the art

3.1 Superplasticizers and their interaction with cement

3.1.1 Types of superplasticizers

The invention of superplasticizers presents one of the most important breakthroughs in concrete technology [19–21]. Superplasticizers used in concrete can significantly increase the workability and fluidity of concrete by dispersing cement particles present in the paste [22]. With the help of modern technology based on superplasticizers, high-performance concrete that includes self-compacting concrete and high-strength concrete can be achieved nowadays [23].

The first commercial application for superplasticizers can be traced back to 1959, when a BNS polycondensate was applied in oil well cementing in Oklahoma. Thereafter, these polycondensates, namely sulfonated melamine formaldehyde resins (PMS) and sulfonated naphthalene formaldehyde polycondensates (BNS) were used in concrete.

Interestingly, the first two polycondensate type superplasticizers were invented separately in Germany by *SKW Trostberg AG* and in Japan by *KAO SOAP* in the same year 1962. The advent of these two types of superplasticizers signified that a completely new era had come which had brought the concrete technology a huge step forward. Applicators also started to realize the important role concrete admixtures can play in the concrete technology which led to the widespread use of superplasticizers beginning in the 1970s [24, 25]. Even though polycondensates have been extremely successful in application, they still revealed some apparent drawbacks. For example, naphthalene-based polycondensates

show a rapid decrease in the dispersing performance (poor slump retention behavior) [26]. Additionally, BNS has a tendency to crystallize and precipitate Na_2SO_4 at low temperatures which requires a purification step to remove the unwanted sulfate. Similarly, the drawbacks of PMS are higher raw materials cost and a reduced performance at low w/c ratios [27]. The synthesis routes for BNS and PMS are shown in **Figure 1** and **Figure 2** respectively.

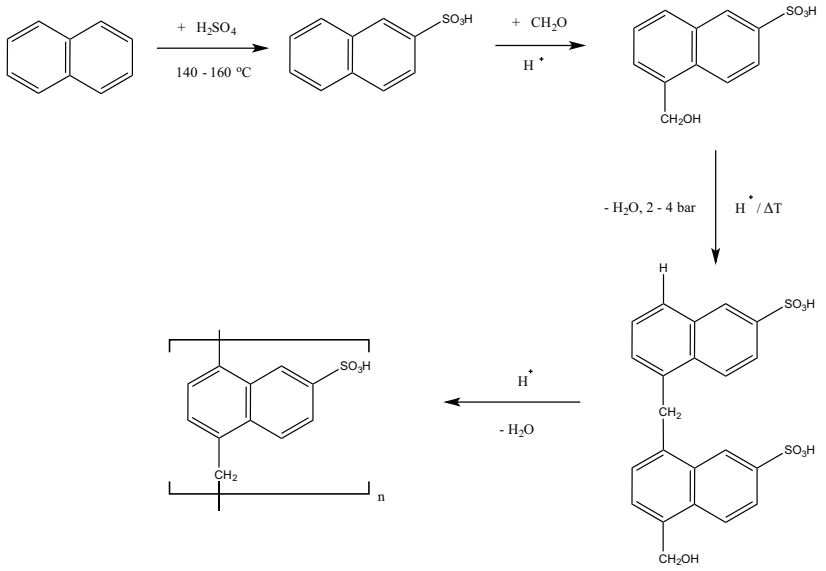

Figure 1: Synthesis route and molecular structure of BNS polycondensate superplasticizer

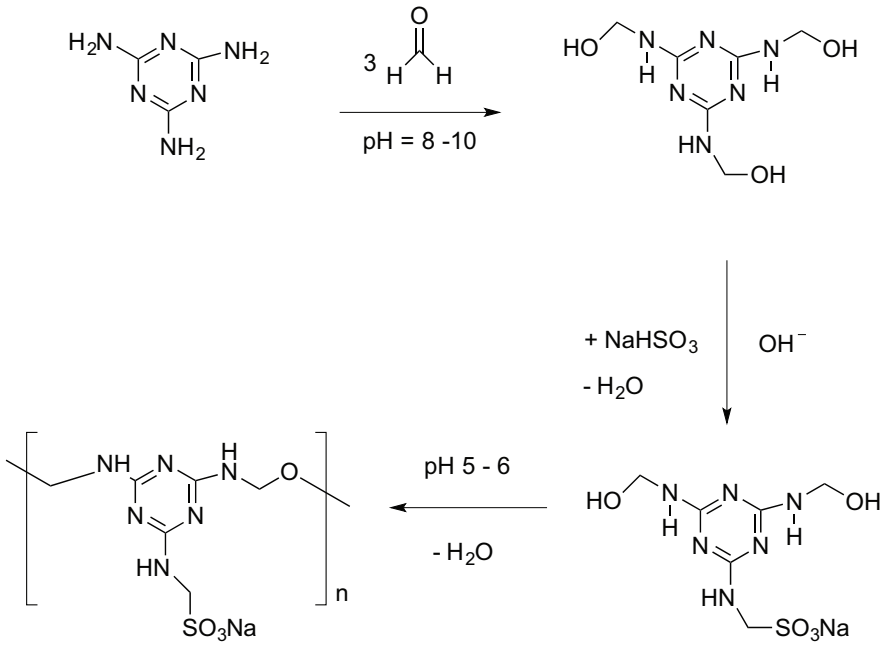

Figure 2: Synthesis route and molecular structure of PMS polycondensate superplasticizer

Another very important polycondensate based admixture is the so-called aliphatic superplasticizer which is produced from acetone, formaldehyde and sulfite via an aldol condensation. The synthesis steps are shown in **Figure 3**. This type of polycondensate was also developed by *SKW Trostberg AG*, Germany, it is generally abbreviated as AFS [28, 29]. Unfortunately, AFS exhibits a characteristic and intense red color which prevented its more wide-spread application in concrete. However, AFS possesses several advantages over the other polycondensates such as inexpensive raw materials, simple synthetic method and no air entrainment which still make it very popular in some countries. For example, in some parts of China it still presents the main kind of superplasticizer being used in concrete due to its robustness towards sand or aggregates which are highly contaminated with clay and silt, its inexpensive raw materials and its mixability with PCEs [27]. In oil well cementing, AFS polycondensate contributes much as the predominant dispersant which is attributed to its high temperature stability, salt tolerance and a synergistic effect with cellulose ethers [30].

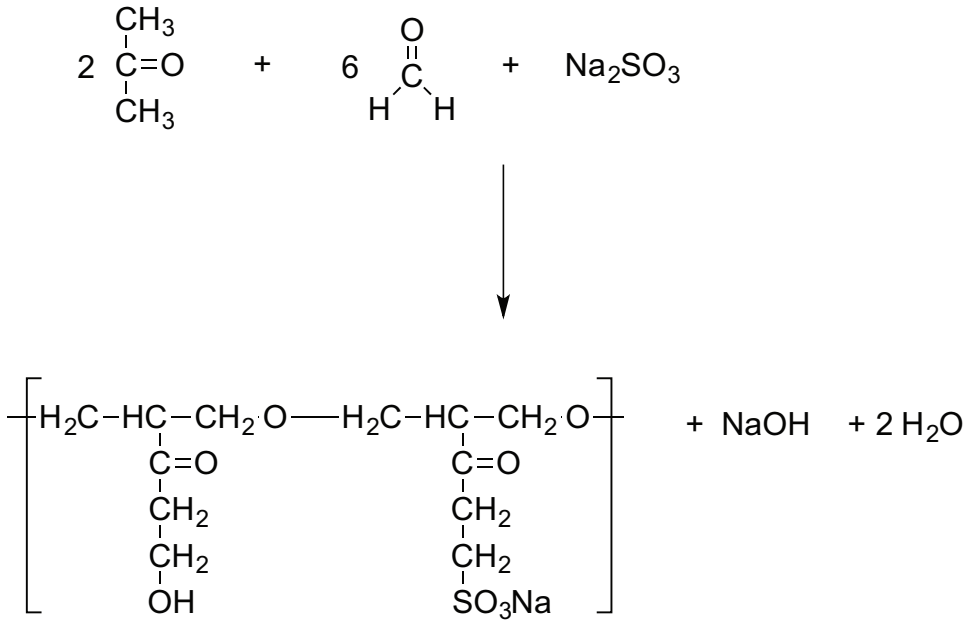

Figure 3: Synthesis route and molecular structure of AFS polycondensate superplasticizer

In China, a relatively low cost new type of polycondensate based on sulfanilic acid, phenol and formaldehyde (SPF) has been developed [31]. It shows similar properties like AFS, only the color is less intensive than from AFS which made it easier for applicators in China to accept. What's more, SPF shows a better slump loss behavior stemming from

a minor retarding effect of the phenolate functionality. The chemical structure of SPF is shown in **Figure 4**.

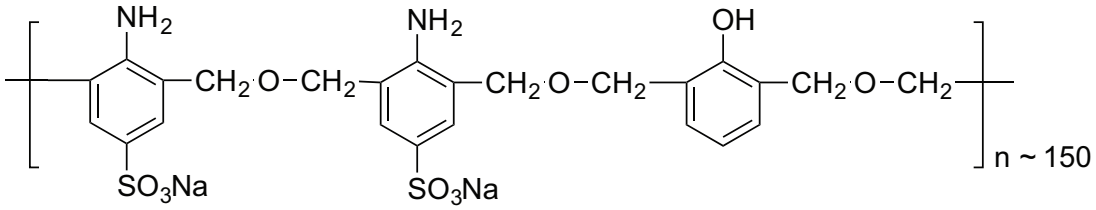

Figure 4: Molecular structure of SPF polycondensate superplasticizer

Recently, a novel cycloaliphatic superplasticizer (CFS) based on cyclohexanone was successfully synthesized from cyclohexanone, formaldehyde and sulfite [22]. Its synthesis procedure is presented in **Figure 5**. It has been proven as an effective cement dispersant and even works at low w/c ratios. However, so far no commercial use has been reported till now.

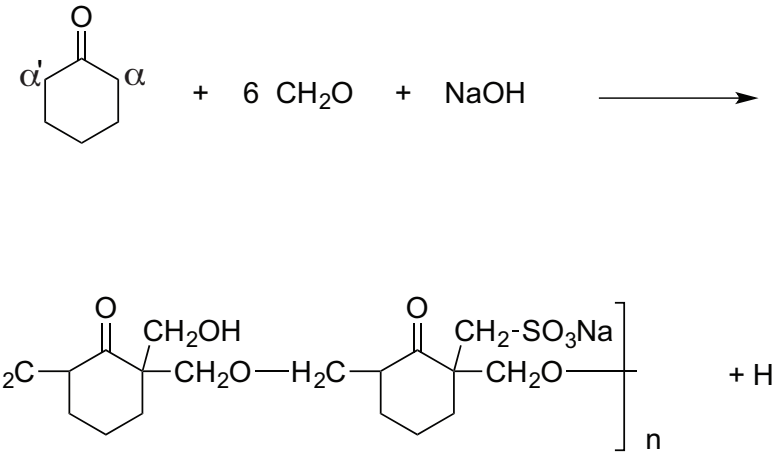

Figure 5: Synthesis route and molecular structure of CFS polycondensate superplasticizer

All polycondensate superplasticizers possess good tolerance to different cement compositions and various aggregate quality. They are mostly prepared from relatively cheap materials, especially BNS, while PMS requires a more sophisticated raw material. These two polycondensates present the main products within their group.

From all the polycondensate superplasticizers we have discussed above, it is obvious that all of them possess specific advantages, but also serious drawbacks, such as poor slump retention ability, inferior dispersing performance at low w/c ratio, and a free formaldehyde content. Thus, in 1981, a new class of superplasticizer based on a completely new

chemistry was introduced by the Japanese company NIPPON SHOKUBAI. Due to the high degree of flexibility in their molecular design, PCE polymers can be prepared such that they can satisfy a broad variety of application fields.

3.1.2 Polycarboxylate-based superplasticizers

Comb shaped PCE polymers are generally composed of hydrophilic polyethylene oxide (PEO) pendant chains grafted onto adsorbing backbone units.

Classification of polycarboxylate superplasticizers

To improve the workability of concrete, numerous modification attempts have been made to achieve polymers of different charge densities [32], side chain lengths [33, 34], backbone variations [35], degree of backbone polymerisation [3, 33] and functional groups [3, 36]. Currently, a great diversity of chemically different PCE products is on the market which includes:

MPEG-type PCEs: made from ω-methoxy poly(ethylene glycol) methacrylate ester (MPEG-MA). MPEG-PCEs can be prepared via two different synthesis approaches:

(a) The so-called grafting process presents the very early synthesis route for MPEG type PCEs. In this case, commercially available ω-methoxy poly(ethylene glycol) is grafted onto a poly(meth)acrylic acid backbone via esterification reaction at the desirable molar ratio to achieve certain properties. Generally, the esterification reaction requires a relatively high temperature (120 – 150 ^{o}C) to speed up the reaction. Different acid catalysts including p-toluenesulfonic acid or hypophosphite are applied. Other methods such as employment of azeotropic solvents (e.g. benzene, cyclohexane etc.) to remove the water from the system increase the reaction efficiency and also improve the conversion rate [37]. The products resulting from this approach typically possess a statistical distribution of side chains along the main chain which means that the PEG lateral chains are relatively regularly distributed along the poly(meth)acrylic acid main chain, see **Figure 6**. It should be noted here that the poly(meth)acrylic acid backbone used in the grafting needs to be rather short, ideally $<$ 4,000 g/mol. This is because PCE polymers built on shorter backbones adsorb fast on cement, thus providing an immediate plasticizing

effect. Furthermore, the molecular masses of PCE products should be limited to insure high water reduction capacity as well as solubility in water. However, the difficulty to control the suitable length of poly(meth)acrylic acid backbone due to the high tendency for (meth)acrylic acid to homopolymerize and form long chains hinders the wide-spread application of this method.

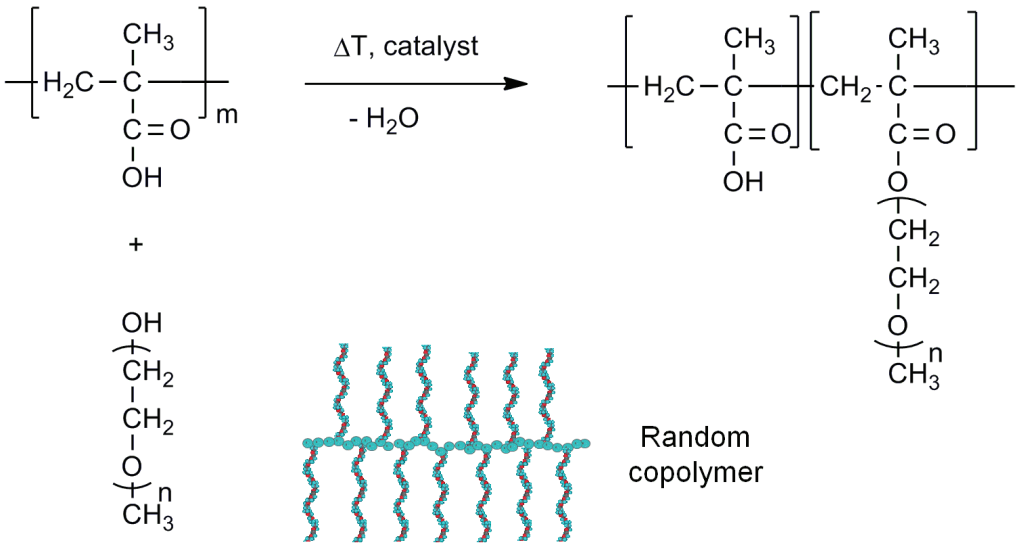

Figure 6: Esterification (grafting) process for the synthesis of MPEG – type PCEs resulting in random copolymers

(b) A more preferable synthesis process for MPEG PCEs is presented by free radical copolymerization whereby a methacrylate ester based macromonomer is reacted with (meth)acrylic acid. Usually a chain transfer agent (e. g. methallyl sulfonic) is used to control the molecular weight. This method is commonly accepted in large scale manufacturing due to its relatively simple procedure. Also no harsh reaction conditions (e.g. high temperature), and no pressurized equipment such as in the case of BNS is required. Furthermore, the specific properties of PCE products can be tailored via modifying the molar ratios of the monomers or adjusting the main chain length by using a chain transfer agent. Researchers carried out a number of studies regarding further improvement of the synthesis procedures, such as batch polymerization and continuous polymerization processes. In batch polymerization, at first the monomers are placed in the reactor at a defined monomer ratio, then initiator is added continuously over time. While in the case of a continuous polymerization process, the monomers and initiator are fed into

the reactor over time. Diversified initiator systems can be employed here, like sodium peroxodisulfate, or redox systems such as Fe^{2+}/H_2O_2, rongalite/Fe^{2+}/H_2O_2 or ascorbic acid/H_2O_2. The reaction is typically carried out at 60 – 80 ^oC. Recently, even a polymerization method which can be performed at room temperature and does not require heating has been developed [38]. Due to the different reactivities of macromonomer and acid-bearing monomer, the PCE polymers resulting from this method exhibit a gradient structure which is characterized by different side chain densities along the trunk of the polymer chain, see **Figure 7**. PCE polymers possessing such unique structure often show superior performance towards high sulfate content in the system which is attributed to the large anionic blocks present in the gradient polymer. These blocks enable the polymer to adsorb more strongly on cement particles. However, this preparation method depends on the local availability of macromonomers which may not always be at hand.

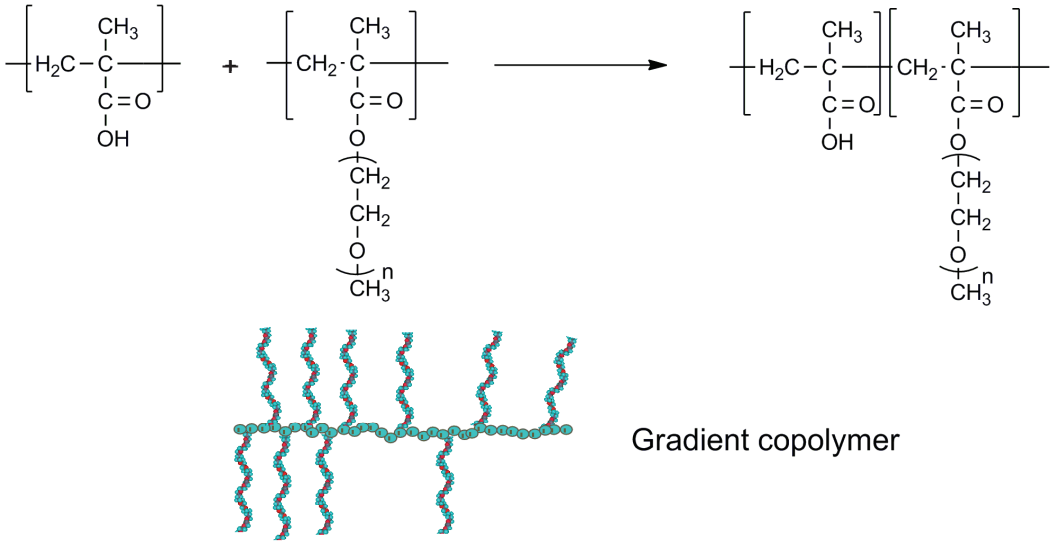

Figure 7: Free radical copolymerisation route for the synthesis of MPEG – type PCEs producing a gradient polymer with large anionic blocks

APEG-type PCEs: prepared from α-allyl-ω-methoxy or ω-hydroxy poly(ethylene glycol) (APEG) ether and maleic anhydride as key monomers via radical copolymerization, either in bulk or in aqueous solution [39]. The APEG macromonomer doesn't homopolymerize due to its mesomeric stabilization which results in a strictly alternating polymer with a well-defined structure (monomer sequence: ABAB ...). Comonomers such as styrene are frequently used as so-called spacer molecules to adjust the conformational flexibility of the trunk chain.

VPEG-type PCEs: they are based on vinyl ethers such as 4-hydroxy butyl-poly(ethylene glycol) vinyl ether which is preferably co-polymerised at low temperatures ($< 30\ ^oC$), e. g. with maleic anhydride [40].

HPEG-type PCEs: they utilize α-methallyl-ω-methoxy or ω-hydroxy poly(ethylene glycol) ether as macromonomer [41]. Compared to the APEG macromonomer, the HPEG macromonomer possesses a much higher reactivity, because resonance stabilization is not possible here. For this reason, the synthesis of PCEs utilizing HPEG macromonomers presents a better and easier approach. Currently, HPEG-type PCEs are the dominant products in China. When HPEG macromonomer reacts with acrylic acid, a lot of reaction heat is released during the polymerization process. Consequently, a process whereby copolymerization is carried out at room temperature utilizing redox initiators has been developed and is widely applied in China [38].

IPEG-type PCEs: (sometimes also referred to as TPEG-type PCE) they are made from isoprenyl oxy poly(ethylene glycol) macromonomers by copolymerisation with acrylic acid, for example according to [42]. Recently, this type of PCE has become very popular because of its easy preparation from versatile raw materials and its high effectiveness in concrete.

XPEG-type PCEs: they represent slightly crosslinked PCEs and are made from monomers which possess two reactive double bonds (e. g. diesters) or diols capable of forming two ester bonds and thus can provide some degree of crosslinking [43]. Their advantage is a sometimes higher dosage - effectiveness.

PAAM-type PCEs: these zwitter-ionic PCEs possess mixed side chains composed of polyamidoamine (PAAM) and PEO segments; this structural feature distinguishes them fundamentally from all other PCEs which exclusively contain PEO/PPO side chains. The PAAM-type PCE is said to fluidify cement at w/c ratios as low as 0.12 [44]. Its disadvantage is the high cost of the PAAM side chain.

Phosphated Comb Polymer: it has been proven that phosphonate acts as even stronger anchor group compared to carboxylate or dicarboxylate group which typically occur in conventional PCE structures [45]. In recent years, several attempts have been made to incorporate phosphate groups into comb structures and good results were achieved [46–50]. By reacting hydroxyethyl methacrylate with phosphoric acid, a phosphate ester is

produced first. In the next step, the phosphated comb polymer is synthesized via free radical copolymerization from the ethylene glycol methacrylate phosphate ester and ω-methoxy poly(ethylene glycol) methacrylate ester (MPEG-MA) as macromonomer. This type of superplasticizer possesses better sulfate robustness and provides high flow speed to concrete or mortar prepared at low w/c ratio.

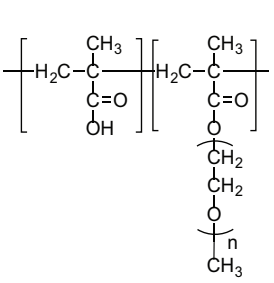

MPEG - type PCEs

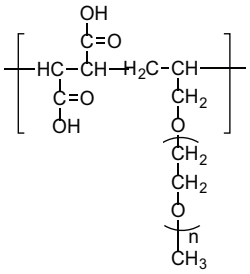

APEG - type PCEs

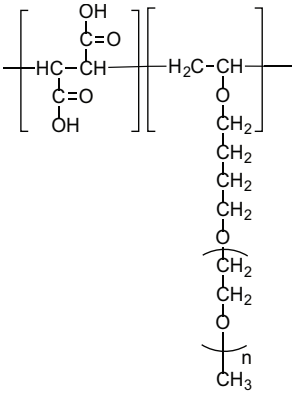

VPEG - type PCEs

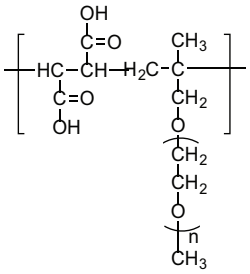

HPEG - type PCEs

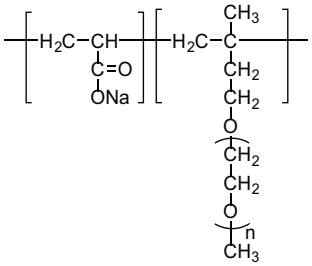

IPEG - type PCEs

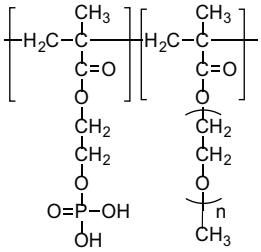

Phosphated Superplasticizer

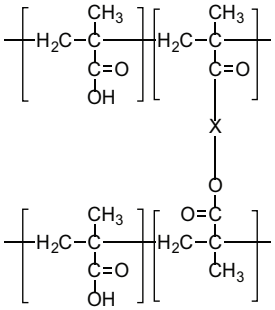

XPEG - type PCEs

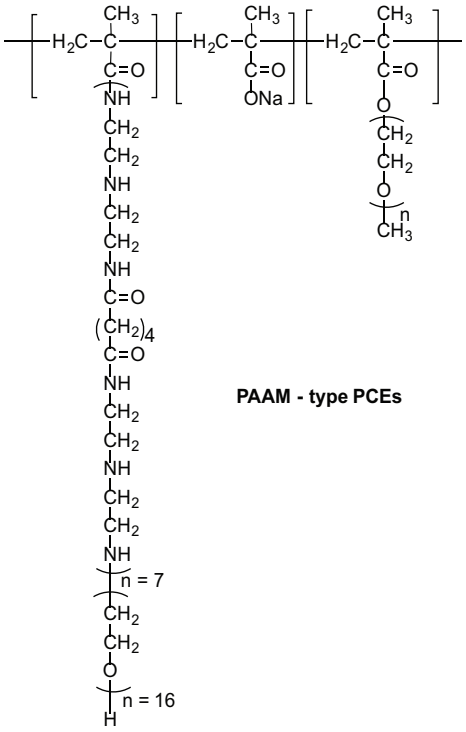

PAAM - type PCEs

Figure 8: Overview of PCE polymers based on different chemical structures

Synthesis of methacrylate ester macromonomers

In Europe, MPEG type PCEs still present the dominant kind of PCEs used. For this reason, the synthesis of the MPEG methacrylate ester macromonomer is described in the following. The most widely applied production process for methacrylate ester macromonomers includes a stepwise method [51]. In the first step, methoxy poly ethylene glycol (MPEG) is obtained by reacting ethylene oxide with a suitable alcohol (typically methanol), see **Figure 9**.

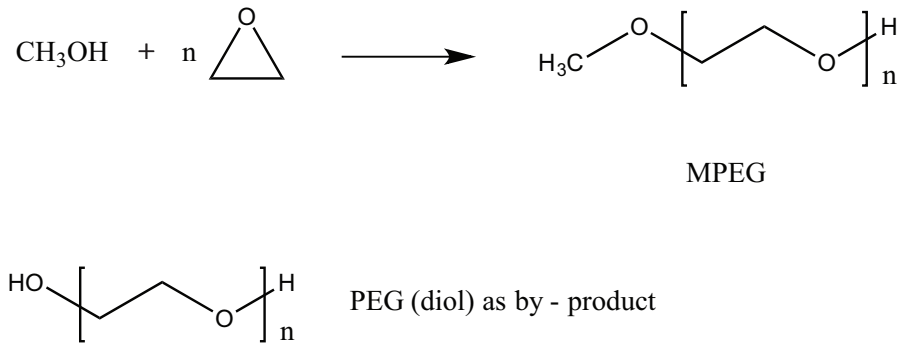

Figure 9: Synthesis of methoxy polyethylene glycol (MPEG)

Subsequently, the methacrylic ester of methoxy polyethylene glycol (methoxy polyethylene glycol monomethacrylate, abbreviated as MPEG-MA) is produced via esterification of methacrylic acid with MPEG in a common manner, see **Figure 10**.

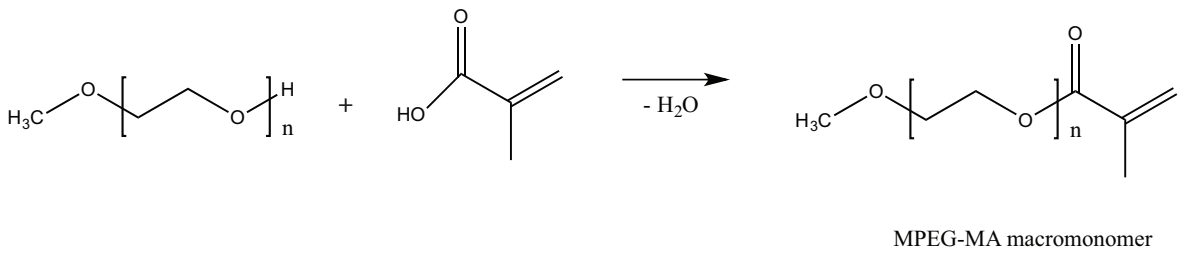

Figure 10: Synthesis of methoxy polyethylene glycol methacrylate ester (MPEG – MA) macromonomer

Residual PEG (diol) from the first step can react further with methacrylic acid to form PEG-di-MA, the diester, see **Figure 11**. However, such PEG-di-MA ester can cause crosslinking of PCE molecules during the copolymerization step (see **Figure 12**) and therefore is highly unwanted [52].

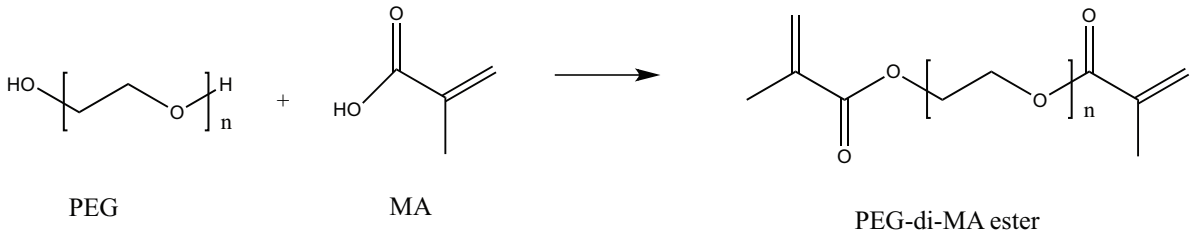

PEG MA PEG-di-MA ester

Figure 11: PEG-di-MA ester is formed from the by - product PEG upon reaction with methacrylic acid

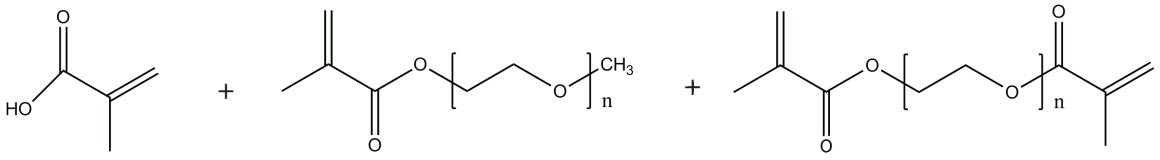

MA MPEG-MA PEG-di-MA

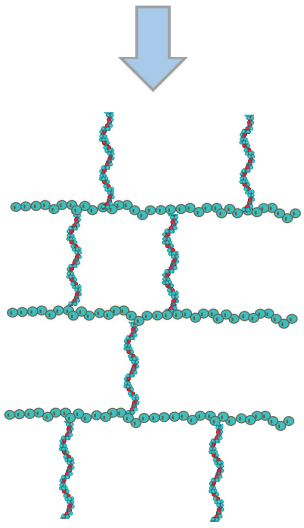

Crosslinked PCE

Figure 12: Formation of a crosslinked MPEG-PCE from MPEG-MA macromonomer which is contaminated with minor amounts of PEG-di-MA ester

An alternative synthesis involving only one reaction step in the preparation of the macromonomer was proposed later which leads to ω-hydroxy poly(ethylene glycol) methacrylate [53], see **Figure 13**. This more direct synthetic approach presents a more efficient and less expensive way by avoiding the second step.

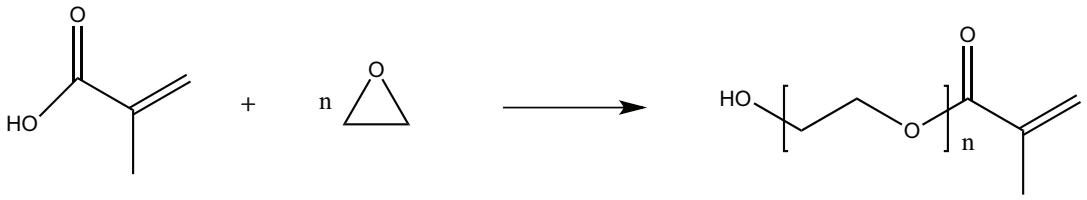

Figure 13: One-step synthesis of the hydroxy terminated methacrylate macromonomer

Synthesis of polyethylene glycol ether macromonomers

The polyethylene glycol ether based macromonomers which have been developed in recent years become more and more popular due to their extraordinary performance in PCEs. They can also be produced in a one-step synthesis via reacting an unsaturated alcohol with ethylene oxide. For example, the VPEG macromonomer is manufactured from 4-vinyloxybutanol and ethylene oxide in the presence of an alkali catalyst. Similarly, the APEG macromonomer is manufactured by reacting allyl alcohol with ethylene oxide; HPEG macromonomer is obtained from methallyl alcohol and ethylene oxide; and TPEG/ IPEG macromonomer can be synthesized from isoprenol and ethylene oxide. Additional terminal group modification can be performed to obtain methoxy terminated macromonomers, see **Figure 14**.

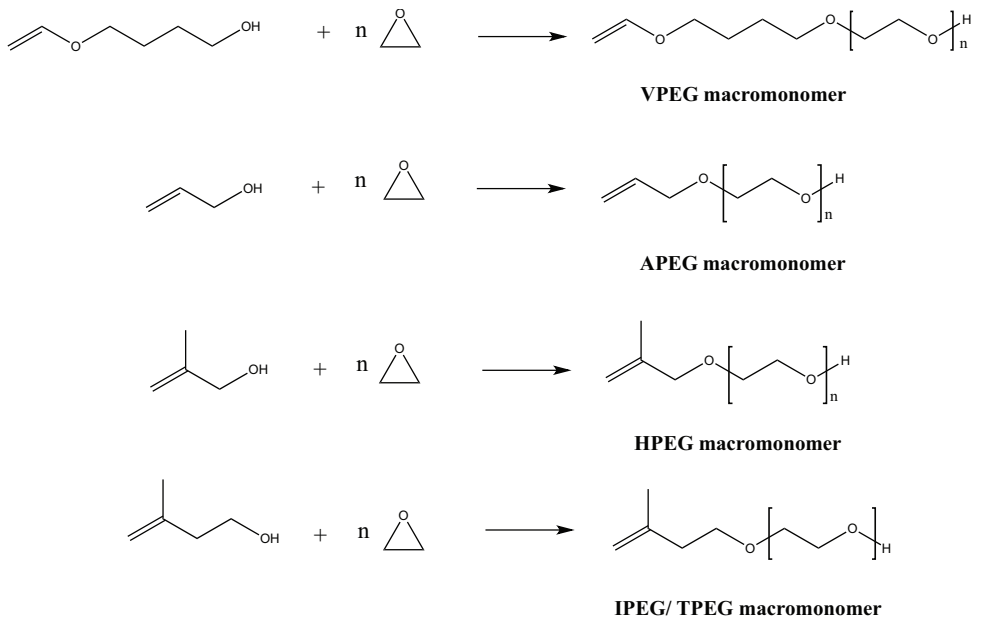

Figure 14: Synthetic approach for the manufacture of VPEG, APEG, HPEG and TPEG/ IPEG macromonomers

3.1.3 Mode of action of superplasticizers

When cement comes in contact with water, cement particles flocculate due to the electrostatic attraction between the positive and negative sites. Between the flocculated cement and water agglomerates are voids that trap part of the mixing water. The addition of superplasticizers can effectively release the trapped water and reduce the yield stress of the cement paste or concrete.

Different dispersing mechanisms have been proposed when superplasticizers possessing different chemical structures adsorb onto the surface of cement particles, see **Figure 15**.

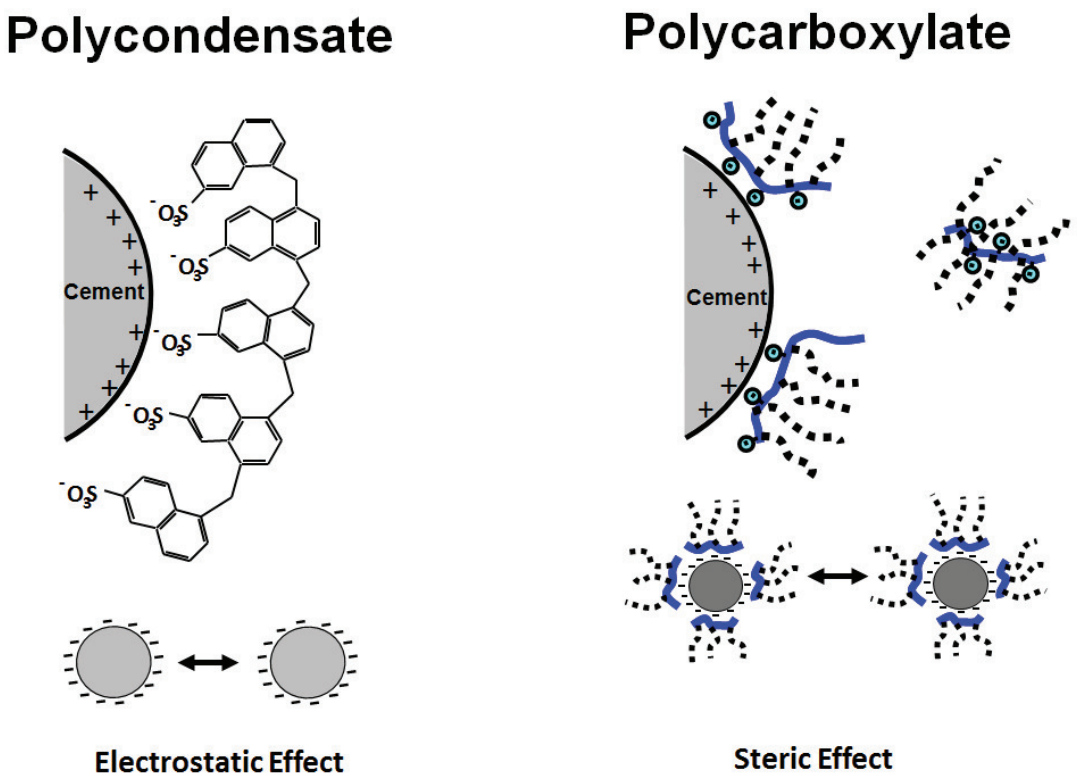

Figure 15: Illustration of the two dispersion mechanisms known for concrete superplasticizers

- Electrostatic repulsion

Superplasticizers based on melamine or naphthalene polycondensates function by electrostatic repulsion. The polymer chains adsorb onto the surface of cement particles via their sulphonate groups, $-SO_3^-$. This way, the cement particles become negatively charged. Consequently, electrostatic repulsion occurs between the cement particles [54–57]. The

cement particle arrangement in a paste matrix offsets the inter-particle attractive forces [58].

- Steric hindrance

Regarding to the dispersion mechanism of PCEs, intensive studies have been carried out [13, 59–61]. The findings suggest another mode of action between PCE polymers and cement particles, namely steric stabilization. It results from the hydrophilic pendant chains which protrude freely into the pore space and contribute the most to the stabilizing force in the system. This effect is augmented by electrostatic repulsion owed to the presence of negatively charged functional groups (-COO^-) in PCEs. This mechanism could also explain why albeit a smaller number of anionic functional groups is present in PCE molecules in comparison with the -SO_3^- groups of PMS or BNS polycondensate, PCEs still show a superior dispersing effectiveness [4, 62]. The steric hindrance effect depends on a number of parameters which are described by the Ottewill - Walker equation (see **Equation 1.1**). There, the adsorbed layer thickness of the PCE molecule presents the most important parameter.

$$V_{steric} = \frac{4\pi kTC_V^2}{3v_1^2p_2^2}(\Psi_1 - k_1)(\delta - a)^2(3R + 2\delta + a/2) \qquad \textbf{Equation 1.1}$$

whereby C_V presents the concentration of the adsorbents in the adsorbed layer, v_1 = molecular volume of the solvent molecules, p_2 = the density of the adsorbent, Ψ and k_1 present the entropy and enthalpy respectively, R the radius of the adsorbed particles, a the distance between two particles and δ represents the adsorbed layer thickness [63, 64].

3.2 Clay contaminants in concrete and mitigation strategies

3.2.1 Brief summary of clay mineralogy

Clay minerals occur in all types of sediments and sedimentary rocks. The basic structure units in layered aluminosilicates are silica sheets and gibbsite or brucite sheets. The former consist of SiO_4^{4-} tetrahedra connected at three edges in the same plane, thus forming a

hexagonal network. The tips of the tetrahedra all point in the same direction. This unit is called the tetrahedral sheet. The gibbsite or brucite sheet consists of two planes of hydroxyl ions between which lies a plane of aluminum or magnesium ions which are octahedrally coordinated by the hydroxyls. This unit is known as the octahedral sheet. These sheets are combined in such way that the oxygens at the tips of the tetrahedra project into a plane of hydroxyls in the octahedral sheet and replace two-thirds of the hydroxyls. Such combination of sheets forms a layer [65–68].

Recently, **M.L. Nehdi** wrote an excellent review paper which covers all the key points relating to clay contaminants occurring in concrete [69]. Based on a thorough literature search, the author covered a broad range of topics including (1) mechanisms of clay swelling [70–72]; (2) possible effects of clay on properties of concrete, such as its influence on water demand, workability, strength, drying shrinkage and freeze–thaw resistance [73–75]; (3) effects of clay on chemical admixtures, especially the interaction with PCE polymers [10, 76]; (4) the dimensional stability of clay - bearing aggregates [77, 78]; (5) typical test methods to determine clay in cement-based materials, i.e. the aggregate durability index [79], sand equivalent test and methylene blue test [80]; (6) researches focusing on making nano-clays and their applications were also summarized [81, 82].

By definition, “clay” is a naturally occurring, non-synthetic material which primarily contains fine-grained minerals. Clay is plastic which makes it possible to be molded, and turns hard after drying or firing [83]. On the other hand, “clay mineral” refers to “phyllosilicate minerals and to minerals which impart plasticity to clay and which harden upon drying or firing” [83]. **Table 1** below explains the difference between “clay” and “clay mineral”. For simplicity reason, in this thesis the term “clay” is used simultaneously also for clay mineral.

Table 1: Criteria in definition of clay and clay mineral [84, 85]

Criteria	Clay	Clay mineral
Origin	Natural	Natural & synthetic
Main constituent	Phyllosilicate	Not restricted to Phyllosilicate, Non-phyllosilicate can be included
Size	Fine grained	Any
Plasticity	Yes	Yes
Hardens upon drying or firing	Yes	Yes

The following describes the subdivisions of layered aluminosilicates which are based upon different combinations of tetrahedral and octahedral sheets. Their principle structures are displayed in **Figure 16**.

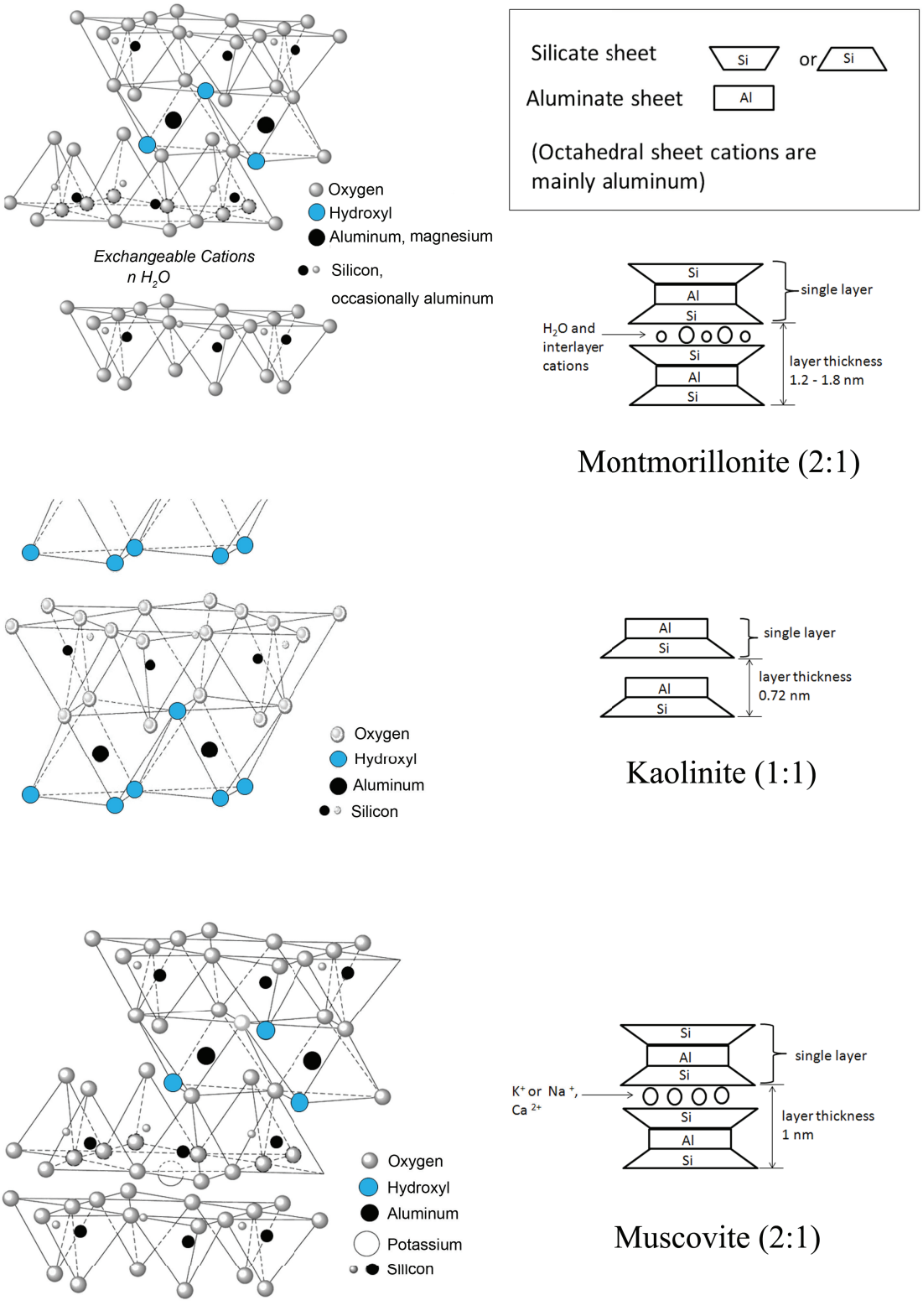

Figure 16: Principle structures of the major clay minerals occurring as contaminant in concrete, after Grim [86].

- 2:1 clay minerals

The 2:1 layer lattice alumo silicates consist of two silicate tetrahedral sheets and one aluminate octahedral sheet. These three sheets form a layer which is approximately 10 Å thick. The oxygens at the tips of the tetrahedra point towards the center octahedral sheet and substitute two-thirds of the octahedrally coordinated hydroxyls. 2:1 clay minerals include the smectite and mica groups which are by far the most abundant among the clay minerals. The pure end members of this type are pyrophyllite, a hydrous aluminum silicate; talc, a hydrous magnesium silicate; and minnesotaite, a hydrous iron silicate [65].

The smectites represent a group of expandable (swelling) 2:1 clay minerals. They exhibit a total negative layer charge of between 0.2 and 0.6 per half unit cell. The octahedral sheet may either be occupied by trivalent cations (dioctahedral smectites) or divalent cations (trioctahedral smectites). Between the 2:1 units is a plane of large cations. These are referred to as interlayer cations. Potassium, sodium and calcium are commonly occurring cations. The general formula for dioctahedral smectites is $(M^{+}_{x+y} \times nH_2O)(R^{3+}_{2-y}R^{2+}_{y})$-$(Si^{4+}_{4-x}Al^{3+}_{x})O_{10}(OH)_2$, and that for the trioctahedral species is $(M^{+}_{x} \times nH_2O)(R^{2+}_{3-y}R^{3+}_{y})$-$(Si_{4-x-y}Al_{x+y})O_{10}(OH)_2$, where x and y indicate the layer charge resulting from substitution in tetrahedral and octahedral sites, respectively; R^{2+} and R^{3+} refer to a divalent and trivalent octahedral cation, respectively; and M^{+} refers to a monovalent interlayer cation. A wide range of cations can occupy tetrahedral, octahedral and interlayer positions [67]. In the structure, successive sheets are bonded together by weak hydrogen bonds. The main representative of dioctahedral smectites is montmorillonite, which is also referred to as bentonite when occurring as natural, impure mineral. And the most important species of trioctahedral smectites are hectorite, saponite and sauconite.

The 2:1 structural unit of mica is similar to that of talc. Generally, the mica group is subdivided depending on whether the species are dioctahedral (muscovite type) or trioctahedral (biotite type). The micas are further characterized by the number of silicate ions in the tetrahedral position. In the structure, successive sheets are strongly bound together. Contrary to montmorillonite, micas belong to the group of non-expandable (non-swelling) clay minerals.

- 1:1 clay minerals

This type of clay mineral consists of one tetrahedral and one octahedral sheet. The two sheets are approximately 7 Å thick. This two-sheet type is divided into the subgroups of kaolinite (dioctahedral) and serpentine (trioctahedral) [65, 86].

Kaolinites exhibit a general composition of $Al_2Si_2O_5(OH)_4$. Their interlayer is occupied by hydroxyl groups and oxygen atoms from the octahedral and tetrahedral sheets connected by weak hydrogen bonds. The kaolinite minerals are all pure hydrous aluminum silicates containing Al and Si with no substitutions. They possess a minimal layer charge and a low base exchange capacity [87]. Kaolinite minerals belong to the group of non-expandable (non-swelling) clay minerals.

The trioctahedral two-sheet minerals are called serpentines. The serpentine minerals (chrysotile and antigorite are the most common ones) consist of a tetrahedral and an octahedral sheet containing magnesium with only minor amounts of aluminum. The other minerals in this subgroup have a wide range of variations in composition. Aluminum, iron, manganese, nickel and chromium can substitute for magnesium in the octahedral sheet and aluminum, ferric iron, and even germanium for silicon in the tetrahedral sheet [65, 88].

- 2:1:1 clay minerals

These clays are made up of regularly stacked, negatively charged 2:1 layers and an additional positively charged interlayer octahedral sheet. They are linked to each other by hydrogen bonds and form a unit which is 14 Å thick [89]. Their main representative is the group of chlorites which exhibits a wide range of compositions because substitution can occur both in the 2:1 layers and in the brucite sheets. Chlorites represent non-expandable clay minerals and seldomly occur in concrete aggregates. For this reason, they were not considered for this study.

3.2.2 Interaction between PCEs and clay contaminants in aggregates

Clays have been viewed as undesirable concrete constituents for a long time. They are harmful to concrete properties due to their high surface area and swelling behavior which consumes more water in the system. A higher water demand in turn reduces workability, strength, durability and increases dry shrinkage [75]. Besides, clay minerals also show negative effects on the performance of PCE superplasticizers [6, 7, 90, 91]. Most confusing,

the influence from different clay minerals which may be present in natural aggregates (sand or gravel) differs from case to case. Sometimes, the effect is very pronounced whereas in other cases the effect is negligible or can be solved by simply adding slightly more PCE. Obviously, depending on the type of clay which can vary with respect to their composition and their physicochemical attributes, PCEs can be affected very differently by these minerals.

Generally, clays can interact with PCE polymers in two different ways:

- Surface (physical) adsorption

Clays (montmorillonite, kaolin, muscovite) exhibit an overall negative charge on their basal planes. For this reason, cationic polymers such as amines or amides can adsorb on the surfaces of those clay platelets [92, 93].

As for PCE polymers which possess anionic charges, they can also adsorb on the surfaces of the clay particles as a result of charge reversal to positive, owed to the adsorption of Ca^{2+} ions from cement pore solution onto the basal planes of the clays [76, 94–98]. This mechanism applies to all different types of clays, however to different extents with respect to the surface charges. **Figure 17** illustrates the surface adsorption of PCEs on the surface of a clay platelet.

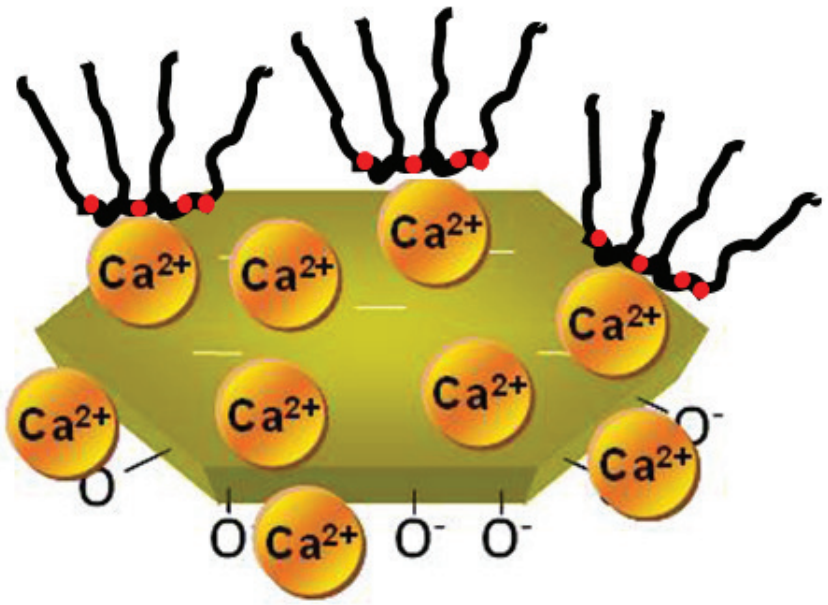

Figure 17: Illustration of physical adsorption of PCE molecules on the surface of a clay platelet

- Chemisorption (intercalation)

In this case, PCE molecules are trapped in between the interlayer region of the clay structure (typically of swelling clays such as smectites) through a process called intercalation, see **Figure 18**. The mechanism behind is that the polyethylene glycol side chains anchor on the silanol groups present on the surfaces of the aluminosilicate layers via H-bonding using water as the mediator. This effect applies to clays which hold cations between the aluminosilicate layers, i.e. clays which possess a high cation exchange capacity, such as montmorillonite [99].

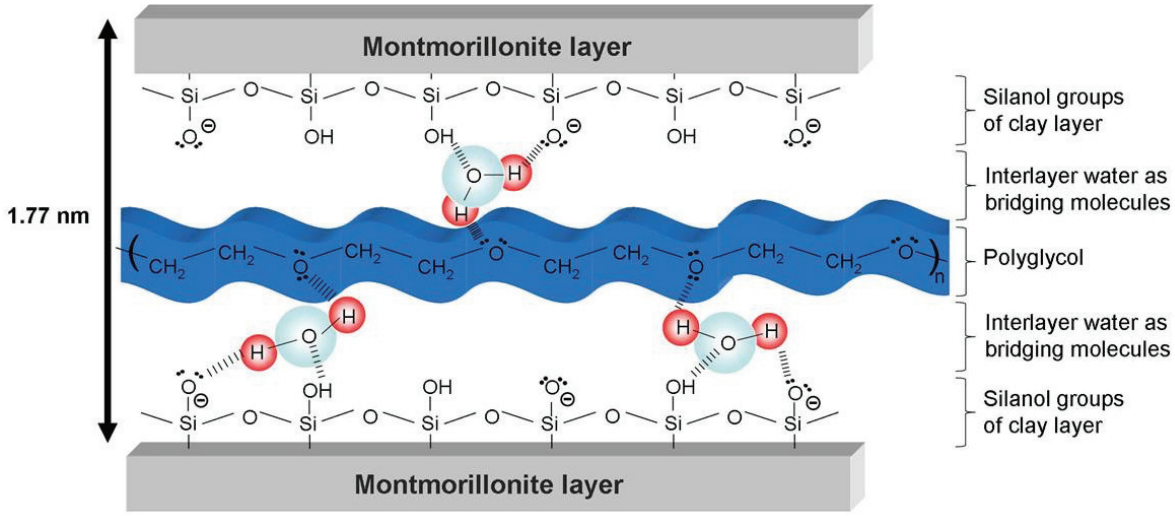

Figure 18: Intercalation of a PCE molecule via its PEG side chain into the interlayer region of montmorillonite, from [76]

3.2.3 Mitigation strategies

Researchers from academic and industrial fields devote huge efforts to solve the sensitivity problem of PCE against clays. Several methods mentioned below have been developed to reduce or solve the negative effect from clays:

- Use of sacrificial agents:

Literatures from oil well drilling (especially relating to the drilling of shale rock) indicate that polyglycols are incorporated into the interlayer galleries because of favourable intermolecular interactions, leading to increased desorption of water and hence a reduced tendency for the clay to swell [100–102]. A similar trend was found for PCEs due to their

PEG side chains. Generally, PEGs have a much higher tendency to intercalate than PCEs because of their negatively charged backbone which is repelled by the negatively charged aluminosilicate main sheet of the clay. Such repulsion causes a disturbed stacking order of the montmorillonite lattice [103]. Based on those findings, pure PEG/ MPEGs can be used as sacrificial agents to block the interlayer region of montmorillonite because of their preferred tendency to intercalate, while PCE molecules can be saved to provide dispersing force in the cementitious system.

- Use of a cationic compound:

Another method includes introducing cationic polymers which can inhibit the swelling of clay entirely [70, 104]. In this case, the hydration of clay would not be possible, thus zero water consumption becomes realistic. In addition, the interlayer galleries in the clay lattice are occupied by cationic compounds and thus blocked for the uptake of PCE molecules [105].

- Use of clay - tolerant PCEs:

Based on the previous findings, the PEG pendant chains of PCE polymers are responsible for the sensitivity problem. The concept of novel PCE structures possessing clay tolerance was brought up. Compared to the other two solutions mentioned above, applying more clay tolerant PCEs appears to be the better remedy. For this purpose, a novel PCE structure based on hydroxy alkyl methacrylate ester as replacement for conventional PCEs which contain PEG side chains has been proposed [10, 106]. To investigate the type of interaction between the novel PCEs and clay, sorption measurement and XRD analysis were carried out. According to TOC measurements, those PCEs holding the novel side chains exhibit extremely low sorption on clay ($\sim$ 25 mg polymer/g clay) whereas PCEs carrying conventional PEG side chains sorb $\sim$ 10 times the quantity of that of the novel PCEs. Additionally, XRD analysis confirmed that no change in the interlayer distance (d value) of montmorillonite was found when PCEs possessing the novel structure were added. Superior dispersing effectiveness can be observed in the presence of e. g. bentonite clay.

3.3 Incompatibility cement – PCE superplasticizer

In high performance concrete which is characterized by a low water-to-cement ratio, applicators often noticed an incompatibility problem between cement and the superplasticizer used to improve the fluidity of cement [107–109]. The typical phenomenon of incompatibility includes poor fluidity (i.e. low or no performance from the superplasticizer), flash setting, delayed setting, rapid slump loss, improper strength gain, and cracking etc. [110–116]. These phenomena in turn have negative effect on the physical properties of hardened concrete. On the market, we have numerous different cement brands from different suppliers exhibiting various phase compositions, and at the same time, a huge number of superplasticizers differing in chemical structure are also available which enhances the incompatibility problem even further.

Incompatibility could arise from various reasons related to the cement, the superplasticizer, the sulfate source in cement (type of calcium sulfate) etc. [12]. **Figure 19** shows the complicated nature of the incompatibility issue. The individual factors are discussed below:

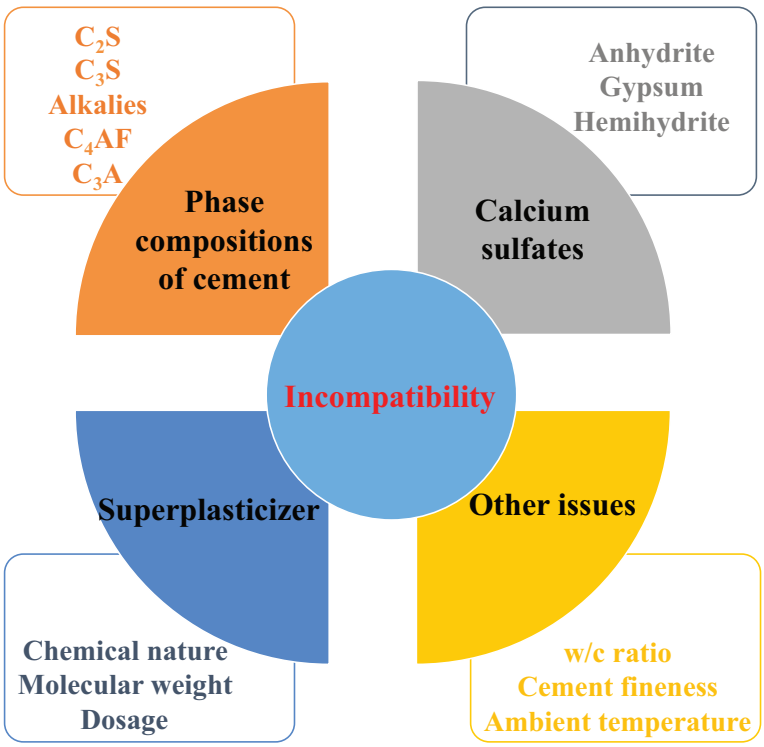

Figure 19: Schematic diagram showing the complexity of the incompatibility problem between cement and PCE superplasticizer and the related parameters

3.3.1 Chemical and phase composition of cement

Alite, Belite, Aluminate and Ferrite are the four main mineral phases present in Portland cement clinker. As the most important component there, Alite has the chemical composition of tricalcium silicate (Ca_3SiO_5, C_3S). In industrial clinker, this phase (doped C_3S) can vary in composition and crystal structure by ionic substitutions. Belite is dicalcium silicate (Ca_2SiO_4, C_2S), also modified by ionic substitutions. Normally, it is present wholly or largely as the β polymorph. Aluminate is tricalcium aluminate ($Ca_3Al_2O_6$, C_3A) which is substantially modified in composition and structure by ionic substitutions, especially with K_2O. Ferrite is tetracalcium aluminoferrite ($2(Ca_2AlFeO_5)$, C_4AF), again substantially modified in composition by variation in the Al/ Fe ratio and ionic substitutions [117]. They develop different surface charges. C_3S and C_2S exhibit a positive surface charge whereas C_3A and C_4AF possess a negative surface charge which determines their different interaction with anionic superplasticizers. Among the four main phases, C_3A plays a crucial role for the cement compatibility of PCE superplasticizers. As we discussed earlier, the dispersing force originates from the adsorption of anionic anchor groups on C_3A or its early hydration products, calcium monosulfoaluminate (AF_m) and ettringite (AF_t) [13, 55, 115]. Previous studies show that the speed of hydration of C_3A and the corresponding ettringite formation present the key factors for the compatibility between cement and PCE polymers [118].

3.3.2 Calcium sulfates

In order to delay the immediate set of cement paste, mortar or concrete, calcium sulfate is used in the system. There are three different chemical forms which could supply SO_4^{2-}, namely calcium sulfate dihydrate ($CaSO_4 \cdot 2H_2O$, gypsum), hemihydrate ($CaSO_4 \cdot 1/2H_2O$) or anhydrite ($CaSO_4$). The three calcium sulfate forms have different solubilities and dissolution rates of the SO_4^{2-} ions. On one hand, hemihydrate and anhydrite exhibit a higher solubility than gypsum, on the other hand, anhydrite is very slowly soluble. Literatures reveal that the type of calcium sulfate can also influence the interaction between cement and superplasticizers [107, 119].

It is of great importance that there are sufficient amounts of soluble calcium and sulfate

ions in the cement pore solution to assure the formation of the AF_t phase and to prevent, or limit, the tricalcium aluminate phase of the cement from reacting directly with water to form large platy crystals of C_2AH_8 and C_4AH_{13} which lead to a flash set [107]. If there is not enough SO_4^{2-} present, then flash setting can occur due to the formation of AF_m. On the contrary, if there is too much soluble SO_4^{2-} present (e. g. hemihydrate which dissolves very fast), then there is a high possibility of a false set resulting from the spontaneous crystallization of gypsum (hemihydrate converts to gypsum). In order to achieve a reasonable workability of the cement paste, a proper ratio of C_3A to SO_4^{2-} is critical. Quickly soluble alkali sulfates (especially K_2SO_4) also influence the C_3A to SO_4^{2-} ratio. But an excess of soluble alkali sulfates can result in competitive adsorption with PCE polymers and thus negatively affect the rheology of the cement paste [16].

3.3.3 PCE polymers

A significant amount of research has been devoted toward a better understanding of the interaction mode between cement and superplasticizers [3, 33, 34, 36]. Apparently, the type, dosage, chemical composition and molecular structure of superplasticizer influence the rheological properties (see **Figure 20**). Several trends were found in experimental investigations [3]:

- PCE polymers carrying higher anionic charges require lower dosages to achieve the same fluidity

- PCE polymers with higher side chain density give better slump retention property, but need higher dosages

- PCE polymers possessing longer PEG chains require lower dosage to achieve the same fluidity, but exhibit a relatively big slump loss over time

- PCE polymers exhibiting a shorter backbone require lower dosages to achieve the same fluidity, but exhibit a relatively longer setting time

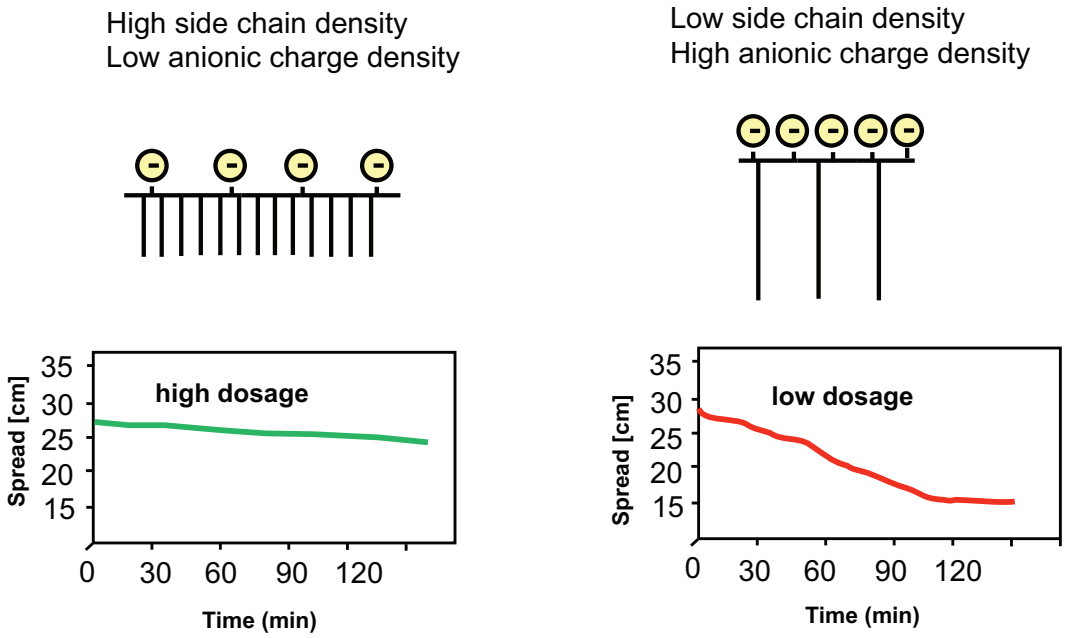

Figure 20: Schematic diagram showing the correlation between different PCE structures and rheological properties of cement pastes

These differences in the rheological properties (fluidity, slump loss) of cement pastes originate from the adsorption of PCE polymers on the surfaces of cement grains. The molecular architecture (molecular weight, main chain length, side chain length, side chain density, charge density) affects the adsorption behavior of the PCE polymers. From experiments, it is well established that polymers with higher charge density adsorb to a larger extent compared to polymers with lower charge density. This trend correlates very well with the results from rheological measurements. Whereas polymers with high side chain density adsorb in low amount and exhibit a slow adsorption rate which translates into higher initial dosage and long slump retention.

In addition, the molecular structure also determines the adsorption conformation of PCE polymers. Generally, PCE molecules can adsorb in three different confirmations, namely train, loop and tail, as is shown in **Figure 21**. Even more difficult is to assess how the molecular architecture influences the adsorption speed of the PCE polymers. It should be noted here that the adsorption process consists of two parts: the first one induces depletion of the PCE polymers from the cement pore solution, while the second part is controlled by the diffusion speed of the PCE polymers in cement pore solution. These two highly interesting research topics remain as unexplored area which need to

be studied to further advance the understanding of the adsorption process and also the dispersing mechanism [32].

An early report on cement - superplasticizer interaction was provided by W. Prince et al. They reported that BNS can work as morphological catalyst for ettringite [18]. Accordingly, BNS molecules do not only adsorb on the clinker phases, but also on the clusters and nuclei of the first hydrates of ettringite, thus they are prohibited from further growth which results in much smaller ettringite crystals. However, when there is no superplasticizer present in the system, ettringite can grow to normal size without any disturbance [18, 120]. As for PCE molecules, a similar phenomenon can happen, and the resulting change in ettringite morphology may affect the compatibility between cement and PCE. As part of this thesis we have carried out some experiments to study this phenomenon. Since ettringite crystallizes immediately after the cement gets in contact with water (around a few seconds), it is very difficult to study this early crystallization process. For this reason, the idea of investigating ettringite formation under more controlled condition, namely zero gravity where only diffusion dependent crystallization can happen, was developed. This topic will be discussed in the next section.

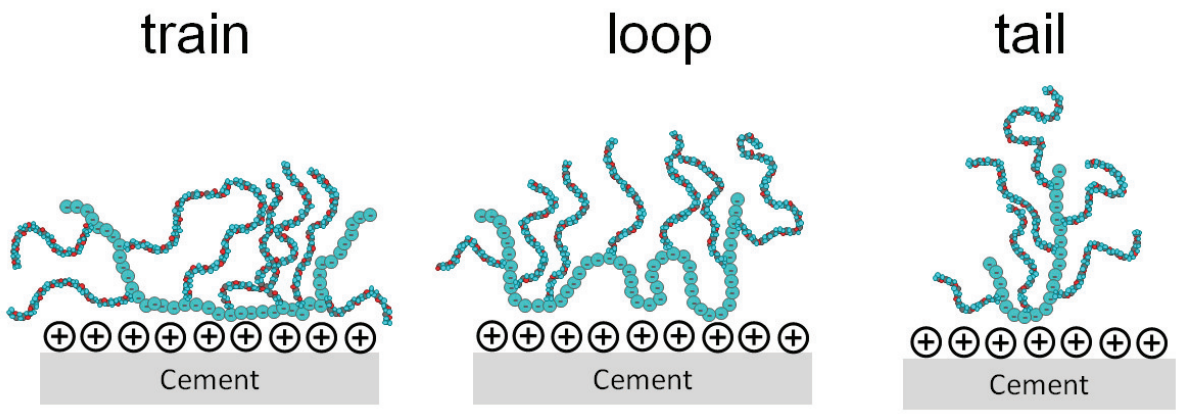

Figure 21: Potential adsorbed confirmations of PCE polymers

3.3.4 Other parameters

Other parameters such as w/c ratio, fineness of cement and ambient temperature can also influence the compatibility [121]. These issues are not our focus, therefore they will not be discussed here.

3.4 Crystallization of ettringite

As discussed in the previous section, ettringite, with the chemical formula $[Ca_3Al(OH)_6 \cdot 12H_2O]_2 \cdot (SO_4)_3 \cdot 2H_2O$ can form in the presence of enough soluble SO_4^{2-} ions in the very early stage of cement hydration.

Ettringite crystals are based on two basic structural units: $[Ca_6[Al(OH)_6]_2 \cdot 24H_2O]^{6+}$ serves as central column which is surrounded by units of $[(SO_4)_3 \cdot 2H_2O]^{6-}$ (**Figure 22**). Inside every pillar, each calcium ion is coordinated with four hydroxyl ions shared with the $Al(OH)_6$ octahedra and four water molecules, thus CaO_8 polyhedra are formed. $Al(OH)_6$ octahedra alternate with triplets of calcium ions from edge-sharing CaO_8 polyhedra [117, 122–124]. Ettringite can also be prepared in a simple precipitation reaction from aqueous $Ca(OH)_2$ and $Al_2(SO_4)_3$ solutions. Within a few seconds, the mixture becomes turbid and then white ettringite crystals precipitate from the solution. The ettringite crystals can be analyzed via scanning electron microscopy. There, they exhibit the characteristic hexagonal acicular morphology.

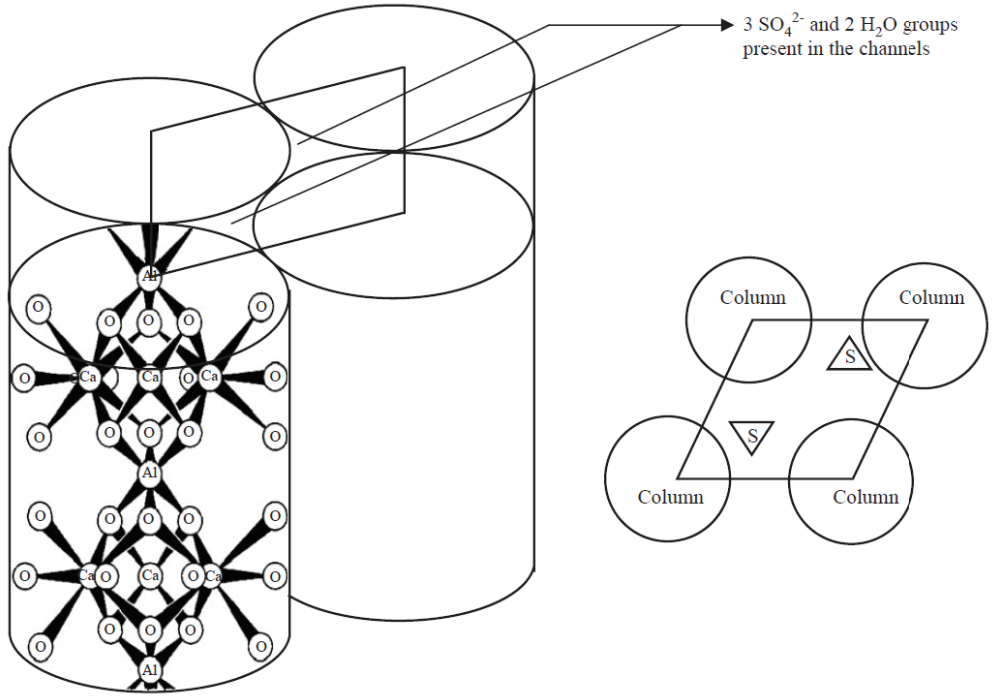

Figure 22: Sketch of the crystal structure of ettringite (left) and part of a single column projected on (1120) (right), from [124].

3.4.1 Nucleation and crystallization

Crystallization presents one of the most important techniques to obtain useful materials such as nanomaterials for the supplementation of bones and teeth. The methods to grow crystals cover quite a huge range, varying by complexity of the process, time consumption etc. Depending on the phase transitions during the process, the methods to achieve crystal growth can be divided into three categories, namely solid growth, liquid growth and vapor growth [125]. The growth of crystals by precipitation from aqueous solution presents one of the earliest and simplest method. However, the mechanism behind this crystallization has been poorly studied and elaborated so far.

Any crystallization process consists of two stages [126]. The first stage which is called nucleation includes the birth of early clusters, and refers to the beginning of the phase separation process. The next stage of the crystallization process requires these nuclei to grow larger by the addition of solute ions or molecules from the supersaturated solution. This part of the crystallization process is known as crystal growth. From an energy point, the free energy of the initial solution phase is greater than the sum of the free energies of the crystalline phase plus the final solution phase [127]. In order to utilize crystallization technique to produce useful materials, a better understanding of the nucleation being the critical stage is necessary.

Classic Nucleation Theory (CNT)

Nowadays, the most accepted theory about nucleation is the classic nucleation theory (CNT) brought up by **J.W. Gibbs**. The key point of this theory is that an activation energy barrier needs to be overcame to achieve crystal growth. And only the nuclei reaching a critical radius can grow further.

The nucleation process includes the conglomeration of atoms or molecules to form the first sub-microscopic speck or nucleus of the solid crystal [128]. Nucleation can be homogeneous, in the absence of foreign particles or crystals in the solution, or heterogeneous, in the presence of foreign particles in the solution. Both types of nucleation are collectively known as primary nucleation. Secondary nucleation takes place when nucleation is induced by the presence of crystals of the same substance [129].

The origin of nucleation is metastability of the old phase [130]. To be more specific, the driving force to form a cluster of a number n of molecules comes from the lowering of the free energy of the system during the phase transformation. The free energy change between the solid and the liquid is $\Delta\mu$, as is shown in **Equation 1.2**:

$$\Delta\mu \quad = \quad \mu_s - \mu_c \qquad \textbf{Equation 1.2}$$

where μ_s is the free energy of a molecule in solution and μ_c is the free energy of the molecule in the bulk crystal.

By rearranging **Equation 1.2** via introducing the Gibbs-Thomson relation **Equation 1.3** is generated:

$$\Delta\mu \quad = \quad KT \cdot \mathrm{lnS} \qquad \textbf{Equation 1.3}$$

where K is the Boltzmann constant, T is the absolute temperature and S is the supersaturation ratio.

The free energy of the system decreases for each unit volume of the solid created, while at the same time a solid-liquid interface is formed. The surface presents a different cause due to the lower attraction among molecules compared to those in bulk crystals, therefore the contribution of the surface to the free energy is quite substantial. The difference in free energy per molecule between the bulk crystals and the surface is defined as interfacial energy (designated as σ) which is a positive term and has a tendency to destabilize the nucleus. The free energy of the whole system increases by the interfacial energy for each unit area of the solid-liquid interface formed. Thus, the change in **Gibbs** free energy of a system in its final and initial stages can be expressed by **Equation 1.4**.

$$\Delta G_T \quad = \quad -n\Delta\mu \quad + \quad 4\pi \cdot r^2\sigma \qquad \textbf{Equation 1.4}$$

In **Equation 1.4**, when each molecule in the crystal occupies a volume V, then the amount of molecules in a nucleus can be calculated as $4/3\pi\mathrm{r}^3/\mathrm{V}$, and **Equation 1.5** can be evolved from **Equation 1.4**:

$$\Delta G_T \quad = \quad -4/3(\pi r^3)/V \cdot \Delta\mu \quad + \quad 4\pi \cdot r^2\sigma \qquad \textbf{Equation 1.5}$$

For simplicity, the formation of a typical spherical nucleus of radius r nucleating in the solution, as illustrated in **Figure 23**, is looked at:

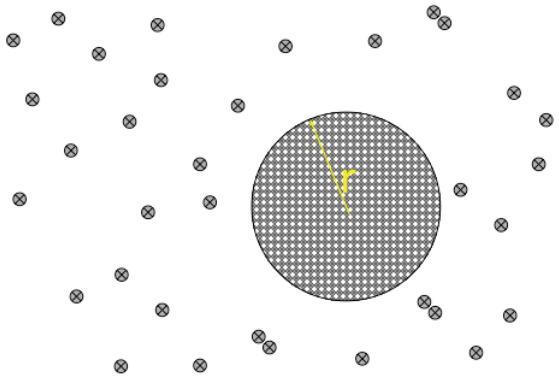

Figure 23: Schematic illustration of the formation of a spherical nucleus of radius r from a solution (redrawn after J. J. De Yoreo [131])

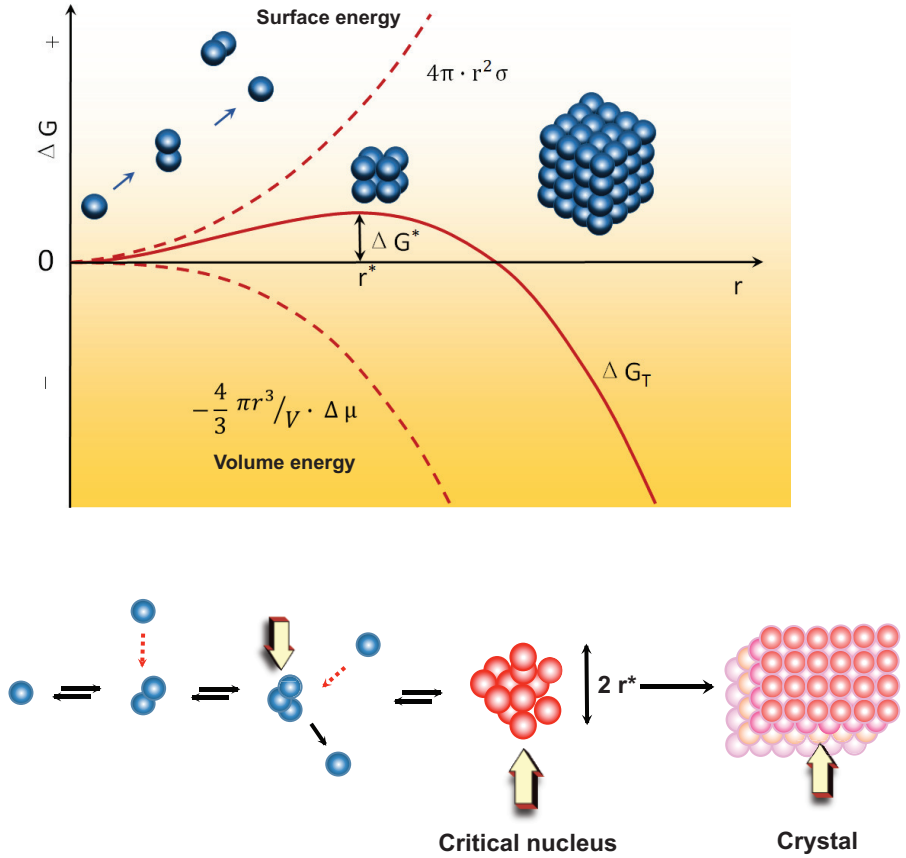

Figure 24: Total Gibbs free energy change as a function of radius r illustrating the nucleation barrier and critical radius (top; redrawn after Ref. [132]); only nuclei surpassing the critical radius can grow further (bottom; redrawn after Ref. [133])

The diagram in **Figure 24** (top) shows a plot of ΔG_T as a function of r. In the function, the total free energy change possesses two terms, the first one represents the volume energy which is negative and changes with r^3, while the second term is positive and varies with r^2. At first, the net free energy change increases with the increase of the radius of the nucleus until a maximum energy is achieved, followed by a decrease with further increase in the size of the nucleus. The sum of both terms produces a maximum value in the function curve, which refers to the energetic barrier to be overcome for nucleation (ΔG^*). The radius which needs to be achieved to propagate growth is defined as the critical radius (r^*). It can be calculated by taking the derivation of ΔG_T for r and set it equal to zero ($d\Delta G_T)/dr = 0$), leading to **Equation 1.6**:

$$r^* = 2\sigma V/\Delta\mu \qquad \textbf{Equation 1.6}$$

Apply **Equation 1.2** here, **Equation 1.6** will then be transformed to **Equation 1.7**:

$$r^* = 2\sigma V/(KTlnS) \qquad \textbf{Equation 1.7}$$

The critical radius (r^*) is the minimum size of nucleus which can grow further whereas counterparts with smaller dimensions will dissolve again into the mother liquor (see **Figure 24** bottom). For them no further growth can be expected, due to the thermodynamic disfavor.

Although the CNT theory exists for a century, very few experimental proofs have been provided so far due to the lacking of a direct observation tool to follow the nucleation process in real. However, in recent years scientists carried out intensive research focusing on simulating or monitoring the nucleation and crystallization in the atomic scale and obtained highly interesting results [134–139]. It is reported that colloidal systems can be used as experimental model systems to investigate the nucleation of crystals. On one hand, colloidal particles behave similar to big "atoms" and their phase diagram is comparable to that of atomic and molecular materials [140–142]; on the other hand, colloidal particles possess much larger particle sizes and a slower time scale which makes them visible by optical microscopy [143].

U. Gasser, **E. R. Weeks** et al. investigated the crystallization of colloidal suspen-

sions via confocal laser scanning microscopy. Both nucleation and growth of crystals were observed via three dimensional imaging. Extremely important parameters such as the critical size of the nuclei, nucleation rates, the average surface tension of the crystal-liquid interface were obtained by continuously following the evolution [143]. In their study, poly(methyl methacrylate) spheres were suspended in a mixture of decahydronaphthalene and cyclohexyl bromide. **Figure 25** illustrates nicely the crystallization process of poly(methyl methacrylate) particles. First, **Figure 25** (A) and (B) show the early time snapshots, whereby the red spheres indicate crystal-like particles arrangement and the blue spheres represent the particles remaining in the mother liquor. Typically, these subcritical nuclei consist of less than 20 particles which most likely shrank and dissolve to the mother liquor again. **Figure 25** (C) and (D) demonstrate that nuclei which have surpassed the critical radium have formed and grow further to big crystallites.

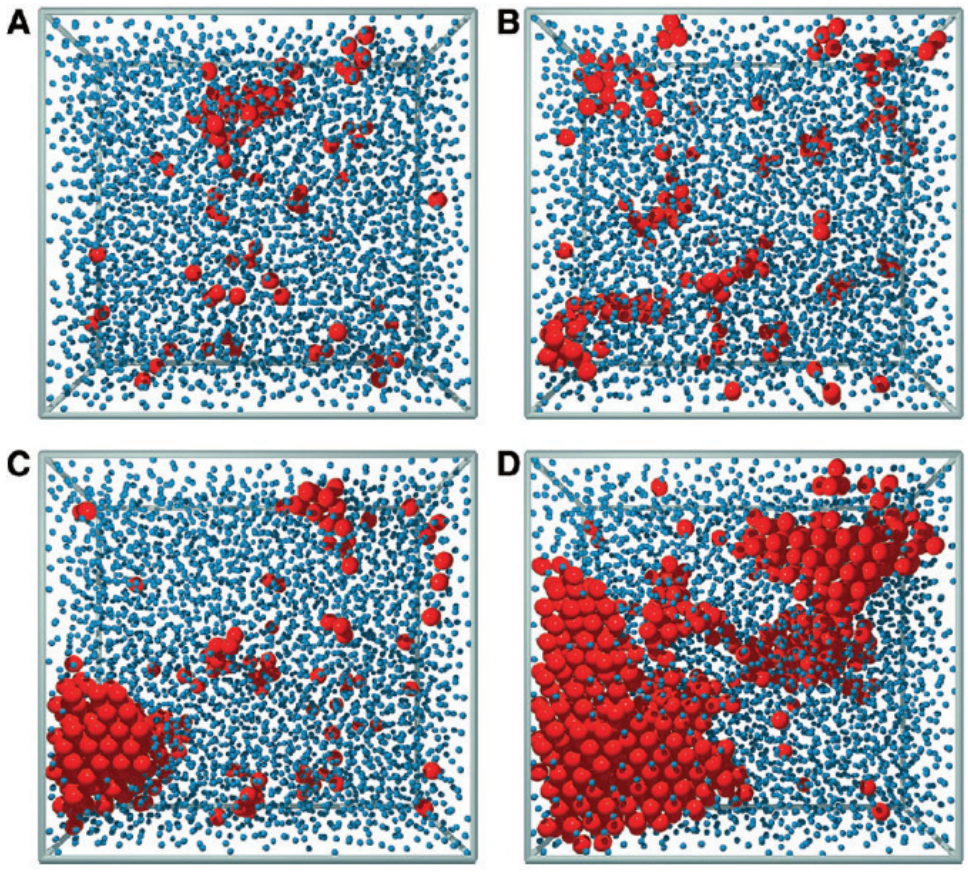

Figure 25: Four snapshots from crystallization of a PMMA sample. The red spheres represent crystal-like aggregates; the blue spheres represent the particles remaining in the mother liquor. (A) Time t = 20 min; (B) t = 43 min; (C) t = 66 min; (D) t = 89 min (from [143]).

However, the limitation of this study is mentioned above is the relatively low resolution of the confocal laser scanning microscopy. Another, more recent study concerning crystallization of colloidal particles was carried out by **X. Y. Liu** & **K. Q. Zhang**. There they reported real-time direct imaging and quantitative measurements of the pre- and post-nucleation processes of colloidal spheres [144, 145]. In their study, the thermodynamic driving force was well defined via applying an alternating electric field (AEF), then the nucleation of charge stabilized polystyrene (PS) spheres was observed via light microscopy. **Figure 26** i - v shows particles accumulated on the surface which start to form nuclei. The nuclei cycled in yellow keeps growing while the nuclei (cycled in red) shrunk instead of growing. When they plotted the size of each nucleus against time, the nuclei which succeeded to grow were larger than the critical size, whereas the counterpart shrunk before reaching the critical size (**Figure 26** vi). The successful monitoring of the nucleation process confirmed that this system meets the criteria of the CNT theory that only the nuclei exceeding the critical radius can grow further.

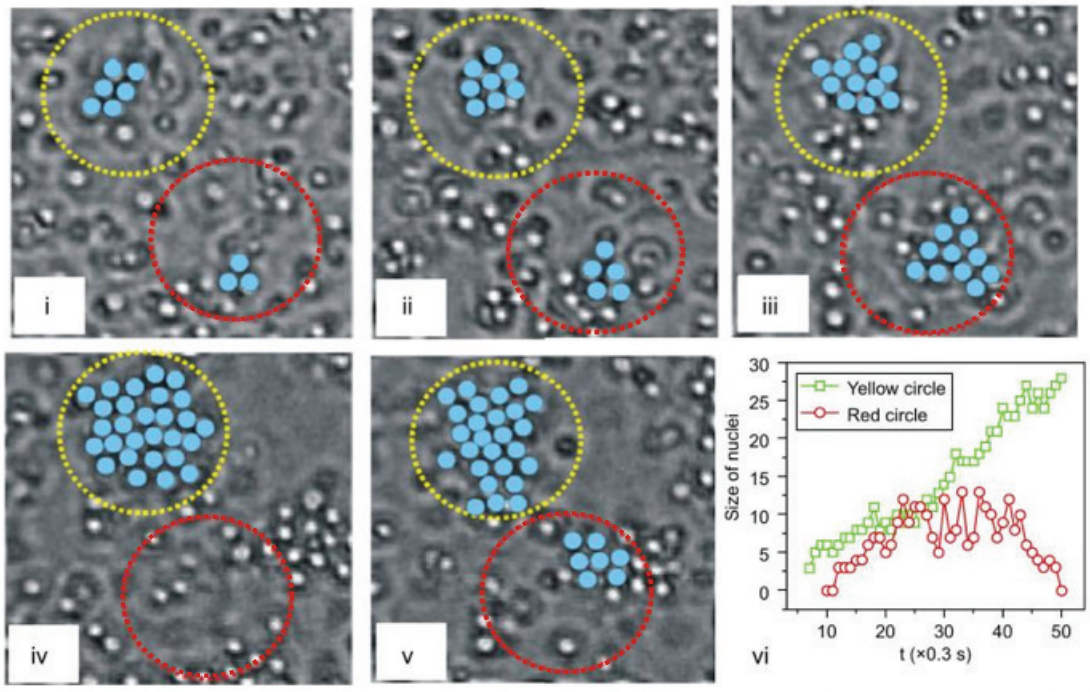

Figure 26: Pre-nucleation process monitored over time (i - v), i) Time t = 10 t_0 (t_0 is the timing interval of images, 0.3 s), ii) 20 t_0, iii) 30 t_0, iv) 40 t_0 , v) 50 t_0; and vi) showing the size evolution of two nuclei, whereby the green curve represents the increasing size of a nucleus in the yellow circle; while the red curve represents the shrinkage of the nucleus in the red circle (from [145])

The examples from above successfully show that CNT can explain the experimental observations, but there are also many cases where CNT failed to mechanistically explain the observation during the nucleation process. The discrepancies between the CNT theory and the experimental data may derive from the basic assumptions of CNT which are summarized below [130, 133]:

- Nuclei are spherical
- Nuclei are identical in structure to an infinite bulk crystal
- The surface tension of a crystal nuclei is identical to that of an infinite bulk crystal
- During the growth, the nuclei incorporate ions or molecules only one-by-one
- The nucleation rate is time dependent

Nonclassic Nucleation Theory (Cluster Theory)

Other nucleation theories were developed to explain these different actual observations [130, 146–149]. For example, **H. Cölfen** et al. proposed a "cluster theory" involving "pre-critical clusters" as a precursor [150]. Different from the CNT, these precritical clusters are stable and can be preserved till the end of the crystallization process. The differences between the two theories are illustrated in **Figure 27**.

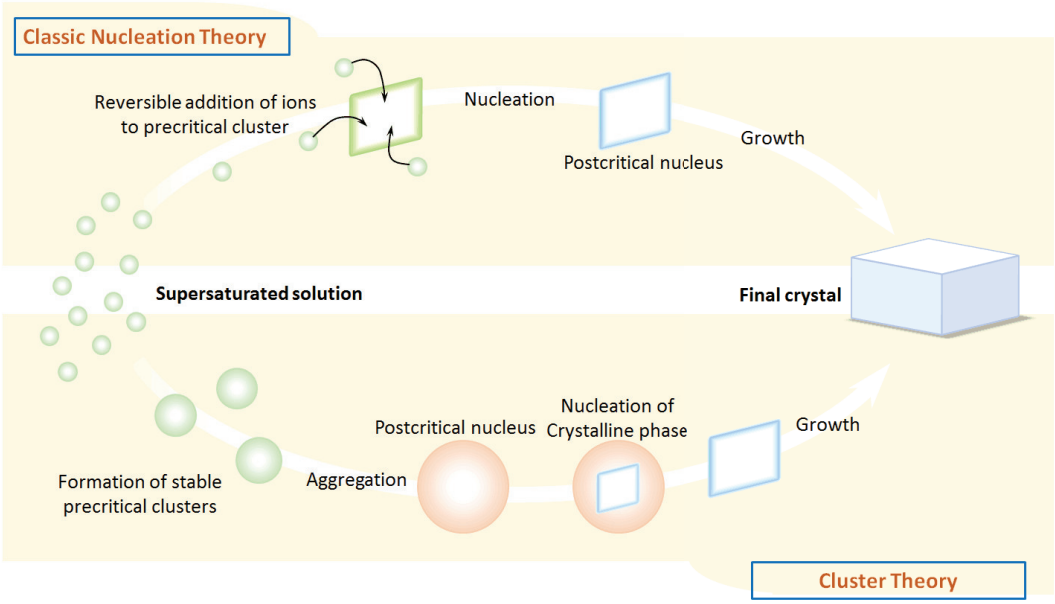

Figure 27: Classic Nucleation Theory versus Cluster Theory (redrawn after **Meldrum** [151])

Ettringite crystallization under zero gravity

Under normal gravity, the necessary transport of building units (ions or molecules) to the initial nuclei or precritical clusters occurs via diffusion and convection processes. In order to understand the crystallization of ettringite under an undisturbed ideal environment, zero gravity experiments were performed. Under such condition, convection was eliminated and no sedimentation can occur. Thus, the crystallization process became solely diffusion dependent, as a consequence, more regular and defect free crystals were expected [152, 153]. Up till now, most of the zero gravity experiments were protein related subjects, in total $\sim$ 200 different samples were tested on 39 US Space Shuttle flights. Only a handful of experiments have been done with inorganic minerals under microgravity which still needs to be explored in depth [154–156]. In 1994, a spectacular experiment was planned and actually started, whereby a large cement sample ($\sim$ 1 kg) was lifted by a U. S. space shuttle and was to be studied on the International Space Station (ISS) with respect to its long term hydration reaction. Unfortunately, during the lift-off, the strong acceleration force destroyed the wood board separating the cement and water, thus no further investigation was possible [157].

3.5 Accelerators

When mixed with water, cement gradually sets and then hardens. The setting and hardening are associated with the interaction of water with the components of the clinker (cement hydration) and the formation of new hydrated phases.

Under certain circumstances, controlling the hydration rate is of great importance, such as during winter when accelerated hydration is required to favor early strength development, and also to minimize the damage by early age freezing [158, 159]. An accelerated setting and hardening process is also desirable in the manufacturing of prefabricated concrete blocks to shorten the production period. A very effective and practical way to increase the rate of cement hydration is the addition of an accelerator [160].

The chemistry of accelerators

A broad variety of materials (inorganic/ organic compounds) have been reported to

accelerate the hydration of Portland cements.

– **Calcium chloride**

Among various known accelerators used in ordinary Portland cement (OPC) based concrete, calcium chloride ($CaCl_2$) was the first cement accelerator introduced and is applied mainly in cold weather [161]. $CaCl_2$ has the advantage of easy availability and favorable cost-performance relationship which make it the most widely recognized accelerator product in earlier years.

Although $CaCl_2$ has long been known to accelerate in some way, its mechanism is still poorly understood. According to **Rosenberg's** study [161], the mechanism responsible for the enhancement is that calcium chloride acts as a catalyst for the hydration of C_3S. As for the C_3A phase, it does react with calcium chloride to form calcium hydrochloroaluminate ($3CaO{\cdot}Al_2O_3{\cdot}CaCl_2{\cdot}xH_2O$), however the influence on the early hydration is very minor [162].

While, if gypsum is present in the system, a different mode of action takes place. Calcium chloride is found to accelerate the reaction between C_3A and gypsum.

C_3A reacts with gypsum preferentially (see **Equation 1.8**). When all the gypsum has been exhausted, then C_3A starts to react with $CaCl_2$ (see **Equation 1.9**). The sequence of reactions occurring in the system C_3A/ $CaCl_2$/ $CaSO_4$/ H_2O is shown below:

$$C_3A + 3CaSO_4 + 32H_2O \longrightarrow C_3A \cdot 3CaSO_4 \cdot 32H_2O \qquad \textbf{Equation 1.8}$$

$$CaCl_2 + C_3A + 10H_2O \longrightarrow C_3A \cdot CaCl_2 \cdot 10H_2O \qquad \textbf{Equation 1.9}$$

After all the chloride ions have been consumed, the remaining C_3A starts to form $C_3ACa(OH)_2{\cdot}12H_2O$, also trisulfoaluminate converts to the monosulfoaluminate (see **Equation 1.10**)

$$C_3A \cdot 3CaSO_4 \cdot 32H_2O + 2C_3A \cdot Ca(OH)_2 \cdot 12H_2O \longrightarrow$$

$$3C_3A \cdot CaSO_4 \cdot 12H_2O + 20H_2O + 2Ca(OH)_2 \qquad \textbf{Equation 1.10}$$

In the final stage, the hydrates which have a hexagonal structure, namely $C_3A{\cdot}Ca(OH)_2{\cdot}$

$12H_2O$, $C_3A{\cdot}CaCl_2{\cdot}10H_2O$ and $C_3A{\cdot}CaSO_4{\cdot}12H_2O$, form solid solutions [162].

In spite of all the benefits from calcium chloride, applicators find a serious deficiency of $CaCl_2$ over the years. It greatly promotes the corrosion of metallic structural parts imbedded in the concrete. Therefore, the use of calcium chloride in iron reinforced concrete is generally discouraged or prevented. Improved chloride-free accelerators were then discovered.

A number of other compounds, such as calcium formate ($Ca(HCOO)_2$), calcium nitrate ($Ca(NO_3)_2$), calcium nitrite ($Ca(NO_2)_2$) have been proposed as alternatives to $CaCl_2$. But all are less effective or show a lower cost-performance relationship.

Neutral calcium formate can be used as a less corrosive accelerator. It acts in a similar manner to calcium chloride. However, $Ca(HCOO)_2$ possesses very low water solubility (16 g/ 100 g of water), commercially it is supplied only in powder form and is not available as liquid which limits its application. There is a high risk that such accelerator is not distributed uniformly in the cement paste/ concrete, potential uneven setting can be expected [160].

Dodson reported that calcium nitrate ($Ca(NO_3)_2$) is less effective than $CaCl_2$ on both setting and hardening [158].

Calcium nitrite ($Ca(NO_2)_2$) seems to be the best non-chloride admixture, it is commercially available as a 20 wt.% solution, then it easily can be introduced to concrete via usual dispersers [163]. Therefore, calcium nitrite accelerator has become the most widely used non-chloride setting accelerator in America [158]. However, due to its toxicity and environmental problem, its application is discouraged and limited.

Figure 28: Application of shotcrete, cited from [164].

– **Accelerators used in shotcrete**

Different to traditional concrete accelerators which are added during mixing of the concrete at the concrete plant, shotcrete accelerators are introduced in the nozzle of the spray gun. These accelerators can provide instantaneous setting of concrete and early-age strength development [165–168].

Generally, shotcrete accelerators constitute two main types:

- Alkaline accelerators
- Alkali-free accelerators

– **Alkaline accelerators**

Currently available alkaline shotcrete accelerators include the following[167, 169]:

- Carbonates and hydroxides of alkaline earth metals (Na_2CO_3, K_2CO_3 and NaOH, KOH)
- Alkaline silicates (water glass, $nNa_2O{\cdot}SiO_2$, $n \approx 3.3$)
- Alkaline aluminates ($NaAl(OH)_4$, $KAl(OH)_4$)

Alkaline carbonates and hydroxides are applied only in the dry-mix process. The accelerating effect is ascribed to promoting C_3S hydration. The disadvantage of this type of shotcrete accelerator is causing tremendous decrease in final strength, the typical reduction in 28-day strength is $\sim 30 - 40$ %, sometimes even 50 % [170].

Sodium and potassium silicate-based accelerators have been the main type wet-mix accelerators for a long time and are still being used in many applications. Rapid setting is achieved in such a way that the water soluble alkaline silicate reacts with Ca^{2+} in cement pore solution to form a calcium silicate hydrate precipitate. The advantage of this type is that it is compatible with almost all types of cements, besides they are relatively cheap compared to the other shotcrete accelerator types (such as alkali aluminates), therefore they are very well received by the field users. The drawback of alkaline silicates - based accelerators is that they have a high alkali content, their pH is above 11. In this case, the operators need adequate protection during spraying the shotcrete. Similar to alkali carbonate- and hydroxide-based accelerators, alkaline silicates - based accelerators also show significant decrease in final strength - up to a 50 % reduction [167].

Alkaline aluminates can be used both for dry- and wet-mix shotcrete. They are the

most widely used materials among all shotcrete accelerator types. This type of shotcrete accelerators result in a much lower loss in final strength ($\sim$ 20 – 25 % in comparison to plain shotcrete). The mechanism based on the accelerating effect of alkaline aluminates is that they can react with gypsum, thus ettringite formation is prevented, and C_3A reacts directly with water to form C_2AH_8 and C_4AH_{13} leading to a flash set [171].

Alkali-free shotcrete accelerators

Alkali-free accelerators were brought up to cope with the difficulties caused by the alkaline accelerators. Commonly used alkali-free accelerators include aluminum-sulfate- or aluminum-hydroxide-based products. They are often used together with various amines to boost their effectiveness. It was found that the reduction in 28-day strength caused by alkali-free shotcrete accelerator lies at $\sim$ 25 % which is superior compared to the conventional alkaline accelerators. In spite of their advantages, they are not so popular due to their higher rebound rate compared to alkaline materials.

– **Novel accelerator based on C-S-H – PCE Nanocomposites**

All above mentioned accelerators have a common deficiency which is that the early strength development is promoted at the cost of final strength. This problem remained unsolved until recently. In 2011 **L. Nicoleau** introduced a completely novel concept to the market. Calcium aluminate hydrate ($xCaO{\cdot}ySiO_2{\cdot}zH_2O$, C-S-H) which is the main hydration product can be stabilized by polycarboxylate (PCE) superplasticizers, the resulting C-S-H - PCE nanocomposites were found to present effective cement hardening accelerators [172]. This new invention attracted a lot of attention and interests, intensive research were carried out in order to further understand the accelerating mechanism. **Plank's group** synthesized PCE nanocomposites via co-precipitation of Na_2SiO_3 and $Ca(NO_3)_2$ in the presence of anionic PCE copolymers. They revealed that C-S-H - PCE nanocomposites work as seeding material which can significantly reduce the activation energy for the crystallization of C-S-H, thus the formation of C-S-H can be formed earlier than in plain cement [173]. What's more, the 28-day strength is not negatively influenced by the addition of C-S-H - PCE nanocomposites. In spite of the excellent performance, the application of this novel type of accelerator suffers from the high cost.

– **Low cost accelerator based on Nano clay**

After discussing different accelerators based on different chemistry, it is obvious that the different types of accelerators possess specific advantages, but also drawbacks. Therefore, new materials providing a strength enhancing effect need to be discovered or evaluated. In this thesis, commercially available nano clay samples were found to be an effective early strength enhancer for Portland cement. Clay minerals are abundantly available in nature, this makes nano clays very competitive among the different accelerator products.

4 Materials and methods

4.1 Graphical summary of the five research topics

In the following, five diagrams are presented to summarize the key steps in the experimental procedures, and the materials and methods taken in the five main research topics disclosed later.

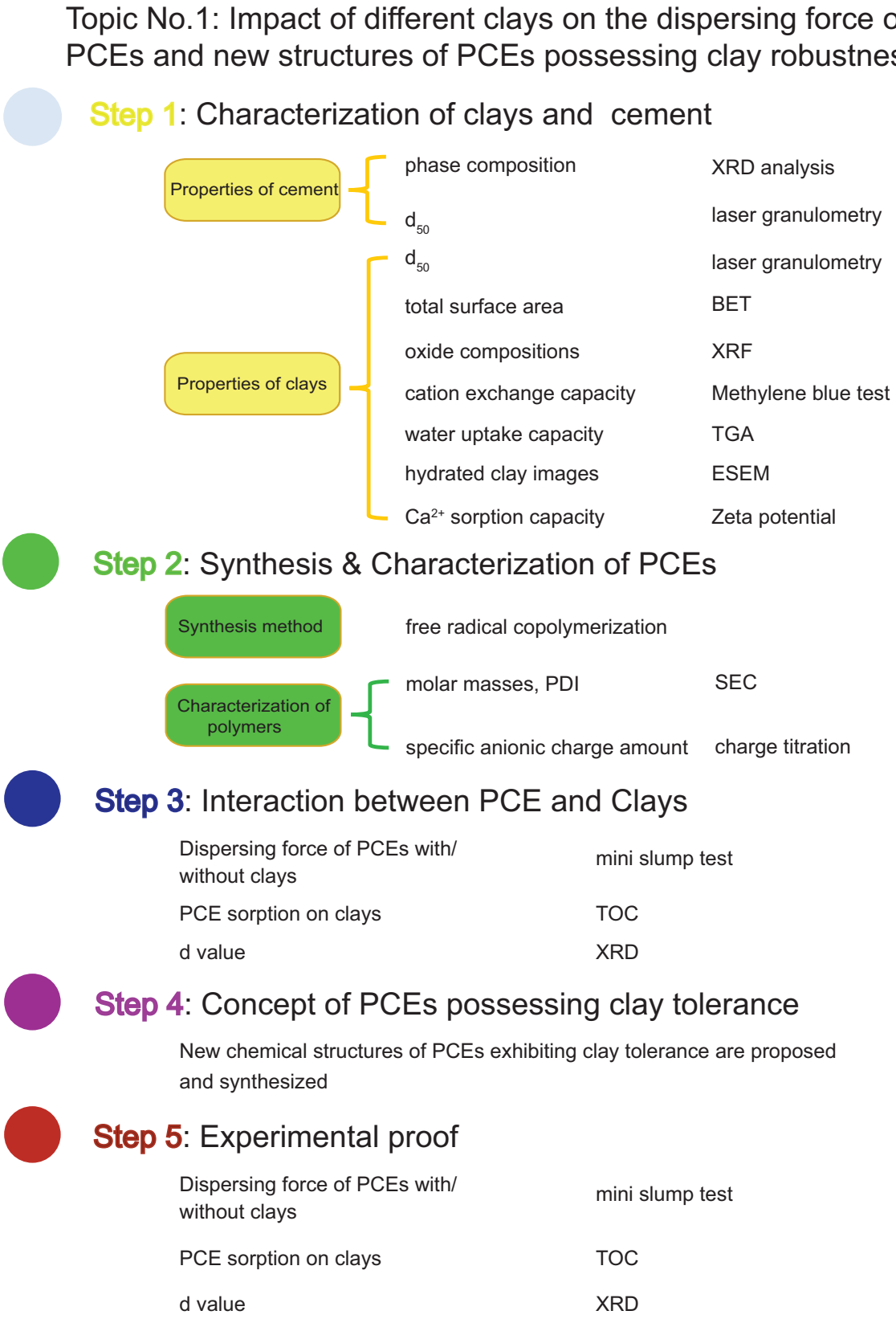

Figure 29: Experimental approach applied in topic no. 1 regarding the impact of different clay minerals on the dispersing force of PCEs & synthesis of clay tolerant PCEs

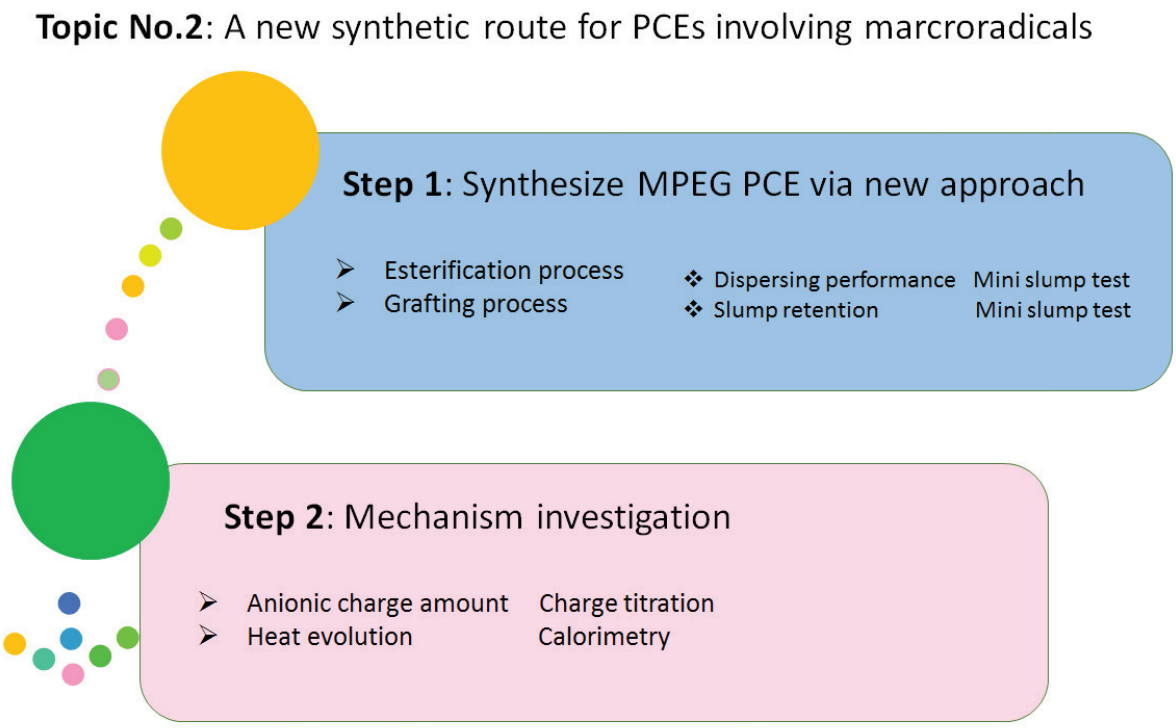

Figure 30: Experimental approach applied in topic no. 2 regarding a new synthesis route for PCEs involving macroradicals

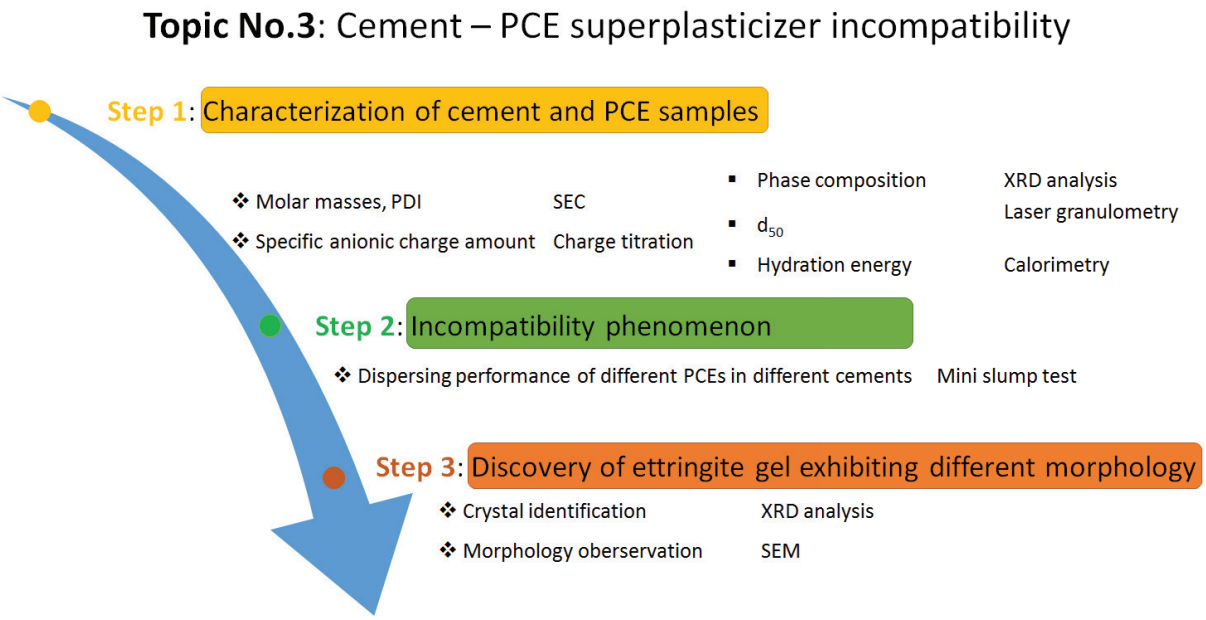

Figure 31: Experimental approach applied in topic no. 3 regarding cement – PCE incompatibility

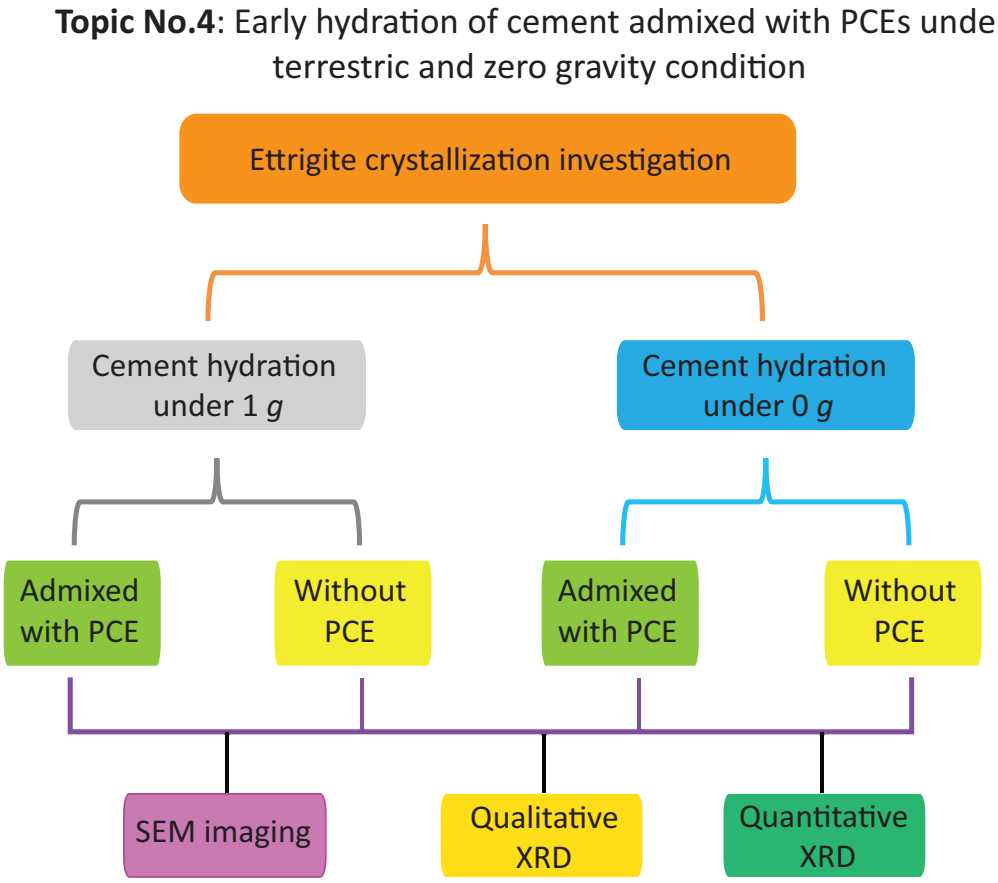

Figure 32: Experimental approach applied in topic no. 4 regarding early hydration of cement admixed with PCEs under terrestric and zero gravity conditions

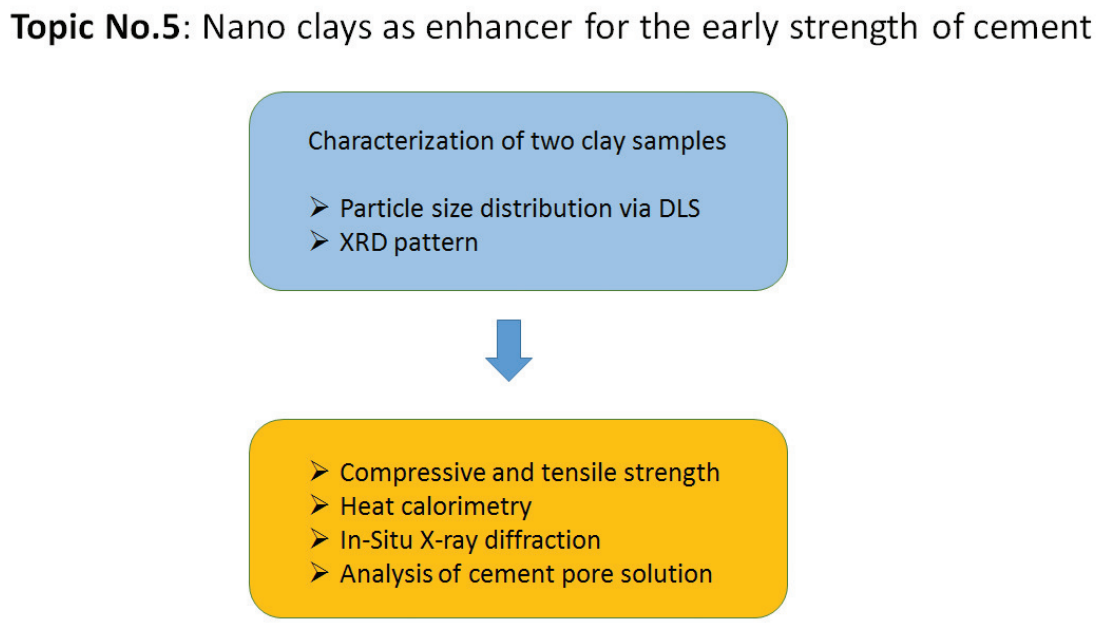

Figure 33: Experimental approach applied in topic no. 5 regarding nano clays as enhancer for the early strength of cement

5 Results and discussion

In this chapter, the key findings of my research regarding the five main topics as below will be presented. Furthermore, the published papers are attached.

- ▷ The interaction of polycarboxylate comb copolymers with different clay minerals;
- ▷ A novel facile preparation method for PCE polymers using macroradicals;
- ▷ A mechanistic investigation of cement – PCE superplasticizer incompatibility;
- ▷ The nucleation and crystallization of ettringite under zero gravity conditions;
- ▷ The use of nano clay for early strength enhancement of Portland cement.

PART I

Peer reviewed SCI(E) journal and conference papers except Paper 5.1

5.1 Impact of different clay minerals on the dispersing force of vinyl ether based polycarboxylate superplasticizers and respective mitigation strategies

L. Lei, J. Plank

Tagung der GDCh-Fachgruppe Bauchemie
October 6 – 8, 2014, Kassel (Germany)
GDCh-Monographie 47 (2014) 84 – 87

This non – reviewed paper presents our first study on PCE – Clay interactions and became the starting point of series of investigations into this subject.

In this paper, the impact of three different clay minerals, montmorillonite, kaolin and muscovite, on vinyl ether (VPEG) - based PCEs was studied. For this purpose, two conventional VPEG PCEs holding PEG side chains were prepared via free radical copolymerization utilizing room temperature synthesis technique. The side chains of the two PCE polymers consisted of 23 EO units (MPEG-1000) and 45 EO units (MPEG-2000) respectively.

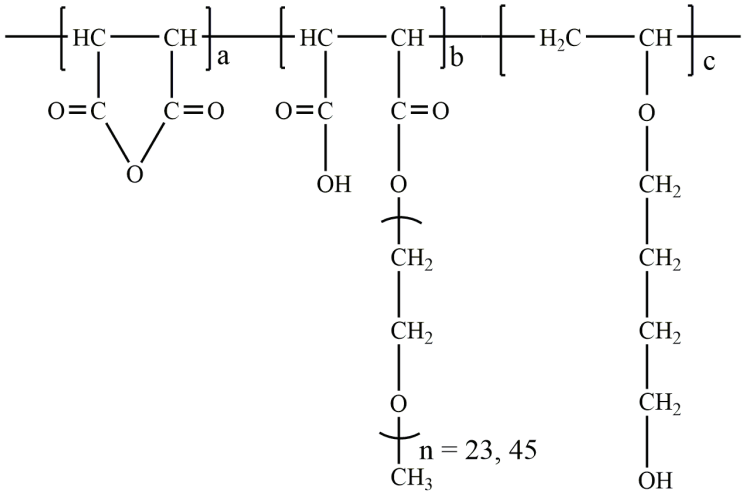

Molecular structure of the synthesized VPEG - PCEs possessing different side chain lengths.

First, the dispersing performance of these PCEs in neat cement paste (no clay present) was evaluated. It was found that their dispersing power was much stronger than that of BNS. However, in the presence of clay minerals, their effectiveness changed completely. When montmorillonite was present, then both VPEG-PCE samples completely lost their dispersing ability. Whereas when kaolin or muscovite were added, then the decrease in spread flow was quite comparable to that from BNS, this suggesting that kaolin and muscovite are much less harmful to PCE superplasticizers than montmorillonite.

A mechanistic study via XRD analysis revealed that strong intercalation of both VPEG-PCE samples into the montmorillonite interlayer gallery had occurred while no such effect was detected for kaolin or muscovite. This result signifies that the especially harmful effect of montmorillonite is owed to its ability to chemically sorb (intercalate) the PCEs via their side chains into the layered structure.

Impact of Different Clay Minerals on the Dispersing Force of Vinyl Ether Based Polycarboxylate Superplasticizers and Respective Mitigation Strategies

L. Lei, J. Plank
Technische Universität München, Chair for Construction Chemicals, Garching, Germany

Introduction

The aim of this study was to compare the effect of three frequently occurring clay minerals (montmorillonite, kaolin, muscovite) on cement pastes admixed with polycarboxylate (PCE) superplasticizers.

Experimental

Synthesis and characterization of synthesized PCE polymers

Two conventional vinyl ether based PCEs were synthesized via free radical copolymerization from maleic anhydride, 4-hydroxy butyl vinyl ether and methoxy polyethylene glycol mono maleate. The number of ethylene oxide units in the methoxy polyethylene glycol was 23 (MPEG-1000) and 45 (MPEG-2000) respectively. Molar masses (M_w, M_n), polydispersity index (PDI) and hydrodynamic radius (R_h) of the PCE samples were determined utilizing size exclusion chromatography (SEC).

Characterization of clays

The cation exchange capacity (CEC) of the clay minerals was determined via adsorption of methylene blue dye by the clay minerals /1, 2/. The water uptake capacity of the clay minerals was obtained via thermogravimetric analysis (TGA).

Dispersing performance test

For determination of the paste flow, a “mini slump test” according to DIN EN 1015 was utilized, for details see /3/. Interaction of the novel superplasticizer with the clays was probed via XRD measurements.

Results and Discussion

Characteristic properties of clay samples

According to the data in **Table 1**, montmorillonite shows the highest MB value. In comparison, the MBV of kaolin and muscovite are much lower, because of the absence of exchangeable interlayer cations.

Table 1. Methylene blue value (MBV) for the clay minerals used in this study

Clay mineral	montmorillonite	kaolin	muscovite
MBV (g/100 g)	8.6	1.9	0.8

According to **Table 2**, montmorillonite exhibits a particularly high water uptake capacity (~77.0 %). In comparison, the water uptake capacity of muscovite is the least at 35.6 %.

Table 2. Water uptake capacity of the clay samples

Clay mineral	montmorillonite	kaolin	muscovite
Water uptake (wt.%)	77.0	49.0	35.6

Characterization of PCE polymers

The molecular properties of the synthesized polymers are presented in **Table 3**.

Table 3. Molar masses (M_w, M_n), polydispersity index (PDI) and conversion rates for the synthesized superplasticizer samples

Polymer sample	M_w (g/mol)	M_n (g/mol)	PDI (M_w/M_n)	Conversion of monomers
VPEG 23	21,390	8,010	2.4	90 %
VPEG 45	53,750	16,180	3.3	85 %
BNS	139,100*	-	-	-

*batch measurement.

Cement dispersion in absence and presence of clay

For this test, the dosages required to achieve a cement paste spread of 26±0.5 cm were determined. The results are displayed in **Fig. 1**. The two vinyl ether based PCE samples exhibit powerful dispersing effectiveness. Dosages of only ~ 0.08 % bwoc are required to achieve the 26 cm spread which are about 2/3 lower than that for BNS.

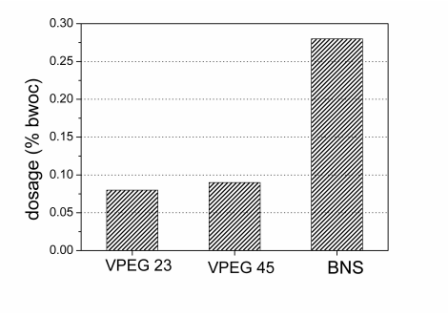

Fig. 1: Dosages of the two synthesized VPEG PCE samples and of the BNS polycondensate required to achieve a cement paste spread of 26±0.5 cm (w/c = 0.45)

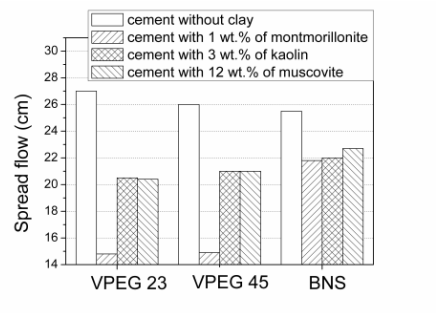

Fig. 2: Spread flow of cement pastes with different superplasticizers, measured in the absence and presence of 1 % of montmorillonite, 3 % of kaolin and 12 % of muscovite, respectively

As is shown in **Fig. 2**, in the cement/montmorillonite system, both VPEG-PCE samples exhibited a strong decrease in performance caused by the presence of 1 wt.% of montmorillonite. The spread flow decreased by 135 %. As for BNS, the spread flow reduction was ~ 50 %.

In the cement/kaolin system, the flow reductions were generally much less. In the presence of 3 wt.% of kaolin, the spread flow for the two VPEG-PCE samples decreased by ~ 72 %, while BNS showed a decrease of ~ 47 %. In the cement/muscovite system, a similar trend was observed.

Mechanistic study - XRD analysis

When hydrated, montmorillonite exhibits a d-spacing of 1.23 nm (**Fig. 3**). For montmorillonite hydrated in the presence of both conventional VPEG PCE polymers, a shift in the d-spacing from 1.23 nm to 1.72 nm was detected. Such d value is characteristic for montmorillonite which contains intercalated polyglycols. Thus, this chemisorption was found to present the main reason for the huge consumption of the conventional PCEs by this type of clay, and in consequence for the strongly decreased fluidity.

For pure hydrated kaolin, a d-spacing of 0.72 nm was detected. After addition of the different superplasticizers, no shift of the d-spacing was found (**Fig. 4**). Similarly, a d-spacing of 0.99 nm for hydrated muscovite was recorded (not shown here). Also here, the d-spacing did not change in the presence of the different superplasticizers. These data

signify that kaolin and muscovite interact with all superplasticizers in a similar manner via surface adsorption only.

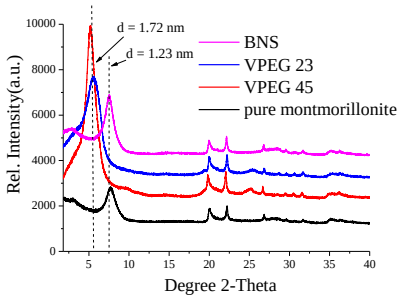

Fig. 3: XRD patterns of montmorillonite dispersed in synthetic cement pore solution holding different superplasticizers (w/clay = 45)

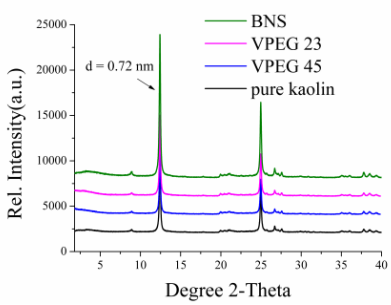

Fig. 4: XRD patterns of kaolin dispersed in synthetic cement pore solution holding different superplasticizers (w/clay = 45)

Conclusion

This study demonstrates that different clay minerals can show completely different impact on the workability of cement and the dispersing effectiveness of PCE superplasticizers. Montmorillonite presents the most detrimental clay mineral. Contrary to this, other clay minerals such as kaolin or muscovite do not so severely impact the performance of VPEG-PCEs. To overcome the sensibility problem of PCE polymers toward clay minerals, applicators should check for the presence and amount of montmorillonite in the aggregates via the MB test. If the MBV is < 1 g/ 100 g, then the clay impurity contained in the aggregates will not cause a significant performance failure of a PCE product. However, when a significant amount of this specific clay mineral is detected (MBV > 1 g/ 100 g), then the use of a PEG-free PCE polymer presents a viable strategy /4/.

Bibliographical references

/1/ AFNOR (1993). Mesure de la quantité et de l'activité de la fraction argileuse (Norme Française NF pp. 68-94). Association française de Normalization (ANFOR), La Défense, Paris, France.

/2/ M. Türköz and H. Tosun, The use of methylene blue test for predicting swell parameters of natural clay soils, Sci. Res. Essays, 6 (2011) 1780-1792.

/3/ L. Lei, J. Plank: „Synthesis, working mechanism and effectiveness of a novel cycloaliphatic superplasticizer for concrete", Cem. Concr. Res., 42 (2012) 118-123.

/4/ L. Lei, J. Plank: „ A Concept For a Polycarboxylate Superplasticizer Possessing Enhanced Clay Tolerance", Cem. Concr. Res. 42 (2012) 118-123.

5.2 Synthesis and properties of a vinyl ether-based polycarboxylate superplasticizer for concrete possessing clay tolerance

L. Lei, J. Plank

Industrial and Engineering Chemistry Research
53 (3), (2014) 1048 – 1055

As shown before, the reduced dispersing performance of conventional PCE superplasticizers in the presence of montmorillonite is mainly owed to the intercalation of the PCE molecules into the expanding lattice of this clay.

In this study, a concept for new PCE structures with enhanced robustness toward clay was probed. The key point was to eliminate the PEG side chains which are most commonly used in PCE structures, and to replace them with 4 - hydroxy butyl vinyl ether (HBVE). This monomer was chosen to provide a non-adsorbing, short side chain. In this case, intercalation has no chance to occur, and the negative impact from montmorillonite should be much reduced.

The first trials to make copolymers from maleic anhydride and HBVE failed because the reactivities of this monomer pair do not match according to the Q-e scheme developed by **Alfrey** and **Price** [174, 175]. Based on this experience, mono alkyl maleates were introduced into the system as auxiliary comonomers which resulted in a successful synthesis. The preparation route is shown below.

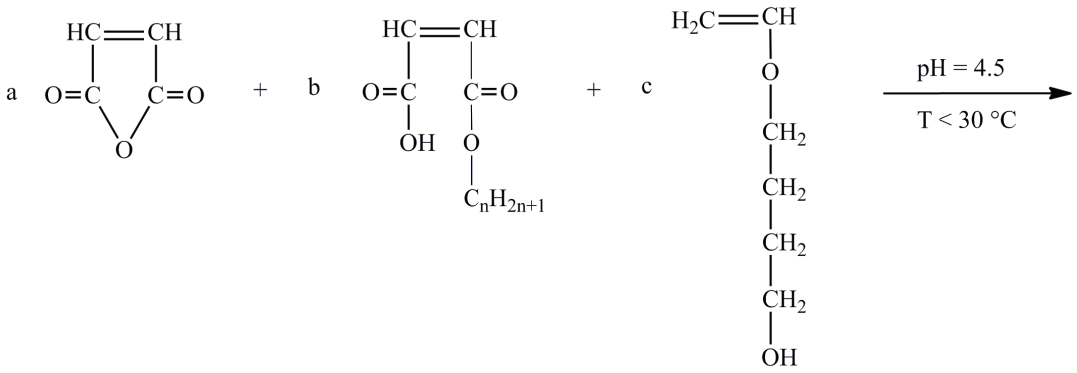

Synthetic route for MA-mono alkyl maleate-HBVE terpolymers

The synthesized terpolymers were tested for their robustness in the presence of a detrimental clay contaminant (montmorillonite). It was found that the novel PCEs required much lower dosages to achieve the standard slump flow compared to that of conventional VPEG-PCEs holding PEG side chains. Thus, our concept of eliminating the PEG pendant groups in the PCE molecule to achieve clay tolerance was confirmed.

Mechanistic studies via TOC and XRD experiments revealed that no intercalation of the modified PCEs into the montmorillonite interlayer gallery had occurred which was in good agreement with the test results from the performance testing.

I&EC research
Industrial & Engineering Chemistry Research

Article

pubs.acs.org/IECR

Synthesis and Properties of a Vinyl Ether-Based Polycarboxylate Superplasticizer for Concrete Possessing Clay Tolerance

Lei Lei and Johann Plank*

Technische Universität München, Lichtenbergstrasse 4, 85747 Garching, Germany

ABSTRACT: Common polycarboxylate ether (PCE) superplasticizers that possess polyethylene glycol (PEG) graft chains exhibit high sensibility toward clay impurities contained in concrete aggregates and limestone powder. The presence of clay greatly weakens their dispersing ability. In this study, modified vinyl ether-based PCEs were synthesized from maleic anhydride (MA) and 4-hydroxy butyl vinyl ether (HBVE). We found that successful copolymerization of these two monomers is dependent on incorporation of at least ~30 wt % of a maleic monoalkyl ester as an auxiliary comonomer. The resulting terpolymers were characterized and tested for their dispersing ability in cement paste in the absence and presence of montmorillonite. The MA−monoalkyl maleate−HBVE terpolymers are little affected by montmorillonite. Sorption measurements and X-ray diffraction analysis suggest that this novel type of PCE interacts with montmorillonite only via surface adsorption, whereas conventional PCEs possessing PEG graft chains incorporate chemically into the interlayer space of alumosilicates.

1. INTRODUCTION

Polycarboxylate superplasticizers (PCEs) make up a class of cement dispersants that exhibit a comb or brushlike structure. They consist of a trunk chain holding carboxylate groups and of pendant chains that are made of polyethylene or polyethylene/polypropylene glycols. Since their invention in 1981, several types of PCE products have been introduced, and they are manufactured commercially. Their chemical structures are presented in Figure 1. The PCE products include the following.

1.1. MPEG-Type PCEs. They constitute the first type of PCE on the market and were introduced by Nippon Shokubai Co. under the name "FC 600".[1] MPEG-PCEs can be synthesized via esterification of a poly(methacrylic acid) backbone with methoxy poly(ethylene glycol) utilizing an acid or base catalyst (e.g., *p*-toluol sulfonic acid or LiOH) and an azeotrop or vacuum to remove the water;[2] this process produces a highly uniform comb polymer with a statistical distribution of the MPEG graft chains along the polyanionic trunk chain. Alternatively, they can be made via aqueous free radical copolymerization of an ω-methoxy poly(ethylene glycol) methacrylate ester macromonomer with methacrylic acid.[3] Here, gradient polymers are attained that at the beginning of the polymerization exhibit a higher side chain density than toward the end of the reaction. Recently, such gradient polymers possessing specific compositions have been synthesized intentionally by applying the RAFT polymerization technique.[4]

1.2. APEG-Type PCEs. This kind of PCE is industrially manufactured via free radical copolymerization either in bulk or in aqueous solution. Key monomers include α-allyl-ω-methoxy or α-allyl-ω-hydroxy poly(ethylene glycol) ether and maleic anhydride or acrylic acid.[5] Polymerization in bulk works well for side chain lengths of up to ~34 EO units, while polymerization in water typically yields copolymers possessing very short trunk chains ("star polymers") made of ~10 repeating units only. Such polymers were found to exhibit an excellent dispersing performance.

1.3. HPEG-Type PCEs. They constitute a minor modification of the APEG-based PCEs because there instead of allyl ethers, methallyl ethers are utilized.[6] Their synthesis is easier compared to that of APEG-PCEs because the methallyl radical is not resonance-stabilized. Unfortunately, methallyl alcohol is not listed under the REACH scheme in Europe; therefore, its use in the manufacturing of PCEs is excluded there at present.

1.4. IPEG-Type PCEs. This type of PCE (also known as TPEG-PCE) is synthesized from isoprenyl oxy poly(ethylene glycol) ethers and unsaturated carboxylic acids such as acrylic acid via copolymerization.[7] In recent years, this PCE became highly popular, especially in China, because of its excellent performance, which often exceeds that of any other type of PCE, and its simple preparation utilizing free radical copolymerization. A minor drawback of IPEG-PCE technology is that macromonomers possessing very long EO chains (e.g., $n \geq 50$) appear to be difficult to make.

1.5. PAAM-Type PCEs. These zwitterionic PCEs hold mixed lateral chains containing both polyamidoamine (PAAM) and PEO segments. This characteristic feature separates them from all other kinds of PCEs that are composed of only PEO/PPO pendant chains. This type of PCE can fluidize cement pastes at very low water:cement ratios (as low as ~0.12).[8]

The information presented above demonstrates that all industrially manufactured PCE copolymers contain PEO or PEO/PPO side chains that make them subject to strong chemical interaction with clays, as will be shown later.

Vinyl ethers present a class of highly reactive monomers. They can be accessed by a number of synthetic methods. The oldest yet most versatile and industrially practiced route for the synthesis of vinyl ethers is base-catalyzed condensation of

Received: October 24, 2013
Revised: December 30, 2013
Accepted: December 31, 2013
Published: December 31, 2013

dx.doi.org/10.1021/ie4035913 | Ind. Eng. Chem. Res. 2014, 53, 1048−1055

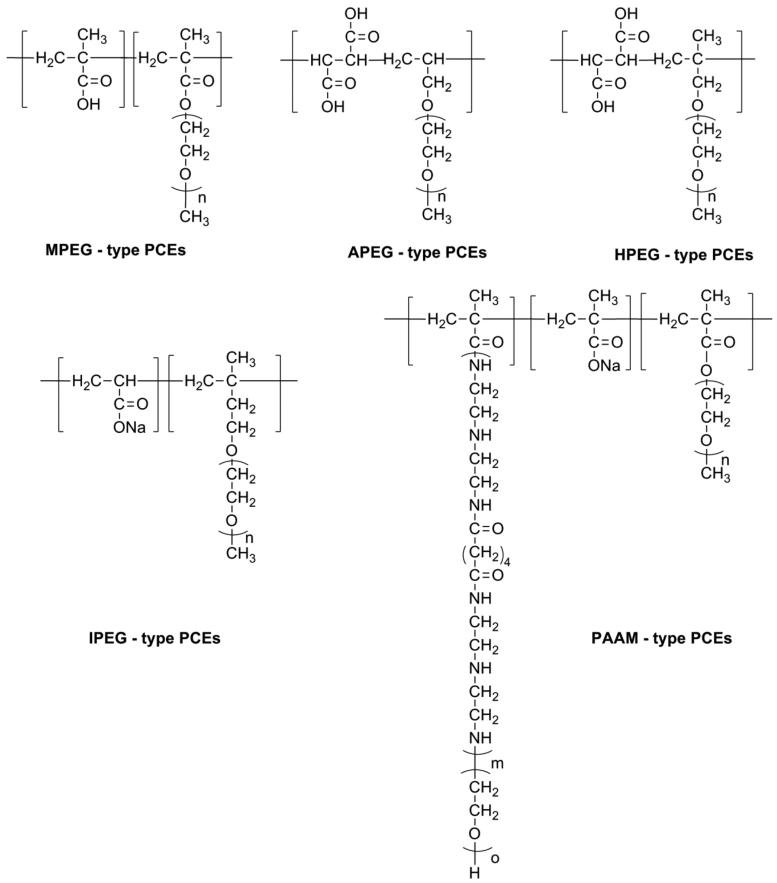

Figure 1. Chemical compositions of MPEG-, APEG-, HPEG-, IPEG-, and PAAM-type PCE polymers.

acetylene with alcohols that was first described by Reppe and co-workers (see Figure 2).[9]

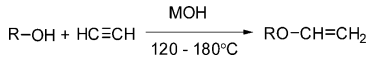

Figure 2. Synthetic route for the preparation of vinyl ether monomers.

During copolymerization, the reactivity of vinyl ethers is particularly high when electron-donating substituents such as hydroxy alkyl groups are linked to the vinyloxy unit. A typical example for such a monomer is 4-hydroxy butyl vinyl ether (HBVE), which is commercially produced in large quantities. From HBVE, it is well-known that partial decomposition can occur during copolymerization, beginning at a temperature of 35 °C, whereby decomposition products, including acetaldehyde, are released. As a result, it is important to polymerize this vinyl ether at ~25 °C. However, under those conditions, many common monomers exhibit low reactivity, even in the presence of strong redox initiators.

Recently, applicators of PCEs reported serious problems when these superplasticizers were used in concrete contaminated with clay and silt, e.g., from insufficiently washed aggregates or limestone powder. Depending on the type and amount of clay contaminant, the dispersing ability of conventional PCEs can be strongly affected by clay. Sometimes even a total loss of the dispersing effect was observed; polycondensate superplasticizers such as BNS (naphthalene-type) or PMS (melamine-type) are less affected.

To overcome this problem, in this study we synthesized a novel type of PCE based on a vinyl ether monomer and probed it with respect to its clay tolerance utilizing the "mini slump" test of cement pastes. Furthermore, interaction of the novel PCE with montmorillonite was studied via adsorption measurement and X-ray diffraction (XRD) analysis, and its behavior was compared to that of a conventional PCE possessing PEG graft chains. From these data, we hoped to gain insight into whether the modified PCE would perform more consistently in the absence and presence of clay.

2. EXPERIMENTAL SECTION

2.1. Materials. *2.1.1. Chemicals.* 4-Hydroxy butyl vinyl ether (>99% pure, purchased from Sigma-Aldrich Chemie, Steinheim, Germany), maleic anhydride (>99% pure, Merck Schuchardt OHG, Hohenbrunn, Germany), methanol, ethanol, and *n*-propyl alcohol (all >98% pure, VWR International, Darmstadt, Germany), sodium hydroxymethane sulfinate (Rongalit C, >98% pure, Sigma-Aldrich Chemie), ferrous sulfate (>98% pure, VWR International), 2-mercaptoethanol (>99% pure, Sigma-Aldrich Chemie), and hydrogen peroxide (30% aqueous solution, VWR International) were used without further purification.

2.1.2. Cement. A Portland cement type CEM I 52.5 N ("Milke® classic" from HeidelbergCement, Geseke plant,

dx.doi.org/10.1021/ie4035913 | Ind. Eng. Chem. Res. 2014, 53, 1048−1055

Germany) was used. Its composition is given in Table 1. It possesses an average particle size (d_{50} value, determined via laser granulometry) of 11.5 μm, and its density was found to be 3.153 g/cm^3 (helium pycnometry). Its specific surface area (BET method, N_2 adsorption) was 1.4 m^2/g.

Table 1. Phase Composition of the CEM I 52.5 N Sample, As Determined by Q-XRD Using Rietveld Refinement

phase	wt %
C_3S, m	54.14
C_2S, m	26.63
C_3A, c	3.28
C_3A, o	4.26
C_4AF, o	2.45
free lime (Franke)	0.1
periclase (MgO)	0.03
anhydrite	2.64
$CaSO_4$ hemihydrate	1.21
$CaSO_4$ dihydrate	0.02
calcite	3.61
quartz	1.16
arcanite (K_2SO_4)	0.46

2.1.3. Clay. The clay sample used in this study was a sodium montmorillonite supplied under the trade name of RXM 6020 by Rockwood (Moosburg, Germany). This clay mineral is a naturally occurring sodium bentonite possessing a specific surface area (BET method, N_2 adsorption) of 38.33 m^2/g and was used as obtained. Table 2 provides its oxide composition as determined via X-ray fluorescence (XRF).

2.1.4. Polymers. 2.1.4.1. Synthesis of the Maleic Anhydride–HBVE Copolymer. At first, 25 mL of deionized (DI) water was placed in a 250 mL four-neck round-bottom flask equipped with a stirrer, a reflux condenser, and two separate inlets for the HBVE monomer (inlet A) and the initiator solution (inlet B). After the water had been purged with N_2 for 30 min, 10.9 g (0.11 mol) of maleic anhydride and 8.3 g of 50% aqueous NaOH were added while the mixture was being stirred, while the temperature was kept below 30 °C by cooling. Subsequently, 30 mg of $FeSO_4{\cdot}7H_2O$ and 6.17 g of 30% aqueous H_2O_2 were fed into the reactor. Using two peristaltic pumps, through inlet A 10.3 g (0.09 mol) of 4-hydroxy butyl vinyl ether was added over 60 min, and at the same time, an aqueous solution of 1.7 g of Rongalit C (initiator) dissolved in 10 mL of H_2O was fed in over 75 min through inlet B. The reaction temperature was carefully kept at 25 °C throughout all additions. Afterward, the mixture was stirred for an additional 30 min. The final product designated as MA–HBVE was a light yellowish, 19 wt % aqueous solution possessing very low viscosity and a pH of ∼4.5. It contained a large amount of unreacted monomers.

2.1.4.2. Monoalkyl Maleate Ester Monomers. Maleic anhydride (4.09 g, 42 mmol) and 32 mmol of either methanol (1.03 g), ethanol (1.48 g), or *n*-propanol (1.9 g) were placed in a 250 mL four-neck round-bottom flask equipped with a stirrer and reflux condenser and heated for 2 h at 55 °C while being constantly stirred. Thereafter, 5 g of DI water was added to the flask, and the resulting solution of the monoalkyl ester of maleic acid was cooled to 20 °C.

2.1.4.3. MA–Monoalkyl Maleate–HBVE Terpolymers. As an example, the synthesis of the MA–monomethyl maleate–HBVE terpolymer is described. A 250 mL four-neck round-bottom flask holding the aqueous solution of the monomethyl maleate prepared as described above equipped with a stirrer, a reflux condenser, and two separate inlets is provided with an inert atmosphere by bubbling N_2 via a bottom valve. The inert atmosphere was maintained over the entire reaction time; ∼7 mL of a 30% KOH solution was added to adjust the pH of the monomethyl maleate solution to ∼4.5. Thereafter, 12.37 g (106 mmol) of 4-hydroxy butyl vinyl ether was added while the mixture was being stirred. Subsequently, 30 mg of $FeSO_4{\cdot}7H_2O$, 40 mg of 2-mercaptoethanol (the first portion of chain transfer agent), and 4.9 g of a 30% H_2O_2 solution were added to the reactor. Next, 0.63 g of Rongalit C (initiator) was dissolved in 10 mL of DI water. This solution was designated solution I. Separately, 4.16 g (42 mmol) of maleic anhydride and 80 mg of 2-mercaptoethanol (second portion of chain transfer agent) were dissolved in 12.5 mL of DI water. This solution was named solution II. Using two peristaltic pumps, solutions I and II were fed separately and continuously into the vessel over periods of 75 min (solution I) and 60 min (solution II) while the temperature was maintained at 25 °C. When the additions were completed, the mixture was stirred for an additional 30 min. The final product designated as the MA–monomethyl maleate–HBVE terpolymer was a slightly reddish, 24 wt % aqueous solution possessing moderate viscosity and a pH of ∼3.9.

The MA–monoethyl maleate–HBVE terpolymer was prepared following the procedure described above except that 10.57 g (32 mmol) of the aqueous solution of monoethyl maleate was used instead of the monomethyl maleate. The sample was designated as the MA–monoethyl maleate–HBVE terpolymer, which exhibited a solid content of 27 wt % and a pH of ∼4.

The MA–monopropyl maleate–HBVE terpolymer was synthesized as described above except that 11 g (32 mmol) of the aqueous solution of monopropyl maleate was used. The resulting terpolymer was a liquid with a solid content of 30 wt % and a pH of ∼4.1.

2.1.4.4. Synthesis of the MA–MPEG-1000 Maleate–HBVE Terpolymer. A conventional vinyl ether-based PCE holding PEG side chains was synthesized via aqueous free radical copolymerization from 4.16 g (42 mmol) of maleic anhydride, 12.37 g (106 mmol) of 4-hydroxy butyl vinyl ether, and 36.2 g (32 mmol) of methoxy polyethylene glycol monomaleate following the description for the monoalkyl maleate-containing terpolymers. 2-Mercaptoethanol was used as the chain transfer agent. The number of ethylene oxide units in the methoxy polyethylene glycol was 23 (MPEG-1000). The resulting terpolymer solution exhibited a solid content of 40 wt % and a pH of ∼4.2 and was a slightly reddish, highly viscous solution.

2.1.4.5. BNS Polycondensate. An industrial superplasticizer sample based on β-naphthalene sulfonate formaldehyde polycondensate (BNS) designated Melcret 500F (BASF

Table 2. Oxide Composition of the RXM 6020 Clay Sample, As Determined by XRF

oxide	SiO_2	Al_2O_3	CaO	MgO	Fe_2O_3	Na_2O	K_2O	TiO_2	LOI	total
wt %	59.7	18.4	0.8	2.3	4.0	2.3	0.1	0.1	12.1	99.8

dx.doi.org/10.1021/ie4035913 | Ind. Eng. Chem. Res. 2014, 53, 1048–1055

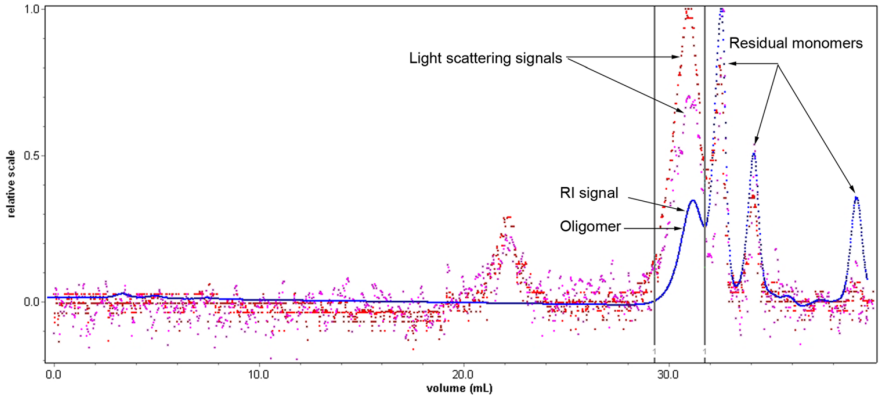

Figure 3. SEC spectrum of the reaction product from copolymerization of maleic anhydride and HBVE.

Construction Polymers GmbH, Trostberg, Germany) was used for comparison. Melcret 500F is a spray-dried BNS powder superplasticizer that possesses a low Na_2SO_4 content (<2 wt %).

2.2. Characterization of Polymers. *2.2.1. Size Exclusion Chromatography (SEC).* Molar masses (M_w and M_n) and the polydispersity index (PDI) of the superplasticizer samples were determined via size exclusion chromatography, which is also known as gel permeation chromatography (GPC). In this study, a Waters Alliance 2695 instrument (waters, Eschborn, Germany) and a three-angle static light scattering detector ("mini Dawn" from Wyatt Technology Corp., Santa Barbara, CA) were employed. Separation of the polymer fractions was achieved by using three Ultrahydrogel columns (120, 250, and 500). An eluent composed of 0.1 M $NaNO_3$ and 0.1 g/L NaN_3 adjusted to pH 12 was used. The value of d_n/d_c applied to calculate the molar masses was 0.135 mL/g (value for polyethylene oxide).[10]

2.2.2. Specific Anionic Charge Amount. Anionic charge densities of all superplasticizer samples were determined in DI water or a synthetic cement pore solution by polyelectrolyte titration using cationic polydiallyl dimethyl ammonium chloride (polyDADMAC) as a titrator. The tests were performed utilizing a PCD 03 pH particle charge detector (Mütek Analytic, Herrsching, Germany). The synthetic cement pore solution was prepared from 1.72 g/L $CaSO_4 \cdot 2H_2O$, 6.959 g/L Na_2SO_4, 4.757 g/L K_2SO_4, and 7.12 g/L KOH dissolved in 1 L of DI water (pH value of 13.06).

2.2.3. Dispersing Performance of the Polymers in Cement. The spread flow of cement pastes containing different superplasticizer samples was determined utilizing a mini slump test following the DIN EN 1015 standard. The test was conducted as follows. First, the water:cement (w:c) ratio of the neat cement paste required for a spread flow of 18 ± 0.5 cm was determined. After that, over a period of 1 min, 300 g of cement was filled into a porcelain cup that contained the specific amount of polymer dissolved in the mixing water. The mixture was allowed to rest for 1 min and then stirred manually for 2 min utilizing a spoon. Immediately after being stirred, the cement paste was poured into a Vicat cone that was placed on a glass plate and filled to the brim and the cone was lifted vertically. The size of the Vicat cone is 40 mm (height) × 70 mm (top diameter) × 80 mm (bottom diameter). The resulting diameter of the paste represents the flow value of the paste. The spread was measured twice, the second measurement being perpendicular to the first, and an average was calculated. All tests were repeated four times, and the average of all measurements is reported as the final spread flow value.

2.2.4. Sorption on Clay. The adsorbed amounts of superplasticizer samples on montmorillonite were determined according to the depletion method. Different dosages of individual superplasticizer samples were added to montmorillonite suspensions that were shaken in a wobbler (VWR International) for 2 min at 2400 rpm and centrifuged for 10 min at 8500 rpm. For quantification of the organic carbon content in the filtrates, a High TOC II apparatus (Elementar, Analysensysteme, Hanau, Germany) was used. Centrifugates were diluted with DI water, and their TOC values were obtained after combustion at 890 °C. The amount of superplasticizer sample adsorbed was calculated by subtracting the concentration of the superplasticizer found in the centrifugate from that contained in the reference sample.

2.2.5. XRD Analysis. The interaction between the superplasticizer samples and montmorillonite was probed via XRD measurements. XRD analysis was performed on montmorillonite samples that were hydrated overnight in the presence and absence of polymers and then centrifuged for 10 min at 8500 rpm. The solid part collected from the centrifuge tube was dried overnight at 80 °C and ground. XRD patterns were obtained on a D8 Advance, Bruker AXS instrument (Bruker, Karlsruhe, Germany) utilizing Bragg−Bretano geometry.

3. RESULTS AND DISCUSSION

Our concept of a more clay-tolerant PCE was based on earlier findings that revealed that the polyethylene glycol (PEG) side chains of conventional PCEs indeed occupy the interlayer space between individual alumosilicate sheets of montmorillonite.[11] Through this chemical sorption (intercalation), the superplasticizer is sequestered from the cement and thus no longer can exert its steric dispersing effect. Consequently, we thought to avoid the detrimental PEG side chains by using HBVE, which presents a versatile monomer and provides a nonsorbing albeit short side chain.

3.1. Copolymerization Behavior of 4-Hydroxy Butyl Vinyl Ether. At first, we attempted to copolymerize HBVE with maleic anhydride at a molar ratio of 1:1.2 and a pH value of 4.5. As expected, this approach failed. The SEC spectrum of the MA−HBVE reaction product reveals that only a small amount of an oligomer possessing a molecular mass (M_w) of <1500 Da was obtained, while ∼75% of the monomers added

were still unreacted (Figure 3). This came as no surprise because the reactivities of the two monomers do not match according to the $Q-e$ scheme developed by Alfrey and Price.[12] There, the reaction rate constant between two monomers is expressed by the parameters Q and e, whereby Q represents the resonance stability and e the polarity, as shown in eqs 1 and 2.

$$r_1 = \frac{Q_1}{Q_2} \times e^{-e_1(e_1-e_2)} \quad (1)$$

$$r_2 = \frac{Q_2}{Q_1} \times e^{-e_2(e_2-e_1)} \quad (2)$$

According to the $Q-e$ scheme, monomers with Q values of >0.35 represent well resonance-stabilized monomers, and those with Q values of <0.35 are poorly resonance-stabilized monomers. Monomers possessing negative e values are electron donors, and monomers with positive e values are electron acceptors. Generally, the copolymerization of monomers possessing similar Q values proceeds best. As shown in Table 3, as for maleic anhydride and an alkyl vinyl ether, their Q values are quite different; therefore, it is very difficult to copolymerize with each other. Thus, to facilitate a reaction between maleic anhydride and HBVE, monoalkyl maleates, namely monomethyl maleate, monoethyl maleate, and monopropyl maleate, were introduced as auxiliary comonomers. Their Q values lie in between those of maleic anhydride and the vinyl ether. Consequently, they can facilitate copolymerization with both monomers.

Table 3. Q and e Values According to the Scheme of Alfrey and Price for Monomers Relevant in This Study[13]

monomer	maleic anhydride	*n*-butyl vinyl ether (approximately for HBVE)	diethyl fumarate (approximately for monoalkyl maleate)
Q	0.86	0.038	0.25
e	3.69	−1.5	2.26

Applying this concept, we successfully synthesized terpolymers from maleic anhydride, monoalkyl maleate, and 4-hydroxy butyl vinyl ether at a molar ratio of 1.6:1:3.3. Figure 4 displays the reaction scheme leading to the terpolymers. Table 4 lists the molecular properties of the newly synthesized terpolymers and of BNS polycondensate. On the basis of the SEC data, the molar masses (M_w) of the PCE samples lie at ~10000 Da. The PDIs of the samples are 1.8−2.7, which indicate a fairly narrow molecular mass distribution. Moreover, turnover rates of >80% were found (Table 4). It should be mentioned here that no particular effort was made to further optimize the conversion rates because synthesizing optimized polymers was not the focus of this study. To exemplify the molecular properties of the polymers prepared, the SEC spectrum of the MA−monoethyl maleate−HBVE terpolymer is shown in Figure 5. There, a large peak signifying the terpolymer as well as three minor peaks representing an oligomer and residual monomers can be observed.

For comparison, a "conventional" vinyl ether-based PCE was synthesized from maleic anhydride, mono polyethylene glycol maleate (nEO = 23), and HBVE (molar ratio of 1.6:1:3.3). Similar to that of the terpolymer containing monoalkyl maleate, high turnover rates were also achieved here. The M_w of this terpolymer was found to be higher (~20 kDa) than those for the monoalkyl ester-based terpolymers, because of the longer side chains.

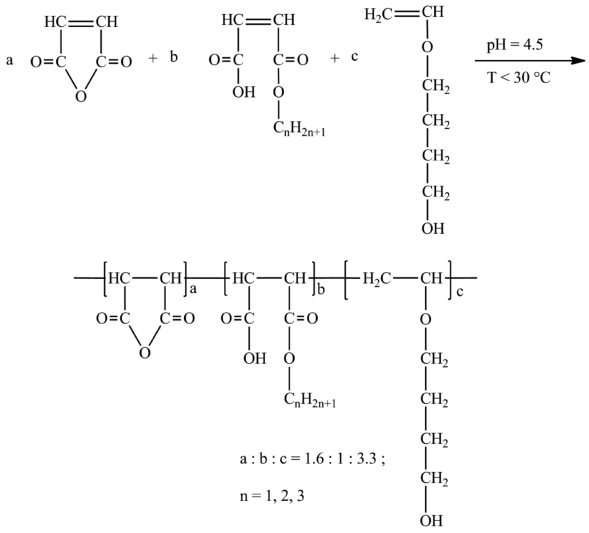

Figure 4. Synthetic route for the preparation of MA−monoalkyl maleate−HBVE terpolymers.

Table 4. Molar Masses (M_w and M_n), Polydispersity Index (PDI) Values, and Conversion Rates for the Synthesized Superplasticizer Samples

polymer sample	M_w (g/mol)	M_n (g/mol)	PDI (M_w/M_n)	conversion rate of monomers (%)
MA−monomethyl maleate−HBVE	10110	5775	1.8	87
MA−monoethyl maleate−HBVE	9000	3334	2.7	83
MA−monopropyl maleate−HBVE	10220	3998	2.7	88
MA−MPEG-1000 maleate−HBVE	21390	8010	2.4	90
BNS (comparison)	139100[a]	–	–	–

[a]Batch measurement.

Next, the specific anionic charge amounts of the synthesized terpolymers were determined in DI water and synthetic cement pore solution. These values signify the tendency of individual polymers to adsorb onto the positive surfaces of cement and/or clay. The results are listed in Table 5. Generally, the anionic charge of all samples tested was lower in the cement pore solution than in DI water. This effect is ascribed to the chelating effect on Ca^{2+} ions present in the cement pore solution that shields some of the negative charge of the polyelectrolytes. Compared to the conventional vinyl ether PCE possessing PEO side chains, the MA−monoalkyl maleate−HBVE terpolymers exhibit higher anionic charge densities, because of their fairly short side chains. Additionally, the specific anionic charge amount of the polycondensate-based superplasticizer BNS was found to be significantly higher at ~4000 μequiv/g.

3.2. Cement Dispersion. Here, the dosages of individual superplasticizer samples required to achieve a spread flow of 26 ± 0.5 cm were compared. The results are displayed in Figure 6. The newly synthesized PCE polymers fluidize cement pastes at surprisingly small dosages [~0.12% by weight of cement (bwoc)], considering their short side chains. Their dosages to

dx.doi.org/10.1021/ie4035913 | Ind. Eng. Chem. Res. 2014, 53, 1048−1055

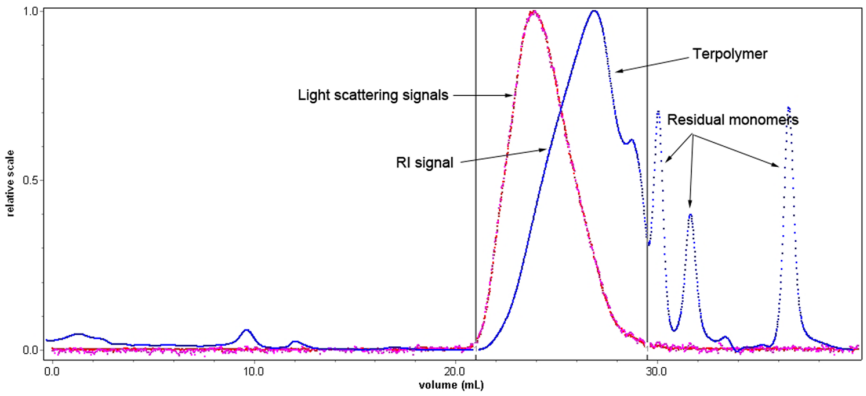

Figure 5. SEC spectrum of the MA−monoethyl maleate−HBVE terpolymer.

Table 5. Specific Anionic Charge Amounts of the Superplasticizer Samples in a DI Water/Cement Pore Solution

	specific anionic charge amount (μequiv/g)				
fluid system	MA−MPEG-1000 maleate−HBVE	MA−monomethyl maleate−HBVE	MA−monoethyl maleate−HBVE	MA−monopropyl maleate−HBVE	BNS
DI water	531	1173	1200	1160	4089
synthetic cement pore solution	145	210	250	348	3911

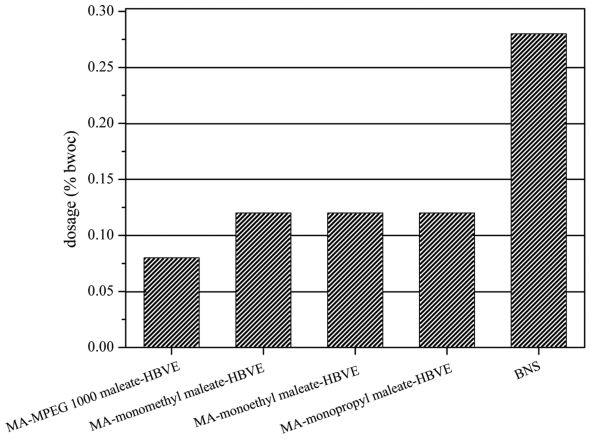

Figure 6. Dosages of MA−monoalkyl maleate−HBVE terpolymers and of comparative superplasticizer samples required to achieve a cement paste spread of 26 ± 0.5 cm (w:c = 0.45).

achieve 26 cm spread are approximately half of that for BNS, which represents the most widely used concrete superplasticizer. Interestingly, we found that the different side chain lengths of the novel terpolymers do not much influence their dispersing performance. The conventional vinyl ether PCE sample possesses a significantly longer side chain made of ~23 ethylene oxide units. Their stronger steric effect allows a dosage of only 0.08% bwoc to achieve the 26 cm spread, thus making it a more powerful dispersant in cement.

3.3. Cement Dispersing Power in the Presence of Clay. This clay mineral was chosen for the experiments because it presents a contaminant that frequently occurs in limestone and sand deposits and because of its well-known huge water sorption (swelling) capacity. The effect of clay contamination on the dispersing performance of the vinyl ether-based superplasticizers was determined on cement that was contaminated with 1 wt % montmorillonite. It was found that for the monoalkyl ester-modified vinyl ether PCEs, the paste spread decreased by ~20%, compared to the reference paste without PCE, whereas the conventional vinyl ether PCE possessing PEG side chains lost 100% of its dispersing force. These data suggest that the replacement of the PEG side chains with alkyl pendants provides a viable method for mitigating the negative effect of clay on PCE superplasticizers.

From an applicator's point of view, however, the decrease in performance is not interesting. Instead, the dosage required to achieve a specific flow value (here 26 cm) of the cement paste is the key criterion. Consequently, the dosages required to achieve this paste spread in the presence of 1% bwoc of montmorillonite were tested, and the results are displayed in Figure 7. There, it is evident that the monoalkyl maleic ester-modified PCEs are most effective whereas the conventional vinyl ether PCE and BNS polycondensate superplasticizers require substantially higher dosages. This result was achieved by the modified PCEs despite their weaker performance in the clay-free system, compared to the conventional PCE (see Figure 6). It signifies that their interaction with clay is much weaker than that of PCEs containing PEG side chains.

3.4. Sorption on Clay. To quantify the interaction between individual PCE samples and montmorillonite, sorption measurements were taken (Figure 8). There, the conventional PCE possessing PEO side chains was found to sorb in extremely large amounts on montmorillonite, with a sorbed amount of ~230 mg/g of clay at the saturation point. On the other hand, the monoalkyl maleic ester-modified terpolymers are sorbed in extremely small amounts (~20 mg/g of clay). These values were even lower than that for the BNS polycondensate that was found at ~50 mg/g of clay. Presumably, the highly anionic BNS (see Table 5) undergoes stronger surface adsorption than the novel PCE polymers. These data explain why the dispersing power of the modified PCEs is significantly less affected by montmorillonite than that of a conventional PCE product. It stems from the enormous

dx.doi.org/10.1021/ie4035913 | Ind. Eng. Chem. Res. 2014, 53, 1048−1055

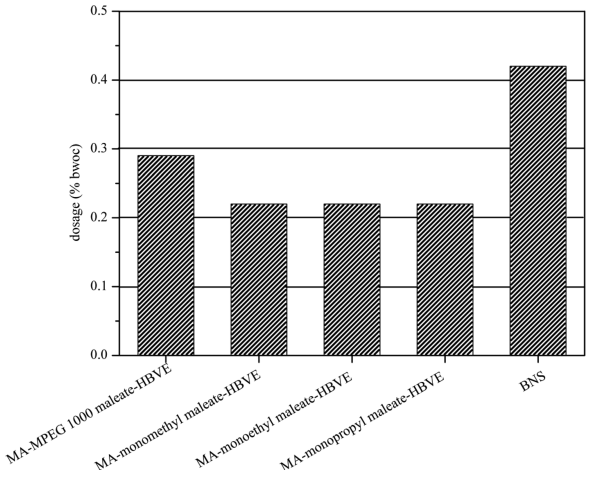

Figure 7. Dosages of superplasticizers required to achieve a spread of 26 ± 0.5 cm, measured in cement pastes (w:c = 0.45) holding 1% bwoc of montmorillonite.

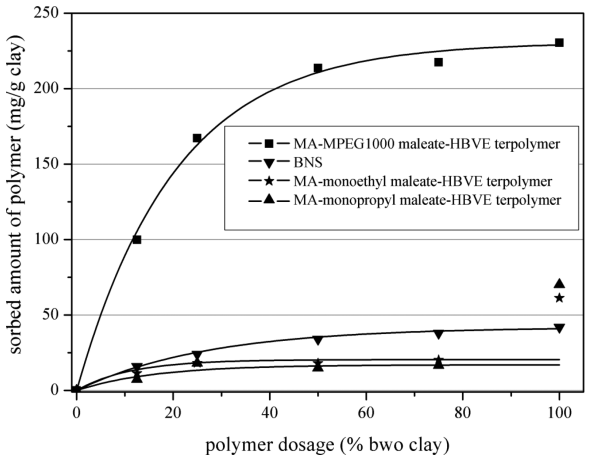

Figure 8. Sorption isotherms for various vinyl ether PCE superplasticizer samples on montmorillonite dispersed in a synthetic cement pore solution (w:c = 45).

consumption of conventional PCE by clay that then no longer is available for cement dispersion. This effect is significantly weaker for the modified PCEs.

3.5. Mode of Interaction with Clay. To investigate the specifics of the interaction between individual PCE samples and montmorillonite, an XRD analysis was performed. Hydrated montmorillonite exhibits a characteristic *d* spacing (distance between the alumosilicate layers) of 1.23 nm[14,15] (Figure 9). Water molecules and various cations (e.g., Na^+) occupy the interlayer space, and successive alumosilicate sheets are bound together by weak hydrogen bonds.[16]

When the conventional VPEG-PCE containing PEG lateral chains was present, the *d* spacing of montmorillonite shifted from 1.23 to 1.72 nm, which implies that intercalation of the polymer between the alumosilicate sheets has occurred. This chemisorption is caused by the high affinity of PEG side chains for the alumosilicate layers present in the montmorillonite structure. In contrast to this, for the monoalkyl maleate-modified PCEs, the *d* spacing of montmorillonite remained

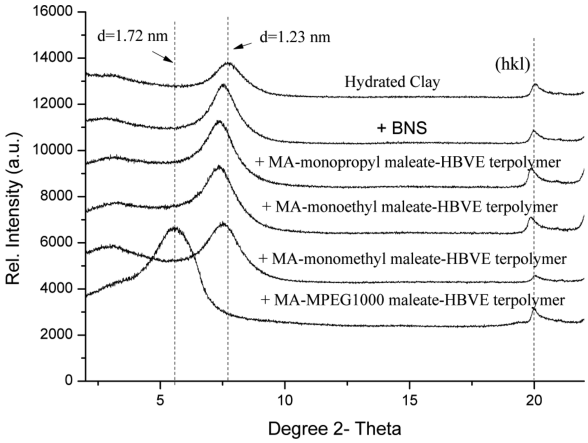

Figure 9. XRD patterns of montmorillonite hydrated in a synthetic cement pore solution holding different superplasticizers (w:c = 45).

constant. The same result was obtained for BNS. There, also no change in the interlayer distance was detected.

The data allow to conclude that because of the unique structure of the modified VPEG-PCEs, their interaction with montmorillonite is limited to surface adsorption, whereas for conventional VPEG-PCE containing PEG pendants, chemical sorption (intercalation) takes place as well and presents the predominant mode of interaction. Through this second mechanism, the dispersing power of conventional PCEs is strongly impeded by montmorillonite.

4. CONCLUSION

A new type of vinyl ether-based PCE has been successfully synthesized from maleic anhydride, monoalkyl maleate esters, and 4-hydroxy butyl vinyl ether utilizing free radical copolymerization. The newly prepared terpolymers containing alkyl ester pendant chains possess high cement dispersing ability and enhanced clay tolerance. Their cement dispersing power might be improved further by increasing the monomer conversion rate to near 100% and by introducing longer yet still sufficiently hydrophilic ester groups. XRD experiments suggest that the newly synthesized terpolymers undergo only weak interaction with clay, opposite to conventional PCE products. Consequently, they allow the formulation of concrete even with aggregates that are contaminated with significant amounts of clay and silt.

Our study demonstrates that modification of the side chains presents the key to achieving clay-tolerant PCE superplasticizers. Conventional PCE molecules holding PEO pendant chains will always be affected by clay unless sacrificial agents with an even stronger tendency to intercalate are used to block the interlayer space for the PCEs.

AUTHOR INFORMATION

Corresponding Author

*Institute for Inorganic Chemistry, Technische Universität München, Garching, Germany. Phone: +49 89 289 13151. Fax: +49 89 289 13152. E-mail: sekretariat@bauchemie.ch.tum.de.

Notes

The authors declare no competing financial interest.

■ ACKNOWLEDGMENTS

L.L. thanks the Jürgen Manchot Foundation for generously providing a scholarship to finance this research at TU München.

■ REFERENCES

(1) Sakai, E.; Ishida, A.; Ohta, A. New Trend in the Development of Chemical Admixtures in Japan. *J. Adv. Concr. Technol.* **2006**, *4*, 211−223.

(2) Guicquero, J. P.; Maitrasse, Ph.; Mosquet, M. A.; Sers, A. (Lafarge Co.). A Water Soluble or Water Dispersible Dispersing Agent. FR Patent 2776285, September 24, 1999.

(3) Plank, J.; Pöllmann, K.; Zouaoui, N.; Andres, P. R.; Schaefer, C. Synthesis and performance of methacrylic ester based polycarboxylate superplasticizers possessing hydroxy terminated poly(ethylene glycol) side chains. *Cem. Concr. Res.* **2008**, *38*, 1210−1216.

(4) Pourchet, S.; Liautaud, S.; Rinaldi, D.; Pochard, I. Effect of the Repartition of the PEG Side Chains on the Adsorption and Dispersion Behaviors of PCP in Presence of Sulfate. *Cem. Concr. Res.* **2012**, *42*, 431−439.

(5) Akimoto, S.; Honda, S.; Yasukohchi, T. (Nippon Oil And Fats Co.). Additives for cement. EP Patent 0291073, March 18, 1992.

(6) Hamada, D.; Yamato, F.; Mizunuma, T.; Ichikawa, H. (Kao Corp.). Additive mixture for cement-based concrete or mortar contains a copolymer of polyalkoxylated unsaturated acid and a mixture of alkoxylated carboxylic acid with a corresponding ester and/or an alkoxylated alcohol. DE Patent 10048139, April 12, 2001.

(7) Yamamoto, M.; Uno, T.; Onda, Y.; Tanaka, H.; Yamashita, A.; Hirata, T.; Hirano, N. (Nippon Shokubai Co.). Copolymer for cement admixtures and its production process and use. U.S. Patent 6,727,315, April 27, 2004.

(8) Amaya, T.; Ikeda, A.; Imamura, J.; Kobayashi, A.; Saito, K.; Danzinger, W.; Tomoyose, T. (Sika Ltd.). Cement Dispersant and Concrete Composition containing the Dispersant. WO Patent 2000039045, July 6, 2000.

(9) Nuyken, O.; Braun, H.; Crivello, J. Poly(vinyl ether)s, Poly(vinyl ester)s, and Poly(vinyl halogenide)s. In *Handbook of Polymer Synthesis*, 2nd ed.; Kricheldorf, H. R., Nuyken, O., Swift, G., Eds.; Marcel Dekker: New York, 2005; pp 151−239.

(10) Teresa, M.; Laguna, R.; Medrano, R.; Plana, M. P.; Tarazona, M. P. Polymer characterization by size-exclusion chromatography with multiple detection. *J. Chromatogr., A* **2001**, *919*, 13−19.

(11) Lei, L.; Plank, J. A Concept For a Polycarboxylate Superplasticizer Possessing Enhanced Clay Tolerance. *Cem. Concr. Res.* **2012**, *42*, 118−123.

(12) Alfrey, T.; Price, C. C. Relative reactivities in vinyl copolymerization. *J. Polym. Sci.* **1947**, *2*, 101−106.

(13) Greenley, R. Z. Q and e Values for Free Radical Copolymerizations of Vinyl Monomers and Telogens. In *Polymer Handbook*, 4th ed.; Brandrup, J., Immergut, E. H., Grulke, E. A., Eds.; Wiley: New York, 2005; pp 309−319.

(14) Suter, J. L.; Coveney, P. V. Computer simulation study of the materials properties of intercalated and exfoliated poly(ethylene)glycol clay nanocomposites. *Soft Matter* **2009**, *5*, 2239−2251.

(15) Svensson, P. D.; Hansen, S. Intercalation of smectite with liquid ethylene glycol resolved in time and space by synchrotron X-ray diffraction. *Appl. Clay Sci.* **2010**, *48*, 358−367.

(16) Lagaly, G. Colloid clay science. In *Handbook of Clay Science*; Bergaya, F., Theng, B. K. G., Lagaly, G., Eds.; Elsevier: Amsterdam, 2006; Vol. *1*, pp 141−245.

5.3 A study on the impact of different clay minerals on the dispersing force of conventional and modified vinyl ether based polycarboxylate superplasticizers

L. Lei, J. Plank

Cement and Concrete Research

60 (2014) 1 – 10.

In previous **section 5.2**, a modified vinyl ether based PCE structure with enhanced clay robustness was introduced. In the next study, the aim was to fully comprehend the interaction mechanism between PCE polymers and different clay minerals, namely montmorillonite, kaolin and muscovite.

First of all, the differences in the physicochemical properties of the clay samples were studied. Experimentally, the methylene blue test was carried out to determine the cation exchange capacity of the clay samples, a thermogravimetric analysis was conducted to probe the water uptake capacity and the Ca^{2+} sorption capacity was determined via zeta potential measurement. The results showed that montmorillonite possessed the most abundant amount of exchangeable interlayer cations and also the highest water uptake capacity.

Furthermore, the dispersing performance of conventional and modified vinyl ether based PCEs was compared in the systems containing different clays. When montmorillonite was present, then the conventional VPEG-PCE sample completely lost its dispersing ability whereas the VPEG-PCEs modified with short alkyl maleate chains were much less affected by montmorillonite. When kaolin or muscovite were added, then the advantage of using the modified VPEG-PCEs was not so obvious. The reason for the much reduced dispersing power of conventional VPEG-PCEs in the presence of montmorillonite was found to be the intercalation of the PCE side chains into the montmorillonite interlayer gallery, as was evidenced by adsorption and XRD measurements. Opposite to this, with kaolin or muscovite, due to their different lattice, no such chemical sorption occurred for conventional as well as modified vinyl ether based PCE polymers.

Based on these results it can be concluded that inactive (non - swelling) clay impurities do not cause a serious problem in cementitious systems. The reason for much reduced or even completely lost PCE performance is presented by active (swelling) clays.

The paper also provides mitigation strategies for concrete producers, such as using sacrificial agents or cationic compounds to inhibit active clays and prevent them from depleting PCE polymers from the pore solution, or to switch to PEG-free PCE polymers exhibiting superior clay robustness.

Cement and Concrete Research 60 (2014) 1–10

Contents lists available at ScienceDirect

Cement and Concrete Research

journal homepage: http://ees.elsevier.com/CEMCON/default.asp

A study on the impact of different clay minerals on the dispersing force of conventional and modified vinyl ether based polycarboxylate superplasticizers

L. Lei, J. Plank *

Technische Universität München, Chair for Construction Chemicals, 85747 Garching, Lichtenbergstraße 4, Germany

ARTICLE INFO

Article history:
Received 10 December 2013
Received in revised form 17 February 2014
Accepted 28 February 2014
Available online xxxx

Keywords:
Dispersion (A)
Workability (A)
Admixture (D)
Concrete (E)
Clay minerals

ABSTRACT

The impact of three different clay minerals (montmorillonite, kaolinite and muscovite) on the dispersing force of vinyl-ether based PCE superplasticizers was studied. At first, a conventional vinyl-ether PCE was synthesized from maleic anhydride (MA), mono methoxy poly(ethylene glycol) ester of MA and 4-hydroxy butyl vinyl ether (HBVE). Additionally, a PEG-free PCE was prepared by substituting MPEG with hydroxyalkyl groups in the ester. Next, the effect of three different clay minerals on the fluidity of cement paste admixed with both PCEs was investigated. It was found that the conventional PCE is negatively affected by the clays in the order: montmorillonite ≫ kaolinite > muscovite. Whereas, the PEG-free PCEs were only slightly affected. The study suggests that conventional PCEs containing PEG reasonably tolerate all types of clay minerals except montmorillonite. When montmorillonite is present as a contaminant, then use of a PEG-free PCE such as described here presents a viable mitigation strategy.

1. Introduction

The invention of polycarboxylate superplasticizers (PCEs) as a new generation of concrete admixtures in the 1980s represents one of the most significant breakthroughs in the history of concrete admixtures. However, recently more and more field users report that under certain conditions PCEs can exhibit a strong sensitivity to clay impurities. Most confusing, in some cases the negative impact of clay minerals on the dispersing force of PCE was very pronounced whereas in other cases, the effect was only minor. Apparently, different types of clay minerals show a completely different impact on the performance of PCEs in relation to variations in their physical and chemical properties.

Clay minerals are hydrous aluminosilicates characterized by crystal sizes of less than 2 μm in diameter. They are phyllosilicates constituted by a layer structure made of sheets of Si-centered tetrahedra alternating with sheets of Al-centered octahedra. Alternatively, they may be constituted by sheets of Si-centered tetrahedra alternating with sheets of Mg-centered octahedra. The presence of trivalent cations (e.g. Al^{3+}) or divalent cations (e.g. Mg^{2+}) in the octahedral sheet brings about a different cation occupancy in the sheet. With divalent cations all sites are occupied, while with trivalent cations only two thirds are occupied.

Clay minerals support extensive isomorphous substitutions in both the tetrahedral and octahedral sheets. The most common ones are Al^{3+} for Si^{4+} in the tetrahedral sheet and Fe^{3+}, Fe^{2+} or Mg^{2+} for Al^{3+} in the octahedral sheet. Where isomorphous substitutions imply cations of different valence, a net charge is acquired by the layer which must be balanced by inter-layer species.

Clays can be categorized depending on the way that tetrahedral and octahedral sheets are combined into layers. The tetrahedral sheets are always bonded to the octahedral sheets through the unshared oxygen vertex substituting a hydroxyl in the octahedral layer. On one side of the octahedral sheet two hydroxyls out of three are replaced by a $(Si_2O_5)^{2-}$ unit. If there is only one tetrahedral and one octahedral sheet in each layer, then the clay is known as a 1:1 clay or a t–o clay. The alternative, known as a 2:1 clay or t–o–t clay, has two tetrahedral sheets, one on each side of the octahedral sheet. The layers are held together by hydrogen bonds (e.g. kaolinite, a 1:1 dioctahedral clay), or by electrostatic forces between the charged layers and the interlayer cations (e.g. illite, a 2:1 dioctahedral clay) [1–3]. Where the layer charge is low in 2:1 clays like in smectites (0.2–0.5 interlayer charge per 11 oxygens, compared to 0.5–0.75 in illites) [4], the interlayer is large and can host variable amounts of water molecules and different kinds of ions. It can easily shrink and swell as the result to changes in relative humidity.

The clay minerals used in the present work have been: kaolinite, a non-swelling 1:1 dioctahedral clay; muscovite, a non-swelling 2:1 dioctahedral clay belonging to the group of illites; and Na montmorillonite, a swelling 2:1 dioctahedral clay belonging to the group of smectites.

The principle structures of the major clay minerals occurring as contaminant in concrete are displayed in Fig. 1.

* Corresponding author. Tel.: +49 89 289 13151; fax: +49 89 289 13152.
E-mail address: sekretariat@bauchemie.ch.tum.de (J. Plank).

http://dx.doi.org/10.1016/j.cemconres.2014.02.009
0008-8846/

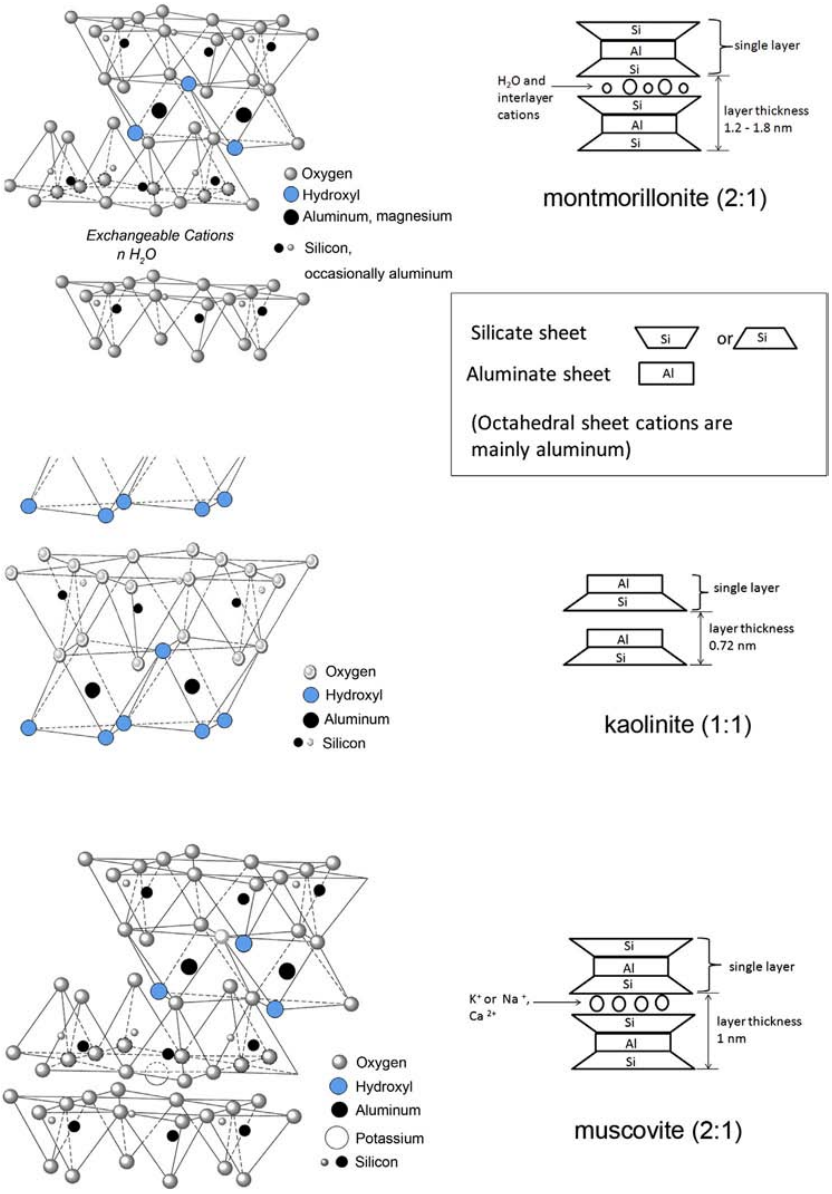

Fig. 1. Principle structure of the major clay minerals occurring as contaminant in concrete, after Grim [5].

The aim of this study was to compare the effect of three most frequently occurring clay minerals (montmorillonite, kaolin, muscovite) on cement pastes admixed with polycarboxylate (PCE) superplasticizers. From this, it was sought to understand the different impacts of differently structured (2:1 and1:1) swelling and non-swelling clay minerals on PCEs. Furthermore, two types of vinyl ether-based PCEs were synthesized, one with a conventional polyethylene glycol (PEG) side chain, and one with hydroxyalkyl pendant groups. For both polymers, their specific modes of interaction with these different clay minerals were assessed via XRD, adsorption and zeta potential measurements. From this mechanistic study it was hoped to obtain an explanation for the different behaviors of clays with PCEs, as reported by field users.

2. Experimental

2.1. Materials

2.1.1. Chemicals

4-Hydroxy butyl vinyl ether (>99% purity, purchased from Sigma-Aldrich CHEMIE, Steinheim, Germany), maleic anhydride (>99%, Merck Schuchardt OHG, Hohenbrunn, Germany), methanol, ethanol, n-propyl alcohol (all >98% purity, VWR International, Darmstadt, Germany), sodium hydroxymethane sulfinate (Rongalit C, >98% purity, Sigma-Aldrich), ferrous sulfate (>98% purity, VWR), 2-mercapto ethanol (>99% purity, Sigma-Aldrich), hydrogen peroxide (30% aqueous solution, VWR) were used without further purification.

2.1.2. Cement

The cement used in this study was an ordinary Portland cement CEM I 52.5 N ("Milke® classic" from HeidelbergCement, Geseke Plant, Germany). Its phase composition as determined via quantitative powder X-ray diffraction (Q-XRD) including *Rietveld* analysis is presented in Table 1. The average particle size (d_{50} value) determined via laser granulometry was found at 11.5 μm. Its density was 3.153 g/cm^3 (helium pycnometry) and its *Blaine* value was 3537 cm^2/g.

2.1.3. Clay minerals

As Na^+ montmorillonite, a commercially available product designated "RXM 6020" supplied by Rockwood, Moosburg, Germany was used. This mineral is a naturally occurring Na bentonite and was used as obtained. Its average particle size (d_{50} value) was found at 0.9 μm and its *BET* value was 38.33 m^2/g. The montmorillonite sample possessed a moisture content of ~6 wt.% (determined on IR balance).

A commercially available kaolin named "Chinafill 800" supplied by Quarzwerke GmbH, Frechen, Germany was used. The average particle size (d_{50} value) was found at 0.7 μm and its *BET* value was 9.78 m^2/g. The kaolin sample exhibited a moisture content of ~0.6 wt.% (determined on IR balance).

A muscovite sample designated "MICA S", supplied by Quarzwerke GmbH, Frechen, Germany was used. The average particle size (d_{50} value) was found at 2.8 μm and its *BET* value was 2.60 m^2/g. The muscovite sample possessed a moisture content of ~0.4 wt.% (determined on IR balance).

The oxide compositions of the clay samples as determined by X-ray fluorescence (XRF) are shown in Table 2.

Table 2
Oxide compositions of the clay minerals, as determined by XRF.

Type of clay	Oxide contents (wt.%)								
	SiO_2	Al_2O_3	CaO	MgO	Fe_2O_3	Na_2O	K_2O	SO_3	LOI
Kaolin	49.71	37.74	0.07	–	0.55	0.14	2.34	0.07	11.40
Montmorillonite	59.20	20.62	0.68	1.94	3.52	2.25	0.08	0.45	11.00
Muscovite	47.37	30.12	0.13	2.79	3.72	0.31	10.24	0.14	4.35

2.1.4. Superplasticizers

2.1.4.1. Synthesis of monoalkyl maleate ester monomers. For the preparation of the modified vinyl ether PCEs, monoalkyl maleate ester monomers are required. Their synthesis was performed as follows.

4.09 g (42 mmol) of maleic anhydride and 32 mmol of either ethanol (1.48 g) or n-propanol (1.9 g) were placed in a 250 mL four-neck round bottom flask equipped with a stirrer and reflux condenser and heated for 2 h at 55 °C under constant stirring. Thereafter, 5 g of DI water was added to the flask and the resulting ~45 wt.% solution of the monoalkyl ester of maleic acid was cooled to 20 °C.

2.1.4.2. Synthesis of MA – mono alkyl maleate – HBVE terpolymers. As an example, the synthesis of MA – mono ethyl maleate – HBVE terpolymer is described. A 250 mL four-neck round bottom flask holding the aqueous solution of the mono ethyl maleate as prepared above equipped with a stirrer, reflux condenser and two separate inlets is provided with an inert atmosphere by bubbling N_2 via a bottom valve. The inert atmosphere was maintained over the entire reaction time. ~7 mL of a 30% KOH solution was added to adjust the pH of the monoethyl maleate solution to ~4.5. Thereafter, 12.37 g (106 mmol) of 4-hydroxy butyl vinyl ether was added under stirring. Subsequently, 30 mg of $FeSO_4 \cdot 7H_2O$, 40 mg of 2-mercapto ethanol (the first portion of chain transfer agent) as well as 4.9 g of 30 wt.% H_2O_2 solution were added to the reactor. Next, 0.63 g of Rongalit C (initiator) was dissolved in 10 mL of DI water. This solution was designated as Solution I. Separately, 4.16 g (42 mmol) of maleic anhydride and 80 mg of 2-mercapto ethanol (second portion of chain transfer agent) were dissolved in 12.5 mL of DI water. This solution was named as Solution II. Using two peristaltic pumps, Solutions I and II were fed separately and continuously into the vessel over the periods of 75 min (Sol. I) and 60 min (Sol. II) while maintaining the temperature at 25 °C through an ice-bath. When the additions were completed, the mixture was stirred for another 30 min. The final product designated as MA – monoethyl maleate – HBVE terpolymer was a slightly reddish, 27 wt.% aqueous solution possessing moderate viscosity and of a pH of ~4.

The MA – monopropyl maleate – HBVE terpolymer was synthesized is the same manner except that here, 11 g (32 mmol) of the aqueous solution of mono propyl maleate was used. The resulting terpolymer was a liquid with a solid content of 30 wt.% and a pH of ~4.1.

2.1.4.3. Synthesis of MA – MPEG-1000 maleate – HBVE terpolymer. A conventional vinyl ether-based PCE holding PEG side chains was synthesized via aqueous free radical copolymerization from 4.16 g (42 mmol) of maleic anhydride, 12.37 g (106 mmol) of 4-hydroxy butyl vinyl ether and 36.2 g (32 mmol) of methoxy polyethylene glycol mono maleate following the description from above for the mono alkyl maleate containing terpolymers. 2-mercapto ethanol was used as chain transfer agent. The number of ethylene oxide units in the methoxy polyethylene glycol was 23 (MPEG-1000). The resulting terpolymer solution exhibited a solid content of 40 wt.%, a pH of ~4.2 and was a slightly reddish, highly viscous solution.

2.1.4.4. BNS polycondensate. An industrial superplasticizer sample based on β-naphthalene sulfonate formaldehyde polycondensate (BNS) designated Melcret® 500F (BASF Construction Polymers GmbH, Trostberg, Germany) was used for comparison. Melcret® 500F is a spray dried BNS powder which possesses a low Na_2SO_4 content (<2 wt.%).

Table 1
Phase composition of the CEM I 52.5 N sample as determined by Q-XRD using *Rietveld* refinement.

Phase	wt.%
C_3S, m	54.14
C_2S, m	26.63
C_3A, c	3.28
C_3A, o	4.26
C_4AF, o	2.45
Free lime (Franke)	0.10
Periclase (MgO)	0.03
Anhydrite	2.64
$CaSO_4$ hemihydrate	1.21
$CaSO_4$ dihydrate	0.02
Calcite	3.61
Quartz	1.16
Arcanite (K_2SO_4)	0.46

2.2. Characterization of clays

2.2.1. Methylene blue test

The cation exchange capacity (CEC) of clay minerals is commonly measured via adsorption of methylene blue dye by the clay mineral. Methylene blue tests performed in this context are based on the French standard Norme Française NF P 94-068 (AFNOR1993) [6]. First, a methylene blue solution is prepared by dissolving 10 ± 0.1 g of methylene blue in 1 L of distilled water in a beaker at room temperature. Separately, a suspension of clay mineral is prepared by dispersing 7.5 g of the clay sample in 50 mL distilled water. Under stirring with a magnetic stirrer, the MB solution is added to this clay suspension in 5 mL increments. After each addition, the suspension is stirred for 1 min before a small drop is taken and placed onto a filter paper. When placing the first drop onto the filter paper, a dark blue spot surrounded by a colorless

moist halo is observed and this is the mark of a negative result of the test. This procedure is continued by adding further 5 mL portions of the methylene blue solution to the clay suspension until a halo of light blue dye surrounds the dark blue spot on the filter paper [7].

The methylene blue value (MBV) represents the amount of MB sorbed by 100 g of clay sample, and is mostly given as g MB/100 g of clay. The MBV is calculated according to Eq. (1).

$$\text{MBV (g/100g)} = \frac{V_{cc}\,(\text{mL}) \times 0.01\,(\text{g/mL})}{f'\,(\text{g})} \times 100 \quad (1)$$

where V_{cc} represents the volume of methylene blue solution (mL) consumed by the clay suspension and f′ is the dry weight of the clay sample (g).

2.2.2. Thermogravimetric analysis (TGA)

The water uptake capacity of the clay minerals was obtained via measuring their weight loss as a function of temperature. A NETZSCH STA 409 instrument was used to carry out the thermogravimetric analysis at a heating rate of 10 °C/min from 300 to 1073 K in an air flow of 30 cm^3/min using alpha-Al_2O_3 as the standard.

2.2.3. Zeta potential measurement

Zeta potential was determined using a model "DT 1200 Electro acoustic Spectrometer" (Dispersion Technology, Inc., Bedford Hills, NY, USA). This instrument measures a vibration current induced by an acoustic wave which causes the aqueous phase to move relative to the cement particles. From that, a potential difference results which can be measured and is designated as zeta potential.

For titration studies, clay samples were dispersed in DI water which was adjusted to pH 12.5 using 20 wt.% aqueous NaOH. A 40 g/L Ca^{2+} solution prepared from 11.1 g $CaCl_2$ dissolved in 100 mL of DI water was titrated to the clay suspensions. Zeta potentials of the clay particles were recorded as a function of Ca^{2+} dosage in alkaline solution.

2.2.4. ESEM

Environmental scanning electron microscopic (ESEM) images of clay particles were captured on a FEI XL 30 FEG microscope (FEI, Eindhoven, Netherlands) equipped with a *Peltier* cooling stage and a gaseous secondary electron detector.

2.3. Characterization of polymers

2.3.1. Size exclusion chromatography (SEC)

Molar masses (M_w, M_n), polydispersity index (PDI) and hydrodynamic radius (R_h) of the polymer samples were determined utilizing size exclusion chromatography (SEC). There, solutions containing 10 g/L of the polymer were applied on a Waters 2695 Separation Module equipped with three Ultrahydrogel™ columns (120, 250, 500), an Ultrahydrogel™ guard column (Waters, Eschborn, Germany) and a 3 angle static light scattering detector ("mini Dawn" from Wyatt Technology Corp., Santa Barbara, CA, USA). Polymer concentrations were monitored with a differential refractive index detector (RI 2414, Waters). 0.1 N aqueous $NaNO_3$ adjusted to pH 12 with NaOH was used as an eluent at a flow rate of 1.0 mL/min. From the SEC measurements, the molar masses (M_w, M_n), the polydispersity index (PDI) as well as the hydrodynamic radius (R_h) were obtained. The value of dn/dc used to calculate M_w and M_n was 0.135 mL/g (value for polyethylene oxide) [8].

2.3.2. Specific anionic charge amount

The values were determined employing a particle charge detector PCD 03 pH (Mütek Analytic, Herrsching, Germany). Here, 0.2 g/L of the polymers was dissolved in DI water or synthetic cement pore solution prepared from 1.72 g/L $CaSO_4 \cdot 2H_2O$, 6.959 g/L Na_2SO_4, 4.757 g/L K_2SO_4 and 7.12 g/L KOH in 1 L of DI water (pH value is 13.06) and titrated against a 0.34 g/L aqueous solution of poly-diallyl dimethyl ammonium chloride (polyDADMAC) until charge neutralization (zero potential) was reached. From the amount of polyDADMAC consumed to reach a zero potential, the amount of negative charge per gram of polymer was calculated.

Table 3
Methylene blue value (MBV) for the clay minerals used in this study.

Clay mineral	Montmorillonite	Kaolin	Muscovite
MBV (g/100 g)	8.6	1.9	0.8

2.4. Cement paste tests

For determination of paste flow, a modified "mini slump test" was utilized and carried out as follows: First, the water-to-cement (w/c) ratio of the paste without polymer was set to produce a spread of 18 ± 0.5 cm. At this w/c ratio, the dosages of the PCE samples required to reach a spread of 26 ± 0.5 cm were determined. Generally, the polymer was added to the mixing water placed in a porcelain cup. The amount of water contained in the polymer solutions was subtracted from the amount of mixing water. Next, 300 g of cement was added to the mixing water and agitated manually for 1 min utilizing a spoon, then rested for 1 min without stirring and was again stirred for 2 min. After the stirring, the cement paste was immediately poured into a Vicat cone (height 40 mm, top diameter 70 mm, bottom diameter 80 mm) placed on a glass plate and the cone was vertically removed. The resulting spread of the paste was measured twice, the second measurement being in a 90° angle to the first and averaged to give the final spread value.

To determine the effect of clay minerals on cement workability, two different experiments were carried out. In the first series, 1 wt.% of each clay was dry blended into the neat cement, and the spread flow was determined. In the second series, the amounts of kaolin or muscovite producing the same flow value than the cement containing 1% montmorillonite were assessed.

2.5. PCE sorption on clays

The amounts of polymers sorbed on the clays were measured using the depletion method. The portion of polymer remaining in solution at equilibrium condition was determined by analyzing the total organic carbon content (TOC) of the solution. In a typical experiment, 0.25 g of clay sample (montmorillonite/kaolin/muscovite), 11.25 g of synthetic cement pore solution and the amount of superplastizer to be tested was filled into a 50 mL centrifuge tube, shaken in a wobbler (VWR International, Darmstadt, Germany) for 2 min at 2400 rpm and then centrifuged for 10 min at 8500 rpm. The supernatant was carefully retrieved using a syringe and then diluted with DI water. For consistent results it is absolutely critical to avoid any shaking or disturbance while taking up the supernatant, as it will immediately lead to redispersion of the nano-sized clay particles and thus produce false results. The TOC of the solution was determined by combustion at 890 °C on a High TOC II instrument (Elementar Analysensysteme, Hanau, Germany). From the difference between the TOC content of the polymer reference sample and the TOC value of the supernatant, the amount of superplasticizer sorbed on clay was calculated. Measurements were generally repeated three times and the average was reported as sorbed amount.

Table 4
Water uptake capacity of the clay samples.

Clay mineral	Montmorillonite	Kaolin	Muscovite
Water uptake (wt.%)	77.0	49.0	35.6

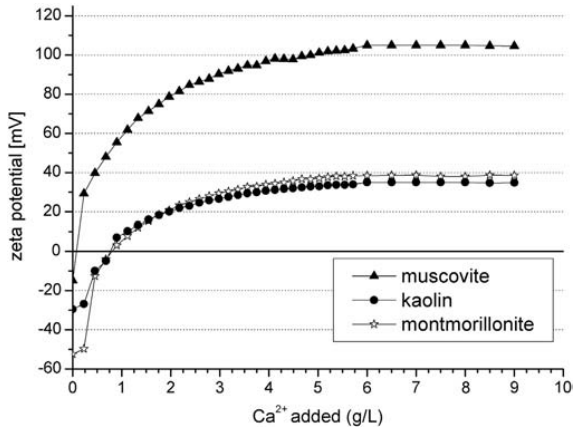

Fig. 2. Zeta potentials of aqueous montmorillonite/kaolin/muscovite suspensions as a function of Ca^{2+} addition measured in alkaline solution (pH = 12.5).

2.6. XRD analysis

To investigate the interaction between different types of clay and the PCE samples, XRD analysis was performed on the clay minerals which were exposed for 12 min to water containing the superplasticizer samples. In a typical experiment, 0.5 g of clay sample and 22.5 g of a 1.11 wt.% polymer solution (w/clay ratio of 45) were filled into a 50 mL centrifuge tube, shaken in a wobbler for 2 min at 2400 rpm and then centrifuged for 10 min at 8500 rpm. The solid residues obtained were dried overnight at 80 °C and ground. XRD scans of all samples were taken at room temperature on a D8 Advance, Bruker AXS instrument (Bruker, Karlsruhe/Germany) utilizing Bragg–Bretano geometry.

Table 5
Molar masses (M_w, M_n), polydispersity index (PDI) and conversion for the synthesized superplasticizer samples.

Polymer sample	M_w (g/mol)	M_n (g/mol)	PDI (M_w/M_n)	Conversion of monomers
MA-monoethyl maleate-HBVE	9000	3334	2.7	83%
MA-monopropyl maleate-HBVE	10,220	3998	2.7	88%
MA-MPEG-1000 maleate-HBVE	21,390	8010	2.4	90%
BNS	139,100[a]	–	–	–

[a] Batch measurement.

3. Results and discussion

3.1. Characteristic properties of clay samples

3.1.1. Cation exchange capacity (CEC)

The cation exchange capacity of the clay samples was assessed by methylene blue test. This test is based on the interaction of the MB dye cation (MB^+) with either exchangeable interlayer cations present in a clay mineral (e.g. in smectites) and/or surface adsorbed cations. Clay minerals possessing exchangeable interlayer cations, a highly negative charge and a large specific surface area exhibit the highest capacity for cation exchange [7,9]. The results for the clay samples studied here are shown in Table 3.

According to the data above, montmorillonite shows the highest MB value, because it possesses abundant exchangeable interlayer cations (Na^+) and exhibits a high surface area. In comparison, the MBV of kaolin and muscovite are much lower, because of the absence of exchangeable interlayer cations. These clay minerals can interact with MB only via surface adsorption.

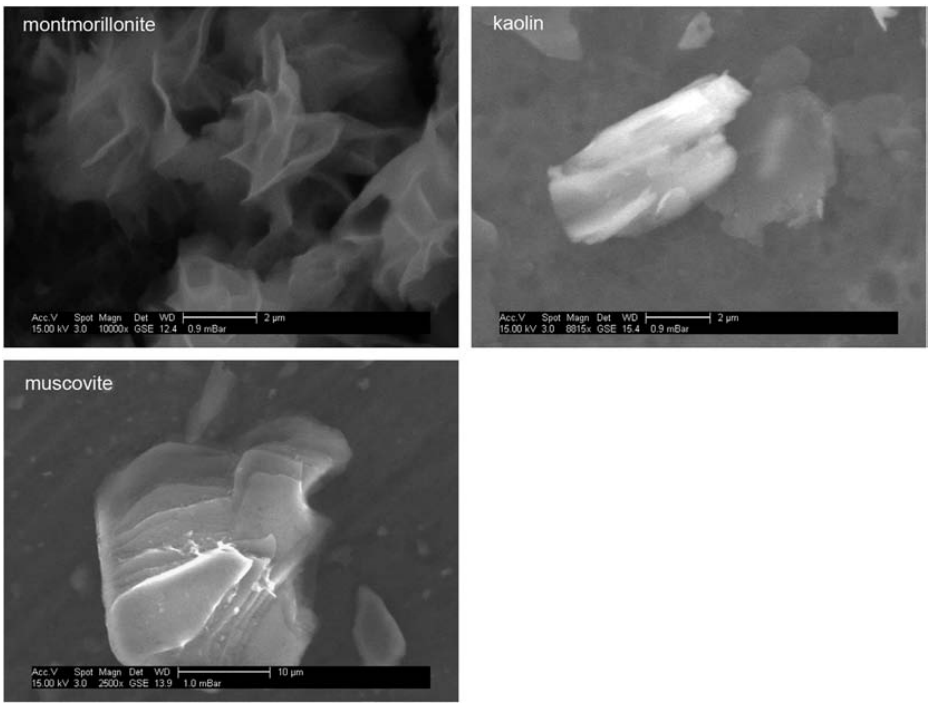

Fig. 3. ESEM micrographs of clay samples dispersed in alkaline solution (pH = 10).

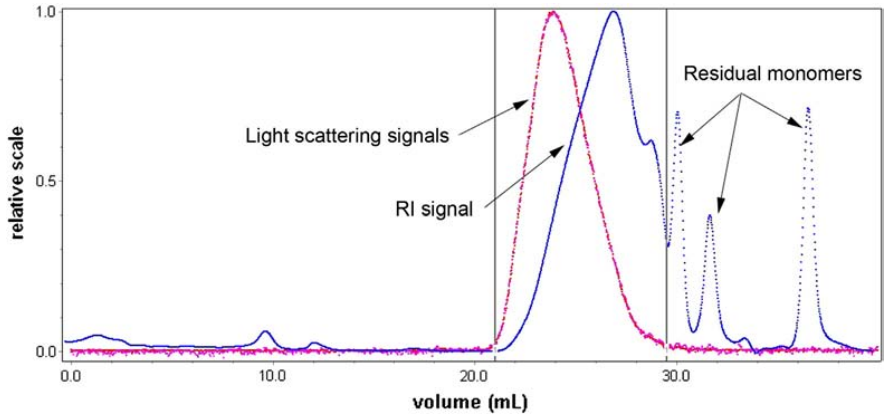

Fig. 4. SEC spectrum of the MA-mono ethyl maleate-HBVE terpolymer.

3.1.2. Water uptake capacity

To determine the actual water uptake capacity, the clay samples were analyzed via thermogravimetry.

According to Table 4, montmorillonite exhibits a particularly high water uptake capacity. It can incorporate 77 wt.% of its weight when it contacts with water. Accordingly, when montmorillonite is present in concrete aggregates as an impurity, a part of the mixing water is consumed leading to reduced workability of the concrete. In comparison, the water uptake capacity of muscovite is much less at 37 wt.%. Surprisingly, the water sorption by kaolin was found relatively high which can be assigned to its high specific surface area (*BET* value 9.78 m^2/g).

3.1.3. Ca^{2+} sorption capacity

When a 40 g/L Ca^{2+} solution was titrated against suspensions of montmorillonite, kaolin or muscovite at pH 12.5, their zeta potentials increased strongly from negative to positive, confirming adsorption of a large amount of Ca^{2+} onto the initially negatively charged surfaces of the clay particles (Fig. 2). Of all clay samples, muscovite showed the lowest initial zeta potential in absolute values of ~ − 14 mV which reversed to positive when more than 0.2 g/L of Ca^{2+} had been added. Upon surface saturation, the zeta potential value stabilized at ~ + 105 mV which is much higher than for the other two clay minerals. As for montmorillonite and kaolin, they exhibited much lower initial zeta potentials in real values. At saturation point, montmorillonite and kaolin showed very similar zeta potentials of ~ + 40 mV, the only difference being the much lower initial zeta potential of montmorillonite at ~ − 52 mV, compared to ~ − 30 mV for kaolin.

Furthermore, the zeta potentials of the clay samples suspended in synthetic cement pore solution (0.4 g/L Ca^{2+}) were probed, There, the suspensions of montmorillonite and kaolin registered a positive zeta potential value of ~ + 15 mV. Again, the muscovite suspension exhibited a much higher positive zeta potential value of ~ + 70 mV. This result signifies that in the presence of cement, charge reversal of the montmorillonite/kaolin/muscovite particles occurs as a result of Ca^{2+} uptake. Additionally, the findings suggest that the positively charged clay particles can decrease cement paste fluidity also via electrostatic interaction with negatively charged parts of the surface of cement, leading to particle agglomeration and flocculation.

3.1.4. ESEM imaging

ESEM is a useful instrument to observe the morphology of clay minerals after contact with water. As for montmorillonite, nano foils (thickness ~ 100 nm) forming a house-of-card structure were obtained (see Fig. 3). Also, the huge surface area of montmorillonite which has been exposed to water becomes evident. On the ESEM images of kaolin and muscovite, stacked clay platelets exhibiting only minor expansion as a result of water sorption are observed. Especially muscovite appears to be practically non-swollen.

3.2. PCE polymers

The molecular properties of the synthesized polymers are presented in Table 5. According to SEC data, the molar masses (M_w) of the modified PCE samples lie at ~10,000 Da while their polydispersity indexes are 1.8–2.7 which indicate a fairly narrow molecular weight distribution. Moreover, yields >80% were found (Table 5). It should be mentioned here that no particular effort was made to further optimize the yields because it was not the focus of this study to synthesize optimized polymers. As an example, the SEC spectrum of MA-monoethyl maleate-HBVE terpolymer is shown in Fig. 4. There, a large peak signifying the terpolymer as well as three minor peaks representing an oligomer and residual monomers can be observed.

For comparison, a conventional vinyl ether-based PCE was synthesized from maleic anhydride, mono polyethylene glycol maleate ($n_{EO} = 23$) and HBVE (molar ratio 1.6:1:3.3). Similar to the terpolymer containing mono alkyl maleate, also here high yields were achieved. M_w of this terpolymer was found at ~20 kDa which is higher than those for the mono alkyl ester based terpolymers, because of the longer side chain.

Next, the specific anionic charge amounts of the synthesized terpolymers were determined in DI water and synthetic cement pore solution, respectively. These values signify the tendency of individual polymers to adsorb onto the positive surfaces of cement and/or clay. The results are shown in Table 6. Generally, the anionic charge of all samples tested was lower in cement pore solution than in DI water. This effect is ascribed to the chelating effect on Ca^{2+} ions present in cement pore solution which shields some of the negative charge of the

Table 6
Specific anionic charge amount of the superplasticizer samples in DI water/cement pore solution.

Fluid system	Specific anionic charge amount [μeq/g]			
	MA-MPEG-1000 maleate-HBVE	MA-monoethyl maleate-HBVE	MA-monopropyl maleate-HBVE	BNS
DI water	531	1200	1160	4089
Synthetic cement pore solution	145	250	348	3911

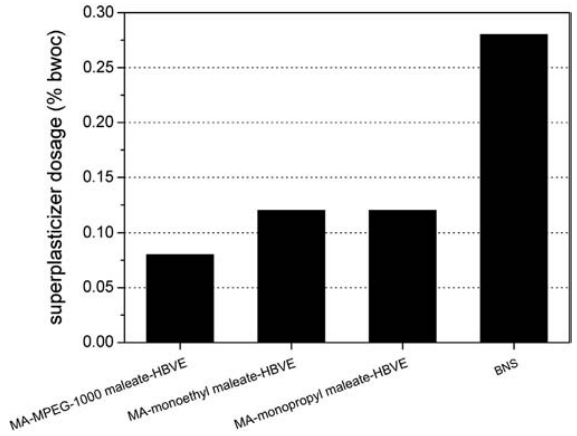

Fig. 5. Dosages of the MA-mono alkyl maleate-HBVE terpolymers and of comparative superplasticizer samples required to achieve a cement paste spread of 26 ± 0.5 cm (w/c = 0.45).

polyelectrolytes. Compared to the conventional vinyl ether PCE possessing PEO side chains, the MA-mono alkyl maleate-HBVE terpolymers exhibit higher anionic charge densities, due to their fairly short side chains. Additionally, the specific anionic charge amount of BNS superplasticizer was found to be significantly higher at ~4000 μeq/g.

3.3. Cement dispersion capacity

To evaluate the dispersing performance of the synthesized MA-mono alkyl maleate-HBVE terpolymers, the dosages required to achieve a cement paste spread of 26 ± 0.5 cm were determined. For this test, a cement paste prepared at a w/c ratio of 0.45 which exhibited a spread of 18 ± 0.5 cm was employed. The results are displayed in Fig. 5. The newly synthesized PCE polymers fluidize cement pastes at surprisingly low dosages (~0.12% by weight of cement), considering their short side chains. Their dosages to achieve a spread of 26 cm are about half of that for BNS which represents the most widely used concrete superplasticizer. Interestingly, we found that the different side chain lengths of the novel terpolymers do not much influence their dispersing performance. The conventional vinyl ether PCE sample possesses a significantly longer side chain made of ~23 ethylene oxide units. Their stronger steric effect allows a dosage of only 0.08% bwoc to achieve the 26 cm spread, thus making it a more powerful dispersant in cement.

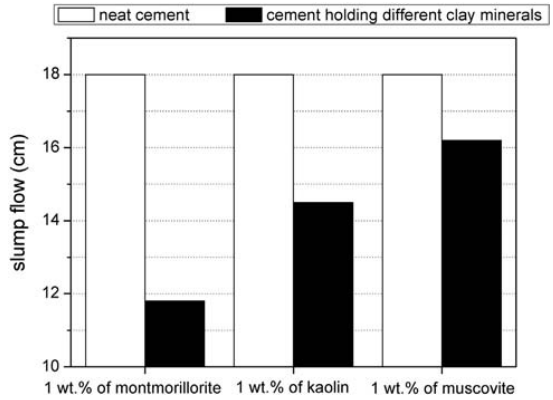

Fig. 6. Spread flow of cement pastes (w/c = 0.45), measured in the absence and presence of 1% by weight of cement (bwoc) of different clay minerals.

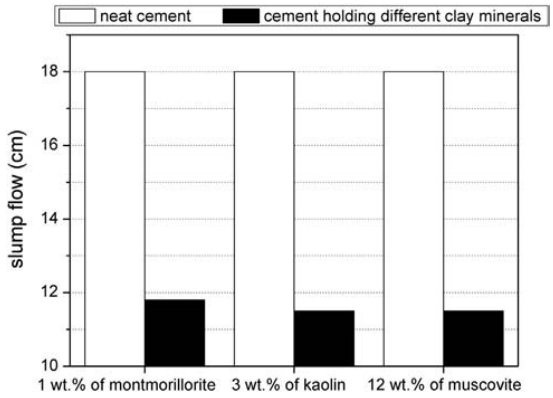

Fig. 7. Spread flow of blank cement pastes (w/c = 0.45), measured in absence and presence of 1% bwoc of montmorillonite, 3% bwoc of kaolin, 12% bwoc of muscovite, respectively.

3.4. Effect of clays on cement fluidity

As shown in Fig. 6, addition of 1 wt.% of montmorillonite strongly affected the flowability of the neat cement paste, the spread flow decreased by 34%. In comparison, the spread flow of the cement pastes containing 1 wt.% of kaolin or muscovite decreased much less by 19% (kaolin) and 10% (muscovite). These data correlate well with the results for the water uptake capacity (Table 4) which showed that montmorillonite possesses the highest water uptake capacity and muscovite the least.

In a separate test, the amounts of kaolin and muscovite respectively required to produce the same reduction in slump flow as caused by the presence of 1 wt.% of montmorillonite was determined. As shown in Fig. 7, this effect was achieved with 3% bwoc of kaolin or 12% bwoc of muscovite. The results signify that with respect to paste fluidity, montmorillonite is about three times as harmful as kaolin, and about 12 times as harmful as muscovite.

3.5. Effect of clays on dispersing effectiveness of PCEs

The PCE dosages applied here were adopted from the previous test using neat cement pastes without clay (see Fig. 5). As shown in Fig. 8, in the cement/montmorillonite system the conventional VPEG-PCE

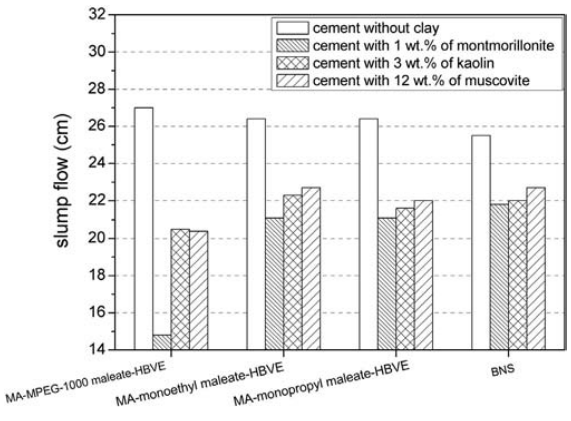

Fig. 8. Spread flow of cement pastes containing different superplasticizers, measured in the absence and presence of 1% bwoc of montmorillonite, 3% bwoc of kaolin, and 12% bwoc of muscovite, respectively.

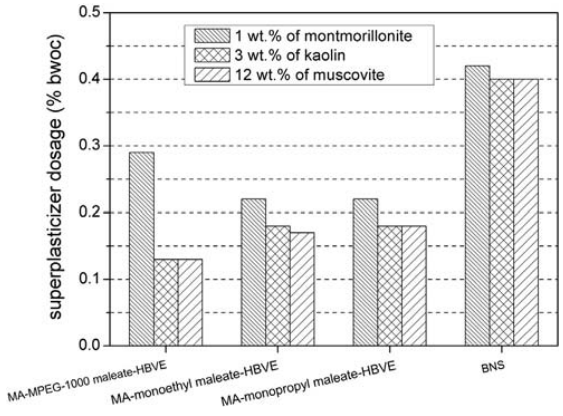

Fig. 9. Dosages of superplasticizers required to achieve a spread of 26 ± 0.5 cm, measured in cement pastes holding 1% bwoc of montmorillonite, 3% bwoc of kaolin and 12% bwoc of muscovite, respectively.

exhibited a strong decrease in performance caused by the presence of 1 wt.% of montmorillonite. The spread flow decreased by 135%, i.e. it became even less than 18 cm registered as for the neat cement paste. Whereas, the newly synthesized vinyl ether based PCEs (MA-monoethyl maleate-HBVE, MA-monopropyl maleate-HBVE) were much less affected by montmorillonite. Their spread flow reductions were ~63% which was comparable to that from BNS.

In the cement/kaolin system, the flow reductions were generally much less. In the presence of 3 wt.% of kaolin, the spread flow from the conventional vinyl ether PCE decreased by ~72%, whereas the newly synthesized vinyl ether based PCEs (MA-monoethyl maleate-HBVE, MA-monopropyl maleate-HBVE) and BNS showed a decrease of ~50%. In the cement/muscovite system, a similar trend was found.

However, for field application the decrease in performance is not the most important concern. Instead, the dosage required to achieve a specific flow value (here 26 cm) of the cement paste is the key criterion. Consequently, these dosages were determined for the pastes containing 1 wt.% of montmorillonite, 3 wt.% of kaolin or 12 wt.% of muscovite. The results are displayed in Fig. 9. For the cement/montmorillonite system it is evident that the mono alkyl maleic ester modified PCEs are most effective while the conventional VPEG-PCE and BNS require substantially higher dosages. It is remarkable that this result was achieved by the modified PCEs in spite of their weaker performance in the clay-free system, compared to the conventional PCE (see Fig. 5). It signifies that their interaction with montmorillonite is much weaker than that of PCEs containing PEG side chains. On the contrary, in the cement/kaolin and cement/muscovite systems, the conventional vinyl ether PCE still required a lower dosage (~0.13% vs ~0.17% for the modified PCEs). These data imply that the newly synthesized vinyl ether PCEs show superior performance only in the presence of montmorillonite.

3.6. Sorption of PCEs on clay samples

To quantify the interaction between the individual PCE samples and the different clay minerals, sorption isotherms were measured. Fig. 10(a) displays the huge difference in sorbed amounts between montmorillonite and the two other clay minerals (kaolin/muscovite) for the conventional PCE possessing PEO side chains. It sorbs in very high amount on montmorillonite, with a sorbed amount of ~230 mg/g

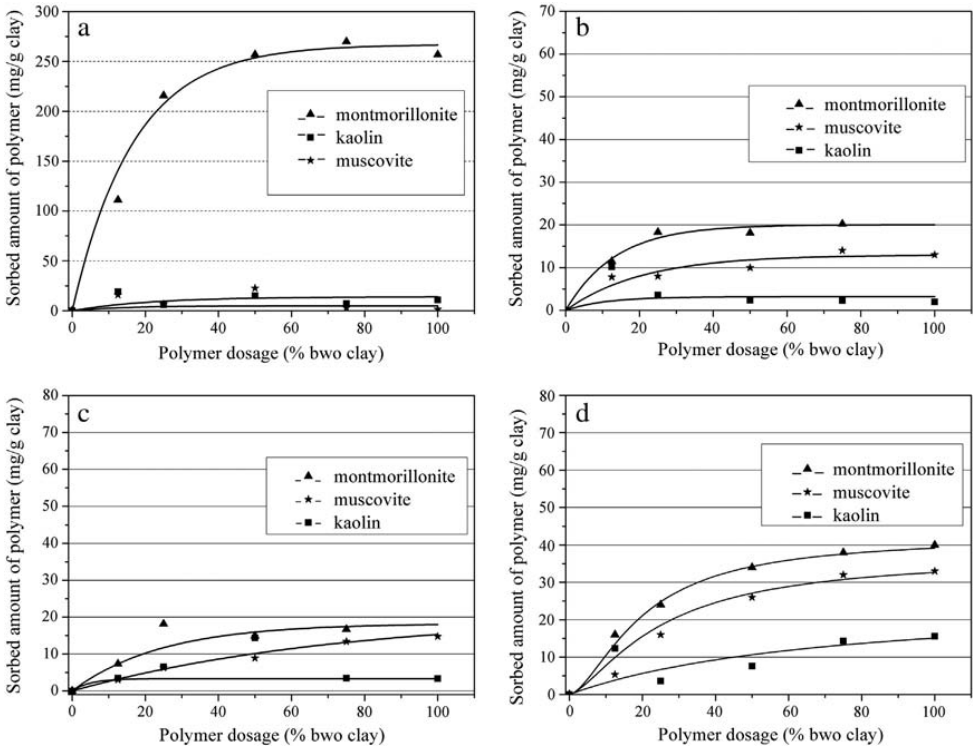

Fig. 10. Adsorption isotherms for (a) MA-MPEG-1000 maleate-HBVE, (b) MA-monoethyl maleate-HBVE, (c) MA-monopropyl maleate-HBVE and (d) BNS samples on different clay minerals dispersed in synthetic cement pore solution (w/clay = 45).

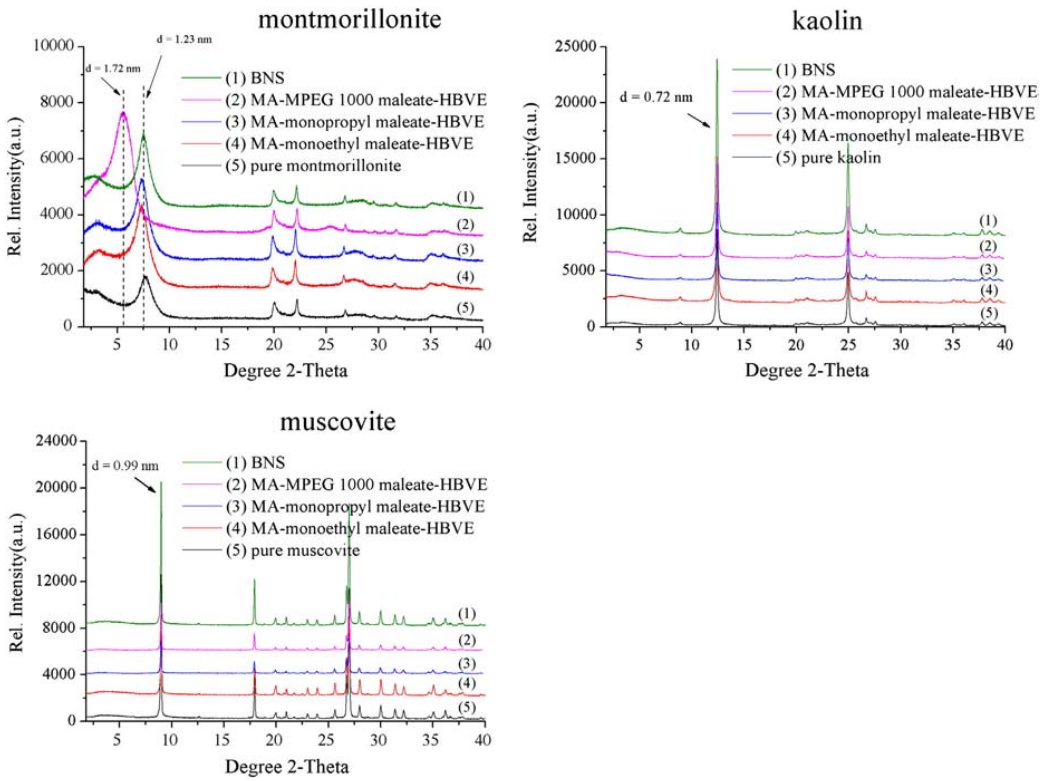

Fig. 11. XRD patterns of montmorillonite/kaolin/muscovite stirred overnight in synthetic cement pore solution, with different superplasticizers (w/clay = 45).

of clay at saturation point. To the contrary, on kaolin or muscovite it sorbs in extremely low amounts (~20 mg/g of clay). This demonstrates again the particularly negative effect of montmorillonite on the performance of conventional PCEs because this clay mineral essentially screens off the PCE from the pore solution, and very few – if any – PCE is left to disperse cement. Fig. 10(b) and (c) shows how the modified MA-monoalkyl maleate-HBVE terpolymers sorb on the different clay minerals. On montmorillonite, sorbed amounts of ~20 mg/g of clay were found at saturation point. Furthermore, on muscovite, the sorbed amounts were ~15 mg/g of clay only, while on kaolin, the sorbed amounts were even less at ~5 mg/g of clay. These data imply weak interaction between the MA-monoalkyl maleate-HBVE terpolymers and all clay samples tested. For BNS (see Fig. 10(d)), a similar behavior was found. The observed trends suggest that for the modified PCEs and BNS, interaction with the clay minerals mainly depends on the specific surface area of the clay mineral after contact with water, while for conventional PCEs, an additional mechanism of interaction comes into play.

3.7. Mechanistic study

To investigate the mechanism of the interaction between the individual PCEs and the different clay minerals, an XRD analysis was performed.

After exposure to water, montmorillonite exhibits a d-spacing (distance between the aluminosilicate layers) of 1.23 nm (Fig. 11). This interlayer space is occupied by Na^+ ions and abundant H_2O molecules. The latter coordinate to the oxygen atoms in the negatively charged silicate layers via hydrogen bonding [10]. For the conventional vinyl ether PCE containing PEG pendants, a shift in the d-spacing from 1.23 nm to 1.72 nm was detected. Such d value is characteristic for montmorillonite which contains intercalated polyglycols [11,12]. As has been reported in previous literature, the PEO side chains present in conventional PCEs exhibit a similar affinity to the aluminosilicate layers than polyglycols [13,14]. Thus intercalation was found to be the main reason for the huge consumption of the conventional PCE by this type of clay, and in consequence for the strongly decreased fluidity. However, when the mono alkyl maleate modified PCEs were added, no change in the d-value was observed. Similarly, when BNS was present, also no shift in the d-spacing was found. These results signify that the modified type of PCE and BNS do not enter into the interlayer space. Hence, interaction of this new type of PCE with montmorillonite is limited to mere surface adsorption while no chemisorption occurs, as it is prevalent for conventional PCEs. Accordingly, the MA-mono alkyl maleate-HBVE terpolymers are not much consumed by this clay. Thus, a sufficient amount of them remains available for adsorption onto and dispersion of cement. Consequently, these findings explain the more robust dispersing performance of the novel terpolymers in the presence of montmorillonite, and their less pronounced effect in the presence of kaolin and muscovite.

After exposure to water, kaolin exhibits a d-spacing of 0.72 nm. After addition of the different superplasticizers, no shift of its d-spacing was found. Similarly, a d-spacing of 0.99 nm for pure muscovite was recorded. Also here, the d-spacing did not change in the presence of the different superplasticizers. These data signify that kaolin and muscovite interact with all PCE polymers in a similar manner via surface adsorption only. This result corresponds well with data on the dispersing performance presented before which indicate that kaolin and muscovite affect the dispersing power of PCE superplasticizers only slightly (see Fig. 8).

4. Conclusions

This study demonstrates that different clay minerals can show completely different impacts on the workability of cement and the dispersing effectiveness of PCE superplasticizers. Montmorillonite is the most detrimental clay mineral and it strongly perturbs the dispersing power of conventional PCE superplasticizers. On the contrary modified PEG-free PCEs exhibit high dispersing ability and robustness even in the presence of smectite clays. The reason is that conventional PCEs undergo chemisorption only with montmorillonite, as was evidenced via adsorption and XRD measurements. Contrary to this, other clay minerals such as kaolin or muscovite do not severely impact the performance of neither conventional nor modified VPEG-PCEs.

The results of this study suggest that contamination of concrete by clay impurities does not pose a serious problem as long as montmorillonite is not present in the contaminants. However, in case of a performance failure of a PCE product, field users might check the presence and amount of montmorillonite in the aggregates using the MB test. When significant amounts of this specific clay mineral are detected (MBV > 1 g/100 g), then a switch to a PEG-free PCE such as those described here presents a viable strategy.

Acknowledgment

L. Lei wishes to thank the Jürgen Manchot Foundation for generously providing a scholarship to finance this research at TU München.

References

[1] C.E. Weaver, L.D. Pollard, The Chemistry of Clay Minerals, Elsevier, Amsterdam, 1973.
[2] D.M. Roy, R. Roy, An experimental study of the formation and properties of synthetic serpentines and related layer silicate minerals, Am. Mineral. 39 (1954) 957–975.
[3] M.F. Brigatti, E. Galan, B.K.G. Theng, Structure and mineralogy of clay minerals, in: F. Bergaya, B.K.G. Theng, G. Lagaly (Eds.), Handbook of Clay Science, Elsevier, Amsterdam, 2006, pp. 19–86.
[4] G. Brown, The X-ray Identification and Crystal Structures of Clay Minerals, Mineralogical Society, London, 1961.
[5] R.E. Grim, Clay Mineralogy, McGraw-Hill Series in the Geological Sciences, McGraw-Hill, New York, 1953.
[6] AFNOR, Mesure de la quantité et de l'activité de la fraction argileuse (Norme Française NF), Association française de Normalization (ANFOR), La Défense, Paris, France, 1993. 68–94.
[7] M. Türköz1, H. Tosun, The use of methylene blue test for predicting swell parameters of natural clay soils, Sci. Res. Essays 6 (2011) 1780–1792.
[8] M. Teresa, R. Laguna, R. Medrano, M.P. Plana, M.P. Tarazona, Polymer characterization by size-exclusion chromatography with multiple detection, J. Chromatogr. A 919 (2001) 13–19.
[9] P.T. Hang, G.W. Brindley, Methylene blue adsorption by clay minerals. Determination of surface areas and cation exchange capacities (clay-organic studies XVIII), Clays Clay Minerals 18 (1970) 203–212.
[10] G. Lagaly, Colloid clay science, in: F. Bergaya, B.K.G. Theng, G. Lagaly (Eds.), Handbook of Clay Science, Elsevier, Amsterdam, 2006, pp. 141–245.
[11] P.D. Svensson, S. Hansen, Intercalation of smectite with liquid ethylene glycol resolved in time and space by synchrotron X-ray diffraction, Appl. Clay Sci. 48 (2010) 358–367.
[12] J.L. Suter, P.V. Coveney, Computer simulation study of the materials properties of intercalated and exfoliated poly(ethylene) glycol clay nanocomposites, Soft Matter 5 (2009) 2239–2251.
[13] S. Ng, J. Plank, Interaction mechanisms between Na montmorillonite clay and MPEG-based polycarboxylate superplasticizers, Cem. Concr. Res. 42 (2012) 847–854.
[14] L. Lei, J. Plank, A concept for a polycarboxylate superplasticizer possessing enhanced clay tolerance, Cem. Concr. Res. 42 (2012) 118–123

5.4 A simplified preparation method for PCEs involving macroradicals

L. Lei, J. Plank

V. M. Malhotra (Ed.), 11th International Conference on Superplasticizers and Other Chemical Admixtures in Concrete (CANMET/ACI)
July 12 – 15, 2015, Ottawa (ON / Canada)
Proceedings, SP-302-12, 155 – 168.

Due to the limitation of both widely used synthesis methods of (meth)acrylate ester-based PCEs, namely aqueous free radical copolymerization and grafting (esterification) reaction, a more simplified synthesis method from maleic anhydride and ω-methoxy poly(ethylene glycol) as sole raw materials is introduced in this study. The synthesized PCE polymers were found to be effective cement dispersants.

As the core of this study, the synthesis mechanism was thoroughly investigated. The synthesis process consists of two steps: esterification and grafting. In the first step, a mono maleate ester is produced via esterification reaction from maleic anhydride and ω-methoxy polyethylene glycol. In the subsequent grafting process, at first free radicals RO• are formed from a peroxide initiator. In the initiation step, the RO• radicals abstract hydrogen from ω-methoxy polyethylene glycol (MPEG). This way, an ω-methoxy polyethylene glycol (MPEG) macroradical is formed. In the propagation step, maleic anhydride and the unsaturated MPEG mono maleate ester can graft onto these macroradicals by forming a comb – shaped PCE structure which again presents a macroradical. Through chain transfer steps, more MPEG macroradicals are produced which then graft with another maleic anhydride and unsaturated MPEG mono maleate ester, and so on. Termination occurs when two ω-methoxy polyethylene glycol macroradicals recombine into a polymer. The proposed structure of the MPEG-PCEs prepared via macroradicals is presented in below:

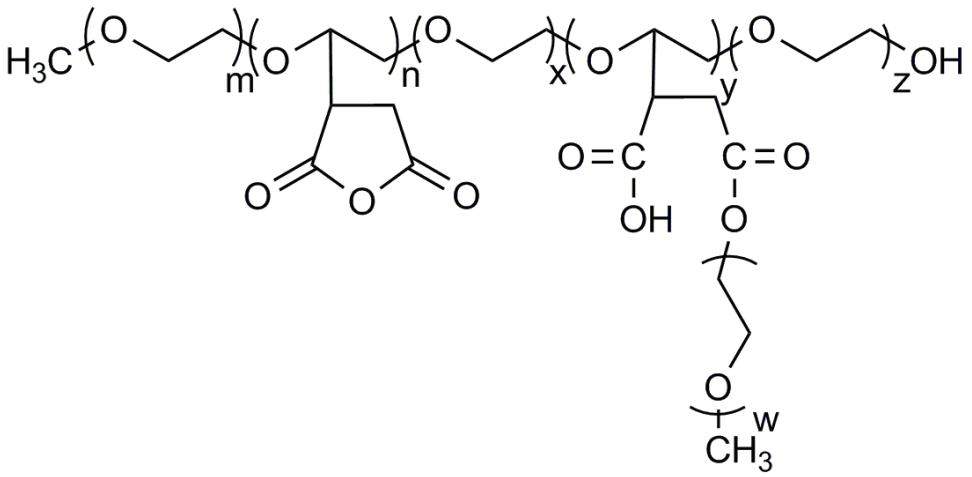

Proposed chemical structure for the newly synthesized MPEG - g - MPEG mono ester/maleic anhydride PCE polymers

A SIMPLIFIED PREPARATION METHOD FOR PCES INVOLVING MACRORADICALS

By

Lei Lei and Johann Plank

Prof. Dr. Johann Plank

Lehrstuhl für Bauchemie, Technische Universität München

Lichtenbergstr. 4, D-85747 Garching, Germany

Tel.: +49 89 289 13151

Fax: +49 89 289 13152

E-mail: sekretariat@bauchemie.ch.tum.de

ID: SP # 036

A SIMPLIFIED PREPARATION METHOD FOR PCES INVOLVING MACRORADICALS

Lei Lei and Johann Plank

Biography:

Lei Lei is a Ph.D. student at the Chair for Construction Chemistry at Technische Universität München, Germany. Her research focuses on the impact of different clay minerals on the performance of polycarboxylate - based superplasticizers and new routes to PCE synthesis.

Johann Plank is full Professor at the Institute of Inorganic Chemistry of Technische Universität München, Germany. Since 2001, he holds the Chair for Construction Chemistry there. His research interests include cement chemistry, chemical admixtures, organic-inorganic composite and nano materials, concrete, dry-mix mortars and oil well cementing.

ABSTRACT

Polycarboxylate superplasticizers are known to be most powerful admixtures which exhibit superior dispersing force even at extremely low water-to-cement ratio. In this study, a simplified one-pot synthesis method for a PCE using only maleic anhydride and methoxy polyethylene glycol as sole raw materials was developed. Compared to conventional synthetic routes, the new method constitutes a much simpler process

which performs esterification and grafting in one reactor. Macromonomers are no longer needed for the synthesis of this PCE. The resulting copolymer was characterized by size exclusion chromatography and anionic charge density measurement. Performance of the polymer in cement was probed via 'mini slump test'. To detect a potential retarding effect of the copolymer, time-dependent heat evolution was monitored. Finally, a model for the formation of this PCE is proposed. According to this, maleic anhydride and MPEG maleate monoester are grafted onto MPEG macroradicals which present the backbone of this PCE.

Key words: Polycarboxylate; Admixture; Synthesis; Graft copolymer; Polymerization mechanism; Dispersion

INTRODUCTION

Polycarboxylate-based superplasticizers (PCEs) have become indispensable admixtures, especially for the production of high performance concretes such as self-compacting (SCC) or ultra-high performance concrete (UHPC)[1, 2]. Nowadays, a broad variety of different PCE products exhibiting diverse chemical compositions are on the market[3]. In literature, they are referred to as ω-methoxy poly(ethylene glycol) methacrylate ester (MPEG), α-allyl-ω-methoxy or ω-hydroxy poly(ethylene glycol) ether (APEG), poly(ethylene glycol) vinyl ether (VPEG), α-methallyl-ω-methoxy or ω-hydroxy poly(ethylene glycol) ether (HPEG) and isoprenyl oxy poly(ethylene

glycol) ether (IPEG or TPEG) type PCEs whereby the acronym indicates the chemical nature of the side chain-bearing unit (for example, MPEG indicates that this PCE contains a poly(ethylene glycol) methacrylate ester as major building block). The general composition of these kinds of PCEs is displayed in **Fig. 1.**

The industrial synthesis of PCEs occurs in different ways. The most common process includes aqueous free radical copolymerization whereby a macromonomer holding the side chain is reacted with an acid-bearing monomer (e.g. acrylic, methacrylic, maleic, itaconic acid etc.) to yield the typical comb structure of PCE[4]. Different initiator systems including peroxodisulfate, redox systems such as Fe^{2+}/H_2O_2, rongalite/Fe^{2+}/H_2O_2 or ascorbic acid/H_2O_2 and chain transfer agents (e.g. methallyl sulphonate or mercapto propionic acid) are utilized to tailor the molecular properties such as molar masses (M_w, M_n) and polydispersity of the PCE to the individual requirements in specific applications. This process of radical copolymerization is fairly easy to carry out in an industrial plant, and even polymerization methods which can be performed at room temperature and do not require heating have been developed[5]. However, this preparation method depends on the local availability of macromonomers which may not always be at hand.

For (meth)acrylate ester-based PCEs, the so-called grafting process presents an alternative synthesis route (**Fig. 2**). There, commonly available ω-methoxy poly(ethylene glycol) is grafted on to a poly(meth)acrylic acid backbone via

esterification reaction, resulting in the desired comb-structure of PCE. Different acid catalysts including p-toluenesulfonic acid or hypophosphite are employed in this reaction to speed up esterification and increase the yield[6]. Typically, such esterification reactions are carried out at relatively high temperatures (120 – 150 °C) and application of azeotropic solvents (e.g. benzene, cyclohexane etc.) or reduced pressure to remove the water helps to accelerate esterification[7]. Compared with free radical copolymerization, the esterification method has the advantage of producing a comb polymer with statistical (rather regular) distribution of the side chains along the polymer backbone whereas free radical copolymerization results in a gradient copolymer with decreasing side chain density along the main chain as copolymerization progresses. This effect is owed to the different reactivities of the ester and the (meth)acrylic acid.

A severe draw-back of the esterification process is the synthesis of short-chain poly(meth)acrylic acid which is utilized as backbone. Its M_w should be less than 7,000 g/mol and ideally even < 4,000 g/mol to avoid extremely long backbones which adsorb only slowly on cement and are not ideally suitable for application in concrete. Additionally, such high molecular weight can lead to reduced water solubility and/or highly viscous solutions which are difficult to handle in the plants of admixture companies. Therefore, inspite of its several advantages the esterification process suffers from the difficulty of preparing a suitable poly(meth)acrylic acid backbone, because of the strong tendency of (meth)acrylic acid to homopolymerize and form

long chains. As a result of this difficulty, the esterification process is less common among MPEG PCE producers, compared to free radical copolymerization.

In order to overcome the problems of both methods we introduce a new preparation method for PCEs which uses macroradicals to achieve the characteristic comb structure of PCE. The target of our study is to prepare a PCE of reasonable performance from simple, easily available raw materials such as maleic anhydride and ω-methoxy poly(ethylene glycol) in a process which is feasible for common chemical plants. For this purpose, different synthesis conditions were evaluated and a suggestion for a typical process is made. Furthermore, the molecular properties and performance in cement paste of the synthesized PCE samples were compared utilizing "mini slump" and slump retention tests and via heat flow calorimetry. Finally, the reaction mechanism underlying the formation of these PCE polymers was investigated using gel permeation chromatography (GPC) and ^{1}H NMR spectroscopy.

RESEARCH SIGNIFICANCE

A new preparation method for PCEs including a simplified process which uses macroradicals to achieve the characteristic comb structure of PCE is presented as an alternative to common free radical copolymerization and esterification processes. The PCE products synthesized according to the new method exhibit competitive dispersing performance although the process has not yet been optimized.

EXPERIMENTAL INVESTIGATION

Materials

Chemicals — maleic anhydride (> 99 %, Merck Schuchardt OHG, Hohenbrunn, Germany), ω-methoxy poly(ethylene glycol) (Polyglycol M350, Polyglycol M500, Polyglycol M2000) (> 99 % purity, Clariant Produkte Deutschland GmbH, Burgkirchen, Germany), H_2SO_4 (98 % purity, SIGMA-ALDRICH CHEMIE, Steinheim, Germany), *tert*-butyl peroxybenzoate (98 % purity, SIGMA-ALDRICH CHEMIE, Steinheim, Germany) were used as is without any further purification.

Reference sample —a self-synthesized polycarboxylate superplasticizer possessing high grafting density, designated 45PC2, was used for comparison. This PCE was prepared from methacrylic acid and ω-methoxy poly(ethylene oxide) methacrylate ester via aqueous free radical copolymerization reaction. The molar ratios of the monomers were 2:1, and the number of ethylene oxide units in the side chain was 45. The synthesis process is described in detail in [4].

Cement — A CEM I 52.5 N (Milke®classic, HeidelbergCement, Geseke plant) was used. Its phase composition as determined by XRD is presented in **Table 1**. The average particle size (d_{50} value, determined by laser granulometry) was found at 11.5 μm. Its density was 3.153 g/cm^3 (Helium pycnometry).

Synthesis of PCE Graft Copolymers

MPEG 350 - *graft* - MPEG 350 mono maleate/maleic anhydride

7.5 g (76 mmol) of maleic anhydride, 25.2 g of MPEG 350 (72 mmol) and 0.15 g of 98 wt.% H_2SO_4 were placed in a 250 mL three-neck round bottom flask equipped with a stirrer and heated for 3 hours at 140 ℃ under constant stirring. Thereafter, 15 g (153 mmol) of maleic anhydride were dissolved in 20.125 g (58 mmol) of MPEG 350. Furthermore, 1.2 g (6 mmol) of *tert*-butyl peroxybenzoate initiator were also added to this homogeneous mixture. Using a peristaltic pump, this solution was fed continuously into the vessel over a period of 60 min while maintaining the temperature at 140 ℃. The viscosity of the mixture increased during the synthesis procedure. When the addition was complete, the mixture was stirred for another 60 min at 140 ℃. After that, the mixture was cooled to ~ 70 ℃ and ~ 65 g of water were added. Then the pH value was adjusted to 7 by addition of 30 wt.% aqueous NaOH solution. The final product was designated as MPEG 350 - *g* - MPEG 350 mono ester/maleic anhydride. It presented a reddish, 34.3 wt.% aqueous solution which was used without further purification.

MPEG 500 - *graft* - MPEG 500 mono maleate/maleic anhydride

7.5 g (76 mmol) of maleic anhydride, 36 g of MPEG 500 (72 mmol) and 0.15 g of 98 wt.% H_2SO_4 were placed in a 250 mL three-neck round bottom flask equipped with a stirrer and heated for 3 hours at 140 ℃ under constant stirring. Thereafter, 15 g (153 mmol) of maleic anhydride were dissolved in 28.8 g (58 mmol) of MPEG 500, then 1.2 g (6 mmol) of *tert*-butyl peroxybenzoate initiator were added to this homogeneous mixture. Using a peristaltic pump, this solution was fed continuously into the vessel

over a period of 60 min while maintaining the temperature at 140 °C. Also here, viscosity of the mixture increased during the synthesis process. All further steps were the same as for the MPEG 350 graft copolymer. The final product was designated as MPEG 500 - *g* - MPEG 500 mono ester/maleic anhydride. It presented a reddish, 43.8 wt.% aqueous solution which was used without further purification.

MPEG 2000 - *graft* - MPEG 2000 mono maleate/maleic anhydride

1.875 g (19 mmol) of maleic anhydride, 36 g of MPEG 2000 (18 mmol) and 0.15 g of 98 wt.% H_2SO_4 were placed in a 250 mL three-neck round bottom flask equipped with a stirrer and heated for 3 hours at 140 °C under constant stirring. Thereafter, 3.75 g (38 mmol) of maleic anhydride were dissolved in 7.2 g (3.6 mmol) of MPEG 2000. Furthermore, 0.6 g (3 mmol) of *tert*-butyl peroxybenzoate initiator were added to this homogeneous mixture. Using a peristaltic pump, this solution was fed continuously into the vessel over a period of 60 min while maintaining the temperature at 140 °C. The rest of the preparation followed the method as described above. The final product was designated as MPEG 2000 - *g* - MPEG 2000 mono ester/maleic anhydride. It presented a reddish, 43.7 wt.% aqueous solution which was used without further purification.

Characterization of PCE samples

Molar masses (M_w, M_n) and polydispersity index (PDI) of the PCE samples were determined utilizing size exclusion chromatography (SEC). Additionally, the anionic

charge density was measured.

Size exclusion chromatography (SEC) — PCE solutions containing 10 g/L of the polymer were prepared for SEC analysis. Measurement was performed on a Waters 2695 Separation Module equipped with three Ultrahydrogel™ columns (120, 250, 500) and an Ultrahydrogel™ guard column from Waters, Eschborn, Germany, and a subsequent 3 angle static light scattering detector ("mini Dawn" from Wyatt Technology Corp., Santa Barbara, CA, USA). The polymer concentration was monitored with a differential refractive index detector (RI 2414, Waters, Eschborn, Germany). Aqueous 0.1 N $NaNO_3$ solution adjusted to pH 12 with NaOH was used as an eluent at a flow rate of 1.0 mL/min. From the SEC measurements, the polydispersity index (PDI) and the molar masses (M_w and M_n) were obtained. The value of *dn/dc* used to calculate M_w and M_n was 0.135 mL/g (value for polyethylene oxide)[8].

Specific anionic charge density — The specific anionic charge densities of the polymers were determined employing a particle charge detector PCD 03 pH (Mütek Analytic, Herrsching, Germany). This instrument allows the experimental determination of the anionic charge of polymers in solution. Here, 0.2 g/L of the polymers were dissolved in DI water and titrated against an aqueous 0.34 g/L solution of poly-diallyl dimethyl ammonium chloride (polyDADMAC) until charge neutralization (zero potential) was reached. From the amount of polyDADMAC consumed to reach a zero potential, the amount of negative charge per gram of polymer was calculated[9].

Calorimetry — To detect a potential retarding effect of the novel PCE samples, time-dependent heat evolution during cement hydration was monitored. There, 4 g of cement were filled into 10 mL glass ampoules, mixed at 21 °C with the appropriate amount of aqueous polymer solution (w/c = 0.3), shaken for 1 min in a wobbler and then placed in an isothermal heat conduction calorimeter (TAMair, Thermometric, Järfälla, Sweden) to monitor the heat flow of the hydration reaction. Data logging was continued for 7 days.

Dispersing performance in cement

For determination of the paste flow, a "mini slump test" modified from DIN EN 1015 was utilized and carried out as follows: First, the water-to-cement (w/c) ratio of the paste without polymer was set to 0.3. At this w/c ratio, the dosages of the PCE samples required to reach a spread of 26±0.5 cm were determined. Generally, the polymer was dissolved in the required amount of mixing water placed in a porcelain cup. When aqueous polymer solutions were used, then the amount of water contained in the polymer solution was subtracted from the amount of mixing water. In preparation, 300 g of cement were added to the mixing water and agitated manually for 1 minute utilizing a spoon, then rested for 1 minute without stirring and were again stirred for 2 minutes. After the stirring, the cement paste was immediately poured into a Vicat cone (height 40 mm, top diameter 70 mm, bottom diameter 80

mm) placed on a glass plate and the cone was removed vertically. The resulting spread of the paste was measured twice, the second measurement being in a 90 ° angle to the first and averaged to give the final spread value.

For the time-dependent flow behavior of the paste, 400 g of cement were mixed with 120 mL of DI water as described in the procedure above. After each measurement, the slurry was transferred back into the cup and covered with a wet towel in order to avoid drying. Before each subsequent measurement, the paste was stirred again for 2 minutes. Measurements were taken every 15 minutes over a total period of 120 minutes.

EXPERIMENTAL RESULTS AND DISCUSSION

Properties of synthesized PCE polymers

In this novel synthesis process, maleic anhydride as well as MPEG mono maleate ester were grafted onto MPEG macroradicals serving as backbone of the PCE polymer. This way, a comb polymer is formed whereby along an MPEG trunk chain, maleic anhydride and MPEG mono maleate pendants are randomly arranged, as will be shown in the mechanistic part of this paper.

The SEC spectra of the synthesized PCE polymers are displayed in **Fig. 3**. According to them, the conversion of the monomers was 71 - 77 %. It should be mentioned here that so far we have not attempted to optimize the yield of polymer. Molar composition of the polymers was confirmed by ^{1}H NMR spectroscopy whereby the peak areas of

the individual protons were integrated (spectra not shown here).

The characteristic molecular properties of the synthesized polymers are presented in **Table 2**. According to the SEC data, the synthesized PCE polymers exhibit relatively low molecular weights (M_w, M_n), compared to a commercial benchmark MPEG PCE product prepared from MPEG - MAA macromonomer via free radical copolymerization. The polydispersity index of the samples lies at ~ 2.5 which indicates a fairly narrow molecular weight distribution.

Next, the specific anionic charge amounts of the synthesized polymers and of the industrial polymer were determined in DI water. The results are exhibited in **Table 3**. From the data, it is obvious that at increasing side chain length of the PCE polymers, the anionic charge density decreases as expected.

Cement dispersion

'Mini slump'test — To probe into the dispersing effectiveness of the newly synthesized PCE samples, the dosages required to achieve a cement paste spread of 26±0.5 cm were determined. For this test, a cement paste prepared at a w/c ratio of 0.3 was employed. According to **Fig. 4,** the newly synthesized polymers work as effective cement dispersants at low w/c ratios. Their effectiveness increases with increased length of the MPEG utilized in the synthesis.

Time - dependent slump loss behavior — Next, time - dependant slump loss behavior of the superplasticizer samples was measured over a period of two hours. In this test, cement pastes prepared at a w/c ratio of 0.3 treated with the superplasticizer dosages as shown in **Fig. 4** were employed. The results are displayed in **Fig. 5.**

According to this data, the synthesized graft polymers maintain workability of the cement paste for a short time period only.

Generally, polymer MPEG 2000 - *g* - MPEG 2000 mono ester/maleic anhydride seems to retain fluidity slightly better than the polymers prepared from the short chain MPEGs (MPEG 350 and MPEG 500). This trend is owed to the specific molecular architecture of the PCE polymers, because PCE molecules with longer side chains are more coiled, adsorb slower and thus can provide better slump retention over time.

Impact on cement hydration — To detect a potential retarding effect of the synthesized graft polymers, time - dependent heat evolvement from a cement paste (w/c ratio = 0.3) holding different polymer samples was monitored. The results are exhibited in **Fig. 6**. There, it is demonstrated that the synthesized graft polymers retard cement hydration, possibly due to the excessive amount of maleic anhydride used in the synthesis which partially did not incorporate into the PCE (see SEC spectra in **Fig. 3**). Again, the polymer containing MPEG 2000 performs better than the two polymers with shorter pendants.

Grafting Mechanism via Macroradicals

Stepwise analysis of the cascade of reactions occurring during this novel synthesis method revealed a mechanism as follows:

In the first step, a mono maleate ester is produced via esterification reaction from ω-methoxy polyethylene glycol and maleic anhydride, as is shown in **Fig. 7**.

In the subsequent grafting process, the peroxide initiator at first undergoes thermal

homolytic cleavage to form radicals RO• (see **Fig. 8**). In a second step, ω-methoxy polyethylene glycol (MPEG) macroradicals are formed through a chain transfer reaction with the radicals RO• whereby hydrogen is abstracted from MPEG. It should be noted that in previous literature, formation of such macroradicals from peroxide initiators has been well documented for polyethylene and polypropylene and successful grafting of maleic anhydride onto these macroradicals is described there as well[10 - 14].

Subsequently, maleic anhydride and the unsaturated MPEG mono maleate ester can graft onto these macroradicals by forming a comb - shaped PCE structure which again presents a macroradical, see step (3) in **Fig. 8**. This reaction is favoured by the strong electron attracting properties of the double bond of maleic anhydride and the mono maleate ester. Through continued chain transfer reactions as shown in step (4) of **Fig. 8,** new MPEG macroradicals are formed which then can undergo the same sequence of grafting reaction as before, thus leading to an MPEG trunk chain which holds multiple maleic acid and MPEG maleate pendant groups. Termination occurs when two ω-methoxy polyethylene glycol macroradicals combine into the final product.

The proposed chemical structure of the final graft copolymer derived from this reaction mechanism is displayed in **Fig. 9**. It should be noted here that due to the complexity of the reaction, the final product likely consists of a mixture of several polymers exhibiting different degrees of grafting (as is also the case in MPEG PCE

synthesis via free radical copolymerization using macromonomers, but this fact is often ignored), thus the structure presented in **Fig. 9** represents only one of several possibilities. Another possibility requiring consideration is the formation of poly(maleic acid) homopolymer. However, the SEC spectra do not provide evidence of its presence. Also, according to literature the homopolymerization of maleic anhydride is inhibited by organic electron donors such as in oxygen or sulfur containing compounds[12, 13]. Consequently, this side reaction was ruled out. Another consideration was the formation of an α - olefin occurring in the initial esterification step from dehydration of MPEG with sulfuric acid. Such α – olefin could then undergo copolymerization. This possibility was checked via ^{1}H NMR spectroscopy of the esterification product. However, no signals characteristic for α - olefinic protons could be detected.

CONCLUSIONS

A new preparation method for PCEs including a simplified process is presented as an alternative to the common free radical copolymerization and esterification processes. Here, the polymerization mechanism relies on the formation of ω-methoxy polyethylene glycol macroradicals which are generated by hydrogen abstraction from the MPEG. Subsequently, maleic anhydride as well as MPEG - mono maleate ester are grafted onto such macroradicals yielding a comb type PCE polymer with carboxylic and EO pendants arranged along the MPEG main chain. SEC data show that the synthesized graft polymers exhibit relatively low molecular weights (M_w, M_n).

Performance tests indicate that this new type of PCE can disperse cement well although it was synthesized from simple raw materials. Future work should focus on further optimization of molar mass and conversion of raw materials to capture the full potential of this novel PCE chemistry.

ACKNOWLEDGMENTS

L. Lei wishes to thank the Jürgen Manchot Foundation for generously providing a scholarship to finance this research at TU München.

REFERENCES

1. Petit, J. Y., Wirquin, E., Khayat, K.H., Vanhove, Y., "Coupled effect of temperature and superplasticizer on rheological properties of SCC mortar", 5th International RILEM Symposium on Self-Compacting Concrete, RILEM Publications SARL, Ghent, Belgium, **2007**, pp. 1099 – 1104.
2. Plank, J., Schroefl, C., Gruber, M., Lesti, M., Sieber, R., "Effectiveness of Polycarboxylate Superplasticizers in Ultra-High Strength Concrete: The Importance of PCE compatibility with Silica Fume", *Journal of Advanced Concrete Technology*, V. 7, No.1, 5-7, **2009**, pp. 5 - 12.
3. Plank, J., "PCE Superplasticizers – Chemistry, Applications and Perspectives",

18. IBAUSIL, Weimar **2012**, V. 1, pp. 91-102.

4. Plank, J., Pöllmann, K., Zouaoui, N., Andres, P. R., Schaefer, C., "Synthesis and performance of methacrylic ester based polycarboxylate superplasticizers possessing hydroxy terminated poly(ethylene glycol) side chains", *Cement & Concrete Research*, V. 38, No. 10, **2008**, pp. 1210-1216.

5. Wang, Z. M., Xu, Y., Wu, H., Liu, X., Zheng, F. Y., Li, H. Q., Cui, S. P., Lan, M. Z., Wang, Y. L., "A Room Temperature Synthesis Method for Polycarboxylate Superplasticizer" CN patent 101974135 B, **2013**, assigned to Beijing University of Technology.

6. Guicquero, J. P., Maitrasse, Ph., Mosquet, M. A., Sers, A., "A water soluble or water dispersible dispersing agent", FR Patent 2,776,285, **1999**, assigned to Chryso.

7. Hirata, T., Yuasa, T., Nagare, K., "Cement admixture and cement composition", US patent 6,166,122, **2000**, assigned to Nippon Shokubai.

8. Teresa, M., Laguna, R., Medrano, R., Plana, M. P., Tarazona, M. P., "Polymer characterization by size-exclusion chromatography with multiple detection", *J. Chromatogr. A.* V 919, **2001**, pp. 13-19.

9. Plank, J., Sachsenhauser, B., "Experimental determination of the effective anionic charge density of polycarboxylate superplasticizers in cement pore solution", *Cement & Concrete Research*, V. 39, **2009**, pp. 1 - 5.

10. Ghaemy, M., Roohina, S., "Grafting of Maleic Anhydride on Polyethylene in a

Homogeneous Medium in the Presence of Radical Initiators", *Iranian Polymer Journal*, V 12, **2003**, pp. 21-29.

11. Gaylord N.G., Mehta R., Kumar V. and Tazi M., "High density polyethylene-*g*-maleic anhydride preparation in presence of electron donors"; *J. Appl. Polym. Sci.*, V 38, **1989**, pp. 359-371.

12. Gaylord N.G. and Mehta R., "Peroxide-catalyzed grafting of maleic anhydride on to molten polyethylene in the presence of polar organic compounds"; *J. Polym. Sci.,Part A, Polym. Chem.*, V 26, **1988**, pp. 1189-1198.

13. Cheng, Q., Lu, Z., Byrne, H., "Synthesis of maleic anhydride grafted polypropylene-butadiene copolymer and its application in PP/OMMT/SBS composite as compatibilizer", *Journal of Applied Polymer Science*, V. 114, No. 3, **2009**, pp. 1820-182.

14. Yin, J. H., Shi, D., Yang, J. H., et al., "Functionalization of isotactic polypropylene with maleic anhydride by reactive extrusion: mechanism of melt grafting", *Polymer*, V. 42, **2001**, pp. 5549-5557.

TABLES AND FIGURES

List of Tables:

Lists of Figures:

Table 1 – Phase composition of the CEM I 52.5 N sample as determined by Q-XRD using *Rietveld* refinement

Phase	wt.%
C_3S, m	54.14
C_2S, m	26.63
C_3A, c	3.28
C_3A, o	4.26
C_4AF, o	2.45
Free lime (Franke)	0.1
Periclase (MgO)	0.03
Anhydrite	2.64
$CaSO_4$-hemihydrate	1.21
$CaSO_4$-dihydrate	0.02
Calcite	3.61
Quartz	1.16
Arcanite (K_2SO_4)	0.46

Table 2 – Molar masses and polydispersity index (PDI) of the synthesized polymers and of a comparative commercial PCE sample

Polymer	M_w (g/mol)	M_n (g/mol)	PDI (M_w/M_n)	Yield
MPEG 350 - *g* - MPEG 350 mono ester/maleic anhydride	9,100	3,349	2.7	77.3 %
MPEG 500 - *g* - MPEG 500 mono ester/maleic anhydride	6,848	2,946	2.3	72.6 %
MPEG 2000 - *g* - MPEG 2000 mono ester/maleic anhydride	16,500	6,163	2.7	71.3 %
Industrial PCE	63,840	28,650	2.2	88.0 %

Table 3 – Specific anionic charge amount of superplasticizer samples tested in pH 12.5 aqueous solution

Fluid System	Specific anionic charge amount [μeq/g]			
	MPEG 350 - *g* - MPEG 350 mono ester/maleic anhydride	MPEG 500 - *g* - MPEG 500 mono ester/maleic anhydride	MPEG 2000 - *g* - MPEG 2000 mono ester/maleic anhydride	45 PC 2
pH 12.5 aqueous	3,239	1,249	1,551	1,033

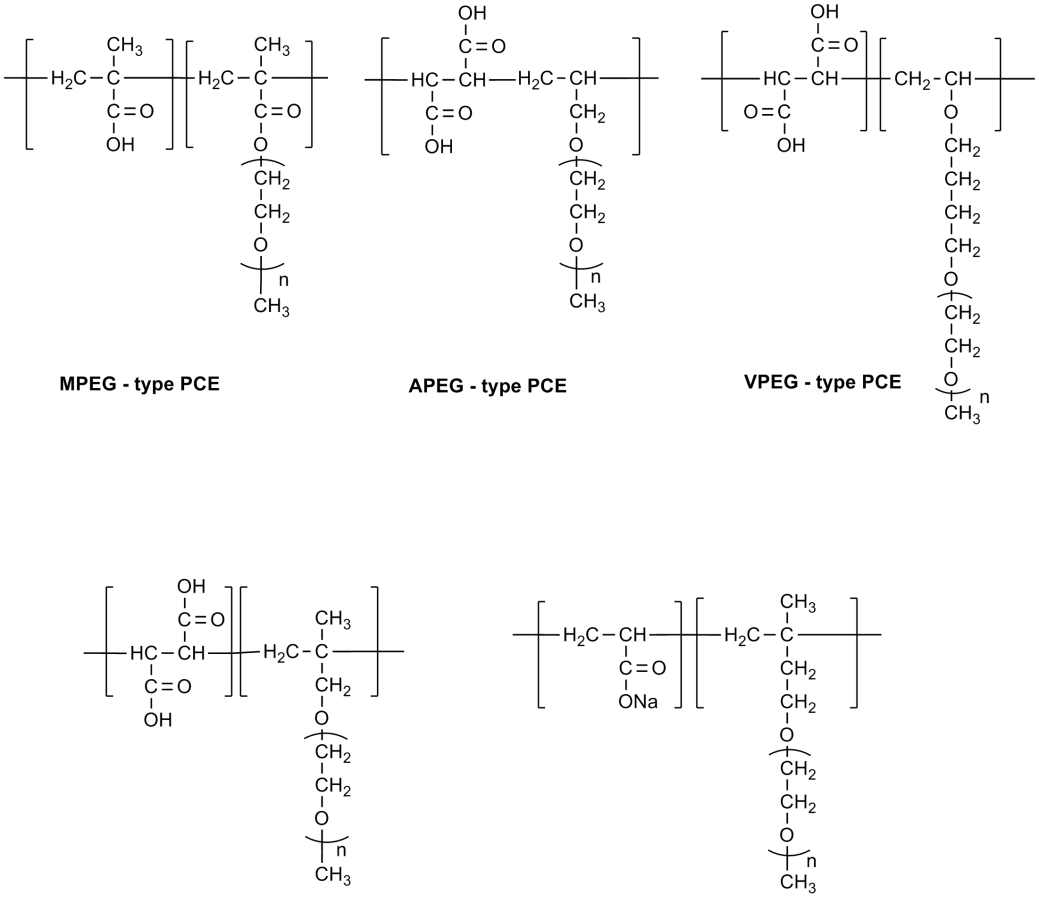

Fig. 1 – General composition of major kinds of PCEs used by the industry

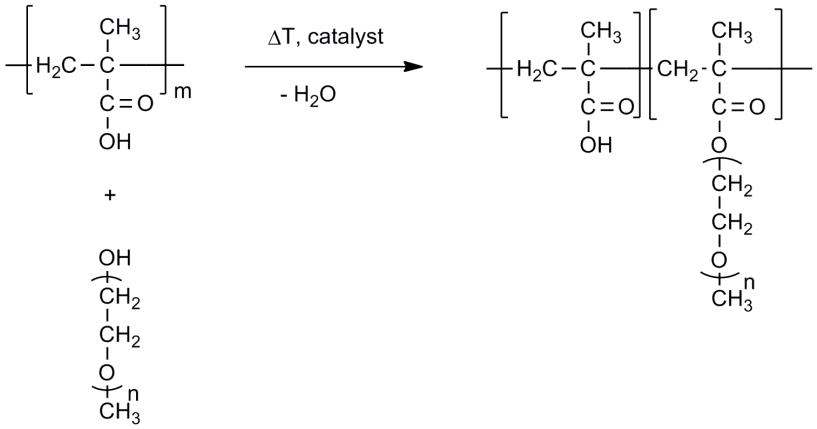

Fig. 2 – Preparation of MPEG PCEs via esterification of poly(methacrylic acid) with ω-methoxy poly(ethylene glycol)

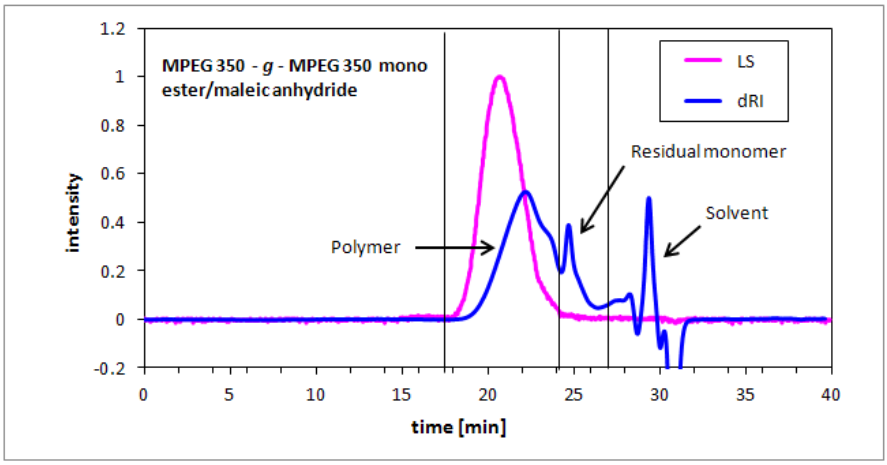

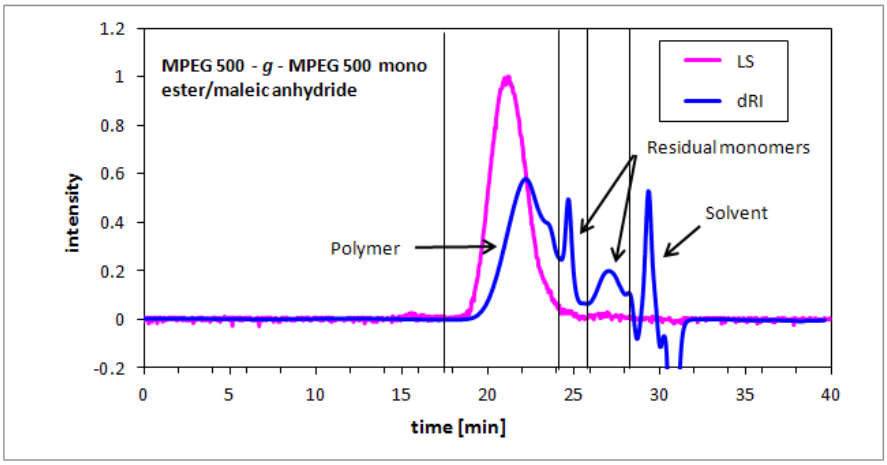

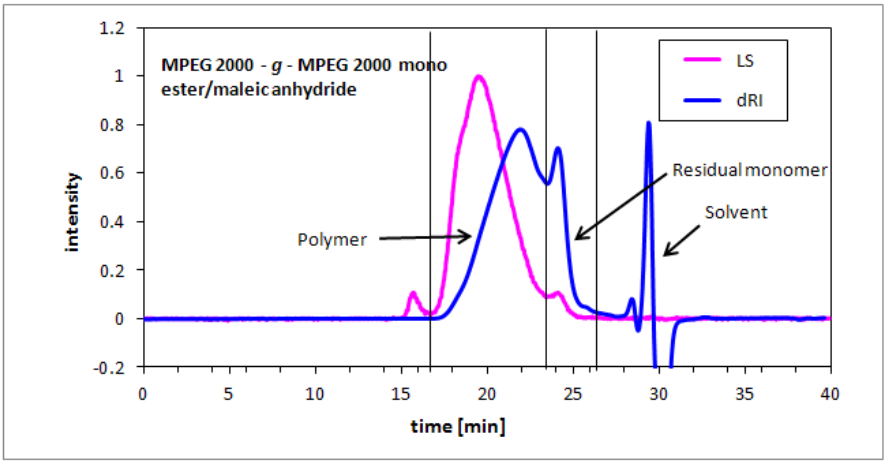

Fig. 3 – SEC spectra of the three synthesized graft polymers

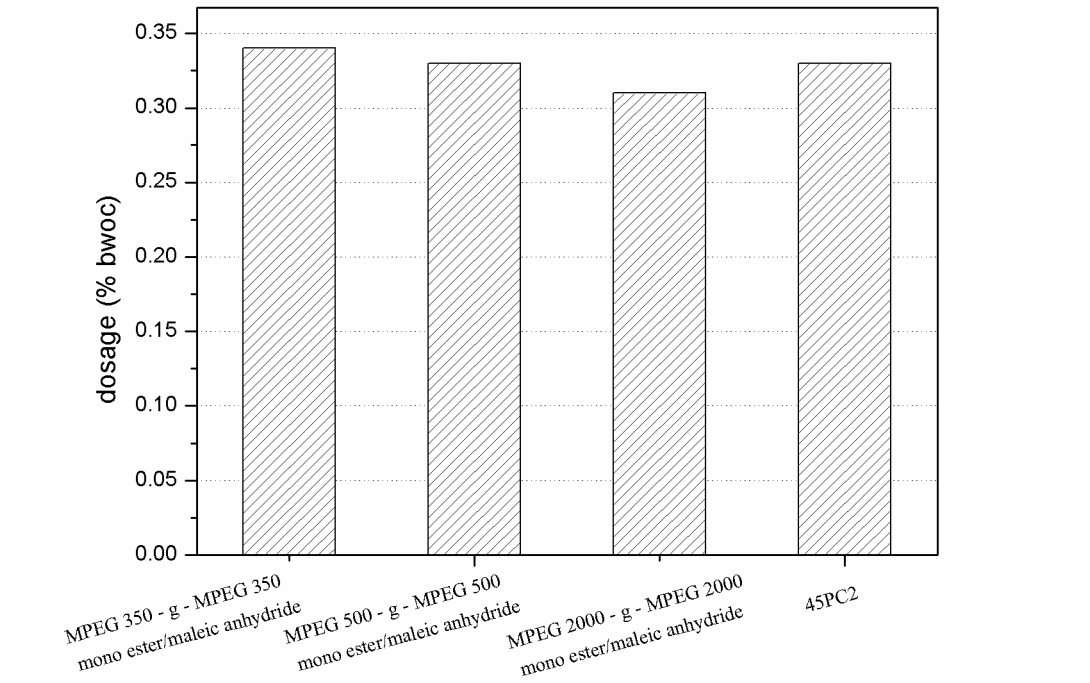

Fig. 4 – Dosages of synthesized graft copolymers required to achieve a paste spread of 26 ±0.5 cm (w/c = 0.3)

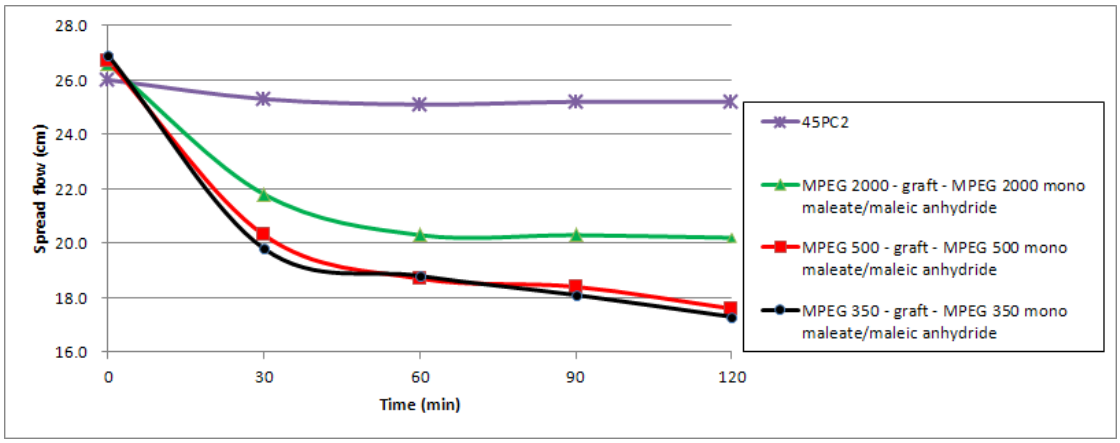

Fig. 5 – Slump loss behavior of cement pastes (w/c=0.3) containing the synthesized graft copolymers

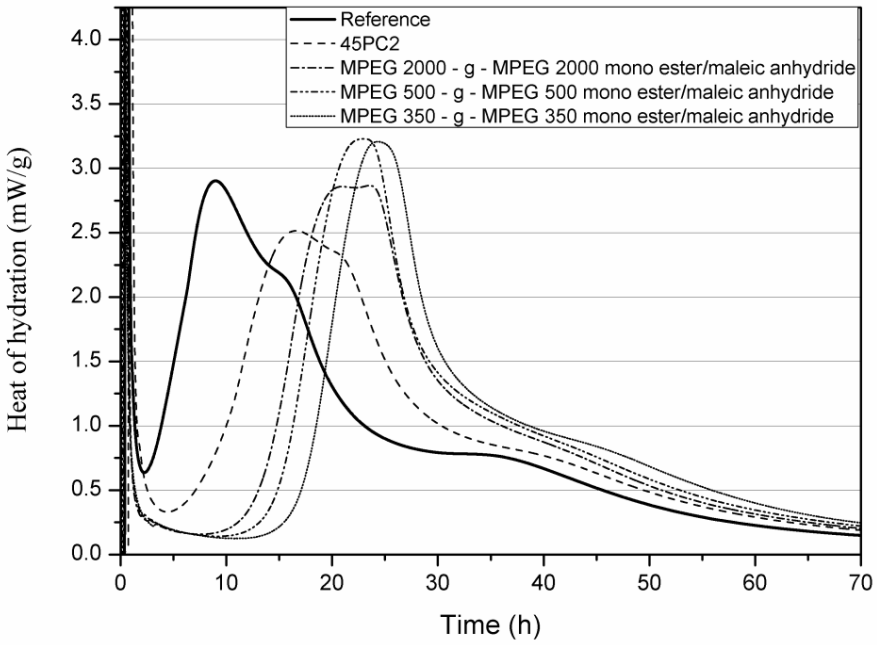

Fig. 6 – Time-dependent heat evolvement from cement paste (w/c = 0.3) holding the synthesized graft polymers

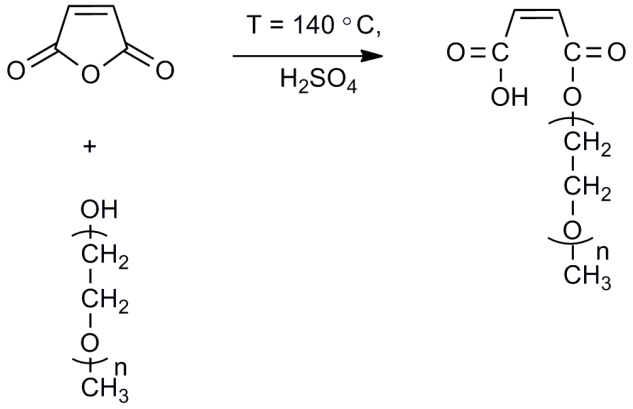

Fig. 7 – Esterification of maleic anhydride with MPEG to yield a mono maleate ester

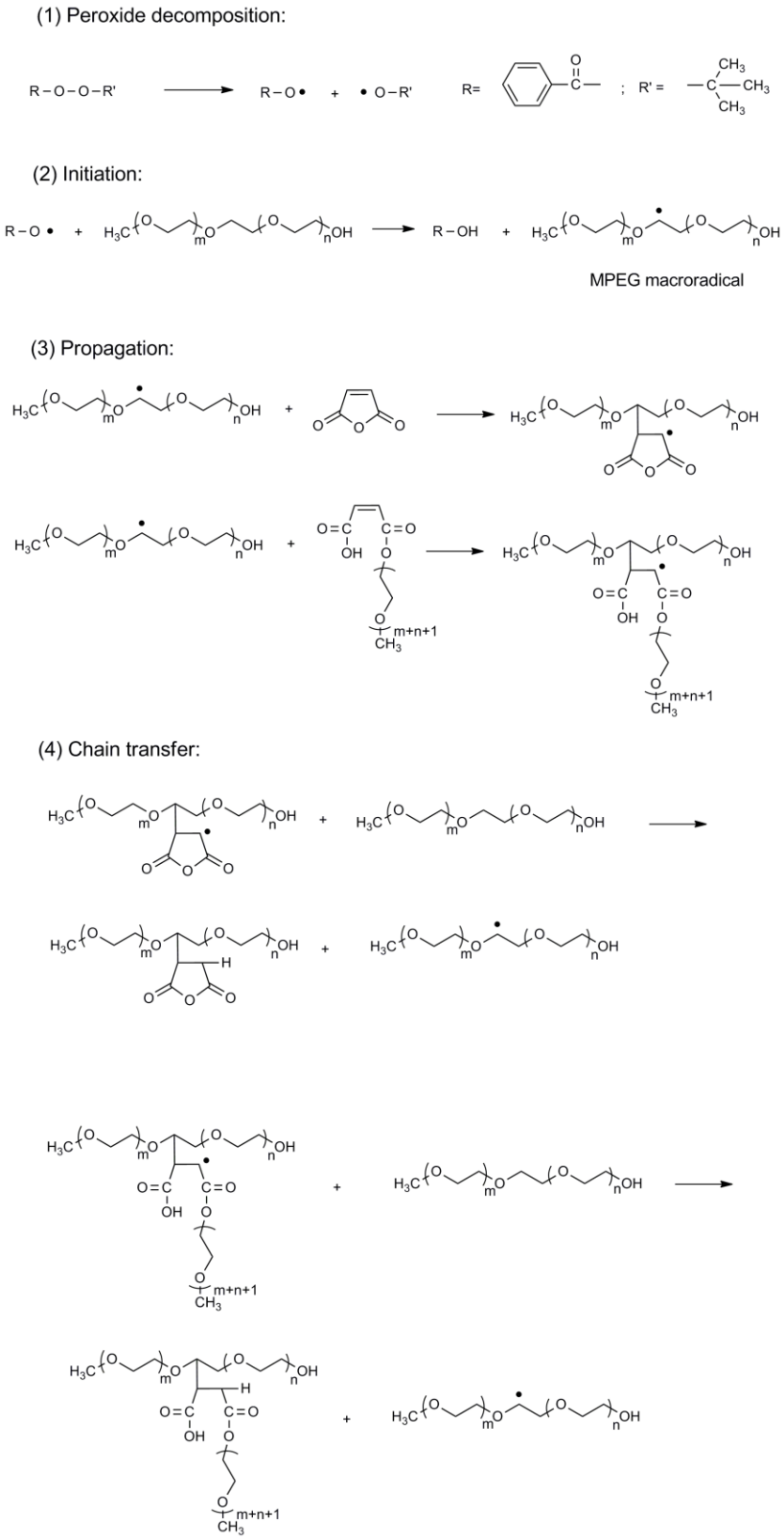

Fig. 8 – Cascade of reactions involved in the grafting of maleic anhydride and MPEG mono maleate ester onto a MPEG macroradical

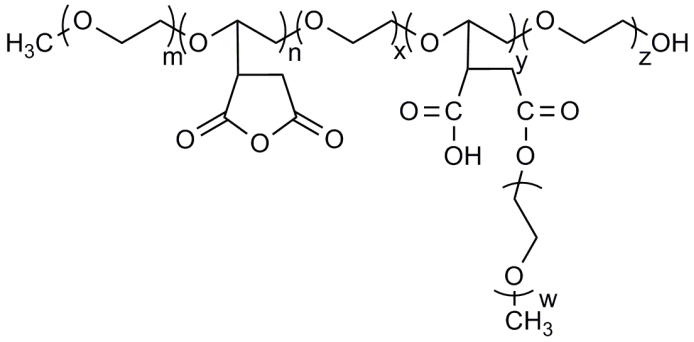

Fig. 9 – Proposed chemical structure for the newly synthesized MPEG - g - MPEG mono ester/maleic anhydride PCE polymers

5.5 Cement compatibility of PCE superplasticizers

A. Lange, **L. Lei**, J. Plank

14th International Congress on the Chemistry of Cement (ICCC)

October 13 – 16, 2015, Beijing, China.

Caijun Shi, Yan Yao (Eds.), Abstract Book, Vol. 1, p. 380

Fullpaper: Proceedings CD, Section 4: Admixtures.

This work was carried out in cooperation with another Ph. D. candidate, **Alex Lange**. In this study, the compatibility of PCE samples exhibiting different chemical structures (MPEG, APEG and IPEG type PCEs) with nine ordinary Portland cements (OPCs) possessing different C_3A content was probed via 'Mini Slump' Test.

It was found that the dispersing performance of PCEs fluctuated tremendously depending on the cement. From our study, it was observed that cements which were difficult to disperse by the PCEs produce large amounts of an ettringite gel as top layer after centrifugation of the cement paste prepared in the presence of the PCE samples. Whereas, a neat cement paste without any PCE polymer did not produce such ettringite gel which suggested that formation of such ettringite gel holding nano-sized ettringite crystals presents the root cause for cement – PCE incompatibility. Apparently, PCEs can act as morphological catalyst which reduces the size of the early ettringite crystals to nano scale, thus exhibiting a huge surface area which attracts a huge amount of PCE molecules and thus results in excessive dosages.

After testing a number of structurally different PCE polymers, i.e. MPEG, APEG and IPEG PCEs, it was found the APEG PCE sample modified with allyl maleate exhibited the best compatibility to different cement samples, even the cements which are most difficult to disperse. This finding indicates that the chemical architecture of PCE polymers plays a critical role with respect to the cement compatibility of a PCE polymer.

Cement Compatibility of PCE Superplasticizers

Lange A., Lei L., Plank J.*
Technische Universität München, Chair for Construction Chemistry, 85748 Garching, Germany

Abstract
It is well known among concrete producers that specific cements seem to be incompatible with almost all PCE products, thus causing excessive PCE dosages or even a total failure of the PCE to disperse cement. This effect is commonly referred to as "cement incompatibility" of PCE polymers. The study here investigates the reasons for such incompatibility.
First, it was found that only cements which form large amounts of ettringite exhibit such incompatibility phenomenon. Their characteristics are elevated C_3A content (> 5 wt.-%) and high initial heat of hydration. Second, it was observed that PCEs strongly influence early ettringite crystallization by acting as morphological catalyst. Most PCEs transform common micro meter-sized ettringite (l ~ 2-10 µm) into nano-sized crystals (l = 200 nm) which brings about a huge surface area and thus requires abnormal dosages of PCE to achieve strong dispersion. Such nano-sized ettringite can be separated from diluted cement pastes by centrifugation whereby a viscous, gel-like top layer is collected.
Furthermore, a broad variety of self-synthesized and chemically different PCE copolymers of methacrylate ester (MPEG), allyl ether (APEG), vinyl ether (VPEG) and isoprenyl ether (IPEG) type were screened with the goal to identify molecules with good tolerance to such "difficult" cements. The best performance with "difficult" cements was found for the IPEG PCE, while the APEG, VPEG and MPEG PCEs were significantly less tolerant. Interestingly, the APEG PCE became highly compatible with a "difficult" cement after allyl maleate was introduced into this PCE as a third comonomer. This result signifies that even relatively minor changes in the chemical composition can make a big difference in the cement compatibility of a PCE polymer. Finally, it was found that "cement compatible" PCEs act as a morphological catalyst for ettringite and enact the formation of larger crystals with less surface area to be occupied by the PCE.
The phenomenon of cement incompatibility mainly occurs in concretes possessing very low water-to-cement ratios and only when the PCE already is present in the mixing water. It disappears when the PCE is added in delayed mode during the mixing of the concrete. This effect is owed to the fact that abundant ettringite precipitation occurs within the very first ~ 30 seconds of cement hydration. Therefore, such incompatibility is most frequently observed in the production of high strength concrete. There, the superplasticizer is generally added to the mixing water to reduce mixing time. Finally, a simple and quick test to identify cement–PCE incompatibility is proposed.

Originality
It is well established among concrete producers that some cements cannot be dispersed well with PCE polymers. Such cements are generally classified as "difficult" cements and are avoided in the manufacturing of high performance concretes. Still, the industry is most interested in a concept which mitigates such incompatibility problem. Our study demonstrates that this phenomenon (1) only occurs with cements which produce enormous amounts of ettringite within the first 30 seconds of cement hydration, and (2) is linked to the ability of most PCE polymers to significantly reduce the size of these early ettringite crystals. This way, PCE polymers act as morphological catalysts for ettringite. Through polymer screening, few specific PCE structures were identified which do not impact much on ettringite morphology and thus exhibit good dispersing ability even with such "difficult" cements.

***Keywords**: Polycarboxylate, High range water reducer, Admixture, Ettringite, Morphology*

*** Corresponding author: sekretariat@bauchemie.ch.tum.de, Tel +49-89-289-13151, Fax +49-89-289-13152**

1. Introduction

Polycarboxylate based superplasticizers (PCEs) are widely used in concrete manufacturing, especially in systems exhibiting low w/c ratios such as ultra-high strength concrete or self-compacting concrete (Okamura H., *et al*, 2003; Sakai E., *et al*, 2009; Plank J., *et al*, 2009). More than 30 years ago PCEs were invented in Japan (Hirata T., 1981) and since then spread out worldwide. Their global production volume increases every year, especially in China. The first PCE products represented copolymers of sodium methacrylate and methoxypolyethylene glycol methacrylate macromonomer (the so-called MPEG type), but nowadays many other PCE products are on the market such as allyl ether (APEG), methallyl ether (HPEG) and isoprenyl ether (IPEG or TPEG) based PCEs (Plank J., 2012).

Common to all PCE structures is an anionic polymer trunk with polyglycol pendants. The dispersing force of PCEs derives from adsorption on parts of the cement particle exhibiting a positive surface charge such as the aluminate and ferrite phases (C_3A and C_4AF), and especially their hydration products ettringite and monosulfo aluminate (Bonen D., *et al*, 1995). The presence of different mineral phases in cement leads to undesired strong agglomeration of the clinker particles (Yoshioka K., *et al*, 1995). Thus, when no superplasticizer is present, a significant part of the mixing water is entrapped between the cement agglomerates causing a stiff consistency of the mortar or concrete. The dispersing effectiveness of PCEs is owed to charge reversal of the initially positively charged domains present on the surface of cement and second to the steric hindrance provided by the polyglycol side chains (Yoshioka K., *et al*, 2005).

PCE easily outperform other superplasticizers such as polycondensates, especially at low w/c ratios. However, applicators sometimes have experienced an incompatibility of PCEs with certain cements, leading to unreasonably high admixture dosages. In some cases it was totally impossible to disperse such cements with PCEs (Agarwal S. K.., *et al*, 2000) It is also well known that clay impurities can hamper the performance of PCE superplasticizers (Lei L., *et al*, 2014), but even in definitively clay-free cements, high dosages were encountered. Previous investigations indicated that such negative effect was owed to interaction of the PCEs with early cement hydration products (Prince W., *et al*, 2003; Aitcin P.-C., *et al*, 1994). Especially in ultra-high strength concrete (UHSC) where the PCE commonly is added to the mixing water to reduce mixing time, incompatibility between PCEs and cement was frequently observed (Schröfl C., *et al*, 2008).

In this study, the compatibility of structurally different PCE superplasticizers with nine specifically selected ordinary Portland cements (OPCs) was analyzed with respect to the dispersing performance of the PCEs in cement paste. Additionally, the initial hydration products were extracted from the cement pastes by centrifugation. Furthermore, the point of addition time of PCE was varied to clarify how fast these initial hydration products are formed in the cement paste and how they interact with the PCE superplasticizers. The initial hydration products were identified using X-ray diffraction, elemental analysis and thermogravimetry. Their morphology was assessed using SEM imaging. Using this data, interaction of the PCE superplasticizers with the early hydration products was elucidated, and

an explanation for the cement incompatibility phenomenon was sought.

2. Experimental

2.1. PCE Samples

A total of five PCE samples were studied. Two of them (samples MPEG-7 and MPEG-25) were methacrylic acid-co-ω-methoxy polyethylene glycol (MPEG) methacrylate ester polymers with side chains holding 7 and 25 EO units respectively. The molar ratio of methacrylic acid and MPEG-MA ester was adjusted in such a way that optimal dispersing performance (i.e. lowest dosage) was achieved. For MPEG-7, the MA : MPEG-MA ratio was 1.2:1 while for MPEG-25 it was 3:1.

Furthermore, two PCE samples (denominated as APEG-34 and APEG-34AM) were allyl ether (APEG) based polycarboxylates with a side chain holding 34 EO units. APEG-34AM contained allyl maleate as additional monomer. The molar ratios between allyl ether, maleic anhydride and allyl maleate were 1:1:0 (for APEG-34) or 1:1:1 (for APEG-34AM) respectively.

The fifth PCE sample (IPEG-25) was a copolymer of acrylic acid and ω-hydroxy polyethylene glycol isoprenyl ether (IPEG) with 25 EO units in the side chain. Again, the molar ratio was adjusted for maximum dispersing performance and was 2.7:1 (acrylic acid : IPEG ether).

All polymers were self-synthesized. For preparation of the MPEG PCEs, two solutions were prepared, one containing the MPEG-MA ester, methacrylic acid and mercaptopropionic acid as chain transfer agent (solution I, 50 wt.-% in DI water). The other solution contained the radical initiator sodium persulfate (3 mol.-% relative to the monomers, 1 wt.-% in DI water, solution II). The reactor was equipped with stirrer, nitrogen inlet and thermometer and charged with a small amount (~30 mL) of DI water. The vessel was then heated to 80 °C. Using peristaltic pumps, both solutions were fed continuously into the reactor, solution I within 3 hours and solution II within 4 hours. After completion of the addition, the mixture was stirred for one more hour, cooled to ambient and neutralized with 30 wt.-% NaOH solution.

In preparation of the APEG-PCEs, all monomers were placed into a round bottom flask equipped with stirrer, heated to 90 °C and polymerized in bulk. Benzoyl peroxide was used as radical initiator. Initiator dosage was 4 mol.-% with respect to the monomers. The radical initiator was added constantly as powder in small portions over 1.5 hours. When the reaction was finished, DI water was added to yield an aqueous solution with a solid content of ~50 wt.-%. After cooling to room temperature, the samples were neutralized with 30 wt.-% NaOH solution.

The IPEG PCE was synthesized by placing the IPEG ether macromonomer as 50 wt.-% solution into the reactor as above and heated to 80 °C. Using peristaltic pumps, acrylic acid was fed into the reactor within 3 hours and the initiator solution (same amount as for MPEG

PCEs) within 4 hours. The final procedure was identical to that for the MPEG PCEs.

The chemical structures of all synthesized PCE polymers are shown in Figure 1.

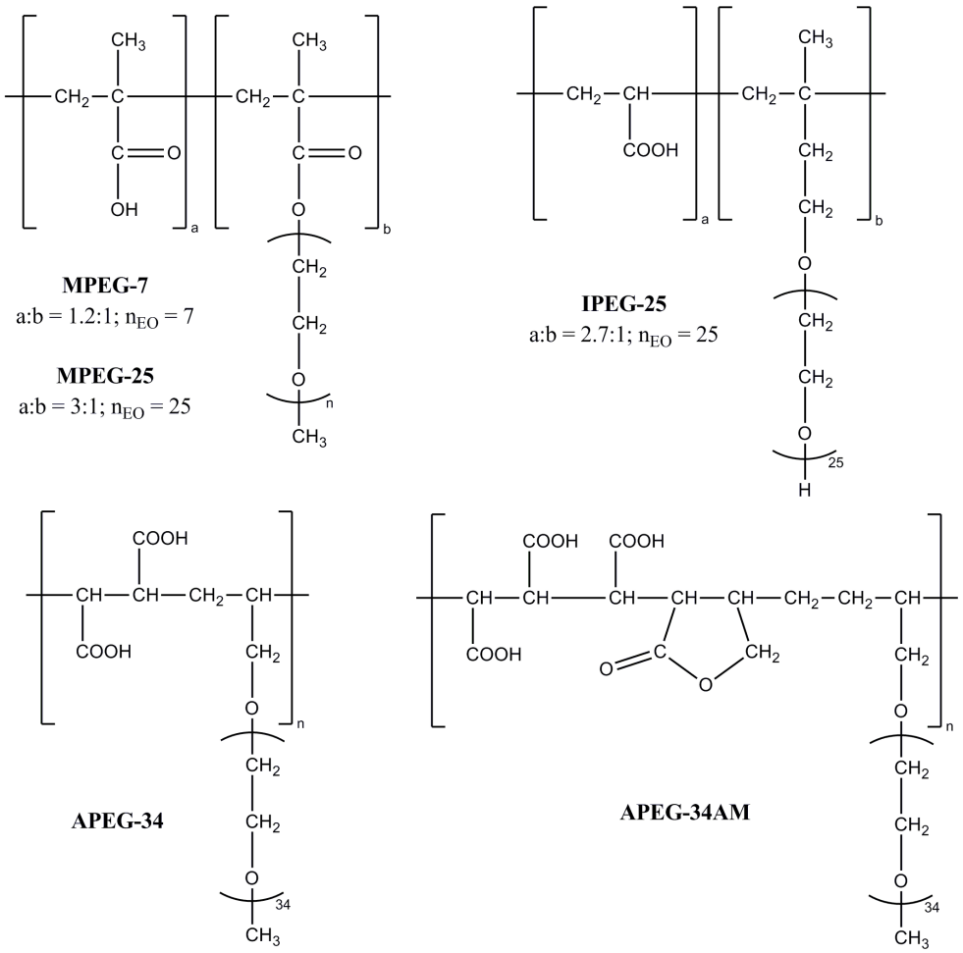

Fig. 1 Chemical structures of the polycarboxylate samples synthesized for this study

All polymer samples were used as is without further purification. The polymers were characterized by gel permeation chromatography using Waters 2695 separation module equipped with 2414 RI detector (Waters) and a Dawn EOS 3 angle light scattering detector (Wyatt Technology). A dn/dc of 0.135 mL/g was used to calculate molar masses relative to polyethylene oxide (Teresa M., *et al*, 2001). The analytical results are shown in Table 1.

Tab. 1 Analytical properties of the synthesized PCE samples

Polymer sample	M_w [g/mol]	M_n [g/mol]	PDI [M_w/M_n]	n_{EO} [mol]
MPEG-7	44,300	23,300	1.9	7
MPEG-25	67,600	28,200	2.4	25
APEG-34	63,100	22,500	2.8	34
APEG-34AM	78,400	24,500	3.2	34
IPEG-25	93,800	36,100	2.6	25

2.2. Cement

Nine different cements were selected for this study. All of them were ordinary Portland cements (CEM I) ranging from 32.5 N to 52.5 R. Additionally, an API Class G oil well cement was tested. Their phase compositions were analyzed by quantitative XRD (Rietveld) and their free lime content was assessed using the Franke method (Franke B., 1941). The cement samples were selected such as to cover a broad range of C_3A contents from 1.2 to 9.85 wt.-% (see Table 2).

Tab. 2 C_3A and CaO contents of cements, initial hydration energies and amount of ettringite gel formed in the presence of 1.0 % bwoc of PCE sample MPEG-25.

Cement sample	C_3A content	CaO (free)	Spec. surf. area (Blaine)	5 min hydration energy	100 min hydration energy	Amount of ettringite gel
	wt.-%	wt.-%	[cm²/g]	[J/g]	[J/g]	
CEM I 32.5 N	1.90	0.11	3,319	1.71	2.86	no gel
CEM I 32.5 R	9.85	0.97	3,589	14.83	23.88	very large
CEM I 42.5 N	6.00	0.15	3,889	11.66	13.65	large
CEM I 42.5 R	7.57	0.04	4,972	22.18	23.95	very large
CEM I 42.5 R HS	1.77	0.06	3,280	0.88	3.11	no gel
CEM I 52.5 N	8.04	0.03	3,299	5.49	9.67	medium
CEM I 52.5 R	8.90	0.10	4,803	25.74	31.28	very large
CEM I 52.5 R HS	1.56	0.27	4,332	0.22	5.65	no gel
API Glass G	1.20	0.10	2,998	1.99	2.75	no gel

2.3. PCE performance test

The dispersing force of the PCE samples was determined using a “mini slump test” carried out as follows: First, a constant water-to-cement ratio (w/c) of 0.3 was chosen. At this w/c ratio, the dosages of the polymers required to reach a spread of 26 ± 0.5 cm were determined. Generally, the polymers were dissolved in the required amount of mixing water placed in a porcelain cup. The amount of water contained in the PCE solution was subtracted from the amount of mixing water. Next, within 5 seconds 350 g of cement were added to the mixing water and thoroughly agitated manually for a total period of 4 minutes. The cement paste was then poured into a Vicat cone (height 40 mm, top diameter 70 mm, bottom diameter 80 mm) placed on a glass plate and the cone was lifted vertically. The resulting spread of the paste was measured twice, the second measurement being in a 90 °angle to the first and averaged to give the spread value.

When PCE was added in a delayed mode, then the cement was first mixed with water only, and the PCE solution was added after 0.5, 1 or 2 minutes respectively. Total mixing time was kept constant at 4 minutes.

2.4. Initial heat of hydration

The initial hydration energy released by the cements was determined in an adiabatic calorimeter for the first 5 minutes of hydration and in an isothermal calorimeter for the first 100 minutes of hydration. The results are presented in Table 2. The amounts of heat measured using the isothermal calorimeter are generally higher than those obtained under adiabatic conditions as hydration time was longer in the isothermal test. For both instruments, a similar trend was found. The heat flow curves obtained from the isothermal test are presented in Figure 2. Note that there, the curves for cement samples CEM I 32.5 N, CEM I 42.5 R HS and API Class G oil well cement are almost identical and therefore cannot be distinguished. In the first 5 minutes of cement hydration, the initial hydration energies vary greatly between the cements tested. They range from almost 0 J/g for CEM I 52.5 R HS to more than 25 J/g for sample CEM I 52.5 R. Furthermore, it became evident that the amount of initial hydration energy correlates well with PCE dosages: Cement samples which release substantial amounts of heat are more difficult to disperse and require higher PCE dosages. Generally, the initial hydration energies of cements possessing a very low C_3A content (< 2 % in CEM I 32.5 N, CEM I 52.5 R HS, CEM I 42.5 R HS and API Class G) are extremely low (2.75 – 5.65 J/g), suggesting that the amount of heat released is linked to this clinker phase. However, one cement exhibiting a high C_3A content of 8.04 % (sample CEM I 52.5 N) exhibits a rather low initial hydration energy of 9.67 J/g. This indicates that the amount of immediately soluble sulfate or the modification of C_3A present plays an additional role here.

The measurements on the initial hydration energy were repeated in the presence of the PCE samples to determine whether any of them affects the amount of heat released. However, no significant differences could be observed. This finding led the authors to conclude that the incompatibility phenomenon is linked to hydration products which crystallize almost immediately after the cement comes into contact with water.

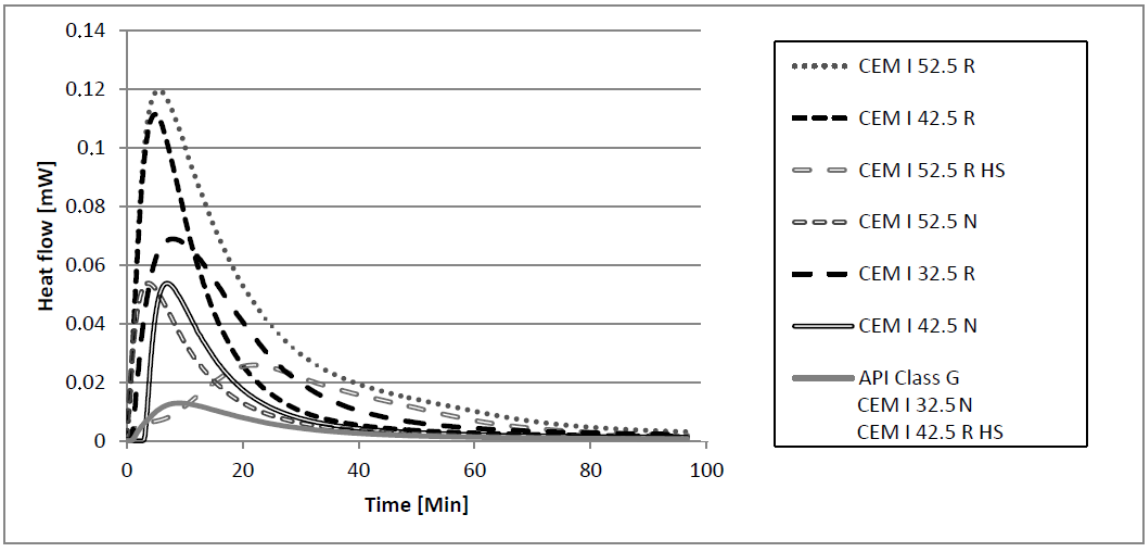

Fig. 2 Heat flow curves of neat cements (w/c = 0.5) hydrated over 100 minutes in an isothermal calorimeter.

2.5. Separation of initial ettringite gel

It was found that the initial hydration products (mainly ettringite) can be separated from the cement via centrifugation (30 minutes at 10.000 g). There, they form a gel-like top layer above the cement residue. For the separation, the same cement paste like in the "mini slump test" was prepared, except that here the w/c ratio was increased to 0.5 and PCE dosages were set constant at 1 % by weight of cement. At this high w/c ratio and PCE dosage, the cement pastes exhibit strong bleeding. After mixing, the cement paste rested for 5 minutes. Then the bleeding water (which is where a significant portion the nano-sized ettringite accumulates) was taken up using a pipette and centrifuged as described above. A gel-like top layer with ~ 85 wt.-% solids content was obtained. The gel layer was carefully removed and dried at 30 °C under atmospheric pressure. It is highly important to mildly dry the product, as ettringite easily can dehydrate to metaettringite which is X-ray amorphous (Zhou Q., *et al*, 2004). The resulting colorless powder was analyzed using X-ray diffraction (Bruker AXS D8 Advance, Karlsruhe, Germany), elemental analysis (Elementar vario EL, Hanau, Germany) and thermogravimetry (Netzsch STA 409 TG-MS, Selb, Germany).

3. Results and Discussion

3.1. Dispersion effectiveness of PCE

The dispersing force of the PCE samples was determined in a "mini slump test" using cement paste. In this test, a paste was prepared at a w/c ratio of 0.3 and the PCE dosage was adjusted to yield a slump flow of 26 ± 0.5 cm. The PCE was dissolved in the mixing water prior to cement addition. This test was carried out for the nine different cement samples and for all five PCE polymers. Table 3 shows significant variations in PCE dosages required for the different cements. Dosages of > 1 % suggest that this PCE is not able to effectively disperse the cement. It is also obvious that PCE sample APEG-34AM exhibits the most consistent performance (i.e. best cement compatibility), followed by IPEG-25. For example, for APEG-34AM the dosages vary between 0.05 and 0.31 %, and for IPEG-25 between 0.05 and 0.51 % by weight of cement (bwoc), thus indicating relatively stable performance with different cement samples. Opposite to this, the three other PCE samples exhibit much higher variations in their dosages, and they cannot fluidize at least two cement samples at all.

The data from Table 3 also clearly indicate that cement samples CEM I 32.5 R and CEM I 42.5 R seem to be most difficult to disperse. Both cements exhibit relatively high C_3A contents (9.85 % and 7.51 %). For the compatibility of PCE with these cements, the order as follows was established (C_3A content in wt.-%): API Class G (1.20 %) > CEM I 42.5 R HS (1.77 %) > CEM I 52.5 N (8.04 %) > CEM I 32.5 N (1.40 %) > CEM I 52.5 R HS (1.56 %) > CEM I 42.5 N (6.00 %) > CEM I 52.5 R (8.90 %) > CEM I 42.5 R (7.57 %) > CEM I 32.5 R (9.85 %). Yet, the C_3A content alone does not seem to represent the only criteria for incompatibility, because one cement sample (CEM I 52.5 N) possesses a high amount of C_3A (8.04 %), but still is easy to disperse.

Tab. 3. PCE dosages required in cement paste to achieve a 26 cm slump flow (w/c ratio = 0.30)

Cement sample	MPEG-7	MPEG-25	APEG-34	APEG-34AM	IPEG-25
	[PCE dosages in % by weight of cement]				
CEM I 32.5 N	0.25	0.11	0.21	0.10	0.10
CEM I 32.5 R	> 1.00	> 1.00	> 1.00	0.25	0.51
CEM I 42.5 N	0.35	0.16	0.29	0.14	0.13
CEM I 42.5 R	> 1.00	> 1.00	> 1.00	0.22	0.35
CEM I 42.5 R HS	0.15	0.09	0.14	0.08	0.08
CEM I 52.5 N	0.22	0.12	0.20	0.12	0.10
CEM I 52.5 R	> 1.00	0.90	0.45	0.31	0.26
CEM I 52.5 R HS	0.31	0.12	0.30	0.12	0.11
API Glass G black l.	0.10	0.06	0.11	0.05	0.05

Furthermore, the dispersing performance of the PCEs was looked at in a delayed addition test. As cement, the "difficult" CEM I 32.5 R sample (C_3A content 9.85 %) was used. In the following, results for PCE sample MPEG-25, a PCE with lowest cement tolerance, will be described. Its dosage was fixed at 0.20 % bowc. At first, the PCE was dissolved in the mixing water, as described above. In the other 3 tests, the PCE was added in a delayed mode after 30 seconds, 1.0 and 2.0 minutes respectively. Figure 3 shows the development of slump flow with increasing delay of PCE addition. It became apparent that the phenomenon of cement incompatibility disappears completely when the PCE sample is added only 1 min after the cement has been mixed with water. similar results were obtained when the other "incompatible" PCE samples were tested with the "difficult" cements.

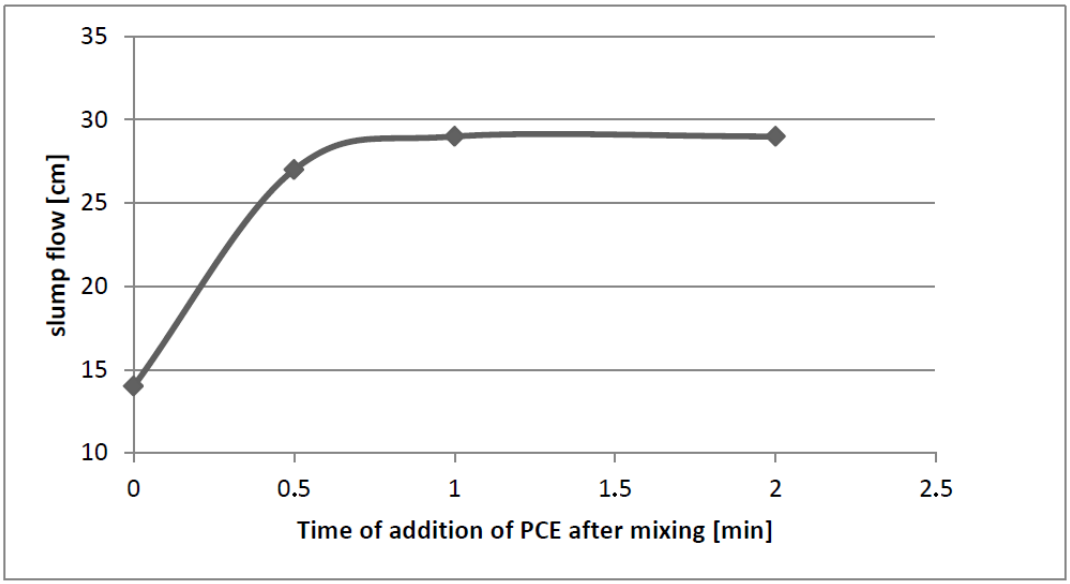

Fig. 3 Slump flow of CEM I 32.5 R (w/c = 0.3) depending on the point of addition of 0.20 % bwoc of MPEG-25 PCE

These findings allow to conclude that the phenomenon of incompatibility between specific cements and PCE polymers can be avoided when PCE is added in a delayed mode. However,

especially when formulating mortars or concretes possessing low w/c ratios, the preferred mode of addition includes placing the PCE in the mixing water to achieve faster wetting of the cement and aggregate particles, thus to reduce mixing time. Consequently, still a need exists for PCE polymers which work well with a broad diversity of cement samples, even when the PCE is placed in the mixing water.

Another conclusion from this test is that the incompatibility phenomenon seems to be linked to processes occurring during the very first seconds of cement hydration. This gave reason to study the morphology of the initially formed hydration products of cement.

3.2. Analysis of colloidal gel

By coincidence it was observed that when centrifuged for 20 minutes at 10,000 g, pastes prepared from "difficult" cements and PCEs form a white, gelous layer on top of the cement residue (Figure 4). Especially PCEs exhibiting poor cement compatibility such as MPEG-25 or APEG-34 produced a significant volume of this layer. Also, the amount of gel was especially high for the samples CEM I 32.5 R, CEM I 42.5 R and CEM I 52.5 R which before were identified as those which are difficult to disperse (Table 3). The amount of gel produced by PCE sample MPEG-25 and the cement samples are exhibited in Table 2. There, it is evident that cements which are difficult to disperse produce large amounts of this gel, and vice versa. For example, from 300 g of cement sample CEM I 32.5 R ~ 6 g of a transparent, waxy gel with a solids content of ~ 85 wt.-% were obtained. Figure 4 displays how the amount of gel can vary with cement composition (mainly the C_3A content) when PCE polymer MPEG-25, a PCE with low cement tolerance, is used.

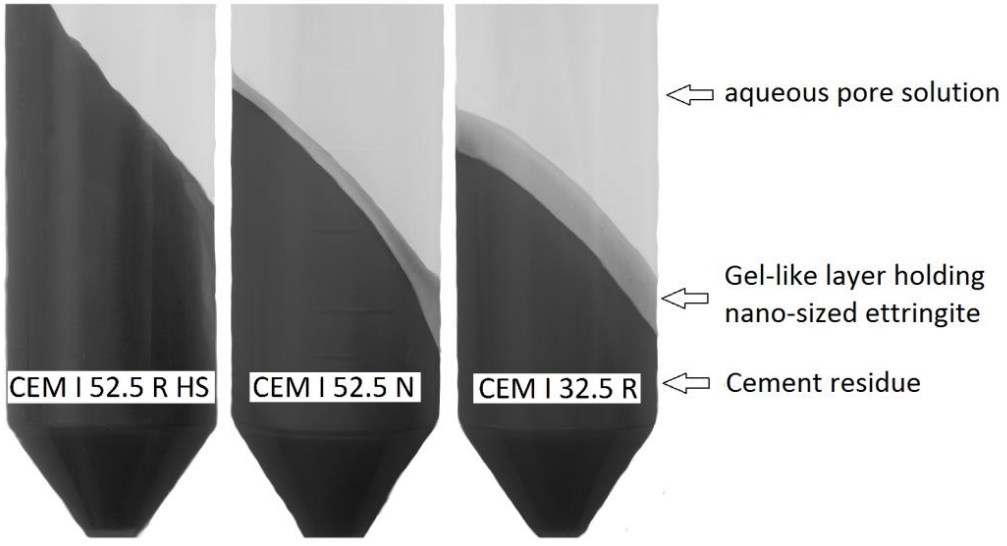

Fig. 4 Comparison of the amounts of ettringite gel obtained as top layer after centrifugation of cement paste (w/c = 0.5) prepared in the presence of 1 % bwoc of PCE sample MPEG-25 using (from left to right): CEM I 52.5 R HS (no gel), CEM I 52.5 N (medium amount) and CEM I 32.5 R (large amount of gel).

Relative to the different PCE samples, the amount of gel was very similar among the MPEG-type PCEs and for APEG-34 (= the less cement compatible PCEs). Whereas, IPEG-25 produced a slightly less volume of gel and for APEG-34AM, hardly any gel formation was detectable. Thus, based on the amounts of gel produced, the order as follows with respect to cement compatibility was established: APEG-34AM > IPEG-25 >> APEG-34 > MPEG-25 > MPEG-7. This order was in perfect agreement with the PCE dosages found ealier to be required for dispersion of those "difficult" cements (see Table 3). It also suggests that even within the same chemical group of PCE, different cement compatibilities can occur.

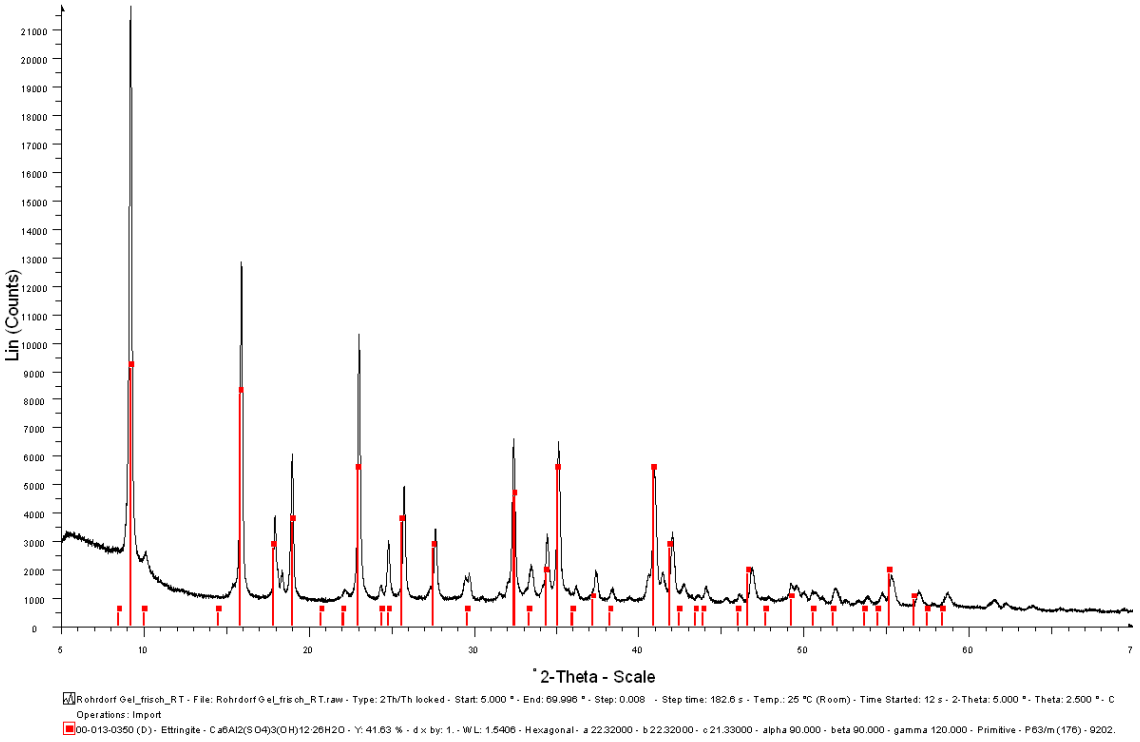

Fig. 5. XRD pattern of the colloidal gel layer formed in the presence of PCE sample MPEG-25 atop CEM I 32.5 R paste after centrifugation.

XRD analysis revealed that this gel contains pure ettringite (Figure 5), as was confirmed also by elemental analysis of the dried powder. However, in the presence of 1 % bwoc of PCE sample MPEG-25, a carbon content of 7.73 wt.-% was detected in the gel, thus indicating significant adsorption of PCE on the surface of the colloidal ettringite. The opaque appearance of the gel indicates that the ettringite crystals must be extremely small and thus can adsorb large amounts of PCE. Furthermore, TG-MS analysis of the ettringite gel containing PCE was performed (Figure 6). Dehydration of ettringite occurs in the temperature range between 100 °C and 180 °C while the PCE begins to decompose above 200 °C as evidenced by the mass signal of m/z = 44 corresponding to the release of CO_2.

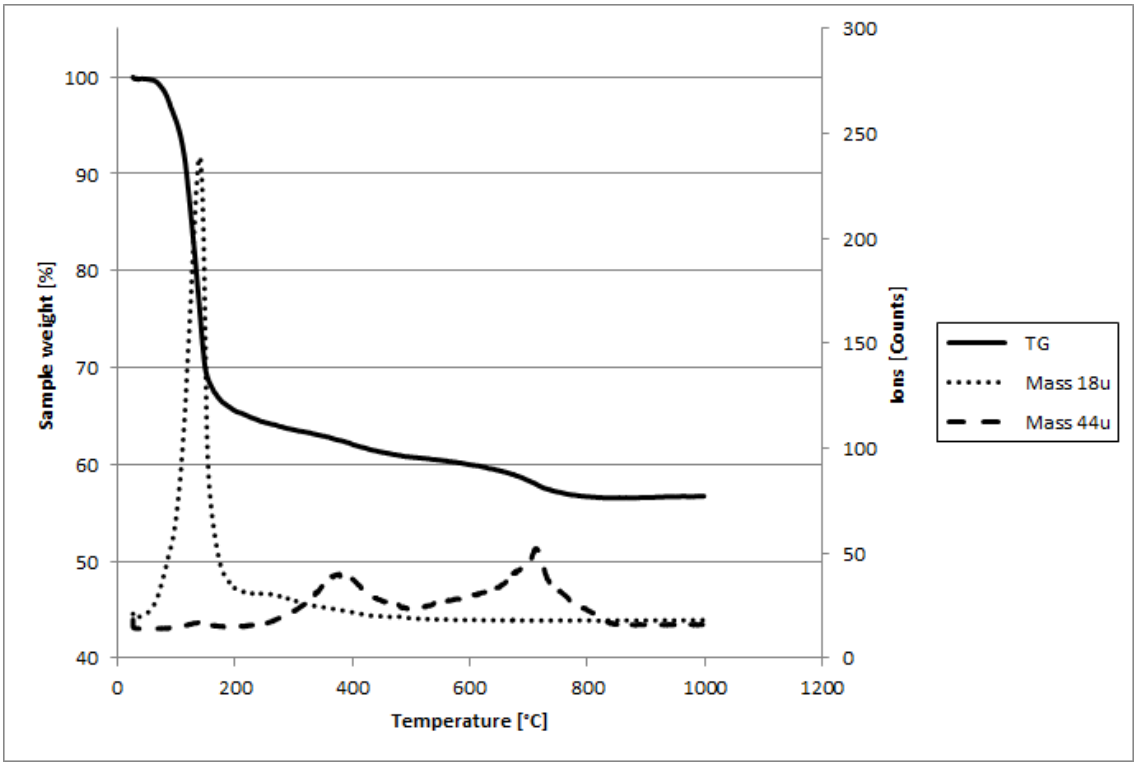

Fig. 6. TG-MS analysis of the ettringite gel produced from CEM I 32.5 R hydrated in the presence of 1 % bwoc of PCE sample MPEG-25.

Generally, an ettringite gel was not observed when no PCE was present in the cement paste. Apparently, the PCE polymers either hinder ettringite formation substantially or – more likely – act as morphological catalyst which reduces the size of the early ettringite crystals to colloidal or even nano scale. This was confirmed by SEM imaging of synthetic ettringite, precipitated in the absence and the presence of different PCE polymers (Figure 7). Please note that according to Figure 7, different PCE polymers affect the crystal size of ettringite differently.

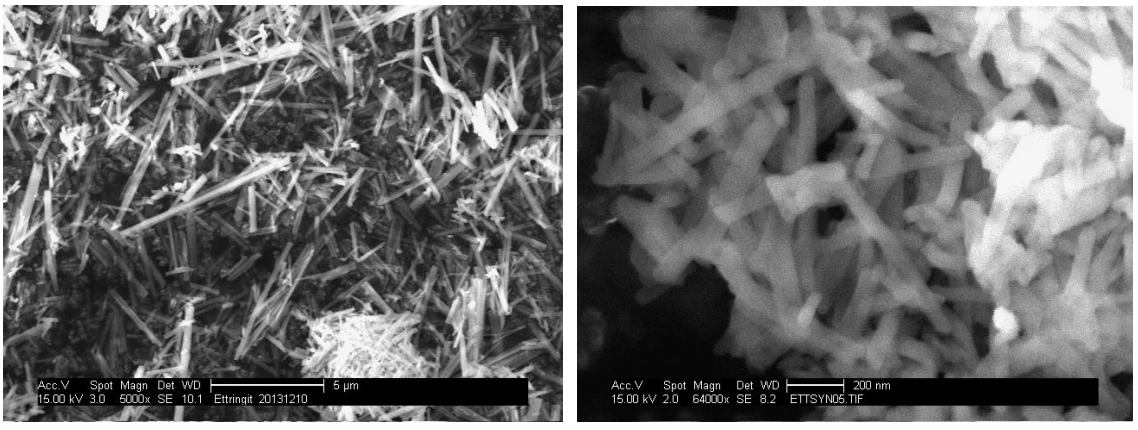

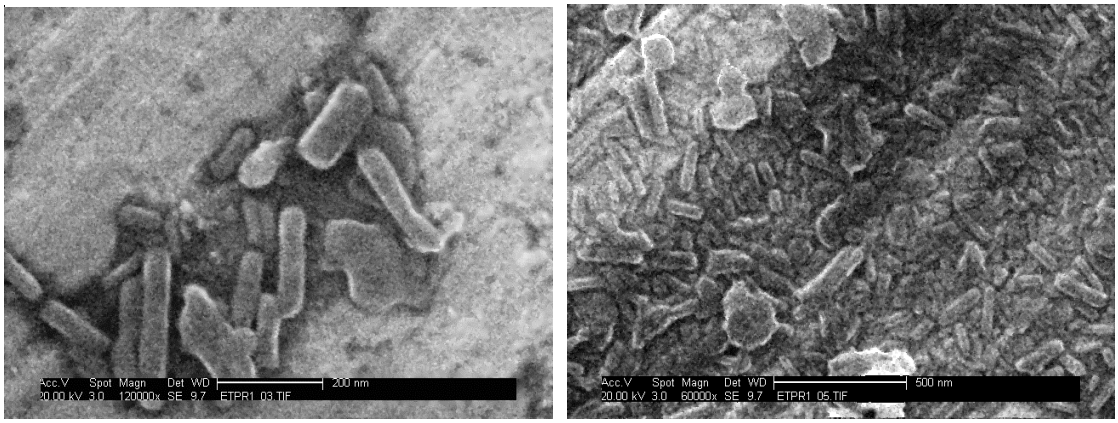

Fig. 7. SEM images of synthetic ettringite precipitated as is (top left), in the presence of PCE samples IPEG 52 (top right), MPEG – 25 (bottom left and right); magnification: 5,000x (top left), 64,000x (top right), 120,000 x (bottom left), 60,000 x (bottom right),

Furthermore, formation of the ettringite gel was studied at delayed addition of PCE sample MPEG-25. However, no ettringite gel was obtained even when the PCE was added only 30 seconds after the cement paste had been mixed. This again instigates that the incompatibility phenomenon is derived from an instantaneous interaction between cement und PCE which occurs as soon as water is added.

To summarize, the amounts of gel formed correlate well with the PCE dosages required in the performance test and also with the C_3A content of the cements. In other words, cements which are difficult to disperse normally are characterized by high C_3A content, large amounts of colloidal ettringite gel and abnormal PCE dosages. The experiments also show that specific PCE molecules can strongly impact ettringite crystallization. They act as morphological catalyst which greatly reduces the aspect ratio of the early ettringite crystals as was confirmed by SEM imaging.

For applicators of PCEs who want to find out whether poor performance of a PCE product is owed to cement incompatibility, the simple test as follows is recommended: mix the cement sample at w/c = 0.5 with water containing 1 wt.-% of your PCE polymer, then centrifuge the bleeding water of the paste for 20 min at 10,000 g. If a significant amount of opaque gel appears at the top of the centrifugate, then incompatibility between this particular cement and the admixture is confirmed. This test allows assessing whether mal-performance of a PCE product is owed to incompatibility with cement, or whether it derives from other factors such as e.g. the presence of clay impurities etc.

4. Conclusions

The study reveals that the incompatibility phenomenon occurring between PCE polymers and certain cements relies on modification of the ettringite crystal morphology. Based on these findings, “incompatibility” between a PCE and cement sample is likely to occur when the following conditions exist:

a) The cement sample exhibits an elevated C_3A content (> 7 wt.-%) and contains significant amounts of immediately soluble sulfates (alkali sulfates, $CaSO_4$ – hemihydrate) to produce large amounts of ettringite.
b) The PCE sample strongly impacts ettringite morphology and produces nano-sized instead of the common meso-sized, large crystals. The nano-sized ettringite possesses a multiple of the surface area of conventional ettringite formed in the absence of PCE, and therefore consumes large amounts of superplasticizer via adsorption.

The authors acknowledge that this study only represents a first step in understanding the complexity of this incompatibility phenomenon. For example, it will be most useful to investigate why specific PCE molecules interact differently with the different surfaces of ettringite crystals. Molecular simulations evidencing the interaction energies might be useful to establish a correlation between PCE molecular structure and ettringite morphology.

Acknowledgements
The authors greatly thank Clariant Deutschland GmbH and Nippon Oil and Fats Company for generously supplying monomers for the PCE synthesis. A. Lange also wishes to thank the "TUM Center for Advanced PCE Studies" for financing the final part of his PhD study.

References

- Agarwal S. K., et al, 2000. Compatibility of Superplasticizers with different cements. *Construction and Building Materials*, 14, 253-259.
- Aitcin P.-C., et al, 1994. Superplasticizers: How they work and why they occasionally don't. *Concrete International*, 16, 45-52.
- Bonen D., et al, 1995. The Superplasticizer Adsorption Capacity of Cement Pastes, Pore Solution Composition, and Parameters Affecting Flow Loss. *Cement and Concrete Research*, 1423 – 1434.
- Franke B., 1941. Bestimmung von Calciumoxyd und Calciumhydroxyd neben wasserfreiem und wasserhaltigem Calciumsilikat. *Zeitschrift für Anorganische und Allgemeine Chemie*, 247, 180-184.
- Hirata T., 1981. *Cement dispersant*, JP1984-18338.
- Lei L., et al, 2014. A Study on the Impact of Different Clay Minerals on the Dispersing Force of Conventional and Modified Vinyl Ether Based Polycarboxylate Superplasticizers. *Cement and Concrete Research*, 60, 1 – 10.
- Okamura, H., *et al*, 2003. Self-Compacting Concrete. *Journal of Advanced Concrete Technology*, V. 1, pp. 5-15.
- Plank J., 2012. PCE Superplasticizers – Chemistry, Application and Perspectives. *18. ibausil, Weimar, 12-15 Sep.* 1, 91 – 102.
- Plank J., et al, 2009. Effectiveness of Polycarboxylate Superplasticizers in Ultra-High Strength Concrete: the Importance of PCE Compatibility with Microsilica. *Journal of Advanced Concrete Technology*, 7, 5-12.
- Prince W., et al, 2003. Ettringite formation: A crucial step in cement superplasticizer compatibility. *Cement and Concrete Research*, 33, 635 – 641.
- Sakai E., *et al*, 2009. Relation between the Shape of Silica Fume and the Fluidity of Cement Paste

at Low Water to Powder Ratio. *Journal of Advanced Concrete Technology*, 7, 13-20.

- Schröfl, C., et al, 2008. Structure-performance relationship of polycarboxylate superplasticizers based on methacrylic acid esters in ultra high performance concrete in: Fehling, E., Schmidt, M., Stürwald, S., Ultra High Performance Concrete (UHPC). *Second International Symposium on Ultra High Performance Concrete, Kassel* 383-390.
- Teresa M., et al, 2001. Polymer characterization by size-exclusion chromatography with multiple detection. *Journal of Chromatography A*, 919, 13-19
- Yoshioka K., et al, 2002. Adsorption characteristics of superplasticizers on cement component minerals. *Cement and. Concrete Research*, 32, 10, 1507-1513
- Yoshioka k., et al, 2005. Role of Steric Hindrance in the Performance of Superplasticizers for Concrete. *Journal of the American Ceramic Society*, 80, 2667-2671.
- Zhou Q., et al, 2004. Metaettringite, a decomposition product of ettringite, *Cement and Concrete Research*, 34, 703-710.

5.6 Early hydration of portland cement admixed with polycarboxylates studied under terrestric and microgravity conditions

L. Lei, M. R. Meier, A. Rinkenburger, B. Zheng, L. Fu, J. Plank

Journal of Advanced Concrete Technology
14(3), (2016) 102-107.

This work was carried out in cooperation with another Ph. D. candidate, **Markus Meier** and a master student **Alexander Rinkenburger**.

Based on the previous finding that PCEs can act as morphological catalyst, in this study the impact of PCE polymers on the early hydration product ettringite formed on the surface of hydrating ordinary Portland cement under normal and zero gravity conditions was investigated utilizing SEM microscopy and X-ray diffraction. For this purpose, two structurally different PCE superplasticizers were selected, one was an ω-methoxypoly(ethylene glycol) methacrylate (MPEG) ester based PCE and the other one was an α-methallyl-ω-methoxypoly(ethylene glycol) (HPEG) ether based PCE. The experiments were performed on parabolic flights sponsored by Deutsches Zentrum für Luft- und Raumfahrt (DLR).

It was found that both PCE polymers cause a particularly strong effect on the morphology of ettringite crystals, which can be summarized as follows:

– Under different gravity conditions (normal gravity and microgravity), both PCE polymers act as morphological catalyst and reduce the size (length, diameter) of the ettringite crystals.

– The aspect ratio of the ettringite crystals obtained from the cement paste admixed with both PCE polymers decreases under microgravity conditions compared to that from 1 g. Furthermore, at 0 g the ettringite crystals became more stocky.

Journal of Advanced Concrete Technology Vol. 14, 102-107 March 2016 / Copyright © 2016 Japan Concrete Institute 102

Scientific paper

Early Hydration of Portland Cement Admixed with Polycarboxylates Studied Under Terrestric and Microgravity Conditions

Lei Lei[1], Markus R. Meier[2], Alexander Rinkenburger[3], Zheng Baicun[4], Fu Lefeng[5] and Johann Plank[6*]

Received 9 October 2015, accepted 10 March 2016 doi:10.3151/jact.14.102

Abstract

The crystallization of ettringite at very early cement hydration (hydration period ~ 10 s) was studied under normal and zero gravity condition utilizing SEM microscopy. Furthermore, the impact of two polycarboxylate superplasticizers (one methacrylate ester-, one methallyl ether - based) on ettringite crystallization was investigated. It was found that under microgravity attained on parabolic flights, generally smaller, but a larger amount of ettringite crystals is formed resulting from the absence of convection and ion diffusion limited crystal growth. Furthermore, the PCE polymers were found to act as morphological catalysts for ettringite even under zero gravity condition.

1. Introduction

The process of nucleation and crystallization of minerals is described by two divergent theories – the "nucleation theory" and the more current "cluster theory" (Gibbs 1876; Frenkel 1939; Zeldovich 1943; Vekilov 2010a). Key parameter of the classical "nucleation theory" is the "critical radius" of an early metastable nucleus. This radius is reached when the volume energy of a nucleus becomes larger than its surface energy. Only nuclei possessing a radius larger than the critical radius can grow, whereas nuclei with a smaller radius dissolve again. The "cluster theory" postulates a mechanism involving "precritical clusters" or "pseudo phases" which act as a precursor. Contrary to the "nucleation theory", these phases are assumed to be stable and already exhibit the final crystal structure. After additional aggregation "postcritical nuclei" are built which form the basis for further crystal growth (Galkin *et al*. 2007; Vekilov 2010b). Under normal gravity, the necessary transport of the building units (ions or molecules) occurs via diffusion and convection. In case of zero gravity, the convection phenomenon disappears and crystal growth becomes diffusion controlled only.

So far, surprisingly few experiments on crystallization under microgravity conditions have been performed, probably because of the high cost of such experiments. They were performed at the international space station (ISS) and include the crystallization of NaCl and of a large number of proteins and viruses (Fontana *et al*. 2011; McPherson 1993). For the latter, much more homogeneous and defect-free crystals were obtained. This was attributed to the absence of convection. Under zero gravity, crystal growth only relies on ion transport via diffusion and thus the growth becomes slower.

Ettringite presents the main anchoring site for superplasticizers (Plank *et al*. 2007). To understand its crystal growth and surface properties constitutes a key to clarify the interaction of such polymers with ettringite and to determine the factors influencing their performance more profoundly. Here, on parabolic flights which produce microgravity conditions for 22 s, the crystal growth and morphology of ettringite crystals were compared with those crystallized in the earth's gravity field. Using ordinary Portland cement admixed with two different PCE superplasticizers based on methacrylate ester and methallyl ether macromonomers we hoped to produce more regular, defect-free ettringite crystals as a result of better controlled growth conditions instead of the flash precipitation which occurs under terrestric conditions. Furthermore, from these experiments it was hoped to obtain a better understanding of cement-admixture interaction.

2. Methods and Materials

2.1 Materials

2.1.1 Cement samples

The cement used in this study was an ordinary Portland

[1]PhD Candidate, Chair for Construction Chemistry, Technische Universität München, Garching, Germany.
[2]PhD Candidate, Chair for Construction Chemistry, Technische Universität München, Garching, Germany.
[3]Master of Science, Chair for Construction Chemistry, Technische Universität München, Garching, Germany.
[4]Professor, Shanghai Sunrise Polymer Materials Co., Ltd Shanghai, China.
[5]PhD, Shanghai Sunrise Polymer Materials Co., Ltd. Shanghai, China.
[6]Professor, Chair for Construction Chemistry, Technische Universität München, Garching, Germany.
*Corresponding author,
E-mail: sekretariat@bauchemie.ch.tum.de

cement CEM I 42.5 R provided by Schwenk Zement KG (Ulm, Germany) from their Allmendingen plant. Its phase composition as determined *via* Q-XRD using *Rietveld* refinement is exhibited in **Table 1**. In the experiments on cement hydration, a water-to-cement ratio of 1.0 was utilized.

2.1.2 Superplasticizer samples

In this study, two commercially available polycarboxylate (PCE) based superplasticizers ("Vivid® 500 A" and "Vivid® 500 C", provided by Shanghai Sunrise Polymer Materials Co., Ltd.) were utilized. These samples were selected because they represent highly effective and commonly used PCE products.

Vivid® 500 A constitutes a MPEG type PCE based on ω-methoxypoly(ethylene glycol) methacrylate ester possessing mixed side chains of MPEG - 1000 ($n_{EO} = 23$) and MPEG - 2000 ($n_{EO} = 45$). The molar ratio of MPEG - 1000 to MPEG - 2000 was 0.8:1 while the molar ratio of methacrylic acid to ω-methoxypoly (ethylene oxide) methacrylate ester was 3.6:1. This sample was designated as S1.

Vivid® 500 C is a HPEG type PCE based on α-methallyl-ω-methoxypoly(ethylene glycol) ether possessing a side chain of HPEG - 2400 (n_{EO} = 54). The molar ratio of acrylic acid to the HPEG macromonomer was 3.2:1. Henceforth, this sample will be labelled as S2.

The molecular properties of the two polymers are presented in **Table 2** and the SEC spectra are shown in **Fig. 1**.

2.2 Experimental methods

The 0 *g* cement hydration experiments were conducted onboard a modified Airbus A 300 aircraft conducting parabolic flight maneuvers. The parabolic flight campaign was initiated by Deutsches Zentrum für Luft- und Raumfahrt (DLR, German Aerospace Center). For the

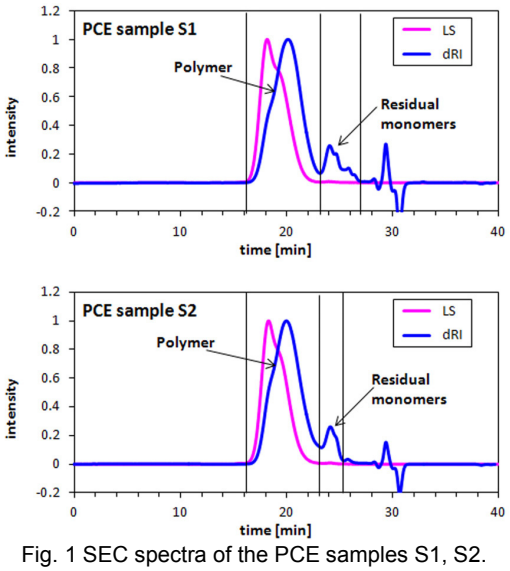

Fig. 1 SEC spectra of the PCE samples S1, S2.

Table 1 Phase composition of the CEM I 42.5 R sample as determined by Q-XRD analysis.

Phases	CEM I 42.5 R
C_3S, m	58.83
C_2S, m	17.01
C_3A, c	3.61
C_3A, o	1.60
C_4AF, o	9.43
Free lime, *Rietveld*	0.09
Free lime, *Franke*	0.06
Periclase	0.66
Anhydrite	1.83
Hemihydrate (TG)	0.27
Dihydrate (TG)	2.42
Calcite	2.80
Quartz	0.36
Arcanite	1.04
Sum	100.02

experiments presented in this work, 15 parabolas were needed. The trajectory and the different gravity periods which occur during one parabola are illustrated in **Fig. 2**. The parabola starts with the plane ascending from an altitude of around 6,000 m to 8,500 m. During this period which last ~ 24 seconds hypergravity occurs in two phases. In the "pull - up" phase, gravity is 1.8 *g* until the airplane reaches an ascending angle of 30°. After this, gravity drops to 1.5 *g*. The hypergravity period ends when the plane achieves a gradient angle of 47°. At this angle (pilot audio command: "injection"), a transition period commences where the gravitational force drops from 1.5 *g* to 0 *g* within ~ 4 seconds. During the following 22 seconds microgravity conditions exist and the experiments were conducted. After the top of the parabola is reached, the aircraft descends and again accelerates strongly whereby hypergravity occurs again. At an inclination angle of 30°, the "pull-out" (pilot audio command) takes place until the plane is reaching a horizontal position. In this section which also lasts around 22 seconds, gravity again becomes ~ 1.8 *g*.

The device developed for conducting the cement hydration experiments onboard consists of three syringes (BD Discardit II 20 mL, Becton Dickinson, Franklin Lakes, New Jersey, USA) connected with a three-way valve (**Fig. 3**). The dead volume was minimized (1 mL) by keeping the pipe lengths as short as possible. Syringe #1 was used as reactor holding the cement (5 g) whereas

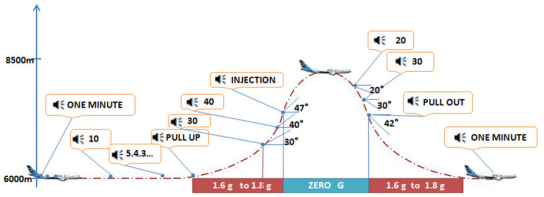

Fig. 2 Flight pattern performed by the air-craft during one parabola.

Table 2 Characteristic properties of the PCE samples S1, S2.

Sample		Yield [%]	M_w [g mol^{-1}]	M_n [g mol^{-1}]	PDI -	Anionic charge density [μeq g^{-1}]
S1	MPEG PCE	87	75,000	31,000	2.4	2,958
S2	HPEG PCE	90	75,000	30,000	2.5	2,024

Table 3 Average length, width and aspect ratio of ettringite crystals obtained from CEM I 42.5 R sample, hydrated for 10 s, 30 s and 60 s under terrestric condition.

Hydration time	Gravity Condition	Length [nm]	Width [nm]	Aspect Ratio
10 s	1 *g*	676 ± 185	192 ± 42	3.6 ± 0.9
30 s	1 *g*	698 ± 144	191 ± 29	3.6 ± 0.9
60 s	1 *g*	758 ± 206	206 ± 67	3.8 ± 0.6

syringe #2 contained the mixing water including the PCE (6 mL, w/c = 1, 1 mL death volume). Syringe #3 contained acetone (10 mL) to stop the hydration reaction. All syringes were loaded at the ground laboratories prior to the flight. To separate the pore solution and retain the cement particles, syringe #1 was equipped with a filter paper (MN520, thickness 1.5 mm, Macherey-Nagel, Düren, Germany).

Figure 4 shows how the experiments were conducted onboard the aircraft, with two experimenters operating the devices and the third one controlling the timing. As the experiments were performed manually it was expected that reaction times might vary at ± 1 sec between different samples. To ensure that such deviations did not impact the results, tests were performed in the laboratory including hydration times of 5 sec, 10 sec, 20 sec, 30 sec, 45 sec and 1 min. There it was found that between 5 sec and 1 min the crystal sizes were the same. There it was found that between 5 sec and 1 min the crystal sizes and amounts were comparable. As examples, **Table 3** presents the data on the crystal dimensions observed after 10 sec, 30 sec and 1 min reaction time. Apparently, ettringite crystallizes instantaneously because of its extreme low solubility (solubility product L = 10^{-44} g^{-3} L^{-3}) and then enters a dormant period.

2.3 Analysis of samples

2.3.1 SEM imaging

This technique was applied to determine the amount of ettringite present on the surface of the cement particles and its morphology as well as crystal size of ettringite present on the surface of the cement particles. SEM images were recorded on a FEI 30 FEG environmental scanning electron microscope from FEI/ Philips, Eindhoven/NL. Each experiment was repeated three times (on parabolic flights) or six times (in the laboratory at 1 *g*) to ensure universality of the results. Furthermore, from every sample at least five different parts were looked at to ensure that only representative images were evaluated. All samples were fixed on the sample holder by using a carbon dispersion. Imaging was carried out at an accelerating voltage of 4 kV (spot size 2) and at working distances of 6 - 7 mm and a tilt angle of 20°. Generally, images were captured at 10,000 x, 20,000 x and 40,000 x magnification.

For quantification of the amount of ettringite formed, images from representative surface areas of cement (12 × 9 μm) at a magnification of 10,000 × were taken, and the amount of ettringite formed from the neat cement at 1 *g* was set as 100 % (reference).

2.3.2 X-ray diffraction

Samples were analyzed in the range of 5 - 70° 2θ using a Bruker AXS D8 Advance instrument (Bruker, Karlsruhe, Germany) with *Bragg-Brentano* geometry and Cu Kα source (30 kV, 35 mA).

For quantification of the amount of ettringite formed, a

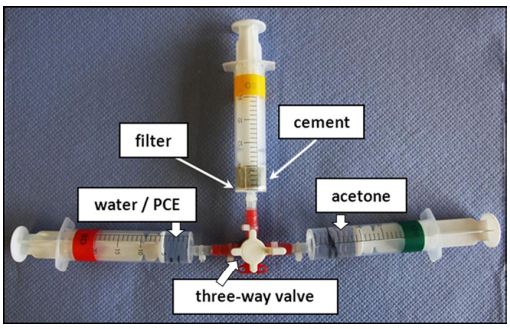

Fig. 3 Experimental device used to perform the cement hydration experiments.

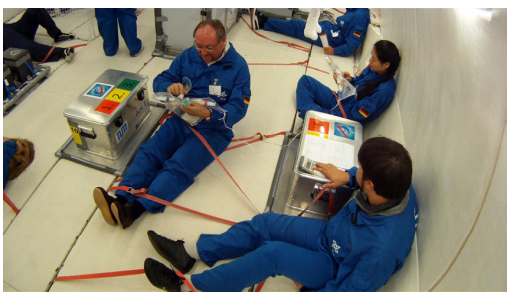

Fig. 4 Conducting the experiment on early ettringite crystallization onboard the zero g airplane. Note that all experimenters are fixed to avoid free floating during the zero gravity period.

method described in the literature for clay minerals was adopted (Bhaskar *et al*. 1994). Here, the characteristic ettringite reflection at 9° 2θ was analyzed with a polynom of 2nd order and smoothed using a 15 point *Savitzky-Golay* filter. The data were then subjected to an impulse analysis. The average intensity from three independent measurements was reported as final value.

3. Results and discussion

3.1 Cement hydrated without PCE

Evaluation of the SEM images revealed that on the surface of the cement sample, even after the very short hydration period of 10 seconds, numerous nano-sized ettringite crystals had formed (**Fig. 5**). The crystals showed the typical hexagonal prismatic shape and were statistically distributed across the surface of the cement particles. XRD analysis (**Fig. 6**) revealed that at 1 *g* and 0 *g* conditions, no other crystalline cement hydrate has been formed apart from ettringite.

Furthermore, by integrating the peak areas in the XRD spectra as described in section 2.3.2, the amount of ettringite produced at 1 *g* and 0 *g* condition revealed that under microgravity, ~ 15 % more crystals were formed (**Fig. 7**).

To characterize the crystal morphology, also the aspect ratio (the ratio between crystal length and width) were looked at (**Fig. 8**). At 0 *g*, both the length as well as the diameter of the crystals decreased significantly (**Fig. 8, left**). However, the aspect ratios did not change much (**Fig. 8, right**).

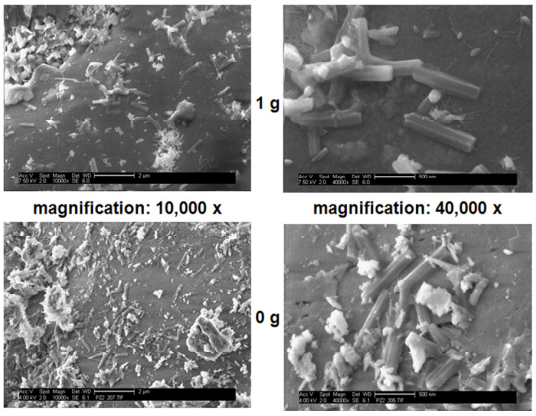

Fig. 5 SEM images of CEM I 42.5 R sample hydrated for 10 s under terrestrial (top) and zero gravity (bottom) conditions.

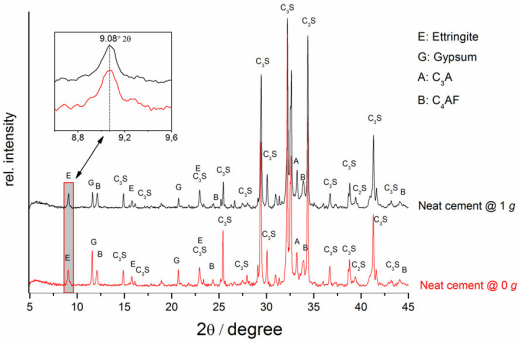

Fig. 6 X-ray diffractograms of CEM I 42.5 R sample, hydrated for 10 s at 1 *g* and 0 *g* (w/c = 1.0).

3.2 Cement hydrated in the presence of PCEs

Recently it has been described that polycarboxylate-based superplasticizers can act as strong morphological catalyst for ettringite, and that they can impact the size as well as the aspect ratio of the crystals (Large and Plank 2015a; Large and Plank 2015b; Dalas *et al*. 2015). In the first work, the authors present that this effect greatly depends on the PCE type and structural specifics. To account for such differences, in this study one ω-methoxypoly(ethylene glycol) methacrylate (MPEG) ester based PCE (sample S1) and one α-methallyl-ω-methoxypoly (ethylene glycol) (HPEG) ether based PCE (sample S2) were selected.

SEM imaging revealed that under normal gravity, the ettringite crystals obtained from the cement paste admixed with polymer S1 exhibit an average length of ~ 600 nm which is smaller than that from the neat cement hydrated in the absence of PCE (~ 800 nm) (**Figs. 9**, **11**). The diameters of the crystals lie at ~ 130 nm which

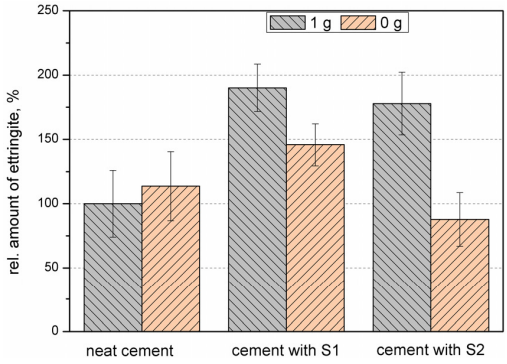

Fig. 7 Relative amounts of ettringite formed from CEM I 42.5 R sample in the absence and presence of the PCE samples S1 and S2, respectively at 1 *g* and 0 *g* condition; 100 % corresponds to the amount of ettringite formed by the neat cement at 1 *g*.

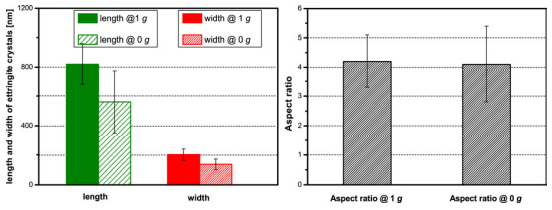

Fig. 8 Average length, width (left) and aspect ratio (right) of ettringite crystals obtained from CEM I 42.5 R under 1 *g* and zero *g*, respectively.

compares with ~ 200 nm for those from the neat cement paste. It is obvious that in the presence of PCE polymers, much smaller ettringite crystals are generated. Similar results were obtained for polymer S2 (**Figs. 10**, **11**). There, both the length and width decreased compared to that grown in the neat cement paste. The experiments suggest that both PCE polymers act as morphological catalyst and reduce the size (length, diameter) of the ettringite crystals by 25 - 30 %.

Similar results were found under zero gravity. The size of ettringite crystals obtained from the cement paste admixed with polymer S1/ S2 decreases compared to the ones grown on the surface of the neat cement paste.

Another observation from SEM imaging was that at zero gravity and in the presence of the PCE polymers, the ettringite crystals became more stocky than those under terrestric gravity, thus suggesting that the aspect ratio had decreased.

Furthermore, compared to 1 *g*, the amount of ettringite produced at 0 *g* decreased when the PCE polymers were present, as is illustrated in **Fig. 7**. This observation was confirmed by quantitative XRD analysis (spectra not shown here).

The experiments allow to conclude that under zero gravity, the presence of PCE polymers generally leads to smaller ettringite crystals as compared to terrestric gravity.

Also, under microgravity the aspect ratio of the crystals grown in the presence of the PCE polymers (S1/S2) had decreased compared to terrestric condition. In other words, the ettringite crystals became more stocky (**Fig. 12**).

Whereas for the neat cement, under different gravity conditions, the aspect ratio had remained nearly constant (**Fig. 12**). Furthermore, in the presence of PCE polymers the amount of ettringite formed at zero gravity is always less than of terrestric gravity, as is illustrated in **Fig. 7**. All this points to the fact that PCE polymers can impact the crystal growth of early ettringite which presents the main anchoring site for most concrete admixtures. Apparently, because at zero gravity condition convection and sedimentation are absent, the transport of PCE

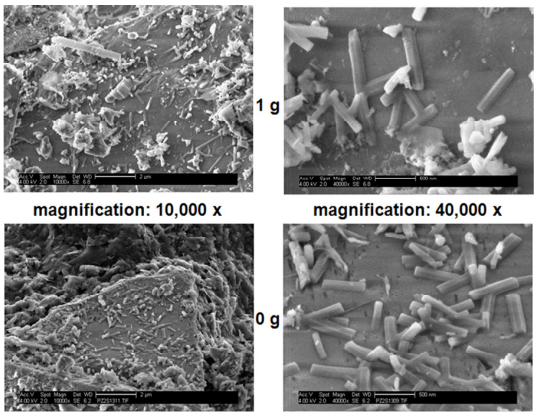

Fig. 9 SEM images of CEM I 42.5 R sample admixed with PCE polymer S1, hydrated for 10 s under terrestric (top) and zero gravity (bottom) conditions.

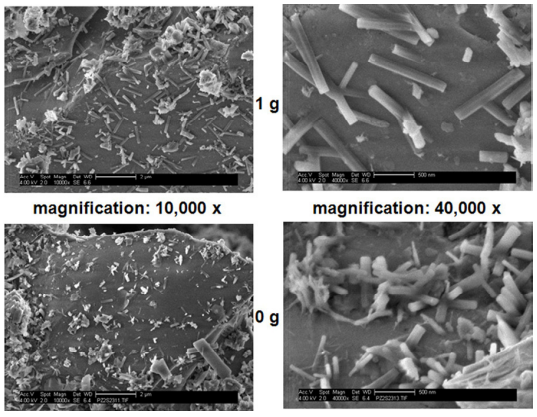

Fig. 10 SEM images of CEM I 42.5 R sample admixed with PCE polymer S2, hydrated for 10 s under terrestric (top) and zero gravity (bottom) conditions.

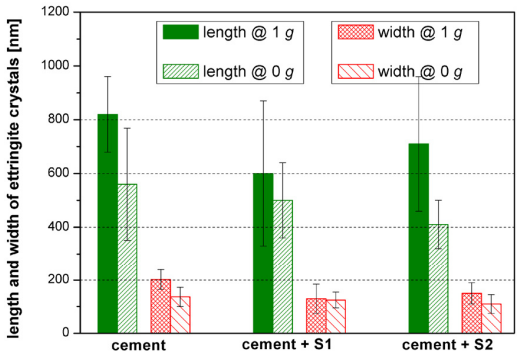

Fig. 11 Average length, width of ettringite crystals obtained from CEM I 42.5 R admixed with PCE polymers S1 or S2 grown under 1 *g* and zero *g* conditions, respectively.

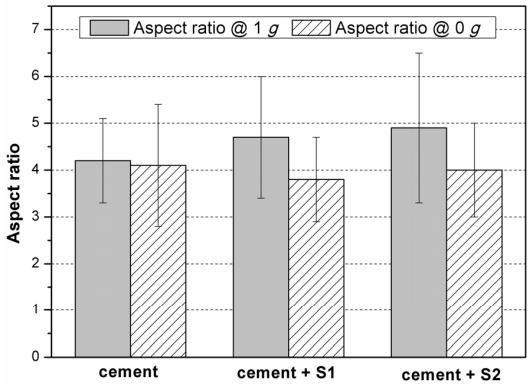

Fig. 12 Average aspect ratios of ettringite crystals obtained from CEM I 42.5 R admixed with PCE polymers S1 or S2, grown under 1 *g* and zero *g* conditions, respectively.

polymers to the surface of the ettringite nuclei is strictly diffusion controlled and therefore crystal growth is decelerated.

It should be noted that the results reported here are linked to the specific cement sample tested. Other cement samples may produce different ion concentrations and pH values in the pore solution which influences the growth of ettringite (Goetz-Neunhoeffer *et al*. 2006). However, the principle findings relative to the difference between the terrestric and micro gravity conditions have been confirmed in a recent flight campaign for other cement samples as well.

4. Conclusions

The impact of polycarboxylate superplasticizers possessing different chemical compositions on ettringite crystallization during early hydration of a CEM I 42.5 R sample was investigated under terrestric and microgravity conditions.

For the neat cement it was found that under microgravity conditions, the ettringite crystals generally become smaller. This is caused by the absence of convection which decelerates crystal growth. The growth rate of the crystals is then limited by ion diffusion. However, for neat cement the aspect ratio of crystals formed at 0 *g* is quite comparable to that under terrestric gravity.

PCE polymers cause a particularly strong effect on the morphology of ettringite crystals, which can be summarized as follows:

1. PCE polymers always (independent of gravity condition) act as morphological catalyst and reduce the size (length, diameter) of ettringite crystals.
2. The aspect ratio of ettringite crystals obtained from the cement paste admixed with PCE polymers under microgravity conditions decreases compared to that from 1 *g*. The ettringite crystals became more stocky.

The results signify that if mankind ever considers to construct on moon or mars by using a crystallizing binder, then experiments investigating the effect of reduced gravity conditions on the microstructure and the mechanical properties of the hardened material need to be checked.

Acklowledgement

The authors are most grateful to DLR for sponsoring the parabolic flight campaign which allowed us to perform these experiments. In this respect, the support received from Dr. Ulrike Friedrich and Dr. Rainer Forke is especially acknowledged. Our thanks also go to Frederic Gai from Novespace, Bordeaux whose advice on the experimental design with respect to feasibility on the aircraft was invaluable. Furthermore, L. Lei wishes to thank the Jürgen Manchot Foundation for generously providing a scholarship to finance her research at TU München.

References

Bhaskar, R., Li, J. and Xu, L., (1994). "A Comparative Study of Particle Size Dependency of IR and XRD Methods for Quartz Analysis." *American Industrial Hygiene Association Journal*, 55(7), 605-609.

Dalas, F., Pourchet, S., Rinaldi, D., Nonat, A., Sabio, S. and Mosquet M., (2015). "Modification of the rate of formation and surface area of ettringite by polycarboxylate ether superplasticizers during early C_3A-$CaSO_4$ hydration." *Cement and Concrete Research*, 69, 105-113.

Fontana, P., Schefer, J. and Pettit, D., (2011). "Characterization of sodium chloride crystals grown in microgravity." *Journal of Crystal Growth*, 324, 297-211.

Frenkel, J., (1939). "A general theory of heterophase fluctuations and pretransition phenomena." *The Journal of Chemical Physics*, 7(7), 538-547.

Galkin, O., Pan, W., Filobelo, L., Hirsch, E., Nagel, R. L. and Vekilov P. G., (2007). "Two-step mechanism of homogeneous nucleation of sickle cell hemoglobin polymers." *Biophysical Journal*, 93(3), 902-903.

Gibbs, J. W., (1876). "Equilibrium of Heterogeneous Substances." *Trans. Connect. Acad. Sci.*, 3, 108-248.

Goetz-Neunhoeffer, F., Neubaue,r J. and Schwesig, P., (2006). "Mineralogical characteristics of ettringites synthesized from solutions and suspensions." *Cement and Concrete Research*, 36, 65-70.

Lange, A. and Plank, J., (2015a). "Formation of nano-sized ettringite crystals identified as root cause for cement incompatibility of PCE superplasticizers." In: Sobolev K, Shah, S. P. (Eds.), *Nanotechnology in Construction - Proceedings of NICOM5,* Chicago (USA), 55-63.

Lange, A. and Plank, J., (2015b). "A study on the cement compatibility of PCE superplasticizers." In: Malhotra, V. M., Gupta, P. R., Holland, T. C. (Eds.), *11th CANMET/ACI Conference on Superplasticizers and Other Chemical Admixtures in Concrete (Proceedings)*, ACI SP-302, Ottawa (Canada), 401-414.

McPherson A., (1993). "Virus and protein crystal growth on earth and in microgravity." *Journal of Physics D - Applied Physics*, 26(8), 104-112.

Plank, J., Chatziagorastou, P., Hirsch, C., (2007). "New model describing distribution of adsorbed superplasticizer on the surface of hydrating cement grain." *Journal of Building Materials* (China) 10, 7-13.

Vekilov, P. G., (2010a). "Nucleation." *Crystal Growth & Design*, 10(12), 5007-5019.

Vekilov, P. G., (2010b). "The two-step mechanism of nucleation of crystals in solution." *Nanoscale*, 2(11), 2346-2357.

Zeldovich, J. B., (1943). "On the theory of new phase formation: cavitation." *Acta Physicochim. URSR*, 18, 1-22.

5.7 Use of a nano clay for early strength enhancement of Portland cement

S. Baueregger, **L. Lei**, M. Perello, J. Plank

5th International Symposium on Nanotechnology in Construction
(NICOM5)
May 24 – 26, 2015, Chicago (USA)
Proceedings, 199 – 206.

This work was carried out in cooperation with another Ph. D. candidate, **Stefan Baueregger**, and Dr. **Margarita Perello** from Dow Europe GmbH, Horgen, Switzerland.

In this paper, the use of commercial nano kaolin as an efficient enhancer for the early strength (16 hours) of cement was studied. At first, the compressive and tensile strengths of mortars prepared from CEM I 52.5 N with the addition of two different nano clay samples were tested.

The results showed that both 16 h compressive and tensile strength were greatly increased due to the addition of the nano clay samples. The reason behind is that nano clay can act as seeding material which can reduce the activation energy to almost zero, thus the formation of C-S-H occurs much earlier than in normal cement. Heat flow calorimetry and X-ray diffraction experiments revealed that the nano clay in particular activates the hydration of the silicate phases C_3S and C_2S. In addition, the early strength enhancing ability directly correlated to the particle size of the nano clay. Only nano sized kaolin possessing a particle size < 250 nm can boost the early strength of Portland cement.

Use of a Nano Clay for Early Strength Enhancement of Portland Cement

Stefan Baueregger, Lei Lei, Margarita Perello, and Johann Plank

Abstract In this study it is reported that additions of kaolin, a natural and abundant clay mineral, can significantly increase the early strength of Portland cements. Its effectiveness greatly depends on the particle size which ideally should be less than 500 nm. For example, 5 % by weight of cement of nano-sized kaolin (d ~ 200 nm) increased the 16 h compressive and tensile strengths of a CEM I 42.5 R sample by 50 % and 60 % respectively. Strength enhancement occurs predominantly in slower reacting cements (CEM I 32.5, 42.5). Analysis via heat flow calorimetry and X-ray diffraction revealed that the nano clay in particular activates the hydration of the silicate phases C_3S and C_2S. Furthermore, rheological measurements evidenced an only minor effect on mortar viscosity. The results suggest that nano-sized kaolin represents an inexpensive additive which can boost the early strength of Portland cement without negatively affecting workability and other properties.

Keywords Cement • Nano kaolin • Strength enhancement

1 Introduction

Nanoparticles (e.g. nano silica) are known to increase the strength and durability of concrete or mortar. Capillary pores present in the cementitious matrix are filled with these nano particles resulting in an optimized packing density of the microstructure. Thus, strength of the hardened cement is enhanced and permeability is decreased by this filling effect. A typical application of micro and nano silica is ultra-high performance concrete (UHPC) where the interstitial spaces between cement and aggregates are filled completely with graded solids [1–5].

S. Baueregger • L. Lei • J. Plank (✉)
Construction Chemistry, Technische Universität München,
Lichtenbergstraße 4, 85747 Garching, Germany
e-mail: sekretariat@bauchemie.ch.tum.de

M. Perello
Dow Europe GmbH, Bachtobelstraße 3, 8810 Horgen, Switzerland
e-mail: mperello1@dow.com

K. Sobolev, S.P. Shah (eds.), *Nanotechnology in Construction*,
DOI 10.1007/978-3-319-17088-6_25

Furthermore, also nano C-S-H crystals (X-Seed®, BASF) prepared through templating with PCE superplasticizers were found to accelerate the silicate reaction of cement significantly and therefore enhance the early strength. The main advantage of this product compared to conventional accelerators is that the final strength is not negatively impacted which is the major drawback of e.g. calcium salts such as $CaCl_2$, $Ca(NO_3)_2$ or $Ca(HCOO)_2$. When dispersed in the cement pore solution these nano C-S-H particles initiate the crystallization of C-S-H by acting as seeding crystals. Owed to this homogeneous nucleation, the activation energy for C-S-H crystallization from cement is reduced, leading to accelerated formation of hydrate phases and early setting [6, 7].

Clay minerals which represent aluminosilicates are known to decrease the workability of concrete or mortar severely. Especially harmful is montmorillonite which can chemically sorb conventional polycarboxylate superplasticizers in its interlayer region [8]. Additionally, clay minerals decrease the final strength of concrete. Their layered structure and high surface area allow the incorporation and sorption of large quantities of water molecules, leading to a swelling of the clay particles. This way, workability is decreased by the significant water consumption and the microstructure is negatively impacted due to the presence of hydrated clay particles.

Upon calcination, the crystalline structure present in most clays is decomposed. Calcined clay minerals (e.g. metakaolinite) are amorphous pozzolanic materials which are known to boost the final strength of cement. These partially or non-crystalline aluminosilicates convert with calcium hydroxide in a pozzolanic reaction to C-S-H phases which contribute to the final strength. Supplementary cementitious materials (SCMs) such as fly ash or blast furnace slag which contain non-crystalline silica show a similar behavior. In composite cements (CEM II and III), these pozzolanic active SCMs are used to partially substitute cement clinker. Unfortunately, these materials possess a low reactivity only and therefore do not increase the early strength of cement [9–12].

Here, we present the possibility to enhance the early strength of Portland cement by adding crystalline nano-sized kaolin clay.

2 Materials and Methods

For investigation of the material properties of Portland cement in the presence of nano clays, two types of kaolin, namely K1 (KaMin HG90, KaMin LLC, Macon, US) and K2 (Chinafill 800, Amberger Kaolinwerke, Hirschau, Germany) were used. Their main difference is the particle size distribution, as is shown in Fig. 1a. Accordingly, the specific surface area and the anionic surface charge of K1 is higher compared to K2, due to the smaller particle size of K1. Table 1 summarizes these results.

The XRD pattern (Fig. 1b) of the kaolin powder samples revealed crystallinity for both K1 and K2. Sample K2 contains minor amounts of illite clay and quarz impurities. SEM analysis of the clay samples (Fig. 2) revealed the characteristic platelet shape of the kaolin particles.

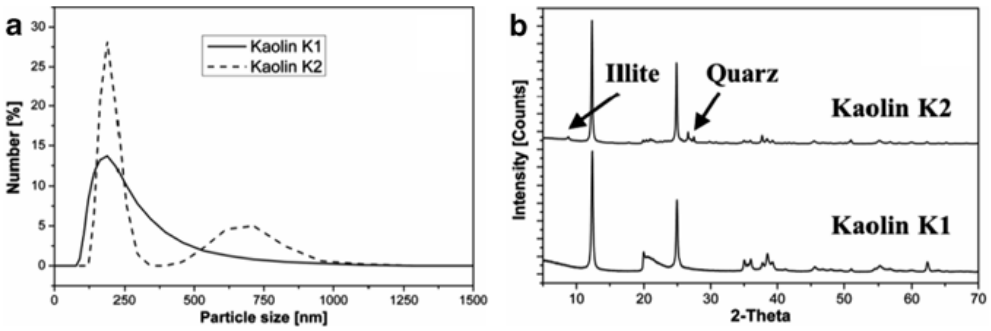

Fig. 1 (**a**) Particle size distribution, measured via dynamic light scattering (DLS), and (**b**) powder XRD pattern of the kaolinite samples K1 and K2

Table 1 pH-dependent anionic charge density and specific surface area (BET) of the kaolinite samples K1 and K2

Sample	Anionic charge amount [C/g]			Specific surface area, BET [m^2/g]
	pH 7	pH 12.5	SCPS	
Kaolin K1	−2.1	−5.9	−3.1	21
Kaolin K2	−1.0	−2.5	−1.6	10

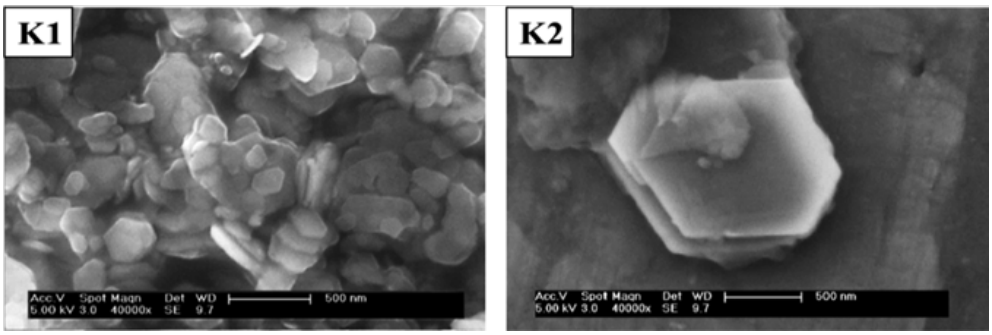

Fig. 2 Scanning electron microscope (SEM) images of dry kaolin samples K1 (*left*) and K2 (*right*)

The cement used in this study was a CEM I 52.5 N (d_{50} = 11.8 µm, HeidelbergCement, Geseke plant, Germany). For comparison, cement samples CEM I 42.5 R (d_{50} = 18.1 µm) and CEM I 52.5 R (d_{50} = 4.5 µm, Schwenk, Allmendingen plant, Germany) were used.

Compressive and tensile strength tests were carried out after 12, 16, 24 h and 28 d. Mortar specimens (nine prisms for each system, size: 160*40*40 mm) were prepared and tested according to DIN EN 196–1 at a w/c ratio of 0.5 for each system. The kaolin was added in two ways: (a) dry-blended together with cement and sand before addition of water and (b) dispersed in the mixing water via sonication.

For further characterization, hydration of OPC pastes in the presence and absence of kaolin was monitored via isothermal heat flow calorimetry at 20 °C and through in-situ XRD measurements. Ion contents present in cement pore solutions were analyzed via atomic absorption spectroscopy (AAS).

3 Results and Discussion

3.1 Compressive and Tensile Strength

The 16 h compressive and tensile strength of mortars prepared from CEM I 52.5 N with the addition of kaolin samples K1 and K2 at dosages of 1, 2 and 5 % bwoc are presented in Fig. 3. It was found that both, the 16 h compressive and tensile strength, were significantly increased when kaolin was present in the mortar.

The effect of strength enhancement depends on the dosage of the kaolin clay – the higher the dosage, the more pronounced is this effect. Additionally, this effect depends on the mode of kaolin addition, whether it is dry-blended together with cement and sand before mixing with water, or whether the clay is dispersed in the mixing water via sonication. The strongest enhancement of early strength can be achieved when kaolin is dispersed in the mixing water. For example, mortars prepared with 5 % of kaolin dispersed in the mixing water revealed a boost of compressive and tensile strength of around 30 % with CEM I 52.5 N.

Upon sonication, the kaolin agglomerates are decomposed and individual kaolin platelets are present in the mixing water. This confirms that the effect of kaolin on strength development much depends on the particle size of the clay mineral.

Table 2 presents the time-dependent results for the compressive and tensile strength of mortars prepared from CEM I 52.5 N and sample K2. Remarkably, by this kaolin strength is only enhanced at a curing time of 16 h. Another interesting effect is that the final strength (28 days) is not negatively influenced by nano kaolin.

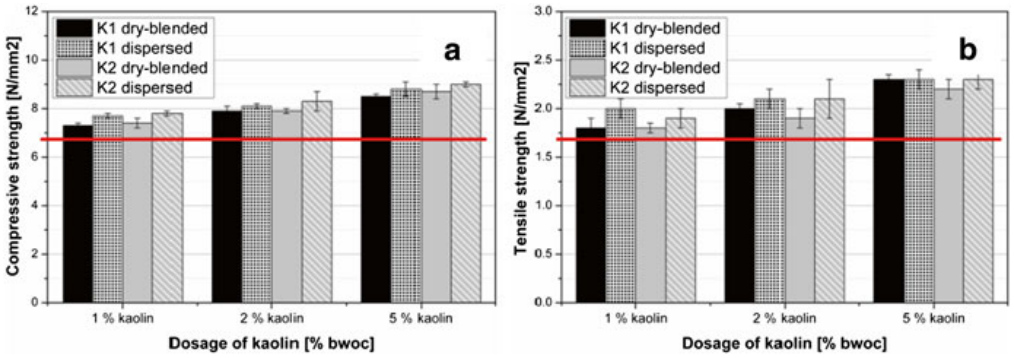

Fig. 3 Compressive (**a**) and tensile (**b**) strength after 16 h of mortar specimens prepared from CEM I 52.5 N containing 1, 2 or 5 % bwoc of kaolin sample K1 or K2. The red line represents the strength of the reference mortar without kaolin

Table 2 Compressive and tensile strength of CEM I 52.5 N after 12, 16, 24 h and 28 d in the presence and absence of 2 % bwoc kaolinite K2 (dispersed)

	Compressive/tensile strength [N/mm²]			
	12 h	16 h	24 h	28 d
CEM I 52.5 N	3.0/0.9	7.1/1.7	14.2/3.5	73.1/8.3
CEM I 52.5 N + 2 % K2	3.0/0.9	8.3/2.1	14.6/3.5	73.4/8.3

Table 3 Sixteen hour compressive and tensile strengths of CEM I 42.5 R and CEM I 52.5 R in the presence and absence of 2 % bwoc of kaolin sample K2 (dispersed)

System	Compressive strength [N/mm²]	Tensile strength [N/mm²]
CEM I 42.5 R	4.5	1.2
CEM I 42.5 R + 1 % K 2	5.1	1.4
CEM I 42.5 R + 2 % K 2	5.9	1.6
CEM I 42.5 R + 5 % K 2	6.6	1.9
CEM I 52.5 R	26.2	5.5
CEM I 52.5 R + 2 % K 2	26.1	6.0
CEM I 52.5 R + 5 % K 2	26.7	5.7

For comparison, the effect of kaolin sample K2 on the 16 h early strength of CEM I 42.5 R and CEM I 52.5 R was tested. As is shown in Table 3, 5 % of K2 increase the compressive strength of CEM I 42.5 R by around 50 % and the tensile strength up to 60 %. For this slowly reacting cement a much stronger effect on the 16 h early strength is observed compared to previous CEM I 52.5 N (Table 2).

In contrast, no enhancing effect of kaolin on the strength of the much faster reacting CEM I 52.5 R can be seen. This result indicates that nano kaolin especially boosts the early strength of cements which exhibit a low reactivity. Here, the ion concentration in pore solution is lower compared to fast reacting cements, thus initiation of crystallization affects the overall hydration rate more.

3.2 Heat Calorimetry

Figure 4 shows the isothermal heat flow curves of cement pastes prepared from CEM I 52.5 N in the presence and absence of 1, 2 and 5 % bwoc of kaolin sample K1 which was dispersed in the mixing water via sonication. The result clearly demonstrates that the overall heat of hydration increases with increasing dosage of the kaolin clay whereas the time of the maximum heat flow is not affected. In the presence of kaolin, the slope in the cumulative heat of hydration curve particularly increases between 12 and 20 h. During this time period, cement hydration is promoted by kaolin K1. A similar trend was found for kaolin K2. These observations explain the results for the compressive and tensile strengths which in the presence of kaolin are especially increased around 16 h.

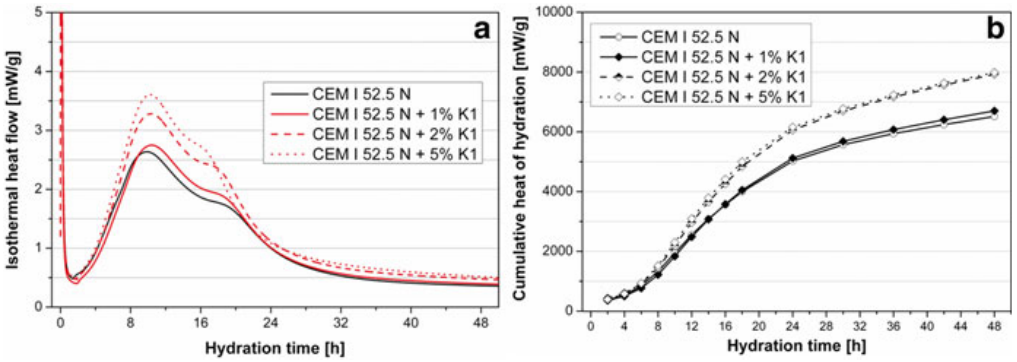

Fig. 4 (**a**) Isothermal heat flow and (**b**) cumulative heat of hydration of cement pastes (CEM I 52.5 N) modified with 1, 2 or 5 % bwoc of kaolin sample K1

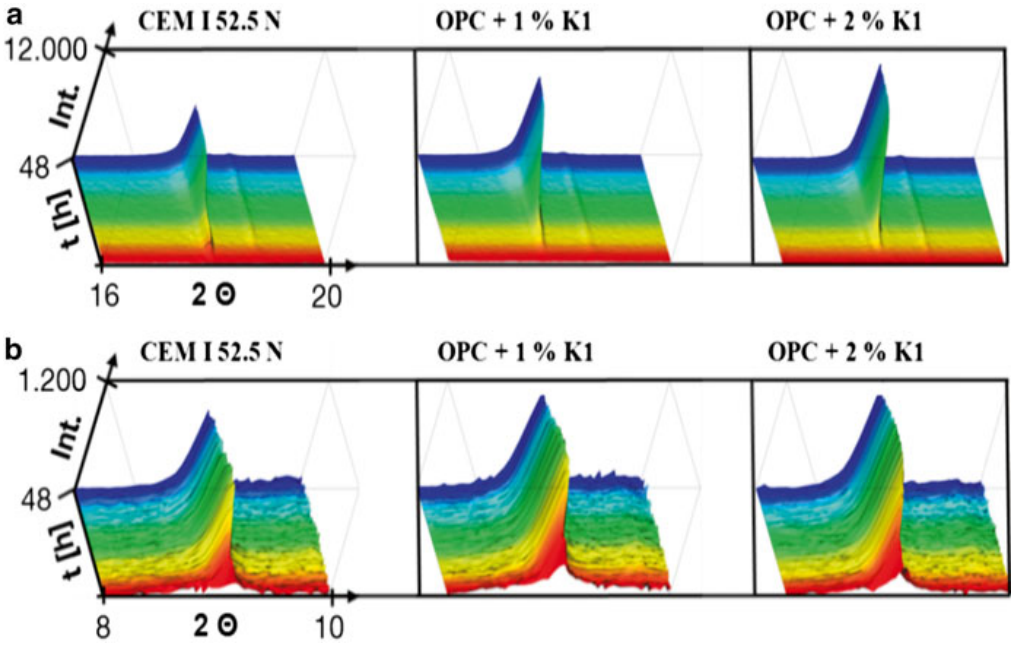

Fig. 5 Time-dependent evolution of (**a**) portlandite and (**b**) ettringite in cement pastes (CEM I 52.5 N) modified with 1 or 2 % bwoc of kaolin K1, measured via in-situ XRD

3.3 In-Situ X-ray Diffraction

Complementary to the calorimetric tests, the formation of crystalline hydrate phases during cement hydration was monitored for the first 48 h via in-situ XRD. Figure 5 presents the time-dependent evolution of the hydrate phases portlandite and ettringite. In the kaolin modified cement pastes, especially portlandite formation is significantly enhanced and ettringite formation is slightly increased. Thus, the XRD results confirm an enhanced silicate reaction which is responsible for strength development. Again, this effect is linked to the dosage of kaolin clay. The higher the

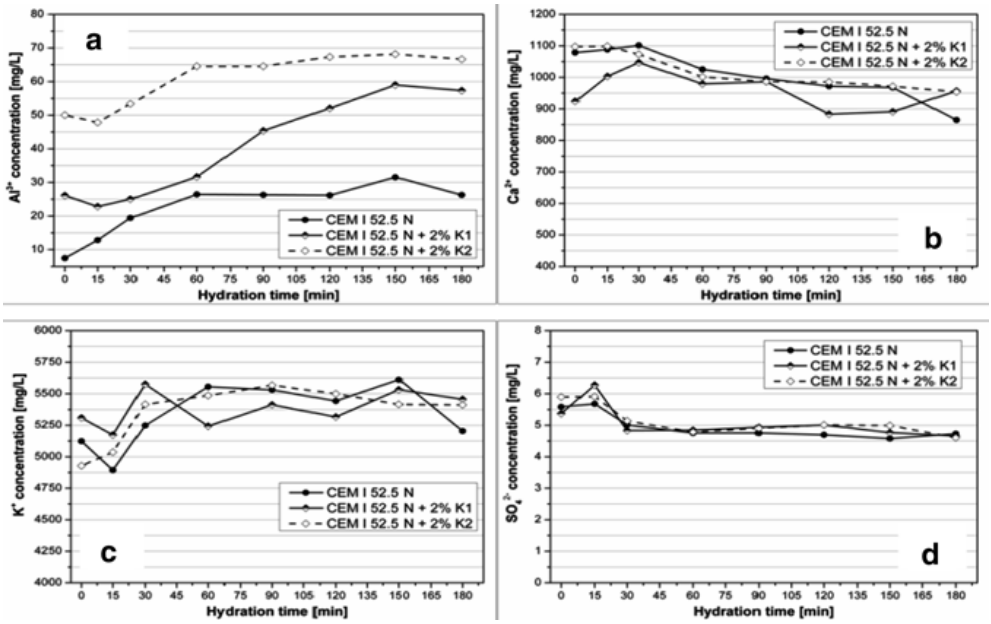

Fig. 6 Time-dependent concentrations of (**a**) Al^{3+}, (**b**) Ca^{2+}, (**c**) K^{+} and (**d**) SO_4^{2-} in cement pore solutions of CEM I 52.5 N in the presence and absence of 2 % bwoc of kaolin samples K1 and K2

dosage, the more pronounced is this effect. These results explain the increased heat flow observed for cement pastes containing kaolin, as presented above (Fig. 4).

3.4 Analysis of Cement Pore Solution

Analysis of the cement pore solution demonstrates that the concentration of Al^{3+} is increased in the presence of kaolin K1 and K2, whereas the concentrations of Ca^{2+}, K^{+} and SO_4^{2-} are not influenced. Obviously, aluminum is leached from the kaolin clay into the alkaline cement pore solution and forms tetra hydroxo aluminate $[Al(OH)_4]^{-}$. This result explains the acceleration of the aluminate reaction in the presence of kaolin (Fig. 6).

4 Conclusion

Our study demonstrates that nano kaolin clay can boost the early 10–24 h compressive and tensile strength of Portland cement without negatively impacting the final strength after 28 d. This effect is not caused by an optimized particle packing of the cementitious matrix (filler effect). Instead, such nano-sized kaolin clay increases the reactivity of the silicate and aluminate phases, as was evidenced via calorimetric and in-situ XRD measurements.

It was found that this effect is linked to the particle size and the mode of addition of the nano clay to mortar (dry-blended into cement or dispersed in the mixing water). A potential explanation for its performance is a seeding effect. Owed to heterogeneous nucleation, the activation energy for the crystallization of cement hydrates is reduced and thus early strength development is promoted. Additionally, aluminum is dissolved from kaolin into the cement pore solution, as was evidenced via AAS. This way, the crystallization of the aluminate hydrates is initiated.

References

1. Shaikh, F., Supit, S., & Sarker, P. (2014). A study on the effect of nano silica on compressive strength of high volume fly ash mortars and concretes. *Materials and Design, 60*, 433–442.
2. Biricik, H., & Sarier, N. (2014). Comparative study of the characteristics of nano silica-, silica fume- and fly ash-incorporated cement mortars. *Materials Research, 17*, 570–582.
3. Oltulu, M., & Sahin, R. (2014). Pore structure analysis of hardened cement mortars containing silica fume and different nano-powders. *Construction and Building Materials, 53*, 658–664.
4. Haruehansapong, S., Pulngern, T., & Chucheepsakul, S. (2014). Effect of the particle size of nanosilica on the compressive, strength and the optimum replacement content of cement mortar containing nano-SiO2. *Construction and Building Materials, 50*, 471–477.
5. Abd El Aleem, S., Heikal, M., & Morsi, W. M. (2014). Hydration characteristic, thermal expansion and microstructure of cement containing nano-silica. *Construction and Building Materials, 59*, 151–160.
6. Bräu, M., Ma-Hock, L., Hesse, C., Nicoleau, L., Strauss, V., Treumann, S., Wiench, K., Landsiedel, R., & Wohlleben, W. (2012). Nanostructured calcium silicate hydrate seeds accelerate concrete hardening: A combined assessment of benefits and risks. *Archives of Toxicology, 86*, 1077–1087.
7. Thomas, J., Jennings, H., & Chen, J. (2009). Influence of nucleation seeding on the hydration mechanisms of tricalcium silicate and cement. *Journal of Physical Chemistry, 113*, 4327–4334.
8. Lei, L., & Plank, J. (2014). A study on the impact of different clay minerals on the dispersing force of conventional and modified vinyl ether based polycarboxylate superplasticizers. *Cement and Concrete Research, 60*, 1–10.
9. Rashad, A. M. (2014). A comprehensive overview about the effect of nano-SiO_2 on some properties of traditional cementitious materials and alkali-activated fly ash. *Construction and Building Materials, 52*, 437–464.
10. Quercia, G., Spiesz, P., Husken, G., & Brouwers, H. (2014). SCC modification by use of amorphous nano-silica. *Cement and Concrete Composites, 45*, 69–81.
11. Morsy, M., Al-Salloum, Y., Almusallam, T., & Abbas, H. (2014). Effect of nano-metakaolin addition on the hydration characteristics of fly ash blended cement mortar. *Journal of Thermal Analysis and Calorimetry, 116*, 845–852.
12. Frias, M., & Martinez-Ramirez, S. (2009). Use of micro-Raman spectroscopy to study reaction kinetics in blended white cement pastes containing metakaolin. *Journal of Raman Spectroscopy, 40*, 2063–2068.

PART II

Non - reviewed conference papers

5.8 A study on the Impact of different clay minerals on the dispersing force of conventional and modified vinyl ether based polycarboxylate superplasticizers

L. Lei, J. Plank

P. Gupta (Ed.), 11th International Conference on Superplasticizers and Other Chemical Admixtures in Concrete (CANMET/ACI)
July 12 – 15, 2015, Ottawa (ON / Canada)
Supplementary Papers, 145 – 159.

In this conference paper, the influence of three clay minerals (montmorillonite, kaolin and muscovite) on the dispersing effectiveness of self-synthesized vinyl ether based PCE superplasticizers was investigated.

At first, one conventional VPEG-PCE sample possessing PEG side chains and two modified VPEG-PCE samples holding novel hydroxyalkyl pendants were prepared in our lab. Then three clay samples (montmorillonite, kaolin and muscovite) were characterized via methylene blue test, thermogravimetric analysis and zeta potential measurement. The 'mini slump' test results showed that for conventional VPEG-PCE samples montmorillonite presents the most detrimental clay mineral, followed by kaolin and then muscovite. Whereas, the two novel modified VPEG PCEs were generally quite tolerant to all three clay minerals.

The different behaviour of the three clay minerals toward the VPEG-PCEs can be attributed to the different interaction mode. As for montmorillonite, both surface adsorption and intercalation on this clay can occur which tremendously affects the dispersing power of conventional VPEG-PCEs holding PEG lateral chains, whereas the modified VPEG-PCE samples were much less affected due to their different side chains which cannot intercalate into the lattice of this clay. As for kaolin or muscovite, their interaction with the VPEG-PCEs possessing different molecular structures is limited to surface adsorption only, therefore the spread flow reduction occurring with all VPEG-PCEs were quite similar for these clays.

A STUDY ON THE IMPACT OF DIFFERENT CLAY MINERALS ON THE DISPERSING FORCE OF CONVENTIONAL AND MODIFIED VINYL ETHER BASED POLYCARBOXYLATE SUPERPLASTICIZERS

By

Lei Lei and Johann Plank

Prof. Dr. Johann Plank

Lehrstuhl für Bauchemie, Technische Universität München

Lichtenbergstr. 4, D-85747 Garching, Germany

Tel.: +49 89 289 13151

Fax: +49 89 289 13152

E-mail: sekretariat@bauchemie.ch.tum.de

ID: SP # 042

A STUDY ON THE IMPACT OF DIFFERENT CLAY MINERALS ON THE DISPERSING FORCE OF CONVENTIONAL AND MODIFIED VINYL ETHER BASED POLYCARBOXYLATE SUPERPLASTICIZERS

Lei Lei and Johann Plank

Biography:

Lei Lei is a Ph.D. student at the Chair for Construction Chemistry at Technische Universität München, Germany. Her research focuses on the impact of different clay minerals on the performance of polycarboxylate - based superplasticizers and new routes to PCE synthesis.

Johann Plank is full Professor at the Institute of Inorganic Chemistry of Technische Universität München, Germany. Since 2001, he holds the Chair for Construction Chemistry there. His research interests include cement chemistry, chemical admixtures, organic-inorganic composite and nano materials, concrete, dry-mix mortars and oil well cementing.

ABSTRACT

It is well-known that polycarboxylate superplasticizers (PCEs) show pronounced sensitivity to clay impurities contained as contaminant in concrete. Here, the impact of different clay minerals (montmorillonite, kaolinite and muscovite) on the

dispersing force of vinyl ether based PCE superplasticizers was studied. At first， a conventional vinyl ether PCE possessing PEG chains and two modified PCEs which do not hold PEG pendants were prepared. Next, the effect of three different clay minerals on the fluidity of cement admixed with the PCEs was investigated. It was found that the conventional PCE is negatively affected by the clays in the order: montmorillonite >> kaolinite > muscovite. Whereas, the modified vinyl ether based PCEs were only slightly affected by all three clay minerals. A mechanistic study revealed that the conventional VPEG PCE interacts chemically with montmorillonite via side chain intercalation. This does not occur for the PEG-free modified PCE.

Key words: Polycarboxylate; Dispersion; Admixture; Concrete; Clay minerals

INTRODUCTION

Polycarboxylate superplasticizers (PCEs) represent one of the most important inventions in the field of concrete admixtures. However, recently more and more field users report that under certain conditions PCEs can exhibit a strong sensitivity to clay impurities. Most confusing, in some cases the negative impact of clay minerals on the dispersing force of PCE is very pronounced whereas in other cases, the effect is only minor. Apparently, different types of clay minerals can show a completely different impact on the performance of PCEs which is owed to variations in their physical and chemical properties. Generally, clay minerals can be classified as 1:1, 2:1 or 2:1:1

type. This classification derives from the fact that they are built of tetrahedral silicate sheets and octahedral aluminate sheets[1-3]. Thus, 1:1 clay consists of one tetrahedral sheet and one octahedral sheet, 2:1 clay of an octahedral sheet sandwiched between two tetrahedral sheets while a 2:1:1 clay is made up of regularly stacked, negatively charged 2:1 layers and an additional positively charged interlayer octahedral sheet. The principle structures of these clay minerals are displayed in **Fig. 1**[4].

The aim of this study was to compare the effect of three most frequently occurring clay minerals (montmorillonite, kaolin, muscovite) on cement pastes admixed with polycarboxylate superplasticizers. From these experiments, it was sought to understand the different impact of differently structured (2:1 and1:1) swelling and non-swelling clay minerals on the PCEs.

RESEARCH SIGNIFICANCE

Different clay minerals occurring in concrete aggregates or limestone powder can show completely different impact on cement pastes admixed with polycarboxylate superplasticizers. In order to understand such different behaviour of various clay minerals with PCEs, a mechanistic study including XRD, adsorption and zeta potential measurements was carried out.

EXPERIMENTAL INVESTIGATION

Materials

Chemicals — 4-Hydroxy butyl vinyl ether (> 99 % purity, purchased from SIGMA-ALDRICH CHEMIE, Steinheim, Germany), maleic anhydride (> 99 %, Merck Schuchardt OHG, Hohenbrunn, Germany), ethanol, n-propyl alcohol (all > 98 % purity, VWR International, Darmstadt, Germany), sodium hydroxymethane sulfinate (Rongalit C, > 98 % purity, SIGMA-ALDRICH), ferrous sulfate (> 98 % purity, VWR), 2-mercapto ethanol (> 99 % purity, SIGMA-ALDRICH), hydrogen peroxide (30 % aqueous solution, VWR) were used without further purification.

Industrial superplasticizer sample — An industrial superplasticizer sample based on β-naphthalene sulfonate formaldehyde polycondensate (BNS) designated Melcret® 500F (BASF Construction Polymers GmbH, Trostberg, Germany) was used for comparison. Melcret® 500F is a spray dried BNS powder which possesses a low Na_2SO_4 content (< 2 wt.%).

Cement — A CEM I 52.5 N (Milke®classic, HeidelbergCement, Geseke plant) was used. Its phase composition as determined by XRD is presented in **Table 1**. The average particle size (d_{50} value, determined by laser granulometry) was found at 11.5 µm. Its density was 3.153 g/cm^3 (Helium pycnometry).

Clay minerals — As Na^+ montmorillonite, a commercially available product designated “RXM 6020” supplied by Rockwood, Moosburg, Germany was used. This mineral is a naturally occurring Na bentonite and was used as per obtained. Its

average particle size (d_{50} value) was found at 0.9 µm and its *BET* value was 38.33 m^2/g.

A commercially available kaolin named "Chinafill 800" supplied by Quarzwerke GmbH, Frechen, Germany was used. The average particle size (d_{50} value) was found at 0.7 µm and its *BET* value was 9.78 m^2/g.

A muscovite sample designated "MICA S", supplied by Quarzwerke GmbH, Frechen, Germany was used. The average particle size (d_{50} value) was found at 2.8 µm and its *BET* value was 2.60 m^2/g.

The oxide compositions of the clay samples as determined by x-ray fluorescence (XRF) are shown in **Table 2**.

Synthesis of VPEG based PCE superplasticizers

Preparation of MA - mono alkyl maleate - HBVE terpolymers

For the preparation of the modified vinyl ether PCEs, monoalkyl maleate ester monomers are required. Their synthesis was performed as follows:

4.09 g (42 mmol) of maleic anhydride and 32 mmol of either ethanol (1.48 g) or n-propanol (1.9 g) were placed in a 250 mL four-neck round bottom flask equipped with a stirrer and reflux condenser and heated for 2 hours at 55 °C under constant stirring. Thereafter, 5 g of DI water were added to the flask and the resulting ~ 45 wt.% solution of the monoalkyl ester of maleic acid was cooled to 20 °C.

As an example for the modified VPEG PCE, the synthesis of the MA - mono ethyl maleate – HBVE terpolymer is described here. A 250 mL four-neck round bottom flask holding the aqueous solution of the mono ethyl maleate as prepared above equipped with a stirrer, reflux condenser and two separate inlets is provided with an inert atmosphere by bubbling N_2 via a bottom valve. The inert atmosphere was maintained over the entire reaction time. ~ 7 mL of a 30 % KOH solution were added to adjust the pH of the monoethyl maleate solution to ~ 4.5. Thereafter, 12.37 g (106 mmol) of 4-hydroxy butyl vinyl ether were added under stirring. Subsequently, 30 mg of $FeSO_4 \bullet 7H_2O$, 40 mg of 2-mercapto ethanol (the first portion of chain transfer agent) as well as 4.9 g of 30 wt.% H_2O_2 solution were added to the reactor. Next, 0.63 g of Rongalit C (initiator) were dissolved in 10 mL of DI water. This solution was designated Solution I. Separately, 4.16 g (42 mmol) of maleic anhydride and 80 mg of 2-mercapto ethanol (second portion of chain transfer agent) were dissolved in 12.5 mL of DI water. This solution was named Solution II. Using two peristaltic pumps, solution I and II were fed separately and continuously into the vessel over periods of 75 min (Sol. I) and 60 min (Sol. II) while maintaining the temperature at 25 ℃ through an ice-bath. When the additions were completed, the mixture was stirred for another 30 min. The final product designated as MA - monoethyl maleate - HBVE terpolymer was a slightly reddish, 27 wt. % aqueous solution possessing moderate viscosity and of a pH of ~ 4.

The MA – monopropyl maleate – HBVE terpolymer was synthesized is the same

manner except that here, 11 g (32 mmol) of the aqueous solution of mono propyl maleate were used. The resulting terpolymer was a liquid with a solid content of 30 wt.% and a pH of ~ 4.1.

Synthesis of MA – MPEG-1000 maleate – HBVE terpolymer

A conventional vinyl ether - based PCE holding PEG side chains was synthesized via aqueous free radical copolymerization from 4.16 g (42 mmol) of maleic anhydride, 12.37 g (106 mmol) of 4-hydroxy butyl vinyl ether and 36.2 g (32 mmol) of methoxy polyethylene glycol mono maleate following the description from above for the mono alkyl maleate containing terpolymers. 2-mercapto ethanol was used as chain transfer agent. The number of ethylene oxide units in the methoxy polyethylene glycol was 23 (MPEG-1000). The resulting terpolymer solution exhibited a solid content of 40 wt.%, a pH of ~ 4.2 and was a slightly reddish, highly viscous solution.

Characterization of clays

Methylene blue test — The cation exchange capacity (CEC) of clay minerals is commonly measured via adsorption of methylene blue dye by the clay mineral. Methylene blue tests performed in this context are based on the French standard Norme Fran çaise NF P 94-068 (AFNOR1993)[5].

Thermogravimetric analysis (TGA) — The water uptake capacity of the clay minerals was obtained via measuring their weight loss as a function of temperature. A NETZSCH STA 409 instrument was used to carry out the thermo gravimetric analysis

at a heating rate of 10°C/min from 300 to 1373 K in an air flow of 30 cm^3/min using alpha-Al_2O_3 as the standard.

Characterization of PCE samples

Molar masses (M_w, M_n) and polydispersity index (PDI) of the PCE samples were determined utilizing size exclusion chromatography (SEC).

Dispersing performance in cement with or without clay minerals

For determination of the paste flow, a "mini slump test" modified from DIN EN 1015 was utilized and carried out, for details see[6].

Sorption on clays

The amounts of polymers sorbed on the clays were measured using the depletion method. The portion of polymer remaining in solution at equilibrium condition was determined by analyzing the total organic carbon content (TOC) of the solution.

XRD analysis

To investigate the interaction between different types of clay minerals and the PCE samples, XRD analysis was performed on the clay minerals which were hydrated overnight with and without polymers.

EXPERIMENTAL RESULTS AND DISCUSSION

Characteristic properties of clay samples

Cation exchange capacity (CEC)

According to the data presented in **Table 3**, montmorillonite shows the highest MB value. In comparison, the MBV of kaolin and muscovite are much lower, because of the absence of exchangeable interlayer cations.

Water uptake capacity

According to **Table 4**, montmorillonite exhibits a particularly high water uptake capacity (~77.0 wt.%). In comparison, the water uptake capacity of muscovite is the least at 35.6 wt.%.

Properties of the synthesized PCE polymers

The molecular properties of the synthesized polymers are presented in **Table 5**. According to SEC data, the molar masses (M_w) of the modified PCE samples lie at ~ 10,000 Da while their polydispersity index is 2.7. For comparison, a conventional vinyl ether-based PCE possessing a polyethylene glycol pendant chain (n_{EO} = 23) was also evaluated. M_w of this terpolymer was found at ~ 20 kDa which is higher than those for the mono alkyl ester based terpolymers.

Cement dispersion

'Mini slump' test — In this test, the dosages required to achieve a cement paste spread of 26±0.5 cm were determined. The results are displayed in **Fig. 2**. The newly synthesized PCE polymers exhibit good dispersing effectiveness. Dosages of only ~ 0.12 % bwoc are required to achieve the 26 cm spread.

Effect of clays on PCE dispersing power — As is shown in **Fig. 3**, in the cement/montmorillonite system, the conventional VPEG-PCE exhibited a strong decrease in performance caused by the presence of 1 wt.% of montmorillonite. The spread flow decreased by 135 %. Whereas for the modified VPEG-PCEs and BNS, the spread flow reduction was ~ 50 % only.

In the cement/kaolin system, the flow reductions generally were much less. In the presence of 3 wt.% of kaolin, the spread flow for the conventional VPEG-PCEs decreased by ~ 72 %, while the modified VPEG-PCEs and BNS showed a decrease of ~ 45 %. For the cement/muscovite system, a similar trend was observed.

Sorption of PCEs on clay samples —To quantify the interaction between the individual PCE samples and the different clay minerals, sorption isotherms were developed. **Fig. 4 (a)** displays the huge difference in sorbed amounts between montmorillonite and the two other clay minerals (kaolin/muscovite) for the conventional PCE possessing PEO side chains. It sorbs in very high amount on montmorillonite, with a sorbed amount of ~ 230 mg/g of clay at saturation point. To

the contrary, on kaolin or muscovite it sorbs in extremely low amounts (~ 20 mg/g of clay). This demonstrates again the particularly negative effect of montmorillonite on the performance of conventional PCEs because this clay mineral essentially screens off the PCE from the pore solution, and very few - if any - PCE is left to disperse cement. **Fig. 4 (b)** and **Fig. 4 (c)** exhibit how the modified MA-monoalkyl maleate-HBVE terpolymers sorb on the different clay minerals. On montmorillonite, sorbed amounts of ~ 20 mg/g of clay only were found at saturation point. Furthermore, on muscovite, the sorbed amounts were ~ 15 mg/g of clay only, while on kaolin the sorbed amounts were even less at~ 5 mg/g of clay. These data imply weak interaction between the MA-monoalkyl maleate-HBVE terpolymers and all clay samples tested. For BNS (see **Fig. 4 (d)**), a similar behavior was found. It suggests that for the modified PCEs and BNS, interaction with the clay minerals mainly depends on the specific surface area of the hydrated clay mineral, while for conventional PCEs, an additional mechanism of interaction comes into play.

XRD analysis —When hydrated, montmorillonite exhibits a d-spacing of 1.23 nm (**Fig. 5**). For montmorillonite hydrated in the presence of the conventional vinyl ether PCE a shift in the d-spacing from 1.23 nm to 1.72 nm was detected. Such d value is characteristic for montmorillonite which contains intercalated polyglycols[7, 8]. However, when the mono alkyl maleate modified PCEs were added, no change in the d-value of the hydrated montmorillonite was observed. Similarly, when BNS was present, also no shift in the d-spacing was found. These results signify that the

modified type of PCE and BNS do not incorporate chemically into the interlayer space.

For pure hydrated kaolin, a d-spacing of 0.72 nm was detected. After addition of the different superplasticizers, no shift of the d-spacing was found (**Fig. 5**). Similarly, a d-spacing of 0.99 nm for hydrated muscovite was recorded (**Fig. 5**). Also here, the d-spacing did not change in the presence of the different superplasticizers. These data signify that kaolin and muscovite interact with all superplasticizers via surface adsorption only.

CONCLUSIONS

This study demonstrates that different clay minerals can show completely different impact on the workability of cement and the dispersing effectiveness of PCE superplasticizers. Montmorillonite presents the most detrimental clay mineral, it strongly perturbs the dispersing power of conventional PCE products. While modified PEG-free PCEs exhibit high dispersing ability and robustness even in the presence of such smectite clay.

To overcome the sensibility problem of PCE polymers toward clay minerals, applicators should check for the presence and amount of montmorillonite in the aggregates via the MB test. If the MBV is < 1 g/ 100 g, then the clay impurity contained in the aggregates will not cause a significant performance failure of a PCE product. However, when a significant amount of this specific clay mineral is detected

(MBV > 1 g/ 100 g), then the use of a PEG-free PCE polymer presents a viable strategy[9, 10].

ACKNOWLEDGMENTS

L. Lei wishes to thank the Jürgen Manchot Foundation for generously providing a scholarship to finance her doctoral research at TU München.

REFERENCES

1. Weaver, C. E., Pollard, L. D., "The chemistry of clay minerals", Elsevier, Amsterdam, **1973.**
2. Roy, D. M., Roy, R., "An experimental study of the formation and properties of synthetic serpentines and related layer silicate minerals", *Am. Mineralogist*, V. 39, **1954**, pp. 957-975.
3. Brigatti, M. F., Galan, E., and Theng, B. K. G., "Structure and mineralogy of clay minerals", in: Bergaya, F., Theng, B. K. G., Lagaly, G. (Eds.), "Handbook of Clay Science", Elsevier, Amsterdam, **2006**, pp. 19-86.
4. Grim, R. E., "Clay mineralogy", McGraw-Hill series in the geological sciences, McGraw-Hill, New York, **1953**.
5. AFNOR (**1993**). Mesure de la quantité et de l'activité de la fraction argileuse (Norme Française NF pp. 68-94). Association française de Normalization

(ANFOR), La Défense, Paris, France.

6. Lei, L., Plank, J., "Synthesis, working mechanism and effectiveness of a novel cycloaliphatic superplasticizer for concrete", *Cem. Concr. Res.*, V. 42, **2012**, pp. 118-123.
7. Svensson, P. D., Hansen, S., "Intercalation of smectite with liquid ethylene glycol resolved in time and space by synchrotron X-ray diffraction", *Appl. Clay Sci.*, V. 48, **2010**, pp. 358–367.
8. Suter, J. L., Coveney, P. V., "Computer simulation study of the materials properties of intercalated and exfoliated poly(ethylene) glycol clay nanocomposites", *Soft mater.*, V. 5, **2009**, pp. 2239–2251.
9. Lei, L., Plank, J., "A Concept For a Polycarboxylate Superplasticizer Possessing Enhanced Clay Tolerance", *Cem. Concr. Res.*, 42, **2012**, pp. 118-123.
10. Lei, L., Plank, J., "Synthesis and Properties of a Vinyl Ether-Based Polycarboxylate Superplasticizer for Concrete Possessing Clay Tolerance", *Ind. Eng. Chem. Res.*, V. 53 (3), **2014**, pp. 1048–1055.

TABLES AND FIGURES

List of Tables:

Lists of Figures:

Table 1 – Phase composition of the CEM I 52.5 N sample as determined by Q-XRD using *Rietveld* refinement

Phase	wt.%
C_3S, m	54.14
C_2S, m	26.63
C_3A, c	3.28
C_3A, o	4.26
C_4AF, o	2.45
Free lime (Franke)	0.1
Periclase (MgO)	0.03
Anhydrite	2.64
$CaSO_4$-hemihydrate	1.21
$CaSO_4$-dihydrate	0.02
Calcite	3.61
Quartz	1.16
Arcanite (K_2SO_4)	0.46

Table 2 – Oxide compositions of the clay minerals, as determined by XRF

Type of clay	Oxide Contents (wt.%)								
mineral	SiO_2	Al_2O_3	CaO	MgO	Fe_2O_3	Na_2O	K_2O	SO_3	LOI
montmorillonite	59.20	20.62	0.68	1.94	3.52	2.25	0.08	0.45	11.00
kaolin	49.71	37.74	0.07	-	0.55	0.14	2.34	0.07	11.40
muscovite	47.37	30.12	0.13	2.79	3.72	0.31	10.24	0.14	4.35

Table 3 –Methylene blue value (MBV) for the clay minerals used in this study

Clay mineral	montmorillonite	kaolin	muscovite
MBV (g/100 g)	8.6	1.9	0.8

Table 4 –Water uptake capacity of the clay samples

Clay mineral	montmorillonite	kaolin	muscovite
Water uptake (wt.%)	84	50	37

Table 5 – Molar masses (M_w, M_n), polydispersity index (PDI) and conversion rates for the synthesized superplasticizer samples

Polymer sample	M_w (g/mol)	M_n (g/mol)	PDI (M_w/M_n)	Conversion rate of monomers
MA-monoethyl maleate-HBVE	9,000	3,334	2.7	83 %
MA-monopropyl maleate-HBVE	10,220	3,998	2.7	88 %
MA-MPEG-1000 maleate-HBVE	21,390	8,010	2.4	90 %
BNS	139,100*	-	-	-

*batch measurement.

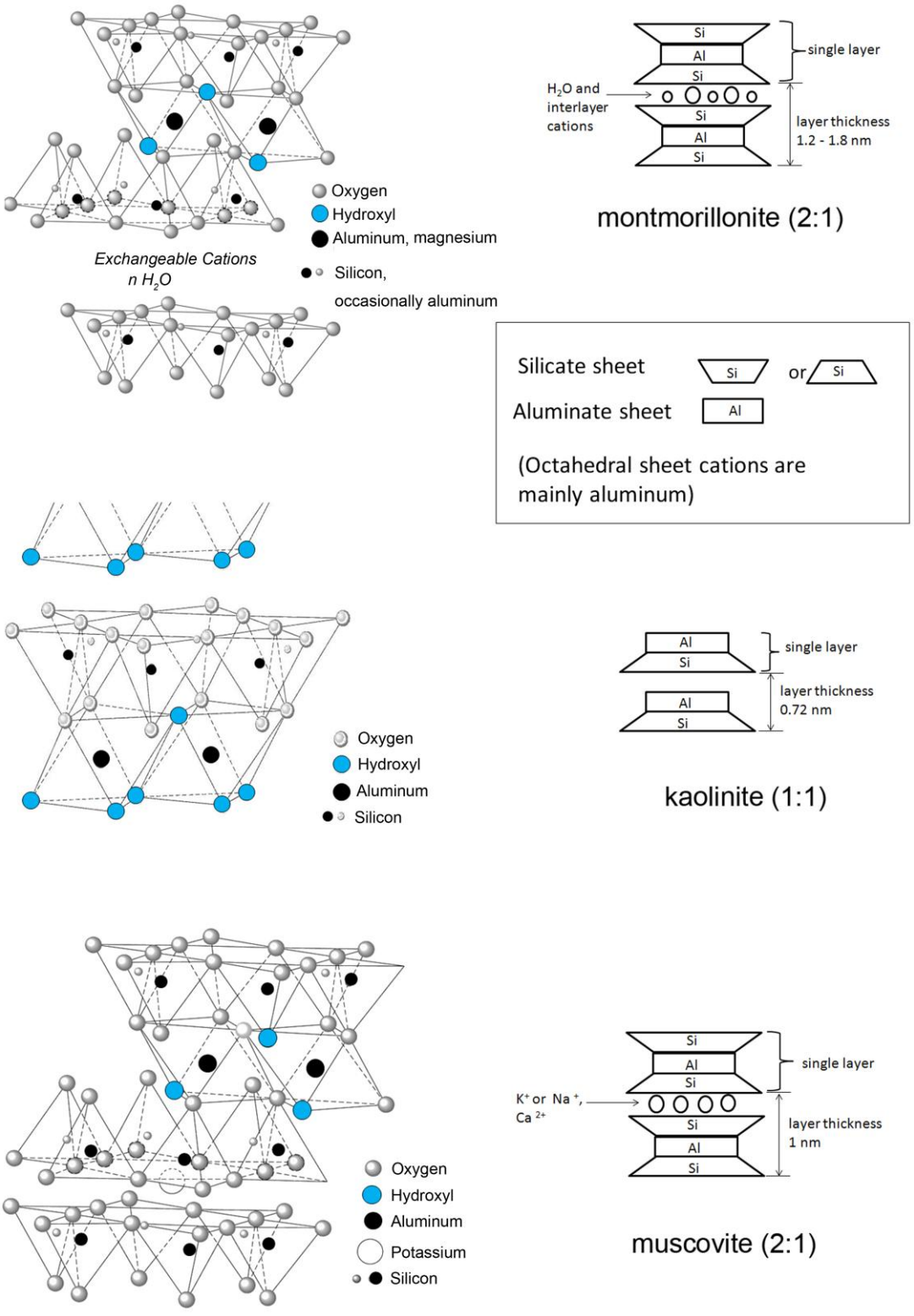

Fig. 1 –Principle structure of the major clay minerals occurring as contaminant in concrete, after Grim [4]

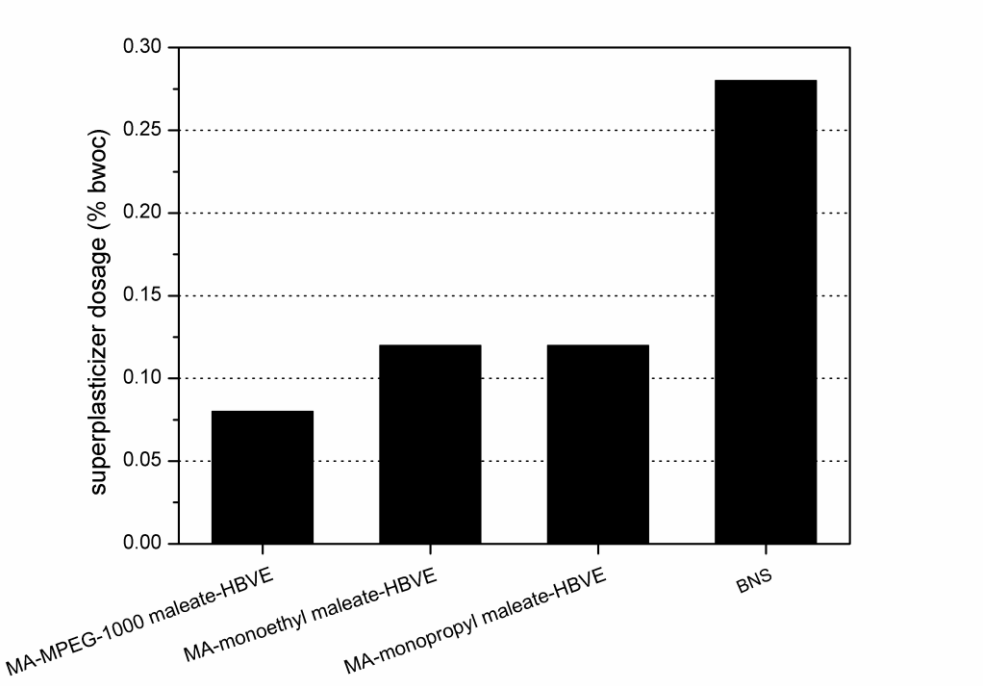

Fig. 2 – Dosages of the MA-mono alkyl maleate-HBVE terpolymers and of comparative superplasticizer samples required to achieve a cement paste spread of 26±0.5 cm (w/c = 0.45)

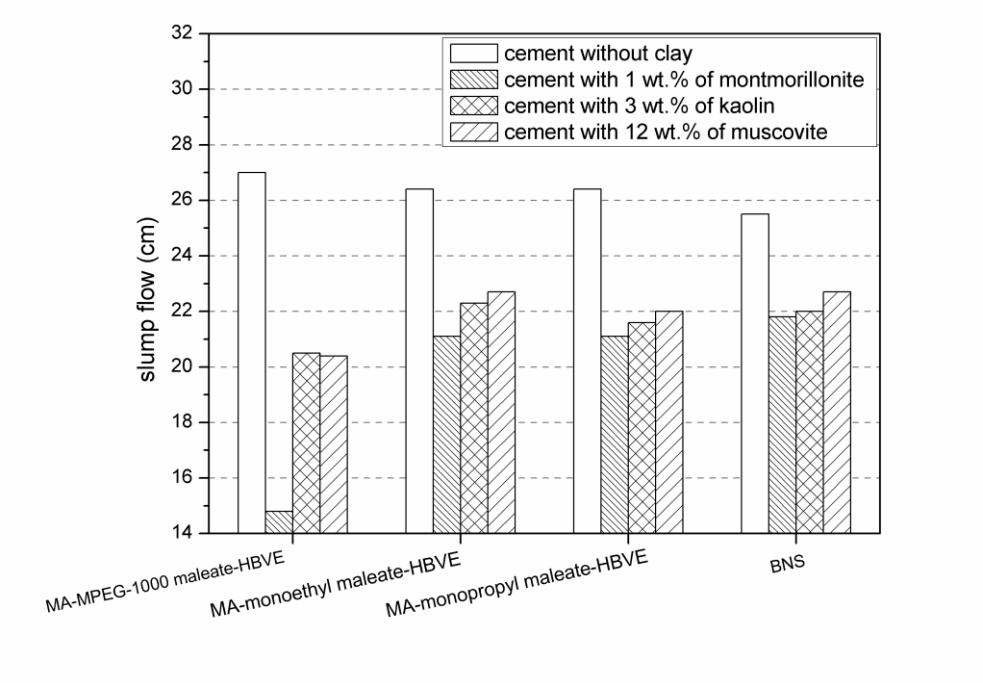

Fig. 3 – Spread flow of cement pastes containing different superplasticizers, measured in the absence and presence of 1 % bwoc of montmorillonite, 3 % bwoc of kaolin, and 12 % bwoc of muscovite, respectively

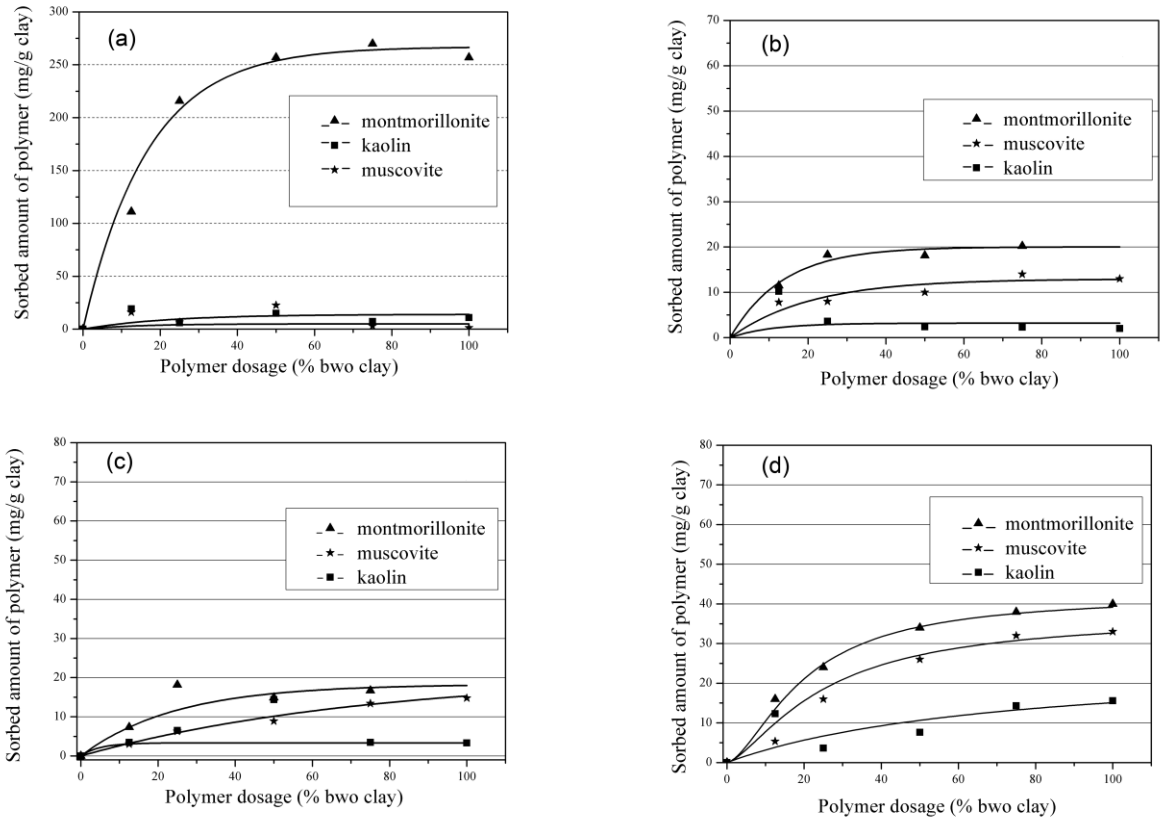

Fig. 4 – Adsorption isotherms for (a) MA-MPEG-1000 maleate-HBVE, (b) MA-monoethyl maleate-HBVE, (c) MA-monopropyl maleate-HBVE and (d) BNS samples on different clay minerals dispersed in synthetic cement pore solution (w/clay = 45)

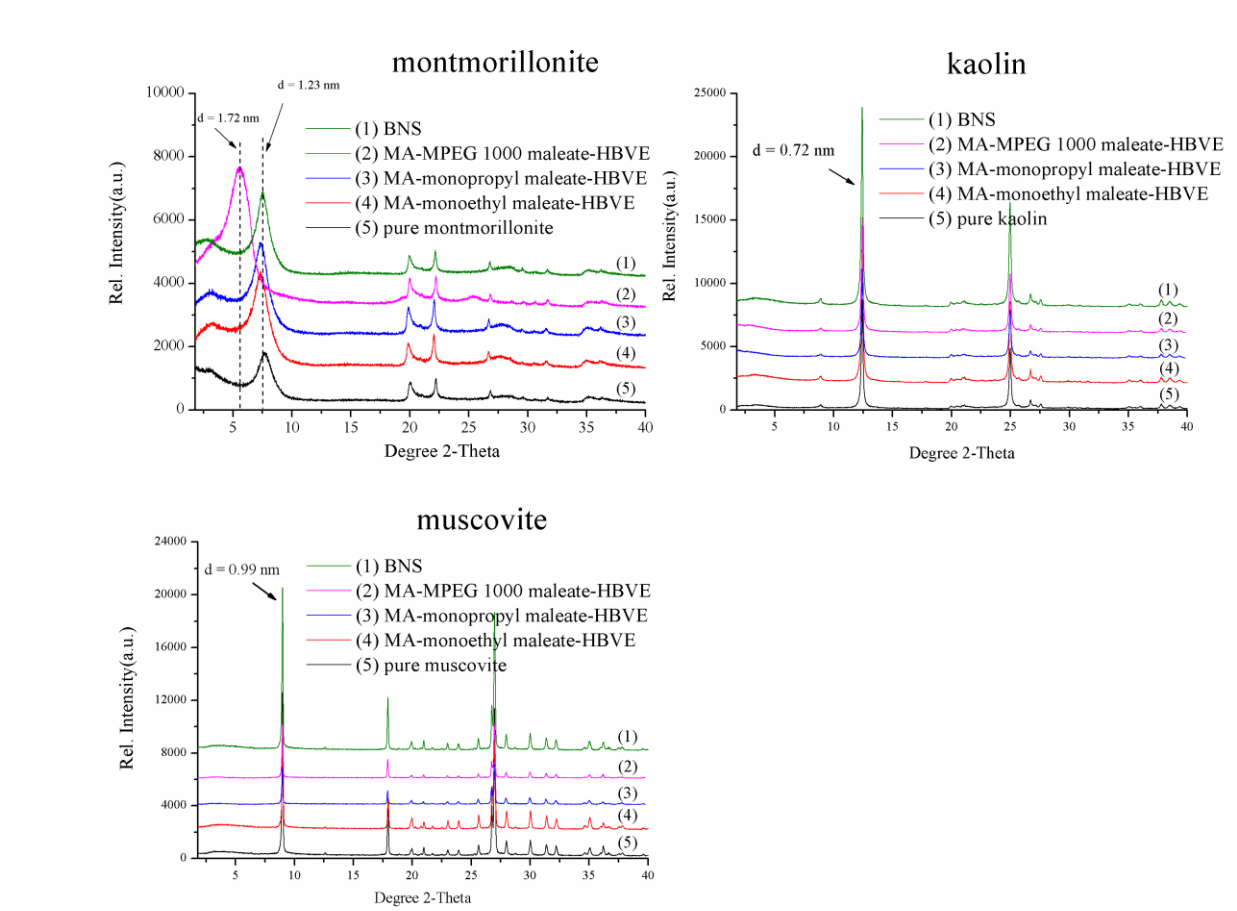

Fig. 5 –XRD patterns of montmorillonite/kaolin/muscovite hydrated overnight in synthetic cement pore solution, holding different superplasticizers (w/clay = 45)

5.9 A study on the sensibility of conventional vinyl ether-based polycarboxylate superplasticizers toward different clay minerals

L. Lei, J. Plank

C. Shi, Z. Ou, K. H. Khayat (Eds.), Design, Performance and Use of Self-Consolidating Concrete (SCC'2014)
Proceedings of the 3rd International Symposium
Xiamen (China), June 5 – 8, 2014
RILEM Publications S.A.R.L., Bagneux (F), 2014, p. 126.

This conference abstract described the different impact of three clay minerals (montmorillonite, kaolinite and muscovite) on the dispersing performance of conventional VPEG-PCE polymers.

This paper was presented as an oral presentation at the conference.

The results revealed that montmorillonite is the most dangerous clay mineral due to its lattice allowing PEG pendants to intercalate. As for kaolinite or muscovite, the interaction with VPEG-PCE polymers was mere surface adsorption. A mechanistic study explained the huge differences in PCE performance for different clay bearing systems.

Third International Symposium on Design, Performance and Use of Self-Consolidating Concrete
SCC'2014-China, June 5-8 2014, Xiamen, China

A STUDY ON THE SENSIBILITY OF CONVENTIONAL VINYL ETHER-BASED POLYCARBOXYLATE SUPERPLASTICIZERS TOWARD DIFFERENT CLAY MINERALS

Lei Lei (1), Johann Plank (1)

(1) Technische Universität München, Chair for Construction Chemicals, 85747 Garching, Lichtenbergstraße 4, Germany

Abstract

The sensibility of conventional vinyl-ether based polycarboxylate (PCE) superplasticizers toward three different clay minerals (montmorillonite, kaolinite and muscovite) was studied. At first, two vinyl-ether PCEs possessing different side chain length were synthesized from maleic anhydride (MA), mono methoxy poly (ethylene glycol) ester of MA and 4-hydroxy butyl vinyl ether (HBVE). Next, the effect of three different clay minerals on the fluidity of cement paste admixed with these PCE samples was investigated. It was found that the PCEs are negatively affected by the clays in the order: montmorillonite >> kaolin > muscovite. The study suggests that vinyl ether-based conventional PCEs containing ethylene glycol side chains reasonably tolerate all types of clay minerals except montmorillonite. When montmorillonite is present as a contaminant, then these PCEs loose their dispersing effectiveness completely. A mechanistic study revealed that such conventional PCEs indeed incorporate into the layer structure of the aluminosilicate. This behavior explains their strongly decreased performance. At the end, some suggestions are made to overcome the sensibility problem of PCEs with clay contaminants.

Keywords: Polycarboxylate, Clay minerals, Dispersion, Sensibility, Concrete

5.10 Synthesis and characterization of a vinyl ether based polycarboxylate possessing clay tolerance

L. Lei, J. Plank

1st International Conference on the Chemistry of Construction Materials
Berlin (Germany), October 7 – 9, 2013
GDCh-Monographie, 46 (2013) 297 – 300.

In this conference paper, a series of VPEG-PCEs possessing alkyl lateral chains introduced by methyl maleate, ethyl maleate and propyl maleate were synthesized and compared with a conventional VPEG-PEG holding PEG side chains.

Firstly, all VPEG-PCE samples were tested in neat cement paste. It was found that the three VPEG-PCE samples containing an alkyl maleate to provide the side chains can fluidize cement pastes at surprisingly low dosages, considering such short lateral chains. In subsequent dispersing performance tests with clay, the VPEG-PCE samples were tested in cement pastes with 1 % bwoc of montmorillonite. All VPEG-PCE samples containing alkyl maleates as building block exhibited much better clay tolerance than the conventional VPEG-PCE sample holding PEG side chains.

The interaction mode between montmorillonite and the VPEG-PCE samples was probed via adsorption (TOC) and XRD measurements. It was confirmed that the conventional VPEG-PCE sample holding PEG side chains can intercalate into the interlayer space of montmorillonite, whereas the VPEG-PCE samples containing alkyl maleates can only be consumed via surface adsorption, due to their novel side chain.

Synthesis and Characterization of a Vinyl Ether Based Polycarboxylate Possessing Clay Tolerance

L. Lei, J. Plank
Technische Universität München, Chair for Construction Chemicals, Garching, Germany

Introduction

In the 1980s, polycarboxylate superplasticizers (PCEs) were introduced as a new generation of concrete admixtures /1, 2/. Recently, applicators have reported serious problems when PCEs were used in concrete contaminated with clay, e.g. from insufficiently washed aggregates or limestone powder. Apparently, PCEs can be strongly affected by clay and sometimes even experience a total loss of their dispersing ability while BNS or PMS superplasticizers are less affected. To overcome the clay problem, a novel type of vinyl ether based PCE was synthesized and tested with respect to its clay tolerance.

Experimental

Synthesis and characterization of MA-HBVE copolymers

Modified vinyl ether based PCEs were synthesized via free radical copolymerization from maleic anhydride, maleic monoester and 4-hydroxy butyl vinyl ether. Their chemical structure is shown in **Fig. 1**. 2-Mercaptoethanol was used as chain transfer agent and Rongalit C was applied as initiator /3/. Molar masses, polydispersity index (PDI) and hydrodynamic radius (R_h) of the PCE samples were determined utilizing size exclusion chromatography (SEC).

Dispersing performance in presence of clay and mechanistic study

For determination of the paste flow, a “mini slump test” according to DIN EN 1015 was utilized, for details see /4/. Interaction of the novel superplasticizer with clay was probed via adsorption and XRD measurements /5/.

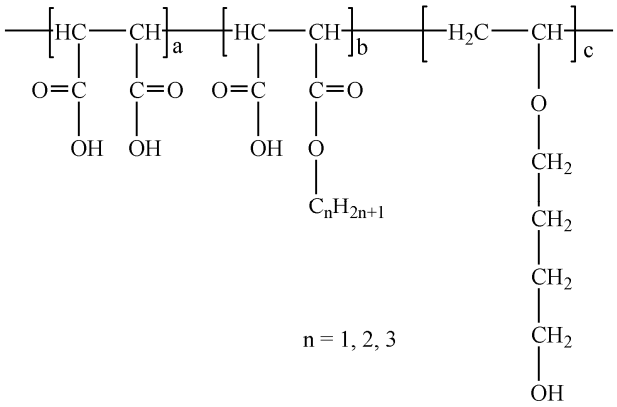

Fig.1: Chemical structure of the synthesized vinyl ether polycarboxylate superplasticizers

Results and discussion

Characterization of MA-HBVE copolymers

The characteristic molecular properties of the synthesized copolymers are presented in **Table 1**. According to the SEC data, the molar masses (M_w) of the PCE samples are ~ 10,000 Da which is lower than for VPEG PCEs possessing conventional PEG side chains which exhibit a M_w of ~ 22,000 Da. The polydispersity index of the samples is 1.8 - 2.7 which indicates a fairly narrow molecular weight distribution.

Table 1: Molar masses, polydispersity index (PDI) of the synthesized superplasticizer samples

PCE	M_w (g/mol)	M_n (g/mol)	PDI (M_w/M_n)
MA-Monomethyl Maleate-HBVE	10,110	5,775	1.8
MA-Monoethyl Maleate-HBVE	9,000	3,334	2.7
MA-Monopropyl Maleate-HBVE	10,220	3,998	2.7
MA-MPEG1000-HBVE	21,390	8,010	2.4
BNS	*139,100	-	-

* batch measurement

Cement dispersion in absence and presence of clay

For this test, a CEM I 52.5 N paste prepared at a w/c ratio of 0.45 was employed (no clay present). The results are displayed in **Fig. 2**. There it shows that the newly synthesized PCE polymers fluidize cement pastes at surprisingly low dosages, considering such short side chains.

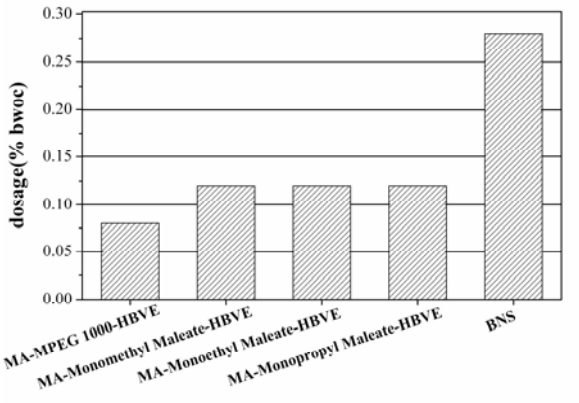

Fig. 2: Dosages of MA-HBVE copolymers and of a comparative PEG-vinylether PCE required to achieve a cement paste spread of 26 cm (w/c = 0.45)

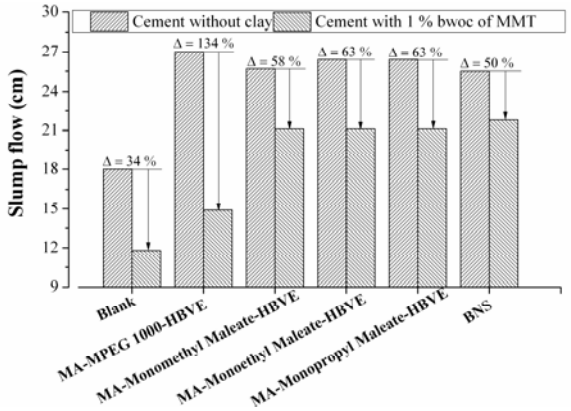

Fig. 3: Spread flow of cement pastes (w/c = 0.45) containing different superplasticizers, measured in absence and presence of 1 % bwoc of clay

As is exhibited in **Fig. 3**, for the neat cement paste addition of 1 % bwoc of montmorillonite clay (MMT) decreases the spread by 34 %. Also, the PCE sample possessing PEO side chains is strongly affected by MMT, its slump flow decreased by as much as 134 %. On the contrary, the MA-HBVE copolymers show much better clay tolerance. Their slump flow decreased by ~ 60 % only, which is comparable to that of the BNS superplasticizer /6/.

Sorption on clay

Sorption isotherms on clay were developed (**Fig. 4**). The VPEG-type PCE possessing a conventional PEO side chain sorbs in very high amount on montmorillonite (~ 230 mg/g of clay at equilibrium). Opposite to this behavior, the MA-HBVE copolymers sorb in extremely low amount on MMT (~ 20 mg/g of clay). This value is even lower than for the polycondensate BNS which lies at ~ 50 mg/g of clay.

PCE/clay interaction

According to **Fig. 5**, when hydrated, pure clay shows a d-spacing (distance between the alumosilicate layers) of 1.23 nm. When MA-MPEG1000-HBVE is present, a shift in the d-spacing from 1.23 nm to 1.72 nm is detected, indicating that such conventional PCE is chemically incorporated into the clay structure /7/. However, when the MA-HBVE copolymers are added, no change in the d-value of the hydrated clay was observed. These results signify that this new type of PCE does not incorporate into the interlayer region. Hence, interaction of these copolymers with clay is limited to mere surface adsorption while no chemical sorption occurs.

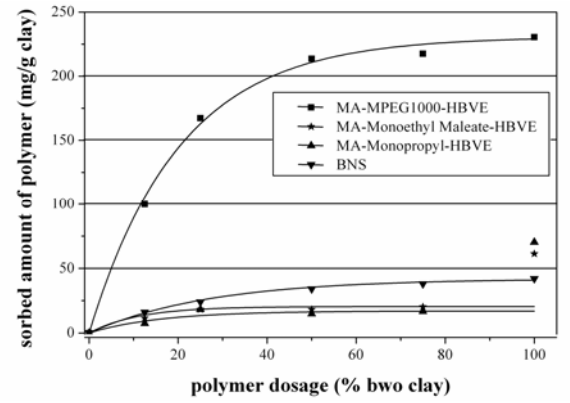

Fig. 4: Sorption isotherms for superplasticizer samples on montmorillonite clay dispersed in synthetic cement pore solution (w/clay = 45)

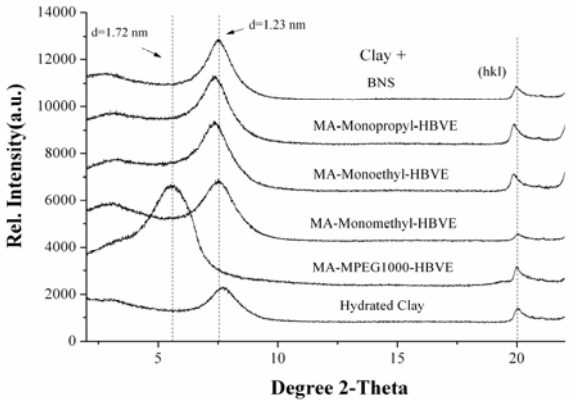

Fig. 5: XRD patterns of montmorillonite clay dispersed in synthetic cement pore solution holding 50 % bwo clay of different superplasticizers (w/clay = 45)

Conclusion

A novel type of vinyl ether modified PCE has been successfully synthesized from maleic anhydride, maleic monoester and 4-hydroxy butyl vinyl ether by radical copolymerization. The newly synthesized copolymers containing alkyl pendant chains possess a high dispersing ability and enhanced clay robustness. According to our findings, the key parameter to obtain a more clay tolerant PCE is modification of the side chain which should not contain polyethylene oxide as is the case in conventional PCEs. Apparently, through chemical modification, there are many possibilities to obtain clay tolerant PCEs.

Bibliographical references

/1/ T. Hirata: Japanese Patent JP 84, 2022 (S59-018338), 1981

/2/ V.S.Ramachandran: „Superplasticizers“, Prog. Cem. Concr. 1 (1992) 345–375.

/3/ G. Albrecht, J. Weichmann, J.Penkner, A. Kern: „Copolymers based on oxyalkyleneglycol alkenyl ethers and unsaturated dicarboxylic acid derivatives”, US Patent 5, 798, 425, 1998, assigned to SKW Trostberg AG.

/4/ L. Lei, J. Plank: „Synthesis, working mechanism and effectiveness of a novel cycloaliphatic superplasticizer for concrete”, Cem. Concr. Res., 42 (2012) 118-123.

/5/ S. Ng, J. Plank: „Interaction Mechanisms Between Na Montmorillonite Clay and MPEG-Based Polycarboxylate Superplasticizers”, Cem. Concr. Res., 42 (2012) 847-854.

/6/ D. Atarashi, E. Sakai, R. Obinata, M. Daimon: „Interactions between Superplasticizers and Clay minerals”, Cem. Sci. Concr. Technol., V. 58, 2004, pp. 387–392.

/7/ S. Liu, X. Mo, C. Zhang, D. Sun, C. Mu: „Swelling Inhibition by Polyglycols in Montmorillonite Dispersions”, J. Disper. Sci. Technol., V. 25, 2004, pp. 63–66.

5.11 A novel type of PCE superplasticizer exhibiting clay tolerance

L. Lei, J. Plank

4th National Conference on Polycarboxylate Superplasticizer and Application Technology, June 18 – 20, 2013, Beijing (China)
in: Polycarboxylate superplasticizers – New progress in preparation, performance and application technology
Beijing Institute of Technology Press, 2013, 58 – 65.

In this conference paper, the synthesis method for a novel PCE structure possessing clay tolerance was disclosed in detail. Different from the conventional VPEG-PCE structure which typically contains PEG as pendent chain, for this novel structure alkyl maleate monomers, namely methyl maleate, ethyl maleate, propyl maleate or butyl maleate were incorporated into the PCE structure.

After successful synthesis of the four VPEG-PCE samples incorporating the novel building block, their robustness against montmorillonite was tested in cement paste via 'mini slump' test. According to the results, the novel PCE polymers exhibited high dispersing effectiveness even in montmorillonite contaminated systems. Mechanistic studies revealed that alkyl maleates present a novel type of side chain which show no affinity to the interlayer gallery of montmorillonite.

一种新型的 VPEG 型聚羧酸系高性能减水剂

雷蕾[1]，J. Plank[1]
[1] 慕尼黑工业大学无机化学系，德国慕尼黑，85747

摘要：传统型聚羧酸系高性能减水剂对混凝土骨料中粘土成分非常敏感，少量的粘土往往会导致 PCE 对水泥分散能力的大幅度降低。本研究合成了一种新型的 4-羟丁基乙烯基醚（VPEG）型聚羧酸系高性能减水剂。水泥净浆流动度测试表明这种新型 4-羟丁基乙烯基醚（VPEG）型 PCE 能够显著地提高水泥浆体的流动性，并且对粘土成分的敏感性较低。TOC 试验结果表明新型（VPEG）型 PCE 在粘土上的吸附量极少，粘土水化物 XRD 表征结果显示新型 4-羟丁基乙烯基醚（VPEG）型 PCE 并没有形成插层结构。这两项试验结果印证了新型 VPEG 型 PCE 对粘土的低敏感性。

关键词：聚羧酸系高性能减水剂，分散能力，吸附，粘土

1 引言

含有聚醚侧链的聚羧酸高效减水剂因具有掺量低，减水率高，保坍性能好、混凝土收缩率低等突出优点，已经成为制造高性能混凝土的一种重要材料，在高速铁路、水利水电、大跨度桥梁、海洋钻井平台、地铁隧道、高层建筑等工程得到广泛应用。但工程应用中发现，聚羧酸系减水剂同传统萘系等缩聚型减水剂相比，相容性问题更加突出，尤其是对骨料中的含泥量特别敏感，导致混凝土初始流动性不足，流动度损失加快。同时优质砂、石资源日益匮乏，开发利用低品位骨料是实现可持续发展的关键。本文合成出一种新型 VPEG 型 PCE 力求在一定程度解决 PCE 对粘土的敏感性难题。

2 实验

2.1 实验材料

（1）马来酸酐，纯度>99%，Merck Schuchardt OHG (Hohenbrunn, Germany)；

（2）4-羟丁基乙烯基醚（VPEG），浓度>99%，SIGMA-ALDRICH CHEMIE (Steinheim, Germany)；

（3）Rongalite，纯度>98%，SIGMA-ALDRICH CHEMIE (Steinheim, Germany)；

（4）硫酸亚铁，纯度>99%，VWR International (Darmstadt, Germany)；

（5）2-巯基乙醇，浓度>99%，SIGMA-ALDRICH CHEMIE (Steinheim, Germany)；

（6）双氧水，浓度 30%，VWR International (Darmstadt, Germany)；

（7）低级醇，纯度>99%，VWR International (Darmstadt, Germany)；

采用标号为 52.5 N 的普通硅酸盐水泥（Milke®classicfrom HeidelbergCement,

[1]雷蕾，女，1988 年 10 月，博士研究生
Technical University Munich, Lichtenbergstr. 4, D-85747 Garching, Germany.
Tel.: (089) 289 13187

Gesekeplant)。使用 XRD 表征得到熟料的矿物组成并列于表 1。水泥颗粒平均粒径（d_{50}）为 10.82 μm。

表 1 水泥熟料的化学成分及矿物组成

Phase	wt.%
C_3S, m	52.0
C_2S, m	27.6
C_3A, c	4.4
C_3A, o	3.6
C_4AF, o	4.3
Free lime (Franke)	0.1
Periclase (MgO)	0.1
Anhydrite	2.1
Hemihydrate*	0.7
Dihydrate*	0.4
Calcite	3.3
Quartz	0.8

*Determined by thermogravimetry

（8）粘土

采用商品名为 RXM 6020 由 Rockwood (Moosburg, Germany)生产的粘土。这种粘土存在于天然的斑脱土中。使用 XRF 表征得到粘土的主要矿物组成并列于表 2 中。

表 2 RXM 6020 粘土的氧化物组成(wt.%)

Oxide	SiO_2	Al_2O_3	CaO	MgO	Fe_2O_3	Na_2O	K_2O	TiO_2
(wt. %)	59.73	18.39	0.79	2.25	3.96	2.32	0.13	0.11

（9）高效减水剂

试验中采取以下高效减水剂与本研究合成的新型VPEG型PCE进行对比。

(a) Melcret®500F萘系高效减水剂（BASF SE, Ludwigshafen, Germany），是一种提纯过的，含少量的Na_2SO_4(<2wt.%) 的粉末状萘系高效减水剂(以下简称BNS)。

(b) 自主合成的2种传统型VPEG型PCE。根据其不同的支链长度，将其分别命名为MA-MPEG1000-HBVE（固含量：40 %）以及MA-MPEG2000-HBVE（固含量：46 %）。

表 3 聚羧酸减水剂的主要物理化学性质

PCE	abbreviation	Side chain n_{EO}	Mw (g/mol)	Mn (g/mol)
MA-MPEG1000 -HBVE	MA- HBVE 1K	23	21,390	8,010
MA-MPEG2000 -HBVE	MA-HBVE 2K	45	53,750	16,180
BNS	BNS	-	139,100*	-

*batch measurement.

2.2 新型 VPEG 型 PCE 的制备

向装有温度计、机械搅拌装置、恒压滴液装置的四口烧瓶中先加入一定量的低级醇和马来酸酐，酯化温度为 60°C，反应时间为 2 小时，制备出马来酸单酯。酯化结束后，在持续搅拌的条件下，往四口烧瓶中依次加入一定量的水，4-羟丁基乙烯基醚，少量硫酸亚铁溶液以及双氧水。再将马来酸酐溶液（含 2-巯基乙醇链转移剂）及始发剂溶液（Rongalite）分别

于 1 小时和 1.5 小时内匀速滴加至四口烧瓶中。整个聚合反应过程中，控制温度低于 25°C。待加液完毕后，持续搅拌 30 min，以完成聚合反应。

表 4 新型 VPEG 型 PCE 的主要物理化学性质

PCE	abbreviation	Side chain	Mw (g/mol)	Mn (g/mol)
MSA-Monomethyl Maleate-HBVE	MA-HBVE 1	Hydroxybutyl	10,110	5,775
MSA-Monoethyl Maleate-HBVE	MA-HBVE 2	Hydroxybutyl	7,727	3,272
MSA-Monopropyl Maleate-HBVE	MA-HBVE 3	Hydroxybutyl	10,220	3,998
MSA-Monobutyl Maleate-HBVE	MA-HBVE 4	Hydroxybutyl	10,100	3,700

2.3 试验方法

2.3.1 净浆流动度

采用“微型坍落度实验”测量水泥浆体的流动度，以此评价减水剂的作用效果。根据 DIN EN 1015 中规定的实验方法，首先确定水泥浆体的水灰比，在水泥、拌合水、无减水剂掺入的系统中，水泥浆体的摊铺直径为 18±0.5 cm 的基准水灰比。在基准水灰比下，测定水泥浆体摊铺直径为 26±0.5 cm 时的减水剂的掺量。

2.3.2 吸附性能测试

称取0.5 g粘土、22.5 g去离子水和不同浓度的PCE溶液，加入50 ml的离心管中，恒温20°C振动2 min (2400 rpm)，然后在8500 rpm的离心机中离心10 min，收集离心管内上清液，使用High TOC II（ElementarAnalysensysteme, Hanau, Germany）测定上清液中有机碳的浓度。继而采用总有机碳量测量法（TOC）计算减水剂于粘土上吸附量。

2.3.3 粘土水化物 XRD 表征

0.5 g 粘土、22.5 g 的 1.11 wt.%减水剂溶液加入 50 ml 的离心管中，恒温振动 20°C 2 min (2400 rpm)，然后在 8500 rpm 的离心机中离心 10 min，倒掉清液，将离心管中的固体物质放入 80°C 真空烘箱中干燥一夜，研磨制样后放入 XRD 衍射仪中进行表征。表征条件为：步长 0.15 s/step，2θ 角扫描范围为 0.6 °到 20 °。

3 结果与讨论

3.1 不同减水剂的饱和掺量

固定 w/c=0.45，在该水灰比下，水泥净浆流动度为 18±0.5cm，测定水泥浆体摊铺直径为 26±0.5 cm 时的不同减水剂的掺量。实验结果如图 1 所示：

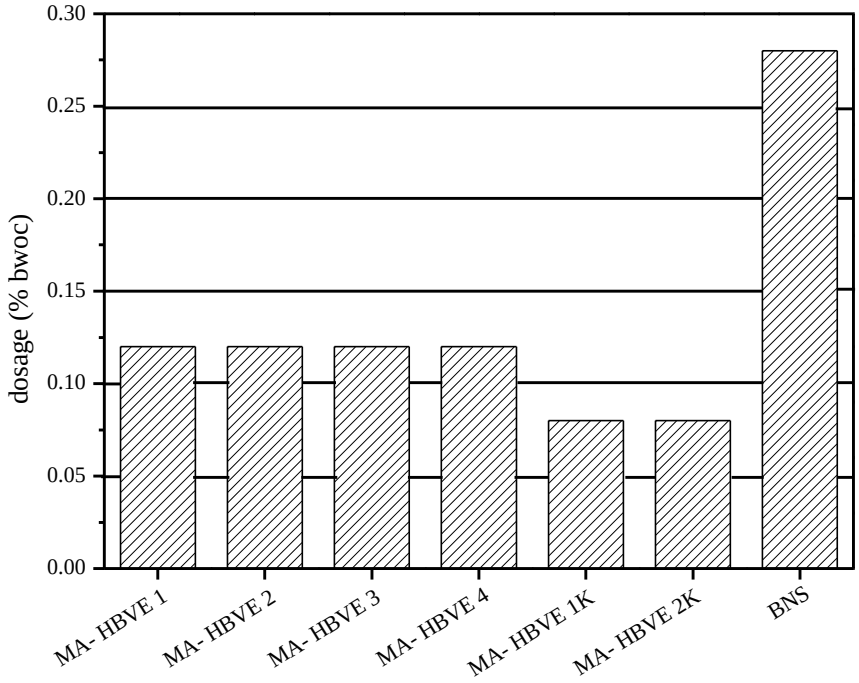

图 1 不同减水剂的饱和掺量

从图 1 可以看出，新型 VPEG 型 PCE 能够显著地提高水泥浆体的流动性。在达到相同的流动度条件下，新型 VPEG 型 PCE 的掺量比传统长支链的 VPEG 型 PCE 略高，远远低于 BNS。

3.2 粘土对 PCE 分散性能的影响

固定 w/c=0.45，在该水灰比下，水泥净浆流动度为 18 cm，当在不掺任何减水剂的水泥浆体中掺入占水泥总量 0.5 %的粘土时，水泥浆体的流动度为 14.5 cm，流动度降低了 20 %。在本实验中，各减水剂的掺量为达到水泥净浆流动度为 26 cm 时的掺量，即新型 VPEG 型 PCE（分别为 MA-HBVE 1，MA-HBVE 2，MA-HBVE 3，MA-HBVE 4）掺量为 0.12 % bwoc。传统长支链 VPEG 型 PCE 掺量为 0.08 % bwoc，BNS 掺量为 0.28 % bwoc。通过测试添加粘土成分后，分别测定掺不同减水剂时水泥净浆流动度的变化，从而考察粘土成分对减水剂性能的影响。

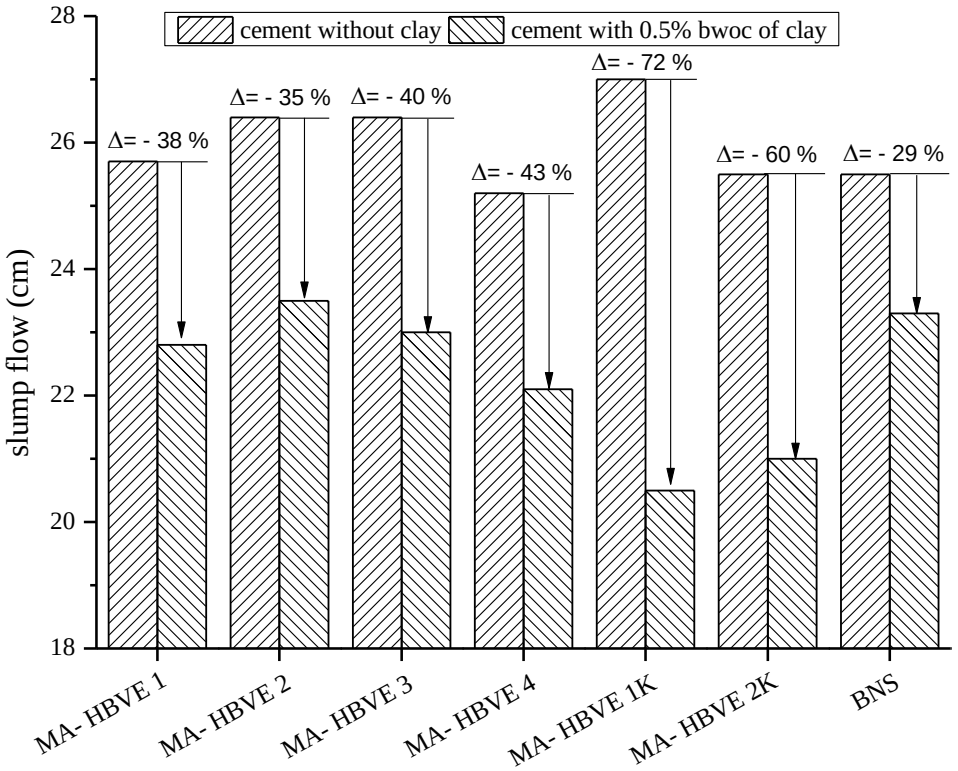

图 2 粘土(0.5 wt.%)对掺不同减水剂水泥浆体流动性的影响

如图 2 所示，作为对比实验，掺传统长支链 VPEG 型 PCE 的水泥浆体，在加入 0.5 wt.%粘土后，净浆流动度分别降低 72 % 和 60 %。由此可以看出，少量粘土的掺入会导致传统型 PCE 对水泥分散能力的显著降低,这可能是由于粘土对传统型 PCE 具有较强的吸附能力，在溶液中与水泥颗粒竞争吸附聚羧酸分子,使得吸附于水泥颗粒表面的聚羧酸分子数量大大减少，从而导致传统型 PCE 对水泥分散能力的降低。而对于掺新型 VPEG 型 PCE 的水泥浆体，在加入 0.5 wt.%粘土后，净浆流动度降低在 35-43 %范围内。由此可见，新型 VPEG 型 PCE 对粘土的敏感度大幅度降低。BNS 的实验结果与新型 VPEG 型 PCE 的实验结果类似，粘土成分对于 BNS 的影响甚小（流动度降低 29 %），这是由于 BNS 为线性缩聚物，无侧链结构，避免了因形成插层结构而损失的减水剂。粘土成分并没有对新型 VPEG 型 PCE 的分散性能产生大的影响，这与新型 VPEG 型 PCE 的分子构型有关， 新型 VPEG 型 PCE 的分子结构中不包含 PEO 支链，避免了插层结构的形成。

3.3 新型 VPEG 型 PCE 在粘土上吸附量

在不同 PCE 掺量下，粘土对新型 VPEG 型 PCE 的吸附量如图 3 所示，同时测定了传统 VPEG 型 PCE，BNS 在粘土上的吸附量作为参照。本实验采用总有机碳量测量法（TOC）计算减水剂于粘土上的吸附量。固定水胶比为 45（w/clay=45）。

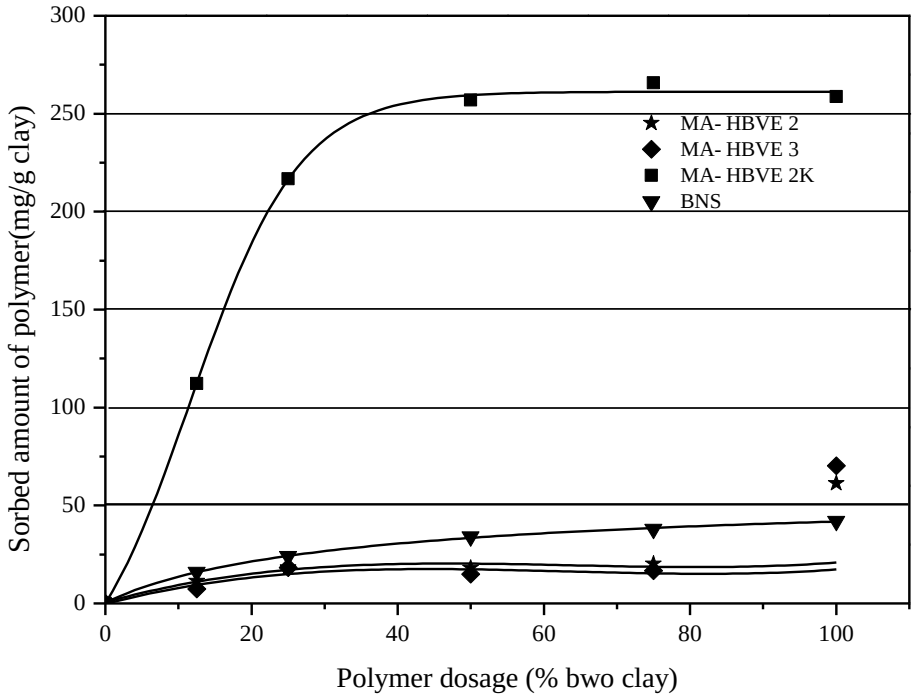

图 3 减水剂分别于粘土系统中的吸附等温线（w/clay=45）

从图 3 可以看出，与 BNS 类似，新型 VPEG 型 PCE(MA- HBVE 2, MA- HBVE 3)在粘土上的吸附量极少（~15mg/g 粘土）。而对于传统长支链的 VPEG 型 PCE(MA- HBVE 2K)，则大量的吸附于粘土上，当 MA- HBVE 2K 掺量为 50 % bwo clay 时，于粘土上的吸附量高达 270 mg/g 粘土。之后，随着减水剂掺量的增加，在粘土颗粒表面的吸附量不再随之增大。新型 VPEG 型 PCE 与传统长支链的 VPEG 型 PCE 于粘土上吸附量差别巨大，由此可以解释新型 VPEG 型 PCE 受粘土成分影响较小而传统 VPEG 型 PCE 的分散能力大大减弱的现象。

3.4 粘土水化产物的 XRD 分析

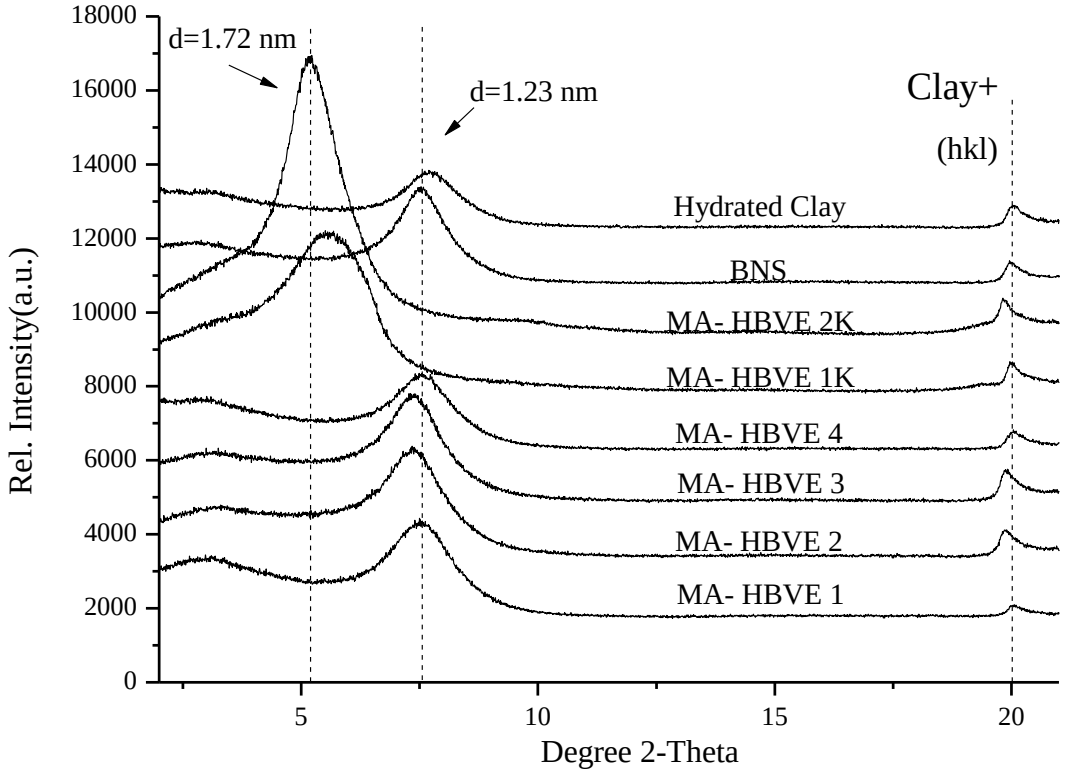

图 4 掺不同减水剂的粘土水化产物的 XRD 图谱（减水剂掺量均为 50 % bwo clay，w/clay = 45）

如图 4 所示，不掺任何减水剂的粘土水化物层间距（d）为 1.23 nm，当粘土中掺入传统长支链 VPEG 型 PCE，其水化物层间距由原本的 1.23 nm 增加至 1.72 nm，证实了其 PEO 侧链插入粘土的层状结构中，从而导致粘土水化物层间距显著增加；与传统长支链 VPEG 型 PCE 不同的是，对于掺新型 VPEG 型 PCE(MA-Monoethyl Maleate-HBVE, MA-Monopropyl Maleate-HBVE)或 BNS 的粘土样品，其水化物的层间距依旧保持在 1.23 nm。说明新型 VPEG 型 PCE 并没有入粘土的层间结构中。这也解释了新型 VPEG 型 PCE 工作性能受粘土成分影响较小的原因。

4 结论

本研究合成了一种新型的 VPEG 型聚羧酸高效减水剂，这种新型高效减水剂的优点是生产工艺简单，常温下即可进行。与 BNS 类似，粘土成分对其分散性能的影响不大，且其掺量远远低于 BNS。与传统型的长支链 VPEG 型 PCE 相较，其对粘土的敏感性大幅度降低。根据实验结果发现，实现粘土抵抗型 PCE，分子结构中一定要避免 PEO 支链，但是传统的聚羧酸分子构型中的 PEO 支链是产生空间位阻效应从而提供分散能力的重要组成部分。XRD 实验结果表明，传统的聚羧酸分子构型中的 PEO 支链极易插入粘土层状结构中，从而大大降低聚羧酸的分散能力。本文中阐述的这种新型 VPEG 型 PCE 的分子构型中不含 PEO 侧链，而改用羟丁基作为支链避免了插层的形成。当然这只是解决聚羧酸对粘土的敏感性问题的一种可能性，在今后的研究中，我们会发现越来越多具备此种性能的聚羧酸产品。

参考文献

[1] 王子明. 聚羧酸系高性能减水剂-制备、性能与应用[M]. 北京：中国建筑工业出版社，2009, 4-14.

[2] 吴中伟，廉慧珍．高性能混凝土[M]．北京：中国铁道出版社，1999, 103-107.

[3] Nathan A. Tregger, Margaret E. Pakula, Surendra P. Shah. Influence of clays on the rheologyof cement pastes[J]. Cement and Concrete Research, 2010, 40(3): 384-391.

[4]齐淑芹，段彬．聚羧酸系高效减水剂在工程应用中的适应性研究[J]．铁道建设，2008, (7): 121-123.

[5] Manning D., "Handbook of Clay Science (Developments in Clay Science, 1)", Bergaya F., Theng B. K. G., Lagaly G. Ed., Elsevier's Science & Technology, 2007: 19–86.

[6] B. Velde, Origin and Mineralogy of Clays: Clay and the Environment, in: B. Velde(Ed.), Springer, 1995.

[7]A.A. Jeknavorian, L. Jardine, C.C. Ou, et al. Interaction of Superplasticizers with Clay-Bearing Aggregates [J], Special Publication ACI/7th CANMET Conference on Superplasticizers and Other Chemical Admixtures, Berlin, Germany, 2003, SP-217, 1293–1316.

[8] E. Sakai, D. Atarashi, M. Daimon, "Interaction between Superplasticizers and Clay Minerals", Special Publication ACI/ 6th CANMET Conference on Superplasticizers and Other Chemical Admixtures, Xi' an, China, 2006,1560–1566.

[9] D. Atarashi, E. Sakai, R. Obinata, M. Daimon, Interactions between superplasticizers and clay minerals[J], Cement Science and Concrete Technology, 2004, 58: 387–392.

[10] R. Magarotto, F. Moratti, N. Zeminian, "Influence of sulfates content in cement on the performances of superplasticizers", ACI/ 8th CANMET Conference on Superplasticizers and Other Chemical Admixtures in Concrete, Sorrento, Italy, 2006, SP-239-15, 215-229.

[11] A.A. Jeknavorian, L. Jardine, C.C. Ou, et al. "Interaction of Superplasticizers with Clay-Bearing Aggregates", Special Publication ACI/ 7th CANMET Conference on Superplasticizers and Other Chemical Admixtures, Berlin, Germany, 2003, SP-217, 1293–1316.

[12] 王子明，程勋，李明东. 不同粘土对聚羧酸系减水剂应用性能的影响[J]. 商品混凝土，2010，(3): 24-26.

[13] 杨勇，冉千平，毛永琳，等. 蒙脱土对聚羧酸超塑化剂的吸附行为[J].建筑材料学报，2012，15(04): 464-468.

[14] S. Ng, J. Plank. Interaction Mechanisms Between Na Montmorillonite Clay and MPEG-Based PolycarboxylateSuperplasticizers[J], Cement and Concrete Research,2012. 42(6): 847-854.

[15] S. Liu, X. Mo, C. Zhang, et al. Swelling Inhibition by Polyglycols in Montmorillonite Dispersions[J], Journal of Dispersion Science and Technology, 2004, 25(1): 63–66.

[16] J. L. Suter, P. V. Coveney, Computer simulation study of the materials properties of intercalated and exfoliated poly(ethylene) glycol clay nanocomposites[J], Soft mater. 2009, 5: 2239–2251.

[17]P. D. Svensson, S. Hansen.Intercalation of smectite with liquid ethylene glycol resolved in time and space by synchrotron X-ray diffraction[J], Appl. Clay Sci. 2010, 48(3): 358–367.

[18] L. Lei, J. Plank., A Concept For a PolycarboxylateSuperplasticizer Possessing Enhanced Clay Tolerance[J],Cement and Concrete Research, 2012, 42(10): 1299–1306.

5.12 Preparation and characterization of a novel polycarboxylate/montmorillonite nanocomposite

L. Lei, J. Plank

18th International Symposium on Intercalation Compounds (ISIC18)
May 31 – June 4, 2015, Strassbourg (France)
Compilation of Abstracts p. 86.

This contribution was presented as an oral presentation and a poster at the conference. Here, a facile method for producing a polymer/clay nano composite with unusual properties by adding an aqueous solution of the anionic polymer (polycarboxylate ether, PCE) to an aqueous suspension of hydrated montmorillonite is described.

Analysis via XRD, IR spectroscopy, elemental analysis and TEM imaging evidenced the successful chemical intercalation of the PCE polymer in between the aluminosilicate layers.

Such composites can be useful materials as filler in plastics and thermal insulation systems.

F14 (P47)

Preparation and characterization of a novel polycarboxylate/montmorillonite nanocomposite

L. Lei[1], J. Plank[1]*

[1] *Technische Universität München, Chair for Construction Chemicals, 85747 Garching, Lichtenbergstraße 4, Germany*

(*)sekretariat@bauchemie.ch.tum.de

Keywords: Polycarboxylate; montmorillonite; nanocomposite; XRD

It is well established that glycols and polyglycols can intercalate between the aluminosilicate layers of montmorillonite, a smectite clay mineral. Here, we present on the intercalation of a highly anionic polyglycol copolymer, namely methacrylic acid– *co* – ω - methoxy poly(ethylene glycol) methacrylate ester into commercial bentonite, resulting in a polymer/clay nano composite with unusual properties.

Synthesis of the nanocomposite can be performed easily by adding an aqueous solution of the anionic polymer (polycarboxylate ether, PCE) to an aqueous suspension of the hydrated clay, stirring for 1 hour at room temperature and centrifugation. Successful chemical intercalation of the PCE polymer in between the aluminosilicate layers was confirmed via XRD, IR spectroscopy, elemental analysis and TEM imaging. From XRD, a d spacing of 1.77 nm characteristic for glycol intercalated into montmorillonite was found. Occurance of intercalation is surprising, considering that the PCE polymer is highly anionic and possesses the same charge as the aluminosilicate layer of bentonite.

The novel nano composite exhibits exceptional stability, e.g. at high pH values (12 - 13). The PCE polymer is not exchanged by K^+ or quaternary ammonium salts. However, it is released when polyglycols are added to an aqueous suspension of the nano composite.

The PCE/bentonite nano composite can be used as filler in plastics whereby different PCE molecules can modify the charge characteristic and properties of the nano composite.

5.13 Impact of polycarboxylate superplasticizers on ettringite crystallization at very early cement hydration stages under zero gravity

L Lei, J. Plank, M. R. Meier

5th National Conference on Polycarboxylate Superplasticizer and Application Technology
June 15 – 17, 2015, Beijing (China)
Proceedings, 45 – 49.

This work was carried out in cooperation with another Ph. D. candidate, **Markus Meier**.

In this study, the early ettringite crystals developed on the surface of hydrating ordinary Portland cement under normal and zero gravity condition was investigated in the presence or absence of PCE polymers utilizing SEM microscopy and X-ray diffraction. The PCE polymer used here was a self-synthesized IPEG-PCE superplasticizer.

According to the SEM images, as for neat cement under zero gravity condition more abundant and smaller ettringite crystals were generated, but no difference regarding the crystal morphology was observed under the different gravity conditions. Whereas, when IPEG-PCE was added, under zero gravity condition not only the amount of ettringite crystals increased, but also the ettringite morphology had changed to a higher aspect ratio (the crystals became slimmer). These observations confirmed that PCE polymers generally act as morphological catalyst because they preferably adsorb on specific faces of the ettringite surface, thus aspect ratio is changed. Furthermore, under zero gravity the period of oversaturation generally seems to last longer, allowing more nuclei to form, and the effect of the IPEG-PCE on ettringite morphology is more pronounced at zero gravity than under terrestric condition.

零重力条件下 PCE 对水泥早期水化产物钙矾石晶化形貌的影响

雷蕾，Johann Plank*，Markus R. Meier
（慕尼黑工业大学无机化学系，德国慕尼黑）

摘要：水泥水化是一个复杂的物理化学过程，其中大部分结晶相是从过饱和溶液中沉淀出来的。作为水泥水化的重要产物和众多混凝土外加剂的主要锚固相，钙矾石晶体在水泥水化的初始阶段（10 s 内）就已形成，其形貌和晶体结构可以采用环境扫描和 X 射线衍射仪进行分析。本文对比了正常重力和零重力条件下聚羧酸减水剂对不同种类水泥早期水化阶段钙矾石晶体的形貌的影响。

关键词：聚羧酸减水剂；钙矾石；水泥水化；零重力条件

0 序言

晶体作用实质上是使质点从不规则排列到规则排列，从而形成晶格的作用。任何晶体的生长均有晶核形成和晶核生长两个阶段，二者受不同因素控制。晶核形成阶段热力学条件起决定性作用，而晶核生长阶段则主要受动力学条件控制。

正常重力场，晶体的生长机理为扩散控制及对流控制。而在零重力特定环境中，对流现象缺失，晶体的生长完全由扩散控制。目前，关于零重力条件下晶体生长的研究大都与蛋白质有关（39 次美国航天飞机飞行，约 200 种不同样品）。仅有少量的零重力试验是针对无机材料的，如 NaCl 及 $Ca_5(PO_4)_3OH$。

钙矾石是水泥水化最早形成的水化产物，钙矾石的结晶过程是水泥水化进程中的一个重要反应。聚羧酸系高性能减水剂是阴离子型表面活性剂，在水泥水化早期，主要吸附在铝酸三钙（C_3A）和钙矾石表面，通过空间位阻效应和静电斥力发挥分散作用，提高混凝土拌合物的流动性。PCE 在 C_3A 和钙矾石表面的吸附会对 C_3A 的水化、溶解和钙矾石晶体的形成产生重要影响。本文对比了在正常重力和零重力条件下水泥样品的早期水化产物钙矾石晶体的形貌，并且分析了聚羧酸减水剂对不同水泥样品的早期水化阶段产物钙矾石晶体的形貌的影响。

1 试验材料

1.1 水泥

试验分别采用了两种包含不同 C_3A 含量的普通硅酸盐水泥，水泥熟料的化学成分及矿

* Johann Plank（1952. 12—）：男，教授，Lichtenbergstr. 4，Garching bei München，85747，电话：+49 89 289 13151。

物组成见表1。

表1 水泥熟料的化学成分及矿物组成

岩相	CEM I 32.5 R	CEM I 42.5 R
硅酸三钙，单斜	53.93	58.83
硅酸二钙，单斜	16.69	17.01
铝酸三钙，立方	5.12	3.61
铝酸三钙，斜方	4.73	1.60
铁铝酸四钙，斜方	8.57	9.43
游离氧化钙，Rietveld 法	—	0.09
游离氧化钙，Franke 法	0.97	0.06
氧化镁	2.06	0.66
无水石膏	2.15	1.83
半水石膏（热重法）	2.00	0.27
石膏（热重法）	—	2.42
方解石	3.04	2.80
石英	0.90	0.36
单钾芒硝	0.80	1.04
共计	100.97	100.02

1.2 聚羧酸减水剂

实验室自主合成的IPEG型PCE。其支链长度为52EO单元，酸醚比为8:1。试验所用聚羧酸减水剂样品信息见表2。

表2 试验所用聚羧酸减水剂样品信息

样品	固含量/%	M_w/(g·mol^{-1})	M_n/(g·mol^{-1})	PDI	阴离子电荷密度/(μeq·g^{-1})
IPEG-52PC8	87	24 000	12 000	2.0	3 237

2 试验方法

所有微重力试验均是在执行抛物线飞行的空客A300飞机上完成的。抛物线飞行试验项目（共飞行5 d，每天31次抛物线飞行）由德国航空航天中心（DLR）资助。抛物线飞行轨迹如图1所示，自0时刻起，飞机加速上升，此时机舱将出现持续大约24 s的（1.5～1.8）g重力环境，即超重期。飞机达到47°的倾斜角度，超重期结束，转而进入到大约持续22 s的0g重力环境，也即为零重力期，此时试验人员在机舱内开始试验。达到抛物线的顶

部后，飞机开始下降，当倾斜角度达到42°时，飞机再次加速，零重力期结束，机舱中再次出现超重期，也持续约22 s。

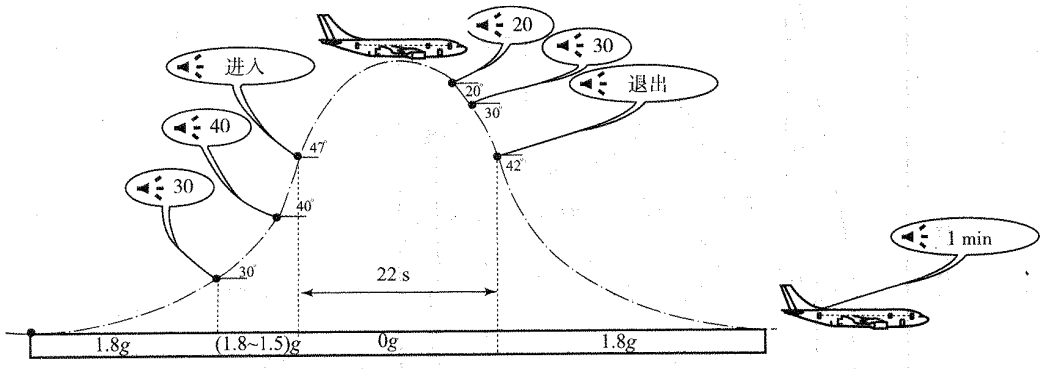

图1　抛物线飞行轨迹

3　结果与讨论

3.1　1g、0g 重力条件下水泥样品的早期水化产物分析

图2所示为1g和0g重力条件下CEM I 42.5 R早期水化产物钙矾石的SEM照片。可见，在非常短的水化时间（10 s）内，纳米尺寸的钙矾石晶体就已形成，晶体形貌为典型的六角柱状。图3中X射线衍射图谱分析表明，此阶段没有其他的水泥水化产物生成。对比不同重力条件下生成的钙矾石晶体发现，在零重力条件下生成的钙矾石数量明显增加，且晶体尺寸较小。此外，相对于正常重力下的钙矾石晶体，零重力情况下生成的钙矾石晶体其形貌并没有发生变化，也即纵横比不变。

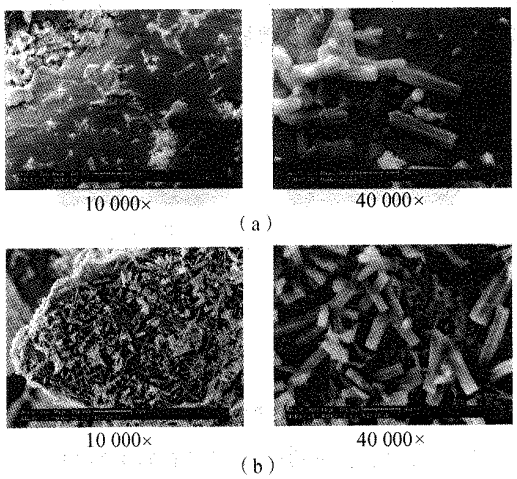

图2　1g和0g重力条件下CEM I 42.5 R早期水化产物钙矾石的SEM照片
(a) 1g; (b) 0g

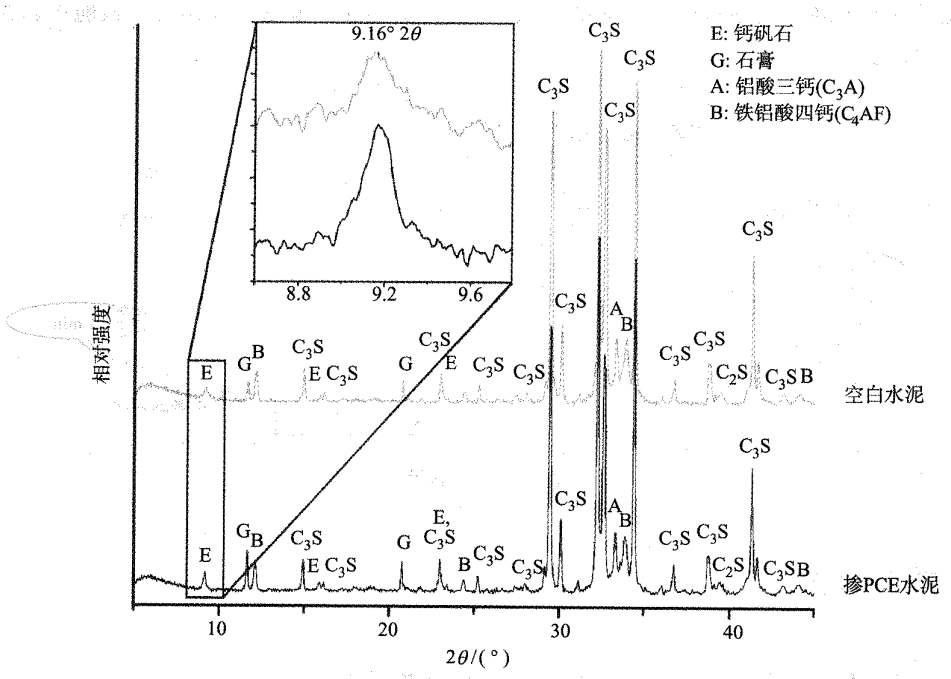

图3 零重力条件下，空白水泥样品（CEM I 42.5 R）及掺 PCE 水泥样品（CEM I 42.5 R）X 射线衍射图谱

3.2 1g，0g 重力条件下掺聚羧酸减水剂水泥样品的早期水化产物分析

图4 所示为 1g 和 0g 重力条件下掺 IPEG 聚羧酸减水剂 CEMI 32.5 R 水泥早期水化产物钙矾石的 SEM 照片。与空白水泥样品类似，零重力条件下掺聚羧酸减水剂的水泥样品生成的钙矾石数量明显增加，并且晶体尺寸也较小。更为重要的发现是，在微重力情况下生成的钙矾石晶体形状发生了变化，晶体的纵横比增加，变得更狭长。

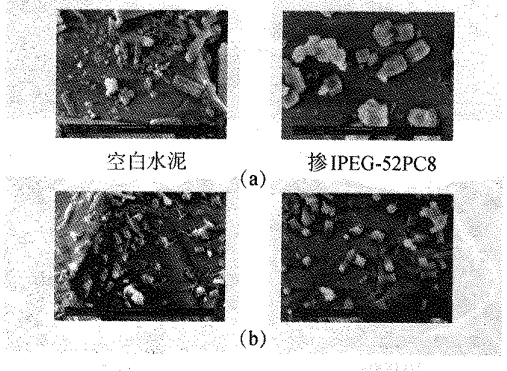

图4 1g 和 0g 重力条件下掺 IPEG 聚羧酸减水剂 CEM I 32.5 R 水泥早期水化产物钙矾石的 SEM 照片

(a) 1g；(b) 0g

4　结论

（1）钙矾石在水泥水化的初始阶段（10 s 内）就已形成，可以采用环境扫描电镜和 X 射线衍射仪对其进行观测分析。

（2）对于空白水泥样品，零重力条件下生成的钙矾石数量比正常重力条件下明显增加，但是晶体的形状并未发生变化。

（3）对于掺加了聚羧酸减水剂的水泥样品，零重力条件下生成的钙矾石不仅数量比正常重力条件下明显增加，而且晶体的纵横比增加，变得更狭长。

参考文献

[1] 钱逸泰. 结晶化学导论 [M]. 合肥：中国科技大学出版社，2005.

[2] 赵旭. 无极晶体结晶过程研究 [D]. 大连理工大学，2009.

[3] McPherson A. Virus and Protein Crystal Growth on Earth and in Microgravity [J]. Journal of Physics D-Applied Physics, 1993, 26 (8): 104 - 112.

[4] DeLucas L J, Moore K M, Long M M, Rouleau R, Bray T, Crysel Weise L. Protein crystal grown in space, past and future [J]. Jounal of Crystal Growth, 2002, 237: 1646 - 1650.

[5] Fontana P, Schefer J, Pettit D. Characterization of sodium chloride crystals grown in microgravity [J]. Journal of Crystal Growth, 2011, 324: 297 - 211.

[6] Lundager Madsen, H E, Christensson F, Polyak L E, Suvorova E I, Kliya M O, Chernov A A. Calcium phosphate crystallization under terrestrial and microgravity conditions [J]. Journal of Crystal Growth, 1995, 152 (3): 191 - 202.

[7] 杨守磊，伍勇华，李国新. 高效减水剂对钙矾石结晶形成影响的研究进展 [J]. 四川建筑科学研究，2012, 38 (3): 237 - 241.

6 Summary and outlook

The work documentted in this thesis includes a wide range of research topics, namely (1) the interaction of polycarboxylate comb copolymers with different clay minerals; (2) a novel facile preparation method for a PCE polymer using macroradicals; (3) a mechanistic investigation of cement – PCE superplasticizer incompatibility; (4) the nucleation and crystallization of ettringite under zero gravity conditions; and (5) the use of nano clay for early strength enhancement of Portland cement.

The investigations on the impact of different clay minerals on the dispersing force of PCEs revealed that different clay minerals exhibit a different influence on the dispersing power of PCEs. Among the three clay minerals which most frequently occur in concrete aggregates, montmorillonite was found to be the most harmful, due to its expanding lattice which allows conventional PCEs to intercalate via their PEG side chains into its interlayer gallery. Whereas, the other clay minerals tested (kaolin or muscovite) showed much less negative impact on the dispersing effectiveness of PCEs. In their case, the interaction with PCE is limited to surface adsorption only.

Based on these findings it can be concluded that inactive (non - swelling) clay impurities do not cause a serious problem in cementitious systems. Opposite to this, the presence of active (swelling) clays such as smectites is responsible for the much reduced or even completely lost dispersing effectiveness of PCEs. Thus, for concrete producers it is necessary to check the presence and quantify the amount of active clays in aggregates via the methylene blue test. When considerable amounts of active clays are found, then suitable mitigation strategies should be taken such as utilizing sacrificial agents or cationic compounds to block the interlayer space for PCE molecules, or use exclusively PCE polymers exhibiting clay tolerance.

Following these considerations, a concept for preparing novel PCE structures possessing

high clay robustness was introduced. The novel clay tolerant PCE structures are characterized by different side chains which replace the PEG side chains present in conventional PCE polymers. Hydroxy alkyl or 4 – hydroxy butyl vinyl ether were identified as non - intercalating side chains. Consequently, by eliminating the PEG side chains, chemisorption can no longer occur. Thus, the PCE polymers with new structures showed much better dispersing effectiveness in clay bearing systems. However, owed to their short side chains the dispersing power of these novel PCE structures in clay - free systems is average. Further work in this field should focus on seeking additional side chain alternatives which do not chemisorb in clay structures. The target should be PCE structures which perform well in both neat and clay-contaminated systems.

Another object of this thesis was to develop a simplified preparation method for MPEG-PCEs. Here, MPEG PCEs from simple raw materials, namely maleic anhydride and ω-methoxy poly(ethylene glycol) as sole raw materials were prepared. The key part in the polymerization process was the generation of ω-methoxy polyethylene glycol macroradicals obtained via hydrogen abstraction from MPEG. The successful synthesis of such MPEG-PCEs utilizing this novel method provides a much more facile route in comparison to the conventional free radical copolymerization methods. In the future, further optimization of the synthesis is proposed to capture the full potential of this novel type of PCE.

The third part of this thesis investigated the incompatibility problem occurring between most PCE polymers and specific cements. The findings suggest that PCE polymers modify the morphology of ettringite crystals to become much smaller, hence a much higher surface area needs to be covered with PCE. In the presence of the PCE polymers, nano-sized ettringite crystals with huge surface area are generated, consequently a higher dosage of PCE is required to achieve high fluidity of the cement paste. Surprisingly, it was found that only few unique PCE structures can avoid the effect on the morphology of ettringite. This behavior is not understood at all, and in future studies molecular simulations should be employed to identify specific structural motifs which can prevent PCEs from becoming a morphological catalyst.

In the fourth part, early ettringite nucleation and crystal growth was investigated. The behavior under idealized zero gravity conditions was studied on parabolic flights which offer 22 seconds of zero gravity. Under these conditions, convection is eliminated and

the crystallization process becomes diffusion governed only. It was found that ettringite crystals grown under zero gravity become smaller, compared to the ones formed under terrestric conditions. Apparently, the PCE polymers again work as morphological catalyst for ettringite. Under zero gravity, when PCE polymers were present the ettringite crystals grown on the surface of cement became smaller and slimmer in comparison to those from neat cement. Due to the excessively high cost of these experiments, only few samples could be studied on the flights. It would be helpful to test a more diversified portfolio of PCE structures. Perhaps then a clear relationship between the PCE molecular structure and ettringite morphology can be established. Another limitation of the experiments was the short hydration time ($\sim$ 20 seconds) of the cement paste which made it impossible to track the crystal growth of ettringite over a longer period of time. Ideally, a larger block of concrete should be prepared on the International Space Station (ISS) and its long - term hydration ($\sim$ 1 year) should be allowed to proceed before it is brought down to earth and its microstructure, crystal sizes, porosity etc. are measured.

In the last part of the thesis, the use of nano kaolin as an efficient, inexpensive enhancer for the early strength of cement was studied. It was found that nano kaolin can boost the 16 h strength by as much as 60 % without sacrificing the final strength which occurs with common cement hydration accelerators. A mechanistic study revealed that this effect is caused by nano clay acting as seeding material which produces a large number of nuclei. They then promote the crystal growth of C-S-H which starts much earlier than in normal cement. In addition, a direct correlation between the early strength enhancement and the particle size of the nano clay was observed. Only nano sized kaolin clay with a particle size $<$ 250 nm can boost the early strength of Portland cement.

7 Zusammenfassung und Ausblick

Die Arbeiten zu dieser Dissertation umfassen einen breiten Themenbereich, nämlich (1) die Wechselwirkung von Polycarboxylat-Kammpolymeren mit verschiedenen Tonmineralien; (2) eine neue, einfache Herstellmethode für PCE-Fließmittel durch Einsatz von Makroradikalen; (3) eine mechanistische Untersuchung zur Unverträglichkeit zwischen bestimmten Zementen und PCE-Fließmitteln; (4) die Keimbildung und Kristallisation von Ettringit unter Schwerelosigkeit; und (5) der Einsatz von NanoKaolin zur Verbesserung der Frühfestigkeit von Portlandzement.

Die Untersuchungen zum Einfluss unterschiedlicher Tonmineralien auf die Dispergierkraft von PCEs ergaben, dass sich verschiedene Tone unterschiedlich auf die Dispergierfähigkeit der Tone auswirken. Unter den drei Tonmineralien, die im Beton am häufigsten vorkommen, wurde Montmorillonit als der schädlichste identifiziert, bedingt durch seine quellfähige Schichtstruktur, welche konventionellen PCEs den Einbau in die Zwischenschichten über ihre PEG-Seitenketten erlaubt. Die beiden anderen Tonmineralien (Kaolin und Muskovit) zeigten hingegen einen deutlich geringeren negativen Einfluss auf die Dispergierwirkung der PCEs. Bei ihnen beruht die Wechselwirkung mit den Tonen lediglich auf einer Oberflächenadsorption.

Anhand der Untersuchungen wurde festgestellt, dass Verunreinigungen an nicht-quellfähigen Tonen im Zement kein Problem darstellen. Im Gegensatz dazu führen quellfähige Tone wie z. B. Smektite zu einer deutlich geringeren oder gar dem vollständigen Verlust der Dispergierwirkung von PCEs. Es ist deshalb für Betonwerke ratsam, ihre Zuschläge auf Anwesenheit und Menge dieser quellfähigen Tone mittels des Methylenblau-Tests zu untersuchen. Sind nennenswerte Mengen an quellfähigen Tonen enthalten, dann sollten Maßnahmen zur Reduzierung ihres schädlichen Effekts ergriffen werden. Diese könnten z. B. den Einsatz von “Opfersubstanzen” oder von kationischen Verbindungen umfassen,

welche den Zwischenschichtraum für die PCE-Moleküle blockieren, oder es werden von vornherein tonresistente PCE-Polymere eingesetzt.

Aufbauend auf diesen Überlegungen wurde ein Konzept zur Herstellung neuartiger Fließmittel mit optimaler Verträglichkeit gegenüber Tonmineralien vorgestellt. Diese neuartigen, tonbeständigen PCE-Strukturen besitzen als charakteristisches Merkmal andere Seitenketten anstelle der PEG-Seitenketten in konventionellen PCE-Polymeren. Hydroxyalkyl- oder 4-Hydroxybutylvinylether-Gruppen wurden als geeignete Seitenketten identifiziert, da sie nicht in die Zwischenschichten des Tons eingebaut werden. Durch den Ersatz der PEG-Seitenketten kann demnach keine schädliche Chemiesorption der PCEs mehr erfolgen. Demzufolge zeigen PCE-Fließmittel mit diesen neuartigen Strukturen eine wesentlich bessere Dispergierwirkung in zementären Systemen, welche mit Tonmineralien verunreinigt sind. Aufgrund der vergleichsweise kurzen Seitenketten ist ihre Dispergierwirkung in tonfreien Systemen jedoch begrenzt. In künftigen Arbeiten sollten deshalb weitere Seitenkettenarten, welche von Tonen nicht chemisorbiert werden können, untersucht werden. Das Ziel sollten PCE-Strukturen sein, welche sowohl in reinen als auch in mit Tonen verunreinigten Zementsystemen gute Wirksamkeit zeigen.

Ein weiteres Ziel dieser Arbeit war die Entwicklung einer vereinfachten Herstellmethode für MPEG-PECs. Gemäß diesem neuartigen Verfahren können MPEG-PECs aus so einfachen Ausgangsstoffen wie Maleinsäureanhydrid und ω-Methoxypolyethylenglykol hergestellt werden. Wesentlicher Punkt dieser neuen Methode ist die Erzeugung von ω-Methoxypolyethylenglykol-Makroradikalen, welche durch H-Abstraktion aus MPEG erhalten werden. Die Synthese derartiger MPEG-PCEs gemäß dieser Methode stellt eine wesentliche Vereinfachung gegenüber den konventionellen Syntheseverfahren (Veresterung oder freie radikalische Copolymerisation) dar. In künftigen Arbeiten sollte die Synthese weiter verfeinert werden, um das volle Leistungspotenzial dieser neuartigen PCE-Fließmittel ausschöpfen zu können.

Im dritten Teil der Dissertation wurde das Problem der Unverträglichkeit der meisten PCE-Polymere mit bestimmten Zementen untersucht. Die Ergebnisse deuten darauf hin, dass PCE-Fließmittel der Morphologie von Ettringitkristallen modifizieren und zu kleineren Kristallen führen, wodurch die PCEs eine größere Oberfläche besetzen müssen. REM-Aufnahmen ergaben, dass bei Anwesenheit von PCEs nanoskalige Ettringitkristalle

mit sehr hoher Oberfläche entstehen, wodurch die zur Erzielung einer hohen Verflüssigung notwendige Dosierung stark ansteigt. Interessanterweise wurde gefunden, dass nur ganz wenige, bestimmte PCE-Strukturen diesen Effekt der Modifizierung der Ettringitmorphologie nicht zeigen. Dieses Verhalten wird derzeit nicht verstanden, weshalb in künftigen Studien z. B. molekulare Simulation eingesetzt werden sollte, um spezifische Strukturmerkmale zu identifizieren, welche die Wirkung von PCEs als morphologischem Katalysator für Ettringit unterbinden.

Im vierten Teil wurden die frühe Keimbildung und das Kristallwachstum von Ettringit untersucht. Dazu wurde das Verhalten unter den idealisierten Bedingungen von Schwerelosigkeit auf Parabelflügen, welche 22 Sekunden lang den Zustand der Schwerelosigkeit herstellen, betrachtet. Unter diesen Bedingungen gibt es keine Konvektion und der Kristallisationsprozess ist ausschließlich diffusionsgesteuert. Es zeigte sich, dass unter Schwerelosigkeit gewachsene Ettringitkristalle kleiner sind als solche, die unter irdischen Bedingungen entstanden sind. Demzufolge wirken hier die PCE-Polymere noch stärker als morphologischer Katalysator. Bei Zementproben, die zehn Sekunden unter Schwerelosigkeit hydratisiert wurden, zeigten sich mehr, jedoch kleinere Ettringitkristalle auf der Oberfläche. Aufgrund der exorbitant hohen Kosten solcher Experimente konnten nur einige ausgewählte Zemente und Fließmittel untersucht werden. Es wäre sinnvoll, in künftigen Versuchen eine größere Anzahl an PCE-Fließmitteln zu testen. Eventuell ergibt sich daraus ein klareres Bild zum Zusammenhang zwischen PCE-Molekülstruktur und Ettringitmorphologie. Eine weitere Einschränkung bei den Versuchen war die kurze Reaktionszeit (ca. 20 Sekunden), welche die Verfolgung des Kristallwachstums über einen längeren Zeitraum unmöglich machte. Hierzu wäre es am besten, wenn ein größerer Betonwürfel auf der Internationalen Weltraumstation (ISS) hergestellt und über den Zeitraum von einem Jahr hydratisieren könnte, bevor er zur Erde zurückgebracht und seine Mikrostruktur, Kristallgröße der Hydrate, Porenverteilung usw. bestimmt werden.

Im letzten Teil der Dissertation wurde der Einsatz von NanoKaolin zur Steigerung der Frühfestigkeit von Zement untersucht. Es wurde gefunden, dass die Zugabe von NanoKaolin die 16 Std.-Frühfestigkeit um bis zu 60 % steigern kann und dies ohne Einbußen bei der Endfestigkeit, was bei konventionellen Beschleunigern üblicherweise der Fall ist. Mechanistische Untersuchungen ergaben, dass dieser Effekt auf der Wirkung von

NanoKaolin als Keimbildner für die C-S-H-Kristallisation beruht, wodurch eine größere Zahl an Keimen entsteht und das C-S-H-Wachstum früher als in normalem Zement einsetzt. Zudem wurde ein direkter Zusammenhang zwischen der Partikelgröße des NanoKaolins und seiner festigkeitssteigernden Wirkung festgestellt. Demnach erhöhen nur nanoskalige Kaolinpulver (d_{50}-Werte von weniger als 250 nm) die Frühfestigkeit von Portlandzement signifikant.

References

[1] P. Aïtcin and M. Baalbaki. Concrete admixtureskey components of modern concrete. In *Concrete Technology: New trends, Industrial applications*, pages 33–47. E&FN Spon, London, 1994.

[2] P. Mehta. Advancements in concrete technology. *Concrete International*, 21:69–76, 1999.

[3] K. Yamada, T. Takahashi, S. Hanehara, and M. Matsuhisa. Effects of the chemical structure on the properties of polycarboxylate-type superplasticizer. *Cement and Concrete Research*, 30:197–207, 2000.

[4] K. Yoshioka, E. Sakai, M. Daimon, and A. Kitahara. Role of steric hindrance in the performance of superplasticizers for concrete. *Journal of the American Ceramic Society*, 80:2667–2671, 1997.

[5] Helena Keller and Johann Plank. Mineralisation of CaCO3 in the presence of polycarboxylate comb polymers. *Cement and Concrete Research*, 54:1–11, 2013.

[6] A. Jeknavorian, L. Jardine, C. Ou, H. Koyata, and K. Folliard. Interaction of superplasticizers with clay-bearing aggregates. *ACI Special Publication*, 217:143–160, 2003.

[7] E. Sakai, D. Atarashi, and M. Daimon. Interaction between superplasticizers and clay minerals. In *Proceedings of the 6th International Symposium on Cement & Concrete*, pages 1560–1566, 2006.

[8] D. Atarashi, E. Sakai, R. Obinata, and M. Daimon. Influence of clay minerals on fluidity of CaCO3 suspension containing comb-type polymer. *Cement and Concrete Science and Technology*, 57:386–391, 2003.

[9] F. Kong, X. Sun, L. Yang, and Z. Sun. Effect of clay content of sand on technical-

economical index of concrete with polycarboxylic high performance water reducer. *Concrete*, 2:95–96,112, 2011.

[10] L. Lei and J. Plank. A concept for a polycarboxylate superplasticizer possessing enhanced clay tolerance. *Cement and Concrete Research*, 42:1299–1306, 2012.

[11] L. Lei and J. Plank. Synthesis and properties of a vinyl ether-based polycarboxylate superplasticizer for concrete possessing clay tolerance. *Industrial & Engineering Chemistry Research*, 53:1048–1055, 2014.

[12] P. Aïtcin. *High performance concrete*. CRC press, 2011.

[13] K. Yoshioka, E. Tazawa, K. Kawai, and T. Enohata. Adsorption characteristics of superplasticizers on cement component minerals. *Cement and Concrete Research*, 32:1507–1513, 2002.

[14] J. Plank and C. Hirsch. Superplasticizer adsorption on synthetic ettringite. In V.M. Malhotra, editor, *7th CANMET/ACI Conference on Superplasticizers and Other Chemical Admixtures in Concrete*, pages 283–298, 2003.

[15] J. Plank, P. Chatziagorastou, and C. Hirsch. New model describing distribution of adsorbed superplasticizer on the surface of hydrating cement grain. *Journal of Building Materials*, 10:7–13, 2007.

[16] S. Han and J. Plank. Mechanistic study on the effect of sulfate ions on polycarboxylate superplasticisers in cement. *Advances in Cement Research*, 25:200–207, 2013.

[17] D. Marchon, U. Sulser, A. Eberhardt, and R. Flatt. Molecular design of comb-shaped polycarboxylate dispersants for environmentally friendly concrete. *Soft Matter*, 9:10719–10728, 2013.

[18] W. Prince, M. Edwards-Lajnef, and P. Atcin. Interaction between ettringite and a polynaphthalene sulfonate superplasticizer in a cementitious paste. *Cement and Concrete Research*, 32:79–85, 2002.

[19] P. Aitcin, C. Jolicoeur, and J. MacGregor. Superplasticizers: how they work and why they occasionally don't. *Concrete International*, 16:45–52, 1994.

[20] V. Ramachandran, V. Malhotra, C. Jolicoeur, and N. Spiratos. *Suplerplasticizers: properties and applications in concrete*. Ottawa : Natural Resources Canada,

Canada Centre for Mineral and Energy Technology, Ottawa, 1997.

[21] E. Sakai and M. Daimon. Mechanisms of superplastification. In *Materials Science of Concrete IV*, pages 91–111. American Ceramic Society, 1995.

[22] L. Lei and J. Plank. Synthesis, working mechanism and effectiveness of a novel cycloaliphatic superplasticizer for concrete. *Cement and Concrete Research*, 42:118–123, 2012.

[23] J. Walraven. High performance concrete: a material with a large potential. *Journal of Advanced Concrete Technology*, 7:145–156, 2009.

[24] V. Malhotra. Innovative applications of superplasticizers in concrete: a review. *Proceeding of the International Symposium 'The Role of Admixtures in High Performance Concrete'*, 5:421–460, 1999.

[25] I. Torresan, R. Magarotto, and R. Khurana. Development of a new betanaphthaline sulfonate-based superplasticizer especially studied for precast application. *ACI Special Publication*, 173:559–582, 1997.

[26] K. Hattori. Mechanism of slump loss and its control. *Journal of the Society of Materials Science, Japan*, 29:240, 1980.

[27] G. Chen, H. Zhu, and G. Huang. Modified aliphatic superplasticizer and preparation method thereof, CN 103113036, 2014.

[28] A. Aignesberger and J. Plank. Saeuregruppen containing thermostable hydrophilic condensation products of aldehydes and ketones, DE 3,144,673, 1981.

[29] J. Plank and A. Aignesberger. Dispersing agent for saline systems, DE 3,344,291, 1981.

[30] J. Plank, F. DugonjićBilić, and N. Lummer. Modification of the molar anionic charge density of acetoneformaldehydesulfite dispersant to improve adsorption behavior and effectiveness in the presence of CaAMPS® – co – NNDMA cement fluid loss polymer. *Journal of Applied Polymer Science*, 111:2018–2024, 2009.

[31] M. Pei, Y. Yang, X. Zhang, J. Zhang, and Y. Li. Synthesis and properties of watersoluble sulfonated acetoneformaldehyde resin. *Journal of Applied Polymer Science*, 91:3248–3250, 2004.

[32] T. Vickers, S. Farrington, J. Bury, and L. Brower. Influence of dispersant structure

and mixing speed on concrete slump retention. *Cement and Concrete Research*, 35:867–873, 2005.

[33] C. Li, N. Feng, and R. Chen. Effects of polyethlene oxide chains on the performance of polycarboxylate-type water-reducers. *Cement and Concrete Research*, 35:867–873, 2005.

[34] F. Winnefeld, S. Becker, J. Pakusch, and T. Götz. Effects of the molecular architecture of comb-shaped superplasticizers on their performance in cementitious systems. *Cement and Concrete Research*, 29:251–262, 2007.

[35] J. Plank, C. Schroefl, M. Gruber, M. Lesti, and R. Sieber. Effectiveness of polycarboxylate superplasticizers in ultra-high strength concrete: the importance of PCE compatibility with silica fume. *Journal of Advanced Concrete Technology*, 7:5–12, 2009.

[36] B. Felekolu and H. Sarikahya. Effect of chemical structure of polycarboxylate-based superplasticizers on workability retention of self-compacting concrete. *Construction and Building Materials*, 22(9):1972–1980, 2008.

[37] J. Guicquero, P. Maitrasse, M. Mosquet, and A. Sers. Water soluble or water dispersible dispersing agent for cement compositions and mineral particle aqueous suspension, and additives containing such dispersing agent. WO 1999047468, 1999.

[38] Z. Wang, Y. Xu, H. Wu, X. Liu, F. Zheng, H. Li, S. Cui, M. Lan, and Y. Wang. A room temperature synthesis method for polycarboxylate superplasticizer, CN 103897119, 2013.

[39] S. Akimoto, S. Honda, and T. Yasukohchi. Additives for cement, US 4946904, 1992.

[40] G. Albrecht, A. Kern, J. Penkner, and J. Weichmann. Copolymers based on oxyalkyleneglycol alkenyl ethers and derivatives of unsaturated dicarboxylic acids, EP 0736553, 1996.

[41] D. Hamada, F. Yamato, T. Mizunuma, and H. Ichikawa. Additive mixture for cement-based concrete or mortar contains a copolymer of polyalkoxylated unsaturated acid and a mixture of alkoxylated carboxylic acid with a corresponding ester and/or an alkoxylated alcohol. DE 10048139, 2001.

[42] M. Yamamoto, T. Uno, Y. Onda, H. Tanaka, A. Yamashita, T. Hirata, and N. Hi-

rano. Copolymer for cement admixtures and its production process and use, US Patent, 6,727,315, 2004.

[43] H. Tahara, H. Ito, Y. Mori, and M. Mizushima. Cement additive, method for producing the same, and cement composition, US Patent, 5,476,885, 1995.

[44] T. Amaya, A. Ikeda, J. Imamura, A. Kobayashi, K. Saito, W. Danzinger, and T. Tomoyose. Cement dispersant and concrete composition containing the dispersant, US 7393886, 2000.

[45] M. Mosquet, Y. Chevalier, S. Brunel, J. Guicquero, and P. Le Perchec. Polyoxyethylene diphosphonates as efficient dispersing polymers for aqueous suspensions. *Journal of Applied Polymer Science*, 65:2545–2555, 1997.

[46] A. Kraus, F. Dierschke, F. Becker, T. Schuhbeck, H. Grassl, and K. Groess. Method for producing phosphated polycondensation products and the use thereof, US 20110281975, 2011.

[47] F. Dalas, A. Nonat, S. Pourchet, M. Mosquet, D. Rinaldi, and S. Sabio. Tailoring the anionic function and the side chains of comb-like superplasticizers to improve their adsorption. *Cement and Concrete Research*, 67:21–30, 2015.

[48] D. Hamada, T. Hamai, M. Shimoda, Y. Kono, Y. Tanisho, Y. Morii, and Y. Naka. Phosphoric ester polymer, WO 2006006732, 2006.

[49] P. Wieland, A. Kraus, G. Albrecht, K. Becher, and H. Grassl. Polycondensation product base on aromatic or heteroaromatic compounds, method for the production thereof, and use thereof, US 20080108732, 2008.

[50] F. Dierschke and A. Kraus. Formulation and its use, US 20110054081, 2011.

[51] T. Hirata, T. Yuasa, K. Shiote, K. Nagare, and S. Iwai. Cement dispersant, method for producing polycarboxylic acid for cement dispersant and cement composition. US 6174980, 2001.

[52] J. Paas, M. Müller, and J. Plank. Influence of diester content in macromonomers on performance of MPEG-based PCEs. In *11th International Conference on Superplasticizers and Other Chemical Admixtures in Concrete (CANMET/ACI)*, 2015.

[53] J. Plank, K. Pöllmann, N. Zouaoui, P. Andres, and C. Schaefer. Synthesis and performance of methacrylic ester based polycarboxylate superplasticizers possess-

ing hydroxy terminated poly (ethylene glycol) side chains. *Cement and Concrete Research*, 38:1210–1216, 2008.

[54] G. Chiocchio and A. Paolini. Optimum time for adding superplasticizer to Portland cement pastes. *Cement and Concrete Research*, 15:805–813, 1985.

[55] P. Andersen, D. Roy, J. Gaidis, and W. Grace. The effects of adsorption of superplasticizers on the surface of cement. *Cement and Concrete Research*, 17:805–813, 1987.

[56] F. El-Hosiny. Physico-mechanical characteristics of admixed cement pastes containing melment. *Silicates industriels*, 1-2:3–7, 2002.

[57] S. El Gamal and H. Bin Salman. Effect of addition of Sikament-R superplasticizer on the hydration characteristics of portland cement pastes. *HBRC Journal*, 8:75–80, 2012.

[58] M. Heikal, M. Morsy, and I. Aiad. Effect of polycarboxylate superplasticizer on hydration characteristics of cement pastes containing silica fume. *Ceramics Silikaty*, 50:5–14, 2006.

[59] M. Mollah, W. Adams, R. Schennach, and D. Cocke. A review of cementsuperplasticizer interactions and their models. *Advances in Cement Research*, 12:153–161, 2000.

[60] R. Flatt and Y. Houst. A simplified view on chemical effects perturbing the action of superplasticizers. *Cement and Concrete Research*, 31:153–161, 2001.

[61] K. Yamada, S. Ogawa, and S. Hanehara. Controlling of the adsorption and dispersing force of polycarboxylate-type superplasticizer by sulfate ion concentration in aqueous phase. *Cement and Concrete Research*, 31:375–383, 2001.

[62] S. Collepardi, L. Coppola, R. Troli, and M. Collepardi. Mechanisms of actions of different superplasticizers for high performance concrete. *ACI Special Publication*, 186:503–524, 1999.

[63] C. Tiemeyer, A. Lange, and J. Plank. Determination of the adsorbed layer thickness of functional anionic polymers utilizing chemically modified polystyrene nanoparticles. *Colloids and Surfaces A: Physicochemical and Engineering Aspects*, 456(1):139–145, 2014.

[64] R. Ottewill and T. Walker. The influence of non-ionic surface active agents on the stability of polystyrene latex dispersions. *Kolloid-Zeitschrift & Zeitschrift fuer Polymere*, 227(1-2):108–116, 1968.

[65] C. Weaver and L. Pollard. *The chemistry of clay minerals*. Elsevier, Amsterdam, 1973.

[66] B. Velde. *Introduction to clay minerals: Chemistry, origins, uses and environmental significance*. Springer Science & Business Media, 2012.

[67] M. Brigatti, E. Galan, and B. Theng. Structure and mineralogy of clay minerals. In F. Bergaya, B. Theng and G. Lagaly, editors, *Handbook of Clay Science*, Chapter 2, 1:19–86, 2006.

[68] L. Fowden, R. Barrer, and P. Tinker. *Clay minerals: their structure, behaviour, and use*, volume 311. The Royal Society Of Chemistry, 1984.

[69] M. Nehdi. Clay in cement-based materials: Critical overview of state-of-the-art. *Construction and Building Materials*, 51:372–385, 2014.

[70] R. Anderson, I. Ratcliffe, H. Greenwell, P. Williams, S. Cliffe, and P. Coveney. Clay swellinga challenge in the oilfield. *Earth-Science Reviews*, 98:201–216, 2010.

[71] A. Posner and J. Quirk. The adsorption of water from concentrated electrolyte solutions by montmorillonite and illite. *Proceedings of the Royal Society of London A: Mathematical, Physical and Engineering Sciences*, 278(1372):35–56, 1964.

[72] R. Mooney, A. Keenan, and L. Wood. Adsorption of water vapor by montmorillonite. II. Effect of exchangeable ions and lattice swelling as measured by X-ray diffraction. *Journal of the American Chemical Society*, 74(6):1371–1374, 1952.

[73] L. Olanitori. Mitigating the effect of clay content of sand on concrete strength. In *31st Conference on Our World in Concrete & Structures*, pages 16–17, Singapore, 2006.

[74] B. Li, J. Wang, and M. Zhou. C60 high performance concrete prepared from manufactured sand with a high content of microfines. In *Key Engineering Materials*, pages 204–211. Trans Tech Publ, 2009.

[75] J. Norvell, J. Stewart, M. Juenger, and D. Fowler. Influence of clays and clay-sized particles on concrete performance. *Journal of Materials in Civil Engineering*,

19:1053–1059, 2007.

[76] S. Ng and J. Plank. Interaction mechanisms between Na montmorillonite clay and MPEG-based polycarboxylate superplasticizers. *Cement and Concrete Research*, 42:847–854, 2012.

[77] A. Shayan. Aggregate selection for durability of concrete structures. In *Proceedings of the Institution of Civil Engineers-Construction Materials*, volume 164, pages 111–121, 2011.

[78] W. Cole and F. Beresford. Evaluation of basalt from Deer Park, Victoria, as an aggregate for concrete: a progress report. In *Australian Road Research Board Conference Proc*, pages 30–59, 1976.

[79] 210-05 AASHTOT. Standard test method for aggregate durability index, 2011.

[80] ASTM C837-09. Standard test method for methylene blue index of clay, 2014.

[81] M. Morsy, S. Alsayed, and M. Aqel. Effect of nano-clay on mechanical properties and microstructure of ordinary Portland cement mortar. *International Journal of Civil & Environmental Engineering*, 10:23–27, 2010.

[82] S. Pavlidou and C. Papaspyrides. A review on polymerlayered silicate nanocomposites. *Progress in Polymer Science*, 33:1119–1198, 2008.

[83] S. Guggenheim and R. Martin. Definition of clay and clay mineral: joint report of the AIPEA nomenclature and CMS nomenclature committees. *Clays and Clay Minerals*, 43:255–256, 1995.

[84] S. Ray. An overview of pure and organically modified clays. In *Clay-Containing Polymer Nanocomposites: From Fundamentals to Real Applications*, pages 1–24. Elsevier Amsterdam, 2013.

[85] F. Bergaya and G. Lagaly. General Introduction: Clays, Clay Minerals, and Clay Science. In Faïza Bergaya and Gerhard Lagaly, editors, *Handbook of Clay Science*, 1: 1–18, 2006.

[86] R. Grim. *Clay mineralogy*. McGraw-Hill, New York, 1953.

[87] K. Satyanarayana and F. Wypych. *Clay surfaces: fundamentals and applications*. Elsevier Academic Press, Amsterdam, 2004.

[88] D. Roy and R. Roy. An experimental study of the formation and properties of

synthetic serpentines and related layer silicate minerals. *American Mineralogist*, 39:957–975, 1954.

[89] G. Brown. *The X-ray identification and crystal structures of clay minerals*. Mineralogical Society, London, 1961.

[90] G. Gao, Y. Wang, L. Wang, and Y. Zhang. The influence of clay to water-reducing effect of polycarboxylic. *Applied Mechanics and Materials*, 357-360:1115–1119, 2013.

[91] X. Liu, Z. Wang, H. Wu, and H. Li. Effects of clay on flow properties of polycarboxylate superplasticizer and its control measure. *Advanced Materials Research*, 690-693:682–685, 2013.

[92] G. Lagaly. Interaction of alkylamines with different types of layered compounds. *Solid State Ionics*, 22:43–51, 1986.

[93] P. LeBaron, Z. Wang, and T. Pinnavaia. Polymer-layered silicate nanocomposites: an overview. *Applied Clay Science*, 15:11–29, 1999.

[94] M. Bolland, A. Posner, and J. Quirk. pH-independent and pH-dependent surface charges on kaolinite. *Clays Clay Miner.*, 28:412–418, 1980.

[95] L. Lei and J. Plank. A study on the impact of different clay minerals on the dispersing force of conventional and modified vinyl ether based polycarboxylate superplasticizers. *Cement and Concrete Research*, 60:1–10, 2014.

[96] S. Iida. Interaction of calcium ion and maleic acid copolymer. *Biophysical chemistry*, 53:219–225, 1995.

[97] P. Daniele, C. De Stefano, M. Ginepro, and S. Sammartano. Salt effects on the protonation of polymethacrylate and Na^+, K^+, Ca^{2+} complex formation. *Fluid Phase Equilibria*, 163:127–137, 1999.

[98] C. Bretti, F. Crea, C. Rey-Castro, and S. Sammartano. Interaction of acrylic-maleic copolymers with H^+, Na^+, Mg^{2+} and Ca^{2+}: Thermodynamic parameters and their dependence on medium. *React. Funct. Polym.*, 65:329–342, 2005.

[99] J. Plank, C. Liu, and S. Ng. Interaction between clays and polycarboxylate superplasticizers in cementitious systems. *GDCh-Monographie*, 42:349–356, 2010.

[100] P. Reid, B. Dolan, and S. Cliffe. Mechanism of shale inhibition by polyols in water based drilling fluids. *SPE International Symposium on Oilfield Chemistry*, pages

155–167, 1995.

[101] A. Bains, E. Boek, P. Coveney, S. Williams, and M. Akbar. Molecular modelling of the mechanism of action of organic clay-swelling inhibitors. *Molecular Simulation*, 26:101–145, 2001.

[102] S. Liu, X. Mo, C. Zhang, D. Sun, and C. Mu. Swelling inhibition by polyglycols in montmorillonite dispersions. *Journal of Dispersion Science and Technology*, 25:101–145, 2004.

[103] S. Ng and J. Plank. Study on the interaction of Na-montmorillonite clay with polycarboxylates. *10th International Conference on Superplasticizers and Other Chemical Admixtures in Concrete*, ACI, SP-288:1–15, 2012.

[104] L. Bailey, M. Keall, A. Audibert, and J. Lecourtier. Effect of clay/polymer interactions on shale stabilization during drilling. *Langmuir*, 10:1533–1549, 1994.

[105] J. Plank, E. Sakai, C. Miao, C. Yu, and J. Hong. Chemical admixturesChemistry, applications and their impact on concrete microstructure and durability. *Cement and Concrete Research*, 78:81–99, 2015.

[106] L. Lei and J. Plank. Synthesis, properties and evaluation of a more clay tolerant polycarboxylate possesing hydroxy alkyl graft chains. In *10th CANMET/ACI Conference on Superplasticizers and Other Chemical Admixtures in Concrete*, Supplementary Papers, pages 1–20, 2012.

[107] V. Dodson and T. Hayden. Another look at the Portland cement/chemical admixture incompatibility problem. *Cement, Concrete and Aggregates*, 11:52–56, 1989.

[108] C. Johnston. Admixture-cement incompatibility. *ACI COMPILATION*, 23, 1993.

[109] P. Aitcin and A. Neville. High-performance concrete demystified. *Concrete International*, 15:21–26, 1993.

[110] M. Polivka and A. Klein. Effect of water-reducing admixtures and set-retarding admixtures as influenced by Portland cement composition. *Symposium on Effect of Water-Reducing Admixtures and Set-Retarding Admixtures on Properties of Concrete*, pages 124–139, 1959.

[111] G. Wallace and E. Ore. *Structural and lean mass concrete as affected by water-reducing, set-retarding agents.* ASTM Special Technical Publication, 1960.

[112] W. Perenchio, D. Whiting, and D. Kantro. Water reduction, slump loss, and entrained air-void systems as influenced by superplasticizers. *ACI Special Publication*, 62:137–156, 1979.

[113] D. Whiting. Effects of high-range water reducers on some properties of fresh and hardened concretes, 1979.

[114] S. Khalil and M. Ward. Effect of sulphate content of cement upon heat evolution and slump loss of concretes containing high-range water-reducers (superplasticizers). *Magazine of Concrete Research*, 32:28–38, 1980.

[115] V. Ramachandran. Absorption and hydration behavior of tricalcium aluminate-water and tricalcium aluminate-gypsum-water systems in the presence of superplasticizers. *ACI Journal*, (May-June):235–241, 1983.

[116] http://www.theconcreteportal.com/compat.html.

[117] H. Taylor. *Cement chemistry*. Academic Press, 1990.

[118] J. Plank. Concrete admixtures where are we now and what can we expect in the future? *19. Ibausil, Tagungsband 1, Bauhaus-Universität Weimar*, pages 27–42, 2015.

[119] F. Basile, S. Biagini, G. Ferrari, and M. Collepardi. Effect of the gypsum state in industrial cements on the action of superplasticizers. *Cement and Concrete Research*, 17:715–722, 1987.

[120] W. Prince, M. Espagne, and P. Atcin. Ettringite formation: a crucial step in cement superplasticizer compatibility. *Cement and Concrete Research*, 33:635–641, 2003.

[121] C. Jolicoeur, P. Nkinamubanzi, M. Simard, and M. Piotte. Progress in understanding the functional properties of superplasticizers in fresh concrete. *ACI Special Publication*, 148:63–88, 1994.

[122] E. Álvarez-Ayuso and H. Nugteren. Synthesis of ettringite: a way to deal with the acid wastewaters of aluminium anodising industry. *Water Research*, 39:65–72, 2005.

[123] H. Taylor. Crystal structures of some double hydroxide minerals. *Mineralogical Magazine*, 39:377–389, 1973.

[124] A. Moore and H. Taylor. Crystal structure of ettringite. *Acta Crystallographica Section B: Structural Crystallography and Crystal Chemistry*, 26:386–393, 1970.

[125] J. Bohm and B. Pamplin. *Crystal growth*. Pergamon Press, 1975.

[126] A. Myerson. *Handbook of industrial crystallization*. Butterworth-Heinemann, 2002.

[127] J. Gibbs. On the equilibrium of heterogeneous substances. *Transactions of the Connecticut Academy*, 3:108–248/343–524, 1876.

[128] E. Kaldis. Principles of the vapour growth of single crystals. In C. H. L. Goodman, editor, *Crystal Growth: Theory and Techniques Vol.1*, pages 49–191. Plenum, London, 1974.

[129] P. Cubillas and M. Anderson. Synthesis mechanism: crystal growth and nucleation. In J. Čejka, A. Corma, and S. Zones, editors, *Zeolites and Catalysis: Synthesis, Reactions and Applications*, pages 1–55. Wiley-VCH Verlag GmbH & Co. KGaA, Weinheim, Germany, 2010.

[130] D. Kashchiev. *Nucleation basic theory with applications*. Butterworth-Heinemann, Oxford, 2000.

[131] J. De Yoreo and P. Vekilov. Principles of crystal nucleation and growth. *Reviews in Mineralogy & Geochemistry - Rev Mineral Geochem*, 54(1):57–93, 2003.

[132] E. Saridakis and N. Chayen. Imprinted polymers assisting protein crystallization. *Trends Biotechnol.*, 31:515–520, 2013.

[133] T. Zhang and X. Liu. Controlled colloidal assembly: experimental modeling of crystallization. In T. Nishinaga, editor, *Handbook of Crystal Growth Fundamentals: Thermodynamics and Kinetics*, pages 561–594. Elsevier, 2014.

[134] M. Trau, D. Saville, and I. Aksay. Field-induced layering of colloidal crystals. *Science*, 272:706–709, 1996.

[135] T. Palberg. Crystallization kinetics of repulsive colloidal spheres. *Journal of Physics: Condensed Matter*, 11:R323–R360, 1999.

[136] A. Larsen and D. Grier. Like-charge attractions in metastable colloidal crystallites. *Nature*, 385:230–233, 1997.

[137] A. Yethiraj and A. van Blaaderen. A colloidal model system with an interaction tunable from hard sphere to soft and dipolar. *Nature*, 421:513–517, 2003.

[138] W. Götze, J. Hansen, D. Levesque, and J. Zinn-Justin. *Liquids, freezing and the glass transition*. North Holland, 1991.

[139] X. Liu and J. Yoreo. *Nanoscale structure and assembly at solid-fluid interfaces: assembly in hybrid and biological systems*. Springer, London, 2004.

[140] D. Aarts, M. Schmidt, and H. Lekkerkerker. Direct visual observation of thermal capillary waves. *Science*, 304:847–850, 2004.

[141] W. Poon. Colloids as big atoms. *Science*, 304:830–831, 2004.

[142] D. Frenkel. Playing tricks with designer "atoms". *Science*, 296:65–66, 2002.

[143] U. Gasser, E. Weeks, A. Schofield, P. Pusey, and D. Weitz. Real-space imaging of nucleation and growth in colloidal crystallization. *Science*, 292:258–262, 2001.

[144] Y. Diao and X. Liu. Controlled colloidal assembly: Experimental modeling of general crystallization and biomimicking of structural color. *Advanced Functional Materials*, 22:1354–1375, 2012.

[145] K. Zhang and X. Liu. In situ observation of colloidal monolayer nucleation driven by an alternating electric field. *Nature*, 429:739–743, 2004.

[146] F. Abraham. *Homogeneous nucleation theory: the pretransition theory of vapor condensation*. Academic Press Inc, New York, 1973.

[147] A. Laaksonen, V. Talanquer, and D. Oxtoby. Nucleation: measurements, theory, and atmospheric applications. *Annual Review of Physical Chemistry*, 46:489–524, 1995.

[148] A. Chernov. *Modern Crystallography: Crystal Growth*. Springer, Berlin, 1984.

[149] R. McGraw and A. Laaksonen. Scaling properties of the critical nucleus in classical and molecular-based theories of vapor-liquid nucleation. *Physical Review Letters*, 76:2755–2757, 1996.

[150] D. Gebauer and H. Cölfen. Prenucleation Clusters and Nonclassical Nucleation. *Nano Today*, 6(6):564–584, 2011.

[151] F. Meldrum and R. Sear. Now you can see them. *Science*, 322:1802–1803, 2008.

[152] L. DeLucas, K. Moore, M. Long, R. Rouleau, T. Bray, W. Crysel, and L. Weise. Protein crystal growth in space, past and future. *Journal of Crystal Growth*, 239:1646–1650, 2002.

[153] A. McPherson. Virus and protein crystal growth on earth and in microgravity. *Journal of Physics D: Applied Physics*, 324:207–211, 2011.

[154] P. Fontana, J. Schefer, and D. Pettit. Characterization of sodium chloride crystals grown in microgravity. *Journal of Crystal Growth*, 324:207–211, 2011.

[155] Y. Zhou, X. Li, S. Bai, and L. Chen. Comparison of space-and ground-grown Bi2Se0.21Te2.79 thermoelectric crystals. *Journal of Crystal Growth*, 312:775–780, 2010.

[156] H. Madsen, F. Christensson, L. Polyak, E. Suvorova, M. Kliya, and A. Chernov. Calcium phosphate crystallization under terrestrial and microgravity conditions. *Journal of Crystal Growth*, 152:191–202, 1995.

[157] M. Bury, L. Jalbert, and S. Mustaikis. Taking concrete to the outer limits. *Concrete Construction*, 40:855–859, 1995.

[158] V. Dodson. Set Accelerating Admixtures. In *Concrete Admixtures*, chapter 4, pages 73–102. Van Nostrand Reinhold, New York, 1990.

[159] R. Rixom and N. Mailvaganam. Accelerators. In *Chemical Admixtures for Concrete*, chapter 5, pages 182-187. E&FN Spon, London, 1999.

[160] D. Berry, B. D. Black, and P. Kirby. Acid formates for use as setting and early strength development accelerators in cementitious compositions, US 4261755, 1981.

[161] A. Rosenberg. Study of the Mechanism Through Which Calcium Chloride Accelerates the Set of Portland Cement. *Journal of the American Concrete Institute*, 61(10):1261–1268, 1961.

[162] R. Edmeades and P. Hewlett. Cement Admixtures. In *Lea's Chemistry of Cement and Concrete*, pages 877–887. Arnold, London, 1998.

[163] R. Rixom and N. Mailvaganam. Accelerators. In *Chemical Admixtures for Concrete*, chapter 5, pages 182–187. E&FN Spon, London, 4th edition, 1999.

[164] http://usstn.com/shotcrete-application-process-video/.

[165] R. Myrdal. Modern Chemical Admixtures for Shotcrete. In N. Barton, editor, *Proceedings from Third International Symposium on Sprayed Concrete*, pages 373–382, Gol, Norway, 1999.

[166] D. Millette and M. Jolin. Shotcrete Accelerators for Wet-Mix, 2014.

[167] R. Rixom and N. Mailvaganam. Air Entraining Admixtures. In *Chemical Admixtures for Concrete*, chapter 6, pages 252–265. E&FN Spon, London, 1999.

[168] V. Ramachandran. Miscellaneous admixtures. In *Concrete Admixtures Handbook. Properties, Science and Technology*, chapter 15, pages 1009–1017. Noyes Publications, 2nd edition, 1995.

[169] R. Myrdal. Accelerating Admixtures for Concrete. State of the Art. Technical report, SINTEF Building and Infrastructure COIN Concrete Innovation Centre, 2007.

[170] J. Blank. Use of Shotcrete for Underground Structural Support. *ASCE and ACI*, SP-45:320–329, 1975.

[171] L. Prudencio. Accelerating Admixtures for Shotcrete. *Cement, Concrete and Composites*, 20:213–219, 1998.

[172] L. Nicoleau, G. Albrecht, K. Lorenz, E Jetzlsperger, D. Fridrich, T. Wohlhaupter, R. Dorfner, H. Leitner, M. Vierle, D. Schmitt, M. Braeu, C. Hesse, S. M. Pancera, Z. Siegfried, and M. Kutschera. Plasticizer-Containing Hardening Accelerator Composition, 2011.

[173] V. Kanchanason and J. Plank. C-S-H PCE Nanocomposites for Enhancement of Early Strength of Portland Cement. In Caijun Shi and Yan Yao, editors, *The 14th International Congress on the Chemistry of Cement*, page 326, Beijing, 2015.

[174] T. Alfrey and C. Price. Relative reactivities in vinyl copolymerization. *Journal of Polymer Science*, 2:101–106, 1947.

[175] J. Brandrup, E. Immergut, E. Grulke, A. Abe, and D. Bloch. *Polymer handbook*. John Wiley & Sons, Inc., 1999.